THE MINOR PLANET BULLETIN

BULLETIN OF THE MINOR PLANETS SECTION OF THE ASSOCIATION OF LUNAR AND PLANETARY OBSERVERS

VOLUME 52, NUMBER 1, A.D. 2025 JANUARY-MARCH

EDITOR'S NOTE

Please join in celebrating and thanking Professor Pilcher for this decades-long series that has been an essential guidepost for minor planet observers.

MINOR PLANETS AT UNUSUALLY FAVORABLE ELONGATIONS IN 2025

Frederick Pilcher
4438 Organ Mesa Loop
Las Cruces, NM 88011 USA
fpilcher35@gmail.com

(Received: 2024 August 5)

A list is presented of minor planets which are much brighter than usual at their 2025 apparitions. For reasons explained, the list in this article is the final installment of a 52-year sequence prepared by the author.

The minor planets in the lists which follow will be much brighter at their 2025 apparitions than at their average distances at maximum elongation. Many years may pass before these planets will be again as bright as in 2025. Observers are encouraged to give special attention to those which lie near the limit of their equipment.

These lists have been prepared by an examination of the maximum elongation circumstances of minor planets computed by the author for all years through 2060 with a full perturbation program written by Dr. John Reed, and to whom he expresses his thanks. Elements are from EMP 1992, except that for all planets for which new or improved elements have been published subsequently in the Minor Planet Circulars or in electronic form, the newer elements have been used. Planetary positions are from the JPL DE-200 ephemeris, courtesy of Dr. E. Myles Standish.

Any planets whose brightest magnitudes near the time of maximum elongation vary by at least 2.0 in this interval and in 2025 will be within 0.3 of the brightest occurring, or vary by at least 3.0 and in 2025 will be within 0.5 of the brightest occurring; and which are visual magnitude 14.5 or brighter, are included. For planets brighter than visual magnitude 13.5, which are within the range of a large number of observers, these standards have been relaxed somewhat to include a larger number of planets. Magnitudes have been computed from the updated magnitude parameters published in MPC28104-28116, on 1996 Nov. 25, or more recently in the Minor Planet Circulars.

Oppositions may be in right ascension or in celestial longitude. Here we use still a third representation, maximum elongation from the Sun, instead of opposition. Though unconventional, it has the advantage that many close approaches do not involve actual opposition to the Sun near the time of minimum distance and greatest brightness and are missed by an opposition-based program. Other data are also provided according to the following tabular listings: Minor planet number, date of maximum elongation from the Sun in format yyyy/mm/dd, maximum elongation in degrees, right ascension on date of maximum elongation, declination on date of maximum elongation, both in J2000 coordinates, date of brightest magnitude in format yyyy/mm/dd, brightest magnitude, date of minimum distance in format yyyy/mm/dd, and minimum distance in AU.

Users should note that when the maximum elongation is about 177° or greater, the brightest magnitude is sharply peaked due to enhanced brightening near zero phase angle. Even as near as 10 days before or after minimum magnitude the magnitude is generally about 0.4 magnitudes greater. This effect takes place in greater time interval for smaller maximum elongations. There is some interest in very small minimum phase angles. For maximum elongations E near 180° at Earth distance Δ, an approximate formula for the minimum phase angle ϕ is

$$\phi=(180°-E)/(\Delta+1)$$

where the units are degrees.

A special list of asteroids approaching the Earth more closely than 0.3 AU is provided following the list of temporal sequence of favorable elongations.

This author has prepared, starting with MPB V.1 No. 3 (1974 January-March), lists of minor planets brighter in the coming year than at most of their oppositions. These lists have now been prepared for 52 consecutive years. In the early years this was done by an ad hoc examination of the Institute for Theoretical Astronomy annual volumes, “Ephemerides of Minor Planets for the Year 19__.” In the 1990’s the author used Windows based 16-bit computers with 1990’s programs to prepare the comprehensive lists that have appeared in this annual Minor Planet Bulletin series. But these lists were prepared only through the year 2025. The year 2025 is now arriving, and the computational facilities to produce listings for 2026 and forward no longer exist.

Therefore, the list in this article is the final installment of a 52-year sequence of “Minor Planets at Unusually Favorable Elongations.” The author thanks users of these articles who have expressed their appreciation to him.

Table I. Numerical Sequence of Favorable Elongations

Planet	Max Elon D	Max E	RA	Dec	Br Mag D	Br Mag	Min Dist D	Min Dist
6	2025/08/25	172.5°	22h32m	-17°	2025/08/26	7.6	2025/08/31	1.025
24	2025/02/26	178.9°	10h37m	+ 9°	2025/02/26	10.7	2025/02/26	1.797
28	2025/02/01	176.5°	8h53m	+13°	2025/02/01	9.8	2025/02/01	1.380
61	2025/09/01	176.9°	22h38m	- 5°	2025/09/01	10.7	2025/09/01	1.490
63	2025/08/03	174.9°	20h56m	-22°	2025/08/02	9.6	2025/07/29	1.122
85	2025/10/16	179.5°	1h27m	+ 9°	2025/10/16	10.1	2025/10/09	1.310
89	2025/08/10	176.1°	21h20m	-11°	2025/08/11	8.8	2025/08/15	1.138
104	2025/11/08	179.6°	2h52m	+16°	2025/11/08	11.6	2025/11/10	1.684
129	2025/08/05	179.0°	21h 1m	-15°	2025/08/05	10.1	2025/07/28	1.503
139	2025/03/21	179.5°	12h 2m	+ 0°	2025/03/21	10.3	2025/03/20	1.322
141	2025/08/08	179.0°	21h13m	-17°	2025/08/08	10.7	2025/08/15	1.285
172	2025/07/25	170.4°	20h24m	-29°	2025/07/25	11.1	2025/07/27	1.128
185	2025/08/31	176.9°	22h43m	-11°	2025/08/31	10.5	2025/09/02	1.445
188	2025/06/07	174.4°	17h 5m	-17°	2025/06/07	12.1	2025/06/13	1.400
200	2025/12/31	171.8°	6h41m	+31°	2025/12/30	11.4	2025/12/27	1.487
226	2025/08/17	174.6°	21h59m	-17°	2025/08/17	12.2	2025/08/12	1.223
244	2025/10/03	178.0°	0h34m	+ 5°	2025/10/03	13.4	2025/10/03	0.878
245	2025/11/12	178.4°	3h12m	+16°	2025/11/12	10.8	2025/11/09	1.511
259	2025/06/01	175.1°	16h37m	-17°	2025/06/01	11.3	2025/06/01	1.715
278	2025/04/27	174.4°	14h27m	- 8°	2025/04/27	12.3	2025/04/27	1.387
312	2025/07/16	165.0°	19h54m	-36°	2025/07/15	11.9	2025/07/13	1.371
313	2025/03/17	179.8°	11h47m	+ 1°	2025/03/17	10.6	2025/03/12	1.037
330	2025/12/02	167.2°	4h40m	+ 9°	2025/12/01	14.4	2025/11/25	0.931
333	2025/10/24	176.3°	1h48m	+15°	2025/10/23	12.8	2025/10/21	1.646
344	2025/05/25	167.4°	16h11m	-33°	2025/05/27	9.7	2025/06/04	0.868
347	2025/04/28	164.6°	14h40m	+ 0°	2025/04/27	11.8	2025/04/24	1.288
352	2025/12/02	179.4°	4h36m	+21°	2025/12/02	11.4	2025/11/27	0.932
364	2025/01/15	178.0°	7h49m	+23°	2025/01/15	11.6	2025/01/09	1.019
373	2025/09/19	176.9°	23h52m	- 4°	2025/09/19	12.6	2025/09/18	1.689
379	2025/09/05	179.4°	22h54m	- 6°	2025/09/05	12.0	2025/09/05	1.577
415	2025/11/02	163.9°	2h50m	- 0°	2025/11/04	11.3	2025/11/07	1.022
419	2025/05/08	179.8°	15h 1m	-17°	2025/05/08	10.1	2025/05/18	1.046
444	2025/09/22	174.9°	23h49m	+ 4°	2025/09/22	10.4	2025/09/20	1.293
469	2025/02/14	177.6°	9h52m	+15°	2025/02/14	12.2	2025/02/18	1.780
471	2025/11/11	164.2°	3h19m	+ 2°	2025/11/11	9.4	2025/11/09	1.261
477	2025/09/30	179.2°	0h26m	+ 2°	2025/09/30	11.9	2025/09/24	1.011
506	2025/02/17	172.1°	9h56m	+ 4°	2025/02/17	12.6	2025/02/14	1.752
531	2025/04/22	159.2°	14h46m	+ 5°	2025/04/24	14.5	2025/04/28	1.332
556	2025/01/13	178.8°	7h40m	+20°	2025/01/13	11.8	2025/01/13	1.228
571	2025/12/02	170.1°	4h26m	+31°	2025/11/30	13.3	2025/11/23	0.922
584	2025/08/24	162.2°	21h56m	+ 6°	2025/08/27	10.4	2025/08/31	0.891
597	2025/09/24	166.6°	0h22m	-12°	2025/09/23	12.3	2025/09/21	1.312
605	2025/09/28	167.1°	0h 1m	+14°	2025/09/27	13.4	2025/09/26	1.610
634	2025/09/02	170.6°	23h 1m	-16°	2025/09/02	12.8	2025/09/02	1.509
649	2025/09/13	176.8°	23h29m	- 6°	2025/09/13	13.5	2025/09/11	0.833
665	2025/06/15	166.0°	17h26m	-37°	2025/06/15	11.7	2025/06/15	1.608
667	2025/02/08	169.4°	9h 9m	+ 5°	2025/02/07	12.6	2025/02/05	1.706
668	2025/08/23	168.4°	21h53m	- 0°	2025/08/23	14.2	2025/08/22	1.141
692	2025/12/04	173.5°	4h39m	+28°	2025/12/04	13.2	2025/12/07	1.943
697	2025/10/07	179.4°	0h53m	+ 5°	2025/10/07	12.5	2025/10/04	1.471
747	2025/09/01	162.9°	23h18m	-22°	2025/09/05	10.7	2025/09/13	1.319
794	2025/07/27	174.0°	20h18m	-13°	2025/07/26	13.5	2025/07/24	1.206
855	2025/04/30	171.1°	14h20m	-23°	2025/04/30	13.6	2025/05/05	0.972
887	2025/01/13	170.8°	7h 8m	+27°	2025/01/12	9.4	2025/01/08	0.082
922	2025/10/12	178.6°	1h 7m	+ 8°	2025/10/12	14.2	2025/10/05	1.285
924	2025/11/04	166.1°	2h55m	+ 2°	2025/11/03	12.8	2025/10/31	1.563
934	2025/09/04	172.6°	22h43m	- 0°	2025/09/05	13.0	2025/09/09	1.279
936	2025/07/09	177.2°	19h17m	-25°	2025/07/09	13.3	2025/07/12	1.618
940	2025/08/22	170.4°	22h19m	-20°	2025/08/22	13.4	2025/08/23	1.822
949	2025/03/01	173.9°	10h39m	+ 1°	2025/03/01	13.0	2025/03/07	1.561
968	2025/02/24	164.7°	10h 7m	- 4°	2025/02/24	13.4	2025/02/25	1.527
969	2025/08/22	177.0°	22h 1m	- 8°	2025/08/22	14.5	2025/08/28	1.067
980	2025/07/02	177.4°	18h45m	-25°	2025/07/02	10.9	2025/07/10	1.479
994	2025/09/19	177.0°	23h51m	- 4°	2025/09/19	12.7	2025/09/17	1.239
1000	2025/07/11	158.9°	19h23m	-43°	2025/07/08	13.0	2025/07/04	1.499
1024	2025/10/28	167.6°	2h19m	+ 0°	2025/10/27	13.4	2025/10/23	1.292
1056	2025/08/18	172.0°	22h 3m	-20°	2025/08/18	13.0	2025/08/15	0.828
1067	2025/01/11	179.4°	7h32m	+21°	2025/01/11	13.8	2025/01/05	1.579
1080	2025/10/04	178.4°	0h40m	+ 6°	2025/10/04	13.6	2025/10/13	0.918
1088	2025/11/10	178.1°	3h 4m	+15°	2025/11/10	12.4	2025/11/04	0.827
1093	2025/05/16	179.3°	15h35m	-19°	2025/05/17	12.1	2025/05/26	1.643
1117	2025/08/11	178.6°	21h22m	-13°	2025/08/11	12.9	2025/08/06	0.805
1122	2025/11/14	178.1°	3h21m	+16°	2025/11/14	12.7	2025/11/09	0.974
1126	2025/01/19	168.5°	8h16m	+31°	2025/01/20	14.0	2025/01/22	0.975
1127	2025/01/10	171.1°	7h19m	+13°	2025/01/09	13.2	2025/01/01	1.126
1146	2025/06/10	157.5°	17h29m	- 0°	2025/06/11	12.8	2025/06/13	1.314
1155	2025/04/15	177.0°	13h40m	- 7°	2025/04/16	13.8	2025/04/20	1.086
1165	2025/08/28	163.9°	22h 1m	+ 5°	2025/08/27	13.8	2025/08/23	1.555
1251	2025/08/16	179.2°	21h46m	-14°	2025/08/16	13.1	2025/08/19	1.335
1318	2025/03/08	168.4°	11h22m	+16°	2025/03/09	13.5	2025/03/13	0.895
1342	2025/02/12	170.4°	9h39m	+ 4°	2025/02/13	12.9	2025/02/18	0.905
1346	2025/10/08	167.5°	1h18m	- 5°	2025/10/09	14.0	2025/10/12	1.258
1463	2025/09/23	173.9°	23h52m	+ 5°	2025/09/24	14.1	2025/09/27	1.682
1475	2025/10/02	178.2°	0h29m	+ 5°	2025/10/02	14.4	2025/10/05	0.999
1493	2025/08/15	179.1°	21h39m	-14°	2025/08/15	13.4	2025/08/16	0.934
1554	2025/11/03	178.5°	2h36m	+13°	2025/11/03	14.3	2025/10/26	1.240
1555	2025/10/29	168.4°	1h58m	+24°	2025/10/28	13.7	2025/10/21	1.020
1591	2025/06/06	163.7°	16h46m	- 6°	2025/06/06	13.7	2025/06/06	0.973
1606	2025/08/09	166.3°	20h58m	- 2°	2025/08/10	13.7	2025/08/13	0.851
1648	2025/07/14	176.6°	19h29m	-18°	2025/07/13	13.5	2025/07/08	0.785
1672	2025/11/14	178.5°	3h18m	+16°	2025/11/14	13.7	2025/11/17	1.340
1708	2025/02/09	171.7°	9h21m	+ 6°	2025/02/08	14.5	2025/01/30	1.286
1714	2025/07/06	175.7°	19h 2m	-26°	2025/07/06	14.2	2025/07/03	1.174
1734	2025/09/09	175.8°	23h 3m	- 1°	2025/09/09	14.0	2025/09/12	1.166
1789	2025/06/22	179.1°	18h 3m	-22°	2025/06/22	14.2	2025/06/29	0.865
1803	2025/05/28	134.4°	15h 7m	-65°	2025/05/23	14.2	2025/05/22	0.910
1916	2025/10/05	158.1°	0h21m	+25°	2025/09/14	14.7	2025/08/26	0.385
1946	2025/09/08	169.9°	23h19m	-15°	2025/09/08	13.0	2025/09/10	0.763
2014	2025/04/18	176.3°	13h54m	- 7°	2025/04/19	13.7	2025/05/01	1.048
2019	2025/05/11	176.9°	15h 9m	-20°	2025/05/11	13.4	2025/05/18	0.940
2071	2025/07/26	179.4°	20h25m	-19°	2025/07/26	14.5	2025/07/26	0.881
2078	2025/12/15	155.3°	4h34m	+45°	2025/12/07	13.2	2025/11/27	0.673
2109	2025/09/28	173.4°	0h33m	- 3°	2025/09/28	13.7	2025/09/25	1.001
2324	2025/06/25	179.5°	18h18m	-23°	2025/06/25	14.3	2025/06/24	1.524
2501	2025/05/05	176.2°	14h45m	-19°	2025/05/05	13.6	2025/05/09	0.943
2525	2025/08/25	175.9°	22h20m	-14°	2025/08/25	14.0	2025/08/28	1.685
3156	2025/01/22	155.3°	8h43m	+43°	2025/01/23	14.5	2025/01/23	1.371
3361	2025/10/30	155.3°	3h54m	+ 6°	2025/11/14	14.2	2025/11/19	0.038
3401	2025/12/14	128.9°	2h42m	+67°	2025/12/11	14.0	2025/12/09	0.694
3444	2025/10/07	173.4°	0h42m	+11°	2025/10/08	14.4	2025/10/15	1.049
3687	2025/09/11	155.7°	22h33m	+17°	2025/09/10	14.3	2025/09/09	1.232
3773	2025/08/18	177.0°	21h56m	-15°	2025/08/18	14.3	2025/08/22	0.781
3813	2025/08/30	177.2°	22h32m	- 6°	2025/08/30	14.4	2025/08/25	0.826
3918	2025/09/19	175.0°	23h58m	- 5°	2025/09/19	14.3	2025/09/19	0.776
3982	2025/06/15	177.4°	17h37m	-20°	2025/06/15	14.3	2025/06/23	0.811
4107	2025/02/08	174.3°	9h18m	+ 9°	2025/02/08	13.8	2025/02/04	1.126
4132	2025/01/18	138.4°	6h58m	-18°	2025/01/08	13.9	2025/01/04	0.956
4155	2025/11/09	173.8°	2h51m	+22°	2025/11/08	14.2	2025/11/01	0.914
4217	2025/10/03	165.1°	0h25m	+18°	2025/10/01	13.9	2025/09/27	0.875
4262	2025/07/16	175.4°	19h36m	-17°	2025/07/16	14.3	2025/07/20	0.799
4287	2025/08/22	167.7°	22h21m	-23°	2025/08/21	14.5	2025/08/17	0.807
4293	2025/12/16	172.2°	5h36m	+31°	2025/12/16	14.3	2025/12/20	1.167
4440	2025/01/19	164.3°	8h 9m	+ 4°	2025/01/20	13.9	2025/01/21	0.818
4520	2025/09/04	170.9°	23h 8m	-15°	2025/09/04	14.1	2025/09/05	0.778
4613	2025/10/29	166.6°	2h33m	+ 0°	2025/10/29	13.4	2025/10/29	0.885
4807	2025/11/21	178.9°	3h45m	+20°	2025/11/21	14.5	2025/11/21	0.851
4820	2025/01/29	171.1°	8h55m	+26°	2025/01/27	13.8	2025/01/17	1.133
4826	2025/07/14	160.9°	20h17m	-38°	2025/07/16	14.2	2025/07/18	0.954
4997	2025/10/12	166.6°	1h 5m	+20°	2025/10/14	14.1	2025/10/20	1.079
5275	2025/09/08	165.4°	22h43m	+ 7°	2025/09/08	14.3	2025/09/07	0.646
5332	2025/02/09	145.9°	7h19m	+ 5°	2025/02/01	13.2	2025/01/26	0.316
5386	2025/06/23	179.5°	18h 6m	-23°	2025/06/23	14.4	2025/06/25	0.924
5438	2025/03/14	136.3°	10h45m	-39°	2025/03/14	14.0	2025/03/14	1.154
5567	2025/09/12	170.1°	23h33m	-13°	2025/09/11	13.7	2025/09/07	1.359
6113	2025/08/09	179.5°	21h14m	-15°	2025/08/09	14.5	2025/08/07	1.116
6361	2025/04/16	171.5°	13h48m	- 2°	2025/04/16	14.2	2025/04/19	1.032
6422	2025/07/25	178.1°	20h17m	-17°	2025/07/25	14.0	2025/07/24	1.217
7369	2025/12/06	154.4°	3h51m	+44°	2025/12/01	14.2	2025/11/25	0.742
7564	2025/03/01	178.6°	10h52m	+ 8°	2025/03/01	14.5	2025/02/28	1.234
7747	2025/06/27	177.2°	18h24m	-26°	2025/06/27	14.2	2025/07/08	0.734
7824	2025/10/06	171.5°	1h 4m	- 2°	2025/10/05	14.5	2025/10/01	0.808
10142	2025/12/08	178.3°	4h58m	+24°	2025/12/07	14.4	2025/11/30	1.209
27174	2025/02/12	175.5°	9h48m	+18°	2025/02/12	14.5	2025/02/04	1.115
47035	2025/02/21	133.1°	10h13m	+57°	2025/02/07	14.4	2025/02/04	0.845
137126	2025/02/20	151.8°	11h58m	- 0°	2025/03/05	13.9	2025/03/08	0.053
152664	2025/09/18	167.7°	0h25m	+ 4°	2025/09/28	13.9	2025/09/29	0.026
163696	2025/05/26	177.8°	16h09m	-19°	2025/05/27	14.2	2025/06/10	0.177
164206	2025/10/27	173.0°	2h35m	+14°	2025/10/29	14.0	2025/11/07	0.112

Table II. Temporal Sequence of Favorable Elongations

Planet	Max Elon D	Max E	RA	Dec	Br Mag D	Br Mag	Min Dist D	Min Dist
1127	2025/01/10	171.1°	7h19m	+13°	2025/01/09	13.2	2025/01/01	1.126
1067	2025/01/11	179.4°	7h32m	+21°	2025/01/11	13.8	2025/01/05	1.579
556	2025/01/13	178.8°	7h40m	+20°	2025/01/13	11.8	2025/01/13	1.228
887	2025/01/13	170.8°	7h 8m	+27°	2025/01/12	9.4	2025/01/08	0.082
364	2025/01/15	178.0°	7h49m	+23°	2025/01/15	11.6	2025/01/09	1.019
4132	2025/01/18	138.4°	6h58m	-18°	2025/01/08	13.9	2025/01/04	0.956
1126	2025/01/19	168.5°	8h16m	+31°	2025/01/20	14.0	2025/01/22	0.975
4440	2025/01/19	164.3°	8h 9m	+ 4°	2025/01/20	13.9	2025/01/21	0.818
3156	2025/01/22	155.3°	8h43m	+43°	2025/01/23	14.5	2025/01/23	1.371
4820	2025/01/29	171.1°	8h55m	+26°	2025/01/27	13.8	2025/01/17	1.133
28	2025/02/01	176.5°	8h53m	+13°	2025/02/01	9.8	2025/02/01	1.380
667	2025/02/08	169.4°	9h 9m	+ 5°	2025/02/07	12.6	2025/02/05	1.706
4107	2025/02/08	174.3°	9h18m	+ 9°	2025/02/08	13.8	2025/02/04	1.126
1708	2025/02/09	171.7°	9h21m	+ 6°	2025/02/08	14.5	2025/01/30	1.286
5332	2025/02/09	145.9°	7h19m	+ 5°	2025/02/01	13.2	2025/01/26	0.316

Planet	Max Elon D	Max E	RA	Dec	Br Mag D	Br Mag	Min Dist D	Min Dist
1342	2025/02/12	170.4°	9h39m	+ 4°	2025/02/13	12.9	2025/02/18	0.905
27174	2025/02/12	175.5°	9h48m	+18°	2025/02/12	14.5	2025/02/04	1.115
469	2025/02/14	177.6°	9h52m	+15°	2025/02/14	12.2	2025/02/18	1.780
506	2025/02/17	172.1°	9h56m	+ 4°	2025/02/17	12.6	2025/02/14	1.752
137126	2025/02/20	151.8°	11h58m	- 0°	2025/03/05	13.9	2025/03/08	0.053
47035	2025/02/21	133.1°	10h13m	+57°	2025/02/07	14.4	2025/02/04	0.845
968	2025/02/24	164.7°	10h 7m	- 4°	2025/02/24	13.4	2025/02/25	1.527
24	2025/02/26	178.9°	10h37m	+ 9°	2025/02/26	10.7	2025/02/26	1.797
949	2025/03/01	173.9°	10h39m	+ 1°	2025/03/01	13.0	2025/03/07	1.561
7564	2025/03/01	178.6°	10h52m	+ 8°	2025/03/01	14.5	2025/02/28	1.234
1318	2025/03/08	168.4°	11h22m	+16°	2025/03/09	13.5	2025/03/13	0.895
5438	2025/03/14	136.3°	10h45m	-39°	2025/03/14	14.0	2025/03/14	1.154
313	2025/03/17	179.8°	11h47m	+ 1°	2025/03/17	10.6	2025/03/12	1.037
139	2025/03/21	179.5°	12h 2m	+ 0°	2025/03/21	10.3	2025/03/20	1.322
1155	2025/04/15	177.0°	13h40m	- 7°	2025/04/16	13.8	2025/04/20	1.086
6361	2025/04/16	171.5°	13h48m	- 2°	2025/04/16	14.2	2025/04/19	1.032
2014	2025/04/18	176.3°	13h54m	- 7°	2025/04/19	13.7	2025/05/01	1.048
531	2025/04/22	159.2°	14h46m	+ 5°	2025/04/24	14.5	2025/04/28	1.332
278	2025/04/27	174.4°	14h27m	- 8°	2025/04/27	12.3	2025/04/27	1.387
347	2025/04/28	164.6°	14h40m	+ 0°	2025/04/27	11.8	2025/04/24	1.288
855	2025/04/30	171.1°	14h20m	-23°	2025/04/30	13.6	2025/05/05	0.972
2501	2025/05/05	176.2°	14h45m	-19°	2025/05/05	13.6	2025/05/09	0.943
419	2025/05/08	179.8°	15h 1m	-17°	2025/05/08	10.1	2025/05/18	1.046
2019	2025/05/11	176.9°	15h 9m	-20°	2025/05/11	13.4	2025/05/18	0.940
1093	2025/05/16	179.3°	15h35m	-19°	2025/05/17	12.1	2025/05/26	1.643
344	2025/05/25	167.4°	16h11m	-33°	2025/05/27	9.7	2025/06/04	0.868
163696	2025/05/26	177.8°	16h09m	-19°	2025/05/27	14.2	2025/06/10	0.177
1803	2025/05/28	134.4°	15h 7m	-65°	2025/05/23	14.2	2025/05/22	0.910
259	2025/06/01	175.1°	16h37m	-17°	2025/06/01	11.3	2025/06/01	1.715
1591	2025/06/06	163.7°	16h46m	- 6°	2025/06/06	13.7	2025/06/06	0.973
188	2025/06/07	174.4°	17h 5m	-17°	2025/06/07	12.1	2025/06/13	1.400
1146	2025/06/10	157.5°	17h29m	- 0°	2025/06/11	12.8	2025/06/13	1.314
665	2025/06/15	166.0°	17h26m	-37°	2025/06/15	11.7	2025/06/15	1.608
3982	2025/06/15	177.4°	17h37m	-20°	2025/06/15	14.3	2025/06/23	0.811
1789	2025/06/22	179.1°	18h 3m	-22°	2025/06/22	14.2	2025/06/29	0.865
5386	2025/06/23	179.5°	18h 6m	-23°	2025/06/23	14.4	2025/06/25	0.924
2324	2025/06/25	179.5°	18h18m	-23°	2025/06/25	14.3	2025/06/24	1.524
7747	2025/06/27	177.2°	18h24m	-26°	2025/06/27	14.2	2025/07/08	0.734
980	2025/07/02	177.4°	18h45m	-25°	2025/07/02	10.9	2025/07/10	1.479
1714	2025/07/06	175.7°	19h 2m	-26°	2025/07/06	14.2	2025/07/03	1.174
936	2025/07/09	177.2°	19h17m	-25°	2025/07/09	13.3	2025/07/12	1.618
1000	2025/07/11	158.9°	19h23m	-43°	2025/07/08	13.0	2025/07/04	1.499
1648	2025/07/14	176.6°	19h29m	-18°	2025/07/13	13.5	2025/07/08	0.785
4826	2025/07/14	160.9°	20h17m	-38°	2025/07/16	14.2	2025/07/18	0.954
312	2025/07/16	165.0°	19h54m	-36°	2025/07/15	11.9	2025/07/13	1.371
4262	2025/07/16	175.4°	19h36m	-17°	2025/07/16	14.3	2025/07/20	0.799
172	2025/07/25	170.4°	20h24m	-29°	2025/07/25	11.1	2025/07/27	1.128
6422	2025/07/25	178.1°	20h17m	-17°	2025/07/25	14.0	2025/07/24	1.217
2071	2025/07/26	179.4°	20h25m	-19°	2025/07/26	14.5	2025/07/26	0.881
794	2025/07/27	174.0°	20h18m	-13°	2025/07/26	13.5	2025/07/24	1.206
63	2025/08/03	174.9°	20h56m	-22°	2025/08/02	9.6	2025/07/29	1.122
129	2025/08/05	179.0°	21h 1m	-15°	2025/08/05	10.1	2025/07/28	1.503
141	2025/08/08	179.0°	21h13m	-17°	2025/08/08	10.7	2025/08/15	1.285
1606	2025/08/09	166.3°	20h58m	- 2°	2025/08/10	13.7	2025/08/13	0.851
6113	2025/08/09	179.5°	21h14m	-15°	2025/08/09	14.5	2025/08/07	1.116
89	2025/08/10	176.1°	21h20m	-11°	2025/08/11	8.8	2025/08/15	1.138
1117	2025/08/11	178.6°	21h22m	-13°	2025/08/11	12.9	2025/08/06	0.805
1493	2025/08/15	179.1°	21h39m	-14°	2025/08/15	13.4	2025/08/16	0.934
1251	2025/08/16	179.2°	21h46m	-14°	2025/08/16	13.1	2025/08/19	1.335
226	2025/08/17	174.6°	21h59m	-17°	2025/08/17	12.2	2025/08/12	1.223
1056	2025/08/18	172.0°	22h 3m	-20°	2025/08/18	13.0	2025/08/15	0.828
3773	2025/08/18	177.0°	21h56m	-15°	2025/08/18	14.3	2025/08/22	0.781
940	2025/08/22	170.4°	22h19m	-20°	2025/08/22	13.4	2025/08/23	1.822
969	2025/08/22	177.0°	22h 1m	- 8°	2025/08/22	14.5	2025/08/28	1.067
4287	2025/08/22	167.7°	22h21m	-23°	2025/08/21	14.5	2025/08/17	0.807
668	2025/08/23	168.4°	21h53m	- 0°	2025/08/23	14.2	2025/08/22	1.141
584	2025/08/24	162.2°	21h56m	+ 6°	2025/08/27	10.4	2025/08/31	0.891
6	2025/08/25	172.5°	22h32m	-17°	2025/08/26	7.6	2025/08/31	1.025
2525	2025/08/25	175.9°	22h20m	-14°	2025/08/25	14.0	2025/08/28	1.685
1165	2025/08/28	163.9°	22h 1m	+ 5°	2025/08/27	13.8	2025/08/23	1.555
3813	2025/08/30	177.2°	22h32m	- 6°	2025/08/30	14.4	2025/08/25	0.826
185	2025/08/31	176.9°	22h43m	-11°	2025/08/31	10.5	2025/09/02	1.445
61	2025/09/01	176.9°	22h38m	- 5°	2025/09/01	10.7	2025/09/01	1.490
747	2025/09/01	162.9°	23h18m	-22°	2025/09/05	10.7	2025/09/13	1.319
634	2025/09/02	170.6°	23h 1m	-16°	2025/09/02	12.8	2025/09/02	1.509
934	2025/09/04	172.6°	22h43m	- 0°	2025/09/05	13.0	2025/09/09	1.279
4520	2025/09/04	170.9°	23h 8m	-15°	2025/09/04	14.1	2025/09/05	0.778
379	2025/09/05	179.4°	22h54m	- 6°	2025/09/05	12.0	2025/09/05	1.577
1946	2025/09/08	169.9°	23h19m	-15°	2025/09/08	13.0	2025/09/10	0.763
5275	2025/09/08	165.4°	22h43m	+ 7°	2025/09/08	14.3	2025/09/07	0.646
1734	2025/09/09	175.8°	23h 3m	- 1°	2025/09/09	14.0	2025/09/12	1.166
3687	2025/09/11	155.7°	22h33m	+17°	2025/09/10	14.3	2025/09/09	1.232
5567	2025/09/12	170.1°	23h33m	-13°	2025/09/11	13.7	2025/09/07	1.359
649	2025/09/13	176.8°	23h29m	- 6°	2025/09/13	13.5	2025/09/11	0.833
152664	2025/09/18	167.7°	0h25m	+ 4°	2025/09/28	13.9	2025/09/29	0.026
373	2025/09/19	176.9°	23h52m	- 4°	2025/09/19	12.6	2025/09/18	1.689
994	2025/09/19	177.0°	23h51m	- 4°	2025/09/19	12.7	2025/09/17	1.239
3918	2025/09/19	175.0°	23h58m	- 5°	2025/09/19	14.3	2025/09/19	0.776
444	2025/09/22	174.9°	23h49m	+ 4°	2025/09/22	10.4	2025/09/20	1.293
1463	2025/09/23	173.9°	23h52m	+ 5°	2025/09/24	14.1	2025/09/27	1.682
597	2025/09/24	166.6°	0h22m	-12°	2025/09/23	12.3	2025/09/21	1.312
605	2025/09/28	167.1°	0h 1m	+14°	2025/09/27	13.4	2025/09/26	1.610
2109	2025/09/28	173.4°	0h33m	- 3°	2025/09/28	13.7	2025/09/25	1.001
477	2025/09/30	179.2°	0h26m	+ 2°	2025/09/30	11.9	2025/09/24	1.011
1475	2025/10/02	178.2°	0h29m	+ 5°	2025/10/02	14.4	2025/10/05	0.999
244	2025/10/03	178.0°	0h34m	+ 5°	2025/10/03	13.4	2025/10/03	0.878
4217	2025/10/03	165.1°	0h25m	+18°	2025/10/01	13.9	2025/09/27	0.875
1080	2025/10/04	178.4°	0h40m	+ 6°	2025/10/04	13.6	2025/10/13	0.918
1916	2025/10/05	158.1°	0h21m	+25°	2025/09/14	14.7	2025/08/26	0.385
7824	2025/10/06	171.5°	1h 4m	- 2°	2025/10/05	14.5	2025/10/01	0.808
697	2025/10/07	179.4°	0h53m	+ 5°	2025/10/07	12.5	2025/10/04	1.471
3444	2025/10/07	173.4°	0h42m	+11°	2025/10/08	14.4	2025/10/15	1.049
1346	2025/10/08	167.5°	1h18m	- 5°	2025/10/09	14.0	2025/10/12	1.258
922	2025/10/12	178.6°	1h 7m	+ 8°	2025/10/12	14.2	2025/10/05	1.285
4997	2025/10/12	166.6°	1h 5m	+20°	2025/10/14	14.1	2025/10/20	1.079
85	2025/10/16	179.5°	1h27m	+ 9°	2025/10/16	10.1	2025/10/09	1.310
333	2025/10/24	176.3°	1h48m	+15°	2025/10/23	12.8	2025/10/21	1.646
164206	2025/10/27	173.0°	2h35m	+14°	2025/10/29	14.0	2025/11/07	0.112
1024	2025/10/28	167.6°	2h19m	+ 0°	2025/10/27	13.4	2025/10/23	1.292
1555	2025/10/29	168.4°	1h58m	+24°	2025/10/28	13.7	2025/10/21	1.020
4613	2025/10/29	166.6°	2h33m	+ 0°	2025/10/29	13.4	2025/10/29	0.885
3361	2025/10/30	155.3°	3h54m	+ 6°	2025/11/14	14.2	2025/11/19	0.038
415	2025/11/02	163.9°	2h50m	- 0°	2025/11/04	11.3	2025/11/07	1.022
1554	2025/11/03	178.5°	2h36m	+13°	2025/11/03	14.3	2025/10/26	1.240
924	2025/11/04	166.1°	2h55m	+ 2°	2025/11/03	12.8	2025/10/31	1.563
104	2025/11/08	179.6°	2h52m	+16°	2025/11/08	11.6	2025/11/10	1.684
4155	2025/11/09	173.8°	2h51m	+22°	2025/11/08	14.2	2025/11/01	0.914
1088	2025/11/10	178.1°	3h 4m	+15°	2025/11/10	12.4	2025/11/04	0.827
471	2025/11/11	164.2°	3h19m	+ 2°	2025/11/11	9.4	2025/11/09	1.261
245	2025/11/12	178.4°	3h12m	+16°	2025/11/12	10.8	2025/11/09	1.511
1122	2025/11/14	178.1°	3h21m	+16°	2025/11/14	12.7	2025/11/09	0.974
1672	2025/11/14	178.5°	3h18m	+16°	2025/11/14	13.7	2025/11/17	1.340
4807	2025/11/21	178.9°	3h45m	+20°	2025/11/21	14.5	2025/11/21	0.851
330	2025/12/02	167.2°	4h40m	+ 9°	2025/12/01	14.4	2025/11/25	0.931
352	2025/12/02	179.4°	4h36m	+21°	2025/12/02	11.4	2025/11/27	0.932
571	2025/12/02	170.1°	4h26m	+31°	2025/11/30	13.3	2025/11/23	0.922
692	2025/12/04	173.5°	4h39m	+28°	2025/12/04	13.2	2025/12/07	1.943
7369	2025/12/06	154.4°	3h51m	+44°	2025/12/01	14.2	2025/11/25	0.742
10142	2025/12/08	178.3°	4h58m	+24°	2025/12/07	14.4	2025/11/30	1.209
3401	2025/12/14	128.9°	2h42m	+67°	2025/12/11	14.0	2025/12/09	0.694
2078	2025/12/15	155.3°	4h34m	+45°	2025/12/07	13.2	2025/11/27	0.673
4293	2025/12/16	172.2°	5h36m	+31°	2025/12/16	14.3	2025/12/20	1.167
200	2025/12/31	171.8°	6h41m	+31°	2025/12/30	11.4	2025/12/27	1.487

Table III. Numerical List of Approaches Closer than 0.3 AU

Planet	Max Elon D	Max E	RA	Dec	Br Mag D	Br Mag	Min Dist D	Min Dist
887	2025/01/13	170.8°	7h 8m	+27°	2025/01/12	9.4	2025/01/08	0.082
3361	2025/10/30	155.3°	3h54m	+ 6°	2025/11/14	14.2	2025/11/19	0.038
137126	2025/02/20	151.8°	11h58m	- 0°	2025/03/05	13.9	2025/03/08	0.053
152664	2025/09/18	167.7°	0h25m	+ 4°	2025/09/28	13.9	2025/09/29	0.026
163696	2025/05/26	177.8°	16h09m	-19°	2025/05/27	14.2	2025/06/10	0.177
164206	2025/10/27	173.0°	2h35m	+14°	2025/10/29	14.0	2025/11/07	0.112

LIGHTCURVE AND ROTATION PERIOD OF 1367 NONGOMA

Stephen M. Brincat
Flarestar Observatory (MPC: 171)
Fl.5 George Tayar Street
San Gwann SGN 3160, MALTA
stephenbrincat@gmail.com

Marek Bucek
Luckystar Observatory (MPC: M55)
Dr. Lučanského 547
Važec, 032 61, SLOVAKIA

Michael Richmond
RIT Observatory (MPC: 920)
Rochester Institute of Technology (RIT)
1 Lomb Memorial Dr
Rochester, NY 14623, USA

Normand Rivard
À la belle étoile Observatory
796, rang des Écossais
Sainte-Brigide-d'Iberville (Québec)
J0J 1X0 CANADA

Charles Galdies
Znith Observatory
Armonie, E. Bradford Street
Naxxar NXR 2217, MALTA

Martin Mifsud
Manikata Observatory
51, Penthouse 7, Sky Blue Court
Dun Manwel Grima Street
Manikata MLH 5013, MALTA

Winston Grech
Antares Observatory
76/3, Kent Street
Fgura FGR 1555, MALTA

(Received: 2024 October 21)

During the 2024 opposition of 1367 Nongoma, an international team of observers worked to improve the asteroid's lightcurve quality. They determined that 1367 Nongoma has a synodic rotation period of 133.485 ± 0.026 h, with an amplitude of 0.65 ± 0.05 mag.

The Asteroid Lightcurve Database (LCDB; Warner et al., 2009; updated 2023 Oct.) gave an adopted period of 94.8 hours for 1367 Nangoma, listing the reliability as U = 1+. Given that Nongoma was at a favorable apparition in 2024 August at a brightness of V ~ 14.9, an international observational campaign was organized to improve the quality of its lightcurve.

Photometric observations were carried out from seven observatories, four of which were located in Malta. The remaining observatories were located in Slovakia, Canada, and the United States. A total of 57 sessions were obtained from 2024 June 8 to August 11, yielding 1770 observations. Table 1 provides the complete equipment list and the observer's total runs.

All images were taken through a clear filter or were unfiltered with an Pan-STARRS r´ bandpass zero point and calibrated using dark and flat-field subtraction. All brightness measurements were based on the Asteroid Terrestrial-impact Last Alert System (ATLAS) catalogue (Tonry et al., 2018).

The equipment used in this study was operated either remotely via the Internet or locally at each telescope. Image acquisition at all Maltese observatories was carried out using *Sequence Generator Pro* (Binary Star Software). In contrast, the Slovakian and Canadian observatories employed *NINA* telescope control software (Berg, 2023) for both image acquisition and telescope automation. RIT Observatory used *Maxim DL* (Version 6.16) for observatory operations and image capture. For image analysis, we employed *MPO Canopus* v10 (Warner, 2017) to perform differential aperture photometry and lightcurve creation. The software's Comparison Star Selector (CSS) feature was used to select comparison stars with near-solar colour.

Observatory	Tel	Camera	Obs Runs
A la belle étoile	0.2-m MK	Moravian G2-1600	3
Antares	0.28-m SCT	SBIG ST-11	1
Flarestar (MPC: 171)	0.25-m SCT	Moravian G2-1600	26
Luckystar (MPC: M55)	0.25-m SCT	Atik 460EX	21
Manikata	0.2-m SCT	ZWO ASI2600MM	1
RIT (MPC: 920)	0.30-m SCT	ASI 6200MM	5
Znith	0.2-m SCT	Moravian G2-1600	2

Table 1 – Instrumentation and Observation Runs. SCT: Schmidt-Cassegrain; MK: Maksutov-Cassegrain.

For this asteroid of the Phocaea family, we estimate the synodic rotation period of 1367 Nongoma to be 133.485 ± 0.0026 h with a lightcurve amplitude of 0.65 ± 0.05 magnitudes. This period differs from the one from Oey (2014), which was constrained by limited coverage of the lightcurve. For our analysis, the Fourier algorithm suggested other candidate periods, but these had higher RMS errors, and none resulted in a valid lightcurve. Although the 267.8-hour solution had a slightly lower RMS, it still failed to produce a viable outcome. This was particularly notable since asteroids with lightcurve amplitudes greater than 0.2 magnitudes typically exhibit a bimodal solution, which was not observed in any of the alternatives.

Number	Name	Family	H	Dkm	*a* (au)	*e*	*i* (deg)	P(yrs)	Discovered by	yyyy/mm
1367	Nongoma	701	12.3	9.37	2.34	0.131	22.48	3.59	C. Jackson	1934/07

Table II. Orbital and discovery information. Fam is the group or family using the LCDB values. An asterisk indicates a generic group, otherwise, the numbers are from Nesvorny et al. (2015). Web Sources: JPL: *https://ssd.jpl.nasa.gov/tools/sbdb_lookup.html#/* MPInfo: *https://minorplanet.info/php/oneasteroidinfo.php*

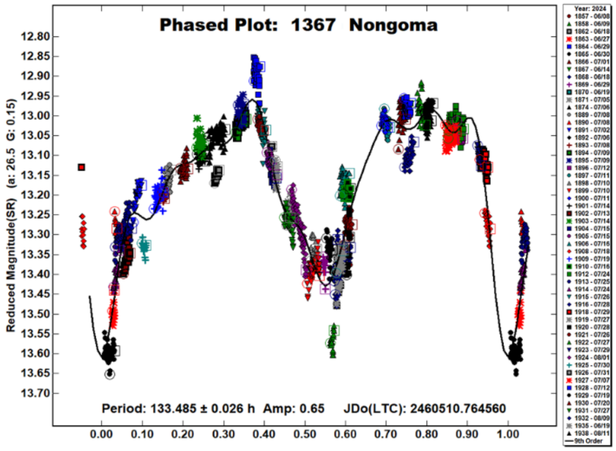

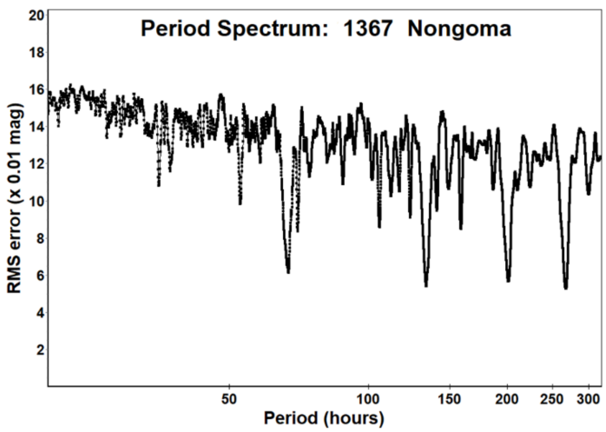

Acknowledgements

We would like to thank Brian Warner for his work in the development of *MPO Canopus* and for his efforts in maintaining the CALL website (Warner, 2016, 2021). This research has made use of the JPL's Small-Body Database (JPL, 2021).

References

Berg, S., (2023). Nightime Imaging 'N' Astronomy (NINA) web site *https://nighttime-imaging.eu/*. Last accessed: 2023 June 29.

JPL (2021). Small-Body Database Browser - JPL Solar System Dynamics web site. Last accessed: 2023 11 July. *http://ssd.jpl.nasa.gov/sbdb.cgi*

Nesvorny, D.; Broz, M.; Carruba, V. (2015). "Identification and Dynamical Properties of Asteroid Families." In Asteroids IV (P. Michel, F. DeMeo, W.F. Bottke, R. Binzel, Eds.). Univ. of Arizona Press, Tucson, also available on astro-ph.

Oey, J. (2014). "Lightcurve analysis of asteroids from Blue Mountains Observatory in 2013." *Minor Planet Bull.* **41**, 276-281.

Tonry, J.L.; Denneau, L.; Flewelling, H.; Heinze, A.N.; Onken, C.A.; Smartt, S.J.; Stalder, B.; Weiland, H.J.; Wolf, C. (2018). "The ATLAS All-Sky Stellar Reference Catalog." *Astrophys. J.* **867**, A105.

Warner, B.D.; Harris, A.W.; Pravec, P. (2009). "The Asteroid Lightcurve Database. *Icarus* **202**, 134-146. Updated 2023 Oct. *http://www.MinorPlanet.info/php/lcdb.php*

Warner, B.D. (2016). Collaborative Asteroid Lightcurve Link website. Last accessed: 2018 September 26. *http://www.minorplanet.info/call.html*

Warner, B.D. (2017). MPO Software, *MPO Canopus* version 10.7.10.0. Bdww Publishing. *https://bdwpublishing.com/*

Warner, B.D. (2021). Asteroid Lightcurve Data Exchange Format (ALCDEF) web site. *https://alcdef.org*

PERIOD OF THE FLAT-TOPPED LIGHTCURVE OF 1510 CHARLOIS

W. Romanishin
1933 Whispering Pines Cir., Norman, OK 73072
wromanishin@ou.edu

(Received: 2024 October 15 Revised: 2024 November 2)

There are three quite different period determinations listed in the latest lightcurve database for 1510 Charlois. One lightcurve shows intriguing broad flat maxima. The author has observed Charlois and derived P = 5.867 ± 0.005 h as the reliable period, which matches one of those previously reported.

1510 Charlois has an orbital period of 4.36 y, a semimajor axis of 2.670 AU, an eccentricity of 0.149, and an orbital inclination of 11.8°. Three incongruous lightcurve periods have been published for this object. Antonini and Roy (2013) report a period of 5.866 h, Bennefeld et al. (2009) report 6.653 h, and Durech et al. report 15.9844 h. All three periods were assigned Q = 2 in the asteroid lightcurve database (Warner et al., 2009).

The author became intrigued by the lightcurve presented by Antonini and Roy (2013), which shows fairly broad flat maxima. A separated close binary asteroid might be expected to show flat maxima as both objects might be fully visible for a length of time at maximum light. In September/October 2024, the author obtained photometry of Charlois on five nights using the 0.43-m T21 iTelescope at the Utah Desert Remote Observatory (IAU code U94). Two-minute exposures through a luminance filter were obtained spanning 17.7 hours in total. Observations of standard stars in the Landolt system (Clem and Landolt, 2013) provided an excellent transformation between the luminance and V system. The lightcurve below presents absolute V mags, H(V), derived assuming G=0.15 (Bowell et al., 1989). The 402 points were fit with a smooth spline curve. The standard deviation scatter around the fit is 0.014 mag.

The observations yield a very reliable period of 5.867 h, which matches that of Antonini and Roy (2013). One of the minima was observed on three nights, the other on two nights, so phasing the observations to various periods resulted in a very narrow window of possible periods around 5.867 h.

The shape of the lightcurve here is significantly different from that presented by Antonini and Roy (2013). The amplitude is little more than half that of the 2013 lightcurve. This is likely due to a significant difference between 2013 and 2024 in the angle between the Earth- object direction and the object rotational axis orientation. As usual, more lightcurves at different orbital positions are needed to determine the rotational axis direction of the object. At its next opposition in January 2026, Charlois will be near the position where the higher amplitude lightcurve was found by Antonini and Roy (2013). In January 2026 Charlois should have a V mag as bright as 14.5 at a declination of +30°, providing an excellent observing opportunity for northern hemisphere observers with small telescopes. Multiple lightcurves at the time of maximum amplitude could help investigate the possible binary nature of the object using the minima timing idea (Romanishin, 2024).

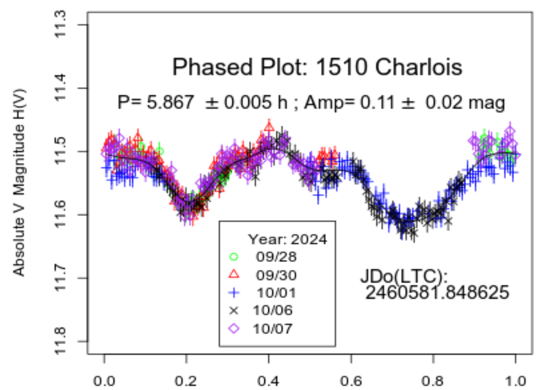

Figure 1. Phased absolute magnitude plot. The observed V mags average around 15.6.

Acknowledgements

This research has made use of data and/or services provided by the Jet Propulsion Laboratory HORIZONS system and the Minor Planet Center of the International Astronomical Union.

References

Antonini, P.; Roy, R. (2013). "Curves of rotation of asteroids and comets, CdR, CdL." *http://obswww.unige.ch/~behrend/r001510a.png*

Bennefeld, C.; Cantu, J.; Holly, V.; Jordan, L.; Martin, T.; Soar, E.; Swinney, T. (2009). "Asteroid Lightcurve Analysis at Ricky Observatory." *Minor Planet Bulletin* **35**, 45-48.

Bowell, E.; Hapke, B.; Domingue, D.; Lumme, K.; Peltoniemi, J.; Harris, A.W. (1989). "Application of Photometric Models to Asteroids." In: Binzel, R.P.; Gehrels, T.; Matthews, M.S. (Eds.), Asteroids II. Univ of Arizona Press, pp. 524-526, Tucson.

Clem, J.L.; Landolt, A.U. (2013). "Faint UBVR Standard Star Fields." *Astronomical Journal,* **146**, 88.

Durech, J.; Hanus, J.; Ali-Lagoa, V. (2018). "Asteroid Models Reconstructed from the Lowell Photometric Database and WISE Data" *Astronomy and Astrophysics* **617**, A57.

Harris, A.W.; Young, J.W.; Scaltriti, F.; Zappala, V. (1984). "Lightcurves and Phase Relations of the Asteroids 82 Alkmene and 444 Gyptis." *Icarus* **57**, 251-258.

Romanishin, W. (2024). "Timing Lightcurve Minima to Look for Candidate Close Binary Asteroids." *Minor Planet Bull.* **51**, 372-373.

Warner, B.D.; Harris, A.W.; Pravec, P. (2009). "The Asteroid Lightcurve Database." *Icarus* **202**, 134-146. Updated 2023 Oct. *http://www.minorplanet.info/lightcurvedatabase.html*

Number	Name	yyyy mm/dd	Phase	L_{PAB}	B_{PAB}	Period(h)	P.E.	Amp	A.E.	Grp
1510	Charlois	2024 09/28-10/07	3.6-6.3	1	8	5.867	0.005	0.11	0.02	MB-M

Table I. Observing circumstances and results. The phase angle is given for the first and last date. If preceded by an asterisk, the phase angle reached an extrema during the period. L_{PAB} and B_{PAB} are the approximate phase angle bisector longitude/latitude at mid-date range (see Harris et al., 1984). Grp is the asteroid family/group (Warner et al., 2009).

13441 JANMERLIN, AN ASTEROID WITH AN EARTH COMMENSURATE ROTATION PERIOD

Alessandro Marchini, Riccardo Papini
Astronomical Observatory, DSFTA - University of Siena (K54)
Via Roma 56, 53100 - Siena, ITALY
marchini@unisi.it

Frederick Pilcher
Organ Mesa Observatory (G50)
4438 Organ Mesa Loop
Las Cruces, NM 88011 USA

(Received: 2024 October 15 Revised: 2024 November 8)

Photometric observations from two different longitudes of the asteroid 13441 Janmerlin were conducted in order to obtain its synodic rotation period, which resulted close to that of Earth. In fact, we obtained P = 23.087 ± 0.002 h with an amplitude A = 0.50 ± 0.03 mag.

CCD photometric observations of the asteroid 13441 Janmerlin were carried out in 2024 September-October from Italy by the Astronomical Observatory of the University of Siena (DSFTA, 2024) and from New Mexico (USA) by the Organ Mesa Observatory. Equipment details are on Table I. Observations from different longitudes became indispensable when, after the first sessions from Italy, we realized that the asteroid had a period close to 24 h.

Data processing and analysis were done with *MPO Canopus* (Warner, 2018). All images were calibrated with dark and flat-field frames and the instrumental magnitudes converted to R magnitudes using solar-colored field stars from a version of the CMC-15 catalogue distributed with *MPO Canopus*. Table II shows the observing circumstances and results.

A search through the asteroid lightcurve database (LCDB; Warner et al., 2009) indicates that our result may be the first reported lightcurve observations and results for this asteroid.

13441 Janmerlin (2098 P-L) was discovered on 1960 September 24 by C.J. Van Houten and I. Van Houten-Groeneveld on Palomar Schmidt plates taken by T. Gehrels. It was named for Jan Merlin (1925-2019), an actor who played cadet Roger Manning in the 1950 TV series Tom Corbett, Space Cadet. He was the astronavigator on the rocket ship's radar deck and was always on the lookout for asteroids and comets. [Ref: *Minor Planet Circ.* 75548] It is a middle main-belt asteroid with a semi-major axis of 2.630 AU, eccentricity 0.261, inclination 11.935°, and an orbital period of 4.27 years. Its absolute magnitude is H = 13.06 (JPL, 2024). The WISE/NEOWISE satellite infrared radiometry survey (Mainzer et al., 2019) found a diameter D = 6.105 ± 0.246 km using an absolute magnitude H = 12.5.

Observations were conducted over five nights and collected 1032 data points. The period analysis, after discarding the unlikely monomodal solution, shows a clear bimodal solution for the rotational period of P = 23.087 ± 0.002 h with an amplitude A = 0.50 ± 0.03 mag.

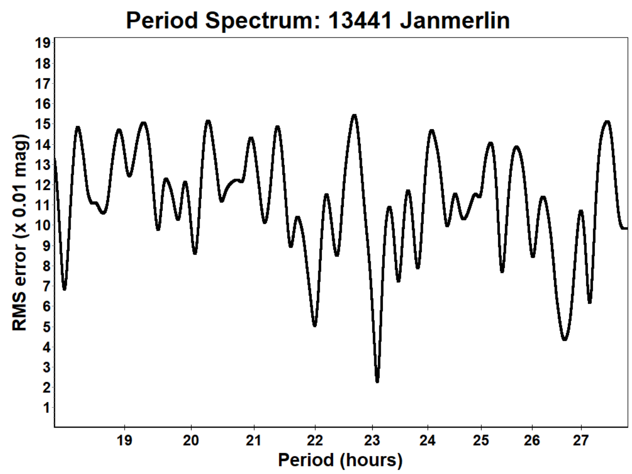

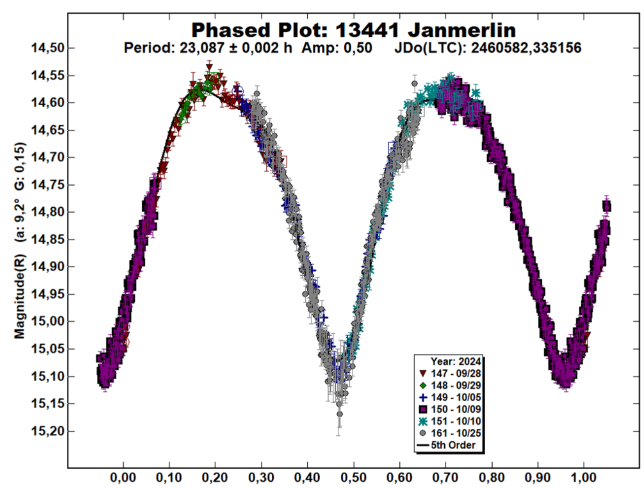

Observatory	Telescope	CCD	Sessions (mm/dd)
Astronomical Observatory University of Siena (K54)	0.30-m MCT f/5.6	SBIG STL-6303E	09/28, 09/29, 10/05, 10/10
Organ Mesa Observatory (G50)	0.35-m SCT f/10.0	SBIG STL-1001E	10/09, 10/25

Table I. Observing equipment. MCT: Maksutov-Cassegrain, SCT: Schmidt-Cassegrain.

Number	Name	2024 mm/dd	Phase	L_{PAB}	B_{PAB}	Period(h)	P.E.	Amp	A.E.	Grp
13441	Janmerlin	09/28-10/25	*9.3,7.1	21	-2	23.087	0.002	0.50	0.03	MB-M

Table II. Observing circumstances and results. The phase angle is given for the first and last date. If preceded by an asterisk, the phase angle reached an extrema during the period. L_{PAB} and B_{PAB} are the approximate phase angle bisector longitude/latitude at mid-date range (see Harris et al., 1984). Grp is the asteroid family/group (Warner et al., 2009).

References

DSFTA (2024). Dipartimento di Scienze Fisiche, della Terra e dell'Ambiente – Astronomical Observatory. *https://www.dsfta.unisi.it/en/research/labs/astronomical-observatory*

Harris, A.W.; Young, J.W.; Scaltriti, F.; Zappala, V. (1984). "Lightcurves and phase relations of the asteroids 82 Alkmene and 444 Gyptis." *Icarus* **57**, 251-258.

JPL (2024). Small-Body Database Browser. *http://ssd.jpl.nasa.gov/sbdb.cgi#top*

Mainzer, A.K.; Bauer, J.M.; Cutri, R.M.; Grav, T.; Kramer, E.A.; Masiero, J.R.; Sonnett, S.; Wright, E.L. (2019). "NEOWISE Diameters and Albedos V2.0." *NASA Planetary Data System, https://doi.org/10.26033/18S3-2Z54*.

Warner, B.D.; Harris, A.W.; Pravec, P. (2009). "The Asteroid Lightcurve Database." *Icarus* **202**, 134-146. Updated 2023 Oct. *http://www.minorplanet.info/lightcurvedatabase.html*

Warner, B.D. (2018). MPO Software, MPO Canopus v10.7.7.0. Bdw Publishing. *http://minorplanetobserver.com*

LIGHTCURVE AND ROTATION PERIOD ANALYSIS OF (1685) TORO

Jiarui Xiong
Xingyuan Observatory
College of Oceanic and Atmospheric Science,
Ocean University of China
Songling Rd. 238, Qingdao, Shandong, CHINA
xiongjiarui@stu.ouc.edu.cn

Yue Lu
Xingyuan Observatory
Xingyuan College, Ocean University of China
Songling Rd. 238, Qingdao, Shandong, CHINA

Chenyang Guo
Xingyuan Observatory
Third Institute of Oceanography, Ministry of Natural Resources, PRC
Daxue Rd. 178, Siming District, Xiamen, Fujian, CHINA

(Received: 2024 August 8)

Ten sets of photometric observations of the near-Earth asteroid 1685 Toro were obtained between 2024 January 26 and February 26. Using *Tycho Tracker* software, we plotted the lightcurve of 1685 Toro and measured its rotation period to be 10.1774 ± 0.012 h with a lightcurve amplitude of 0.51 ± 0.05 mag.

1685 Toro is a near-Earth Apollo asteroid that was discovered in 1948 July by C.A. Wirtanen at Mount Hamiliton. A total of 1875 images were taken on ten nights between 2024 January 26 to February 26. We used an *f*/4 0.2-m reflector and ASI6200MM CCD camera operating at -20 degrees C. Given Toro's large sky motion, exposure times were between 60 and 120 seconds. All of the frames were taken under L band (unfiltered).

Tycho Tracker was used for data analysis and measurement. Bias, flat, and dark frames were applied and the images aligned prior to measuring. The V magnitudes from APASS were used for the comparison stars. According to the asteroid lightcurve database (LCDB; Warner et al., 2009), the mean absolute magnitude is H = 14.48 ± 0.13 if assuming a phase slope parameter G = 0.24 ± 0.11. We used these values in our analysis. A fourth-order Fourier lightcurve was fit to P = 10.1774 ± 0.012 h for a light-time corrected zero-point of JD = 2460336.0.

The rotation period of 1685 Toro is known (Ďurech et al., 2022) to be affected by YORP (Rubincam, 2000) based on data from 1972, 1988 (Hoffmann and Geyer, 1990), 2007 (Higgins, 2008, 2011) and (Higgins et al. 2008), 2013 (Warner, 2013). In the YORP model, a free parameter $v \equiv \frac{d\omega}{dt}$ is used to express rotational acceleration. Assuming a linear model, the period can be calculated as:

$$P(t) = \frac{2\pi P_0}{vP_0(t - T_0) + 2\pi}$$

Where:

- t: the time of observation (JD).
- T_0: the epoch from which the model is propagated.
- P_0: the rotation period of Toro from which the model is propagated.
- P(t): the rotation period of (1685) Toro at a certain time, t.

Tian et al. (2022) suggest YORP acceleration $\nu = (3.2 \pm 0.3) \times 10^{-9}$ rad·day^{-2} (1σ error). Using T_0 = 2441507.0, P = 10.197826 ± 0.000002 hours (Tian et al, 2022). Toro's rotation period at the time of observation is P = 10.197675 ± 0.000165 hours. Meanwhile, this work's result is P = 10.1774 ± 0.012 hours. There is evidence that the rotation rate is accelerating; however, more accurate data are required to analyze if any other effects changed its rotation period.

ID	JD	Period in hours	Author
1	2441507.0	10.197826 ± 0.000002	Ďurech et al., 2002
2	2447379.0	10.1995 ± 0.0018	Hoffmann & Geyer, 1990
3	2454244.0	10.1995 ± 0.0004	Higgins, 2008
4	2454513.9	10.1862 ± 0.0006	Higgins et al. 2008
5	2455324.8	10.199 ± 0.003	Higgins, 2011
6	2456152.8	10.188 ± 0.002	Warner, 2013
7	2260336.0 (This work)	10.1774 ± 0.012	Xiong et al.

Table I. (1685) Toro's rotation period in hours observed from 1972 to present. Note that the uncertainties in IDs 3-6 lack detailed confidence degrees, suggesting they should be given less weight.

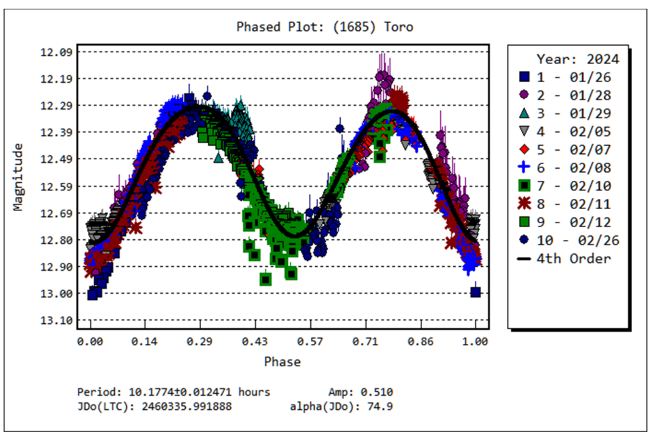

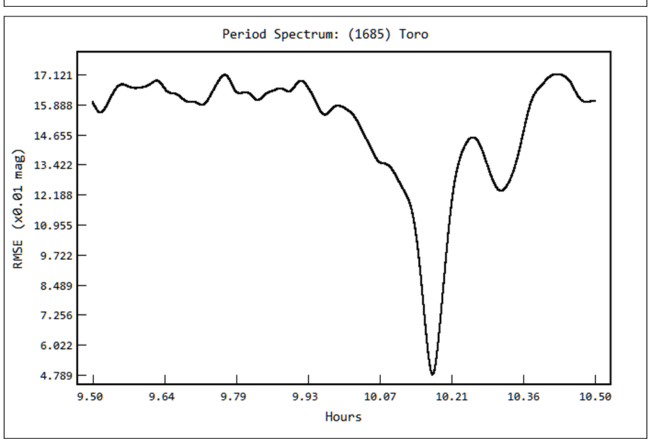

Acknowledgements

This work is supported by Xingyuan College of Ocean University of China. This work is possible in part based on data from AAVSO Photometric All-Sky Survey (APASS) and software *Tycho* v11.0.1 developed by Daniel Parrott. We want to express our special thanks to Dr. Ye Yuan in Pulper Mount Observatory and Astronomical Associations of the Ocean University of China. Thanks to Deng Linxi, Yan Yirou, Jiang Bicong, and Gao Shijie's help checking this article. Thanks Shao Yushuang provided checking in data analysis.

References

Ďurech, J.; Vokrouhlický, D.; Pravec, P. and 28 colleagues (2022). "Rotation acceleration of asteroids (10115) 1992 SK, (1685) Toro, and (1620) Geographos due to the YORP effect." *Astron. Astrophys.* **657**, A5.

Higgins, D. (2008). "Asteroid Lightcurve Analysis at Hunters Hill Observatory and Collaborating Stations: April 2007 - June 2007." *Minor Planet Bull.* **35**, 30-32.

Higgins, D.; Pravec, P.; Kusnirak, P.; Hornoch, K.; Brinsfield, J.W.; Allen, B.; Warner, B.D. (2008). "Asteroid Lightcurve Analysis at Hunters Hill Observatory and Collaborating Stations: November 2007 - March 2008." *Minor Planet Bull.* **35**, 123-126.

Higgins, D. (2011). "Period Determination of Asteroid Targets Observed at Hunters Hill Observatory: May 2009 - September 2010." *Minor Planet Bull.* **38**, 41-46.

Hoffmann, M.; Geyer, E.H. (1990). "Photometric Observations of Three Near-Earth Asteroids." *ACTA Astronomica* **40**, 389-396.

Rubincam, D.P. (2000). "Radiative Spin-up and Spin-down of Small Asteroids." *Icarus* **148**, 2-11.

Tian, J.; Zhao, H.B. Li, B. (2022). "Shape Model and Rotation Acceleration of (1685) Toro and (85989) 1999 JD6 from Optical Observations." *RAA* **22**. 17pp

Warner, B.D.; Harris, A.W.; Pravec, P. (2009). "The Asteroid Lightcurve Database." *Icarus* **202**, 134-146. Updated 2023 Oct. *http://www.minorplanet.info/lightcurvedatabase.html*

Warner, B.D. (2013). "Asteroid Lightcurve Analysis at the Palmer Divide Observatory: 2012 June - September." *Minor Planet Bull.* **40**, 26-29.

LIGHTCURVE AND ROTATION PERIOD OF 4222 NANCITA

Jonathan Chen
Shanghai Jianping High School ECIC
385 Gushan Road
Pudong New Area, 200135 Shanghai, P.R. CHINA
timedevblocker@gmail.com

Jiashuo Zhang
Walton International School
Xuzhou, 221111 Jiangsu, P.R. CHINA

Binyu Wang, Lanhe Ding
Hefei Astronomical Society
Anhui, P.R. CHINA

Jia You, Runwei Xu, Weiye Wang,
Xiaochang Yan
Huanyu Observatory
Hebei, P.R. CHINA

Yuqing Ren
Chongqing Astronomical Society
Chongqing, P.R. CHINA

(Received: 2024 October 15)

Unfiltered CCD photometric observations of 4222 Nancita were obtained in Hebei, China from Dec 2023 to Jan 2024. We report a synodic rotation period of 3.8743 ± 0.0001 hours and an amplitude of 0.800 ± 0.042 magnitudes.

4222 Nancita was discovered by E.F. Helin at Palomar on 1988 March 13. It is a Mars-crosser with a semimajor axis of 2.366 AU, eccentricity 0.297, inclination 3.742°, and an orbital period of 3.64 years. Its absolute magnitude is $H = 12.42$ (*http://ssd.jpl.nasa.gov/sbdb_query.cgi*). The WISE/NEOWISE satellite (Masiero et al., 2014) found a diameter $D = 9.636 \pm 0.121$ km with an absolute magnitude $H = 12.4$.

Photometric observations of 4222 Nancita were conducted at Huanyu Observatory in January 2024 using a 0.13-m *f*/7.7 refractor and ASI 2600MM-Pro CMOS camera. An exposure time of 180 seconds was used for each image. All observations were made unfiltered with 1×1 binning at a plate scale of 0.78 arcsec/pixel. Data reduction and period analysis were performed with *Tycho* (Parrott, 2024). The asteroid and five comparison stars were measured. Comparison stars were selected with color indices within the range of 0.5 < B-V < 0.95, aligning with the typical color range of asteroids.

A total of 85 data points were collected over the period from 2024 January 26 to 2024 January 28. The period analysis shows a synodic rotation period $P = 3.8743 \pm 0.0001$ h with an amplitude $A = 0.800 \pm 0.042$ mag. These results are in perfect agreement with previous results published in the Asteroid Lightcurve Database (LCDB; Warner et al., 2009; Higgins et al., 2006; Ďurech et al., 2018).

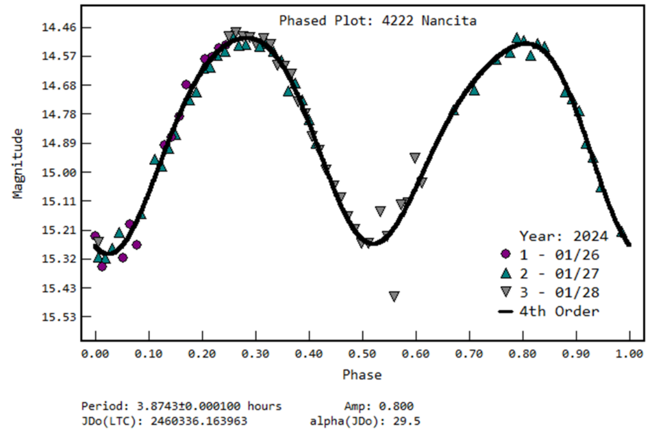

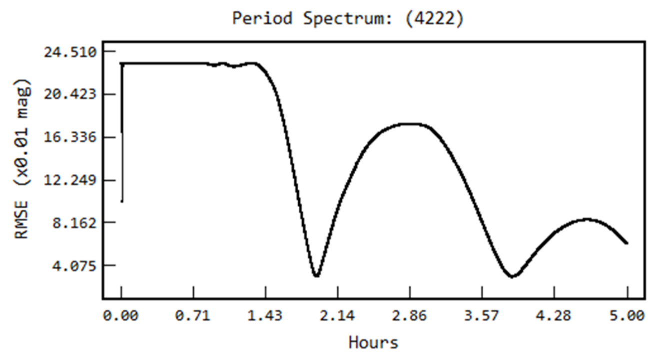

Acknowledgements

The authors would like to express their gratitude to Daniel Parrott, the author of *Tycho*.

References

Ďurech, J.; Hanuš, J.; Ali-Lagoa, V. (2018). "Asteroid models reconstructed from the Lowell Photometric Database and WISE data." *Astronomy & Astrophysics* **617**, A57.

Harris, A.W.; Young, J.W.; Scaltriti, F.; Zappala, V. (1984). "Lightcurves and phase relations of the asteroids 82 Alkmene and 444 Gyptis." *Icarus* **57**, 251-258.

Higgins, D.; Pravec, P.; Kusnirak, P.; Reddy, V.; Dyvig, R. (2006). "Asteroid lightcurve analysis at Hunters Hill Observatory and collaborating stations-summer 2005/6." *Minor Plan Bull* **33**, 64-66.

Masiero, J.R.; Grav, T.; Mainzer, A.K.; Nugent, C.R.; Bauer, J.M.; Stevenson, R.; Sonnett, S. (2014). "Main-belt asteroids with WISE/NEOWISE: Near-infrared albedos." *The Astrophysical Journal* **791(2)**, 121.

Parrott, D. (2024). Tycho software. *https://www.tycho-tracker.com*

Warner, B.D.; Harris, A.W.; Pravec, P. (2009). "The Asteroid Lightcurve Database." *Icarus* **202**, 134-146. Updated 2023 Oct. *http://www.minorplanet.info/lightcurvedatabase.html*

Number	Name	yyyy mm/dd	Phase	L_{PAB}	B_{PAB}	Period(h)	P.E.	Amp	A.E.	Grp
4222	Nancita	2024 01/26-01/28	29.5,29.9	82	-4	3.8743	0.0001	0.80	0.04	MC

Table I. Observing circumstances and results. The phase angle is given for the first and last date. L_{PAB} and B_{PAB} are the approximate phase angle bisector longitude and latitude at mid-date range (see Harris et al., 1984). Exp is the exposure (sec) or average if a range of exposures was used. Grp is the asteroid family/group (Warner et al., 2009).

ROTATION PERIOD DETERMINATION FOR ASTEROID 2024 MK

Nick Sioulas
NOAK Observatory (L02)
Stavraki Ioannina, GREECE
nsioulas@hotmail.com

(Received: 2024 July 21 Revised: 2024 August 8)

Photometric observations of the near-Earth asteroid 2024 MK were conducted from the NOAK Observatory, in Greece to determine its rotation period. Multiple tumbling periods are found: $P = 0.730 \pm 0.003$ h, $A = 1.48$ mag and $P = 0.664 \pm 0.003$ h, $A = 1.38 \pm 0.02$ mag.

All observations of 2024 MK were performed at the NOAK Observatory, Ioannina Greece (MPC-International Astronomical Union code L02), using a 0.25-m Newtonian Skywatcher optical tube operating at f/4.7. The optical tube is mounted on NEQ6 Skywatcher robotic mount and equipped with ATIK 460exm CCD camera. It is a high Quantum Efficiency CCD. No filters used for better signal to noise. Exposure time for all the images was two seconds. The camera was binned at 2×2. The image scale after 2×2 binning was 1.57 arcsec/pixel and the field of view 35.9′× 28.7′. In these fields, the asteroid and five comparison stars were measured for differential photometry.

All images were reduced in the standard manner using nightly flatfield files as well as dark-current and bias images. Photometric measurements and lightcurve analysis were performed using *MPO Canopus* (version 10.8.1.1; Warner, 2019). The *Cartes Du Ciel* was used as the planetarium software with the most recent ephemerides downloaded from the Minor Planet Center and *Artemis Capture* was used for image capture.

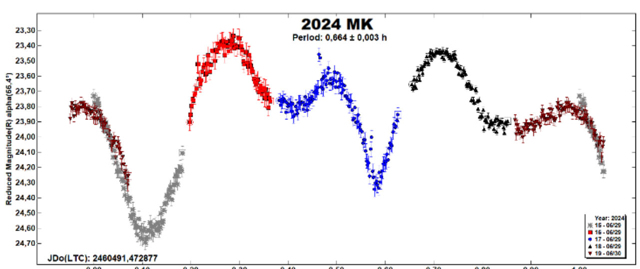

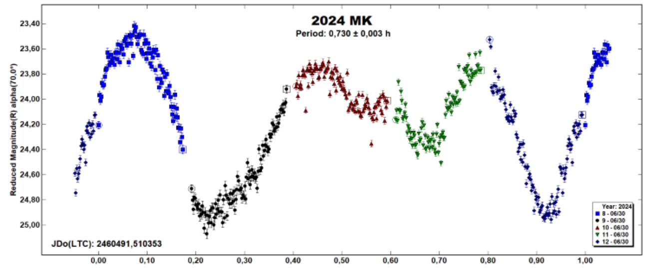

2024 MK (54448601) was discovered by ATLAS South Africa, Sutherland on 2024-06-16. It has an estimated diameter of 141m and passed within 294.000 km of Earth's surface – roughly 77% of the distance between Earth and the Moon. The recording time from the observatory was 2 hours. Within this observation period it was found that the asteroid has 2 rotation periods. This leads to the result that it is a non-principal axis rotator asteroid, a result that agrees with the preliminary analysis performed by the Goldstone Solar System Radar. The first period analysis shows a solution for the rotational period $P = 0.730 \pm 0.003$ h with an amplitude $A = 1.48 \pm 0.02$ mag and the second analysis a rotational period $P = 0.664 \pm 0.003$ h with an amplitude $A = 1.38 \pm 0.02$ mag. It is a Potentially Hazardous Asteroid with a semi-major axis of 2.201AU, eccentricity 0.542, inclination 8.401deg, and an orbital period of 3.266 years. Its absolute magnitude is $H = 22.052$ (JPL, 2024).

References

Goldstone Solar System Radar. *https://echo.jpl.nasa.gov/asteroids/june2024.goldstone.planning.html*

Harris, A.W., Young, J.W., Scaltriti, F., Zappala, V. (1984). "Lightcurves and phase relations of the asteroids 82 Alkmene and 444 Gyptis." *Icarus* **57**, 251-258.

JPL (2020). Small Body Database Browser. *https://ssd.jpl.nasa.gov*

MPC (2020). Database Search. *https://minorplanetcenter.net/db_search/*

Warner, B.D.; Harris, A.W.; Pravec, P. (2009). "The Asteroid Lightcurve Database." Icarus **202**, 134-146. Updated 2019 Aug. *http://www.minorplanet.info/lightcurvedatabase.html*

Warner, B.D. (2019). MPO Software, *MPO Canopus* v10.8.1.1. Bdw Publishing. *http://minorplanetobserver.com*

Number	Name	yyyy mm/dd	Phase	L_{PAB}	B_{PAB}	Period(h)	P.E.	Amp	A.E.	Grp
	2024 MK	2024 06/29	+33.40	264.9	-11.8	0.664	0.003	1.48	0.02	APOLLO[NEO]
	2024 MK	2024 06/30	+70.30	308.6	19.4	0.730	0.003	1.38	0.02	APOLLO[NEO]

Table I. Observing circumstances and results. The phase angle is given for the first and last date. If preceded by an asterisk, the phase angle reached an extrema during the period. L_{PAB} and B_{PAB} are the approximate phase angle bisector longitude/latitude at mid-date range (see Harris et al., 1984). Grp is the asteroid family/group (Warner et al., 2009).

LIGHTCURVE AND ROTATION PERIOD ANALYSIS OF 1908 POBEDA, 2168 SWOPE, AND 5203 PAVAROTTI

Wayne Hawley
Old Orchard Observatory (Z09)
Fiddington, UK
hawley.wayne@gmail.com

Patrick Wiggins
University of Utah (718)

James D. Armstrong
University of Hawaii Institute for Astronomy (L09) (V38)
34 Ohia Ku Street
Pukalani, HI 96768, USA

Paul C. Leyland
Tacande Observatory (J22)
La Palma, SPAIN

Kent DeGroff
Whiskey Creek Observatory (V19)
New Mexico, USA

Steven Arnold
NNHS Drummonds Observatory (Z34)
Northamptonshire, UK

Mohammad Shawkat Odeh
Al Khatim Observatory (M44)
Abu Dhabi, UAE

Tim Haymes
Southside Observatory (Y98)
Steeple Aston, UK

Emmanuel Kardasis, Alexia Takoudi
Pelagia-Eleni Observatory (247)
Athens, GREECE

Grant Privett
LPMR Observatory (Y82)
Broad Chalke, UK

Joan Genebriera
Astropriorat Observatory (M02)
Catalonia, SPAIN

(Received: 2024 October 8)

Photometric observations were made of asteroids 1908 Pobeda, 2168 Swope, and 5203 Pavarotti. From these, we determined the synodic rotation period and lightcurve amplitudes for each asteroid.

CCD photometric observations were obtained by observatories around the globe from 2024 March to June for asteroid 1908 Pobeda and from 2024 August to September for asteroids 2168 Swope and 5203 Pavarotti. Several of the co-authors used their own equipment and some used the Las Cumbres Observatory facilities.

The photometric analysis was performed using *TychoTracker Pro* Version 11.7.5 (*TT*; Parrott, 2024). Standard differential techniques were used on images with the comparison stars selected by *TT* to be within the colour range of +0.50 < (B-V) < +0.90, i.e., near solar color. The Asteroid Terrestrial-impact Last Alert System catalog (ATLAS refcat2; Tonry et al., 2018), was used as the source of magnitudes for the comparison stars.

Period determination in *TT* operates by using user-defined orders of Fourier analysis to find model lightcurves by sampling periods over a user-defined range that best fit the data. The program lists the RMS of the fit for each sample period and uses the values to create a *period spectrum*, which plots RMS versus period. Each object yielded a clear best-fit solution, seen as a well-defined minimum RMS in the period spectrum. In some cases, datapoints used for analysis were created by combining (binning) raw data points in order to improve the signal-to-noise ratio.

The period spectra often exhibit several possible periods, in which case an examination of the rotational phase plot for each of these periods is then conducted to look for a credible lightcurve. Where the object shape is the dominant factor in producing the observed magnitude changes, and especially if the lightcurve amplitude is on the order of >0.2 mag, a bimodal lightcurve, meaning two minimum/maximum pairs per cycle, was usually chosen as the most likely solution. The results are summarized in the Table I.

In this paper, no attempt is made to find an absolute magnitude (*H*) or phase slope parameter (*G*). Instead, we used a default value of $G = 0.15$ throughout the calculations. Time-series magnitude estimates from different nights and observing locations using a variety of imaging equipment were offset in magnitude to bring them into alignment when producing the raw and rotational-phase plots. The same offset was used for each instance of an individual imaging setup.

All the data will be uploaded into the Asteroid Lightcurve Data Exchange Format (ALCDEF) database (*https://alcdef.org*) following publication.

Information given for an object is taken from the NASA Jet Propulsion Laboratory (JPL, 2023) Small-Body Database Lookup webpage.

<u>1908 Pobeda</u> is an outer main-belt asteroid that was discovered on 1972 Sep 11 by N. Chernykh at Nauchnyj. Our data set of 39 observing sessions (404 data points) was obtained between 2024 March and June. Analysis of the data found a synodic period of 150.1 ± 0.1 h; this compares well with the sidereal period of 149.95 h from Durech et al. (2020). The peak-to-peak amplitude of the lightcurve is 0.66 ± 0.09 mag.

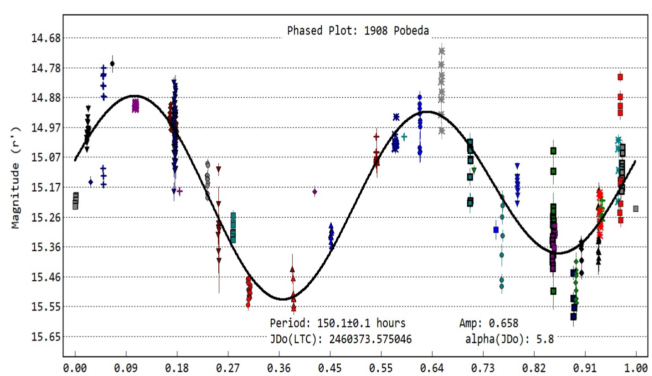

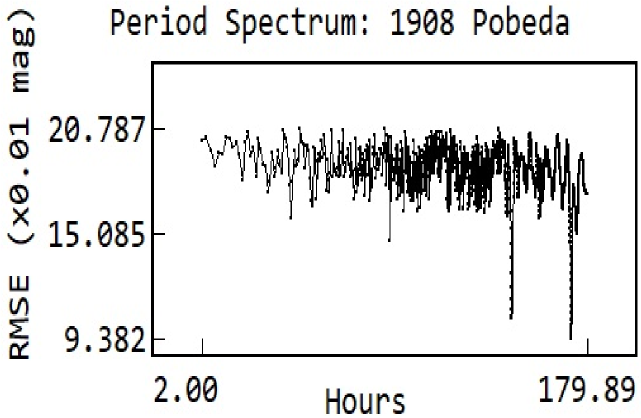

2168 Swope. This is an inner main-belt asteroid discovered on 1955 Sep 14 at Goethe Link Observatory in Brooklyn. It is named after Henrieta Hill Swope, an American astronomer who studied variable stars, particularly the period-luminosity relationship of Cepheids. Our results are based on 31 observing sessions (603 exposures) obtained between 2024 August and September. Our bimodal lightcurve has a period of P = 7.355 ± 0.005 h and amplitude of A = 0.80 ± 0.05 mag.

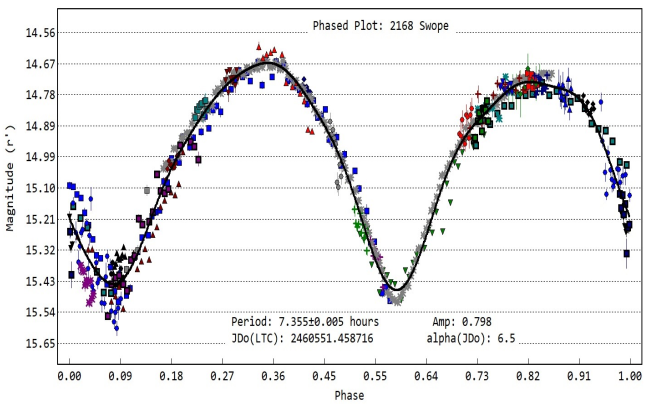

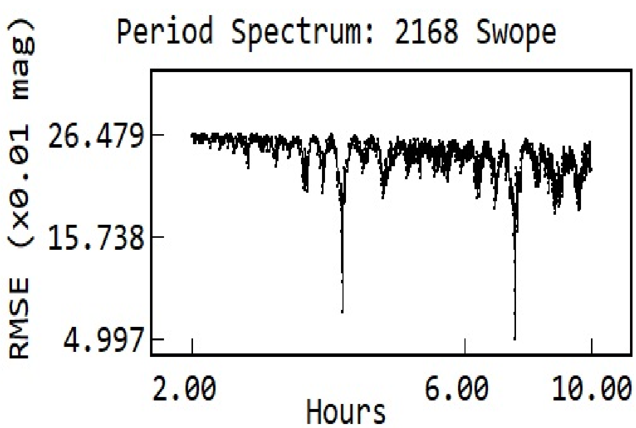

5203 Pavarotti is an inner main-belt that was discovered on 1984 Sep. 27 by Zdeňka Vávrová, a Czech astronomer at the Kleť Observatory. Our results of P = 6.930 ± 0.005 h and A = 0.48 ± 0.04 mag are based on 15 observing sessions (668 exposures) obtained between 2024 August and September.

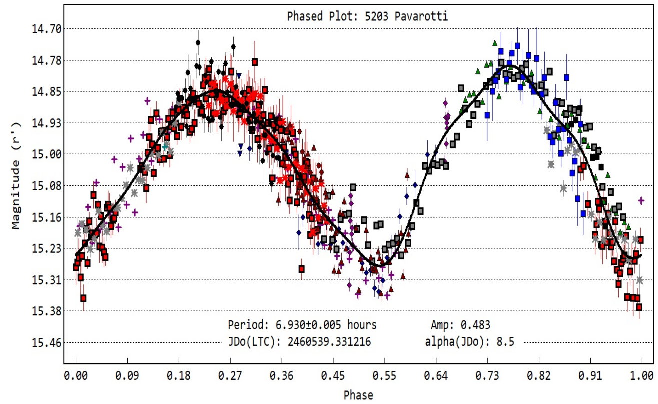

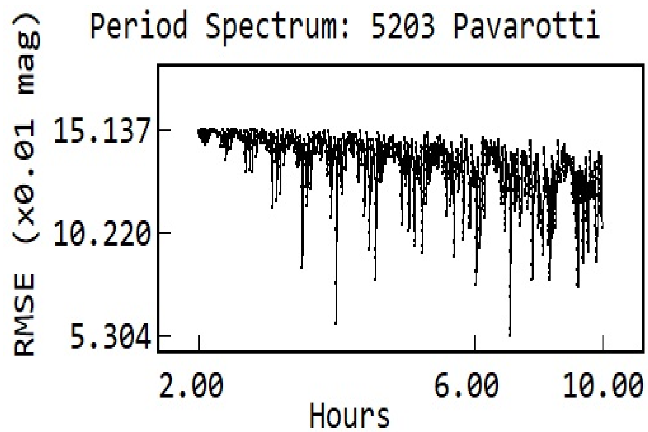

Acknowledgements

Our thanks are extended to Daniel Parrott, author of *TychoTracker Pro*.

This work has made use of data from the Asteroid Terrestrial-impact Last Alert System (ATLAS) project. ATLAS is primarily funded to search for near earth asteroids through NASA grants NN12AR55G, 80NSSC18K0284, and 80NSSC18K1575; byproducts of the NEO search include images and catalogs from the survey area. The ATLAS science products have been made possible through the contributions of the University of Hawaii Institute for Astronomy, the Queen's University Belfast, the Space Telescope Science Institute, and the South African Astronomical Observatory.

The ATLAS refcat2 makes use of the formulae to convert Pan-STARRS gri to BVRI from Kostov and Bonev (2017).

This work makes use of observations from the Las Cumbres Observatory global telescope network.

References

Durech J.; Tonry J.; Erasmus N.; Denneau L.; Heinze A.N.; Flewelling H.; Vanco R. (2020). "Asteroid models reconstructed from ATLAS photometry." *Astronomy and Astrophysics* **643**, A59.

Harris, A.W.; Young, J.W.; Scaltriti, F.; Zappala, V. (1984). "Lightcurves and phase relations of the asteroids 82 Alkmene and 444 Gyptis." *Icarus* **57**, 251-258.

JPL (2023). Small-Body Database Lookup. *https://ssd.jpl.nasa.gov/tools/sbdb_lookup.html*

Kostov, A.; Bonev, T. (2017). "Transformation of Pan-STARRS1 gri to Stetson BVRI magnitudes. Photometry of small bodies observations." *Bulgarian Astron. J.* **28**, 3 (ArXiv:1706.06147v2).

Parrott, D. (2024). Tycho Tracker Pro software. *https://www.tycho-tracker.com/*

Tonry, J.L.; Denneau, L.; Flewelling, H.; Heinze, A.N.; Onken, C.A.; Smartt, S.J.; Stadler, B.; Weiland, H.J.; Wolf, C. (2018). "The ATLAS All-Sky Stellar Reference Catalog." *Astrophys. J.* **867**, A105.

Warner, B.D.; Harris, A.W.; Pravec, P. (2009). "The Asteroid Lightcurve Database." *Icarus* **202**, 134-146. Updated 2023 Oct. *http://www.minorplanet.info/lightcurvedatabase.html*

Number	Name	yyyy mm/dd	Phase	L_{PAB}	B_{PAB}	Period (h)	P.E.	Amp	A.E.	Grp
1908	Pobeda	2024 03/04-06/18	*4.7,21.3	179	1	150.1	0.1	0.66	0.09	9106
2168	Swope	2024 08/29-09/30	*2.4,12.0	346	4	7.355	0.005	0.80	0.05	9104
5203	Pavarotti	2024 08/16-09/12	*2.3, 9.3	336	3	6.930	0.005	0.48	0.04	9104

Table I. Observing circumstances and results. The phase angle is given for the first and last date. If preceded by an asterisk, the phase angle reached a minimum during the period. L_{PAB} and B_{PAB} are the approximate phase angle bisector longitude/latitude at mid-date range (see Harris et al., 1984). Grp is the asteroid family/group (Warner et al., 2009).

Observatory	Telescope	CCD/CMOS	Fil	Object (sessions)
Hawley Old Orchard Observatory (Z09)	0.35-m SCT f/6.7	SX694 Trius Pro (2×2)	SR	1908 (7) 2168 (7) 5203 (5)
Wiggins University of Utah, (718)	0.35-m SCT f/5.5	ST-10XME (3×3)	C	1908 (19) 2168 (19)
Armstrong Sutherland LCO-Aqawan A (L09)	0.4-m f/8	SBIG STL6303 (1×1)	SR	2168 (1)
Armstrong McDonald LCO-Aqawan A (V38)	0.4-m f/8	SBIG STL6303 (1×1)	SR	5203 (1)
Leyland Tacande Observatory (J22)	0.4m Dilworth f/6.5	SX814 Trius Pro (2×2)	V	2168 (2) 5203 (3)
DeGroff Whiskey Creek Observatory (V19)	0.46m Newt f/4.2	QHY 268M	V	2168 (1)
Arnold NNHS Drummonds Observatory (Z34)	0.3m f/3.8	SX694 Trius Pro	C	2168 (1)
Haymes Southside Observatory (Y98)	0.28m f/5.8	QHY 174	C	1908 (1) 5203 (1)
Kardasis Takoudi (5203) Pelagia-Eleni Observatory (247)	0.28m SCT f/10	ASI 183 Pro	V	1908 (8) 5203 (4)
Privett LPMR Observatory (Y82)	0.3m f/4	SX694 Trius Pro	C	1908 (1)
Genebriera Astropriorat Observatory (M02)	0.41m f/8	Moravian G4-16000	V	1908 (3)

Table II. List of observers, equipment, and sessions for each location.

COLLABORATIVE ASTEROID PHOTOMETRY FROM UAI: 2024 JULY-SEPTEMBER

Lorenzo Franco
Balzaretto Observatory (A81), Rome, ITALY
lor_franco@libero.it

Giulio Scarfi
Iota Scorpii Observatory (K78), La Spezia, ITALY

Nello Ruocco
Osservatorio Astronomico Nastro Verde (C82), Sorrento, ITALY

Matteo Lombardo
Zen Observatory (M26), Scandicci, ITALY

Maura Tombelli, Matteo Lombardo, Marco Iozzi
Beppe Forti Astronomical Observatory (K83)
Montelupo Fiorentino, ITALY

Gianni Galli
GiaGa Observatory (203), Pogliano Milanese, ITALY

Marco Iozzi
HOB Astronomical Observatory (L63)
Capraia Fiorentina, ITALY

(Received: 2024 October 10)

Photometric observations of four asteroids were made in order to acquire lightcurves for shape/spin axis modeling. Lightcurves were acquired for 1394 Algoa, 8577 Choseikomori, 21088 Chelyabinsk, and (66251) 1999 GJ2.

Collaborative asteroid photometry was done inside the Italian Amateur Astronomers Union (UAI; 2024) group. The targets were selected mainly in order to acquire lightcurves for shape/spin axis modeling. Table I shows the observing circumstances and results.

The CCD observations of four asteroids were made in 2024 July-September using the instrumentation described in the Table II. Lightcurve analysis was performed at the Balzaretto Observatory with *MPO Canopus* (Warner, 2023). All the images were calibrated with dark and flat frames and converted to standard magnitudes using solar colored field stars from CMC15 and ATLAS catalogues, distributed with *MPO Canopus*. For brevity, "LCDB" is a reference to the asteroid lightcurve database (Warner et al., 2009).

1394 Algoa is a low albedo inner main-belt asteroid. Collaborative observations were made over three nights. The period analysis shows a synodic period of $P = 2.7681 \pm 0.0001$ h with an amplitude $A = 0.21 \pm 0.01$ mag. The period is close to the previously published results in the LCDB.

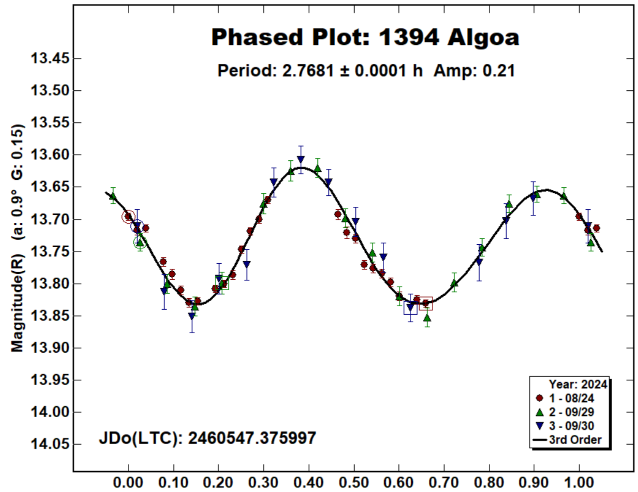

8577 Choseikomori is a medium albedo inner main-belt asteroid. Collaborative observations were made over nine nights. The period analysis shows a synodic period of $P = 5.574 \pm 0.001$ h with an amplitude $A = 0.21 \pm 0.03$ mag. The period is close to the previously published results in the LCDB.

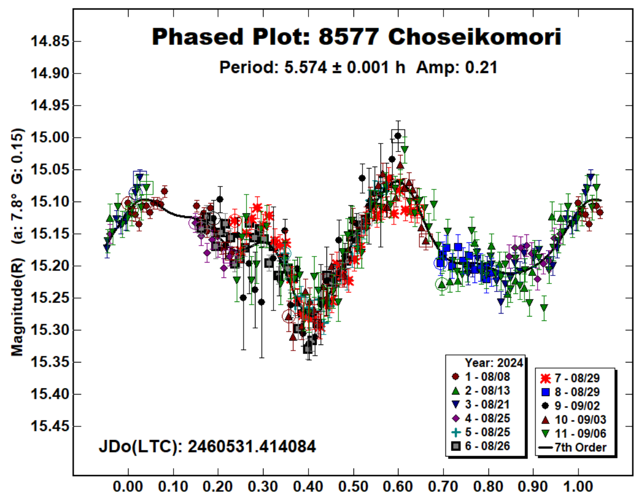

21088 Chelyabinsk is an Amor Near-Earth asteroid. Collaborative observations were made over seven nights. The period analysis shows a synodic period of $P = 11.234 \pm 0.003$ h with an amplitude $A = 0.34 \pm 0.03$ mag. The period is close to the previously published results in the LCDB. Multiband photometry was made by G. Scarfi (K78) on 2024 August 12. We found V-R = 0.47 ± 0.05. This color index is consistent with a S-type asteroid (Shevchenko and Lupishko, 1998; 0.49 ± 0.05).

Number	Name	2024 mm/dd	Phase	L_{PAB}	B_{PAB}	Period(h)	P.E.	Amp	A.E.	Grp
1394	Algoa	08/24-09/30	0.9,16.8	333	1	2.7681	0.001	0.21	0.01	MB-I
8577	Choseikomori	08/08-09/06	*7.8,14.2	324	8	5.574	0.001	0.21	0.03	MB-I
21088	Chelyabinsk	07/23-08/12	28.4,40.8	317	28	11.234	0.003	0.34	0.03	NEA
66251	1999 GJ2	09/27-09/28	15.6,15.8	357	8	2.464	0.003	0.10	0.03	NEA

Table I. Observing circumstances and results. The first line gives the results for the primary of a binary system. The second line gives the orbital period of the satellite and the maximum attenuation. The phase angle is given for the first and last date. If preceded by an asterisk, the phase angle reached an extrema during the period. L_{PAB} and B_{PAB} are the approximate phase angle bisector longitude/latitude at mid-date range (see Harris et al., 1984). Grp is the asteroid family/group (Warner et al., 2009).

Observatory (MPC code)	**Telescope**	**CCD**	**Filter**	**Observed Asteroids (#Sessions)**
Iota Scorpii(K78)	0.40-m RCT f/6.1	CMOS QHY 268 (bin 4×4)	V,Rc,C	21088(6), 66251(1)
Osservatorio Astronomico Nastro Verde (C82)	0.35-m SCT f/6.3	SBIG ST10XME (bin 2×2)	C	1394(1), 8577(4)
Zen Observatory (M26)	0.30-m RCT f/7.4	ATIK 383L+	C	8577(2), 21088(3)
Beppe Forti Observatory (K83)	0.40-m RCT f/8.0	SBIG ALUMA 4040	C	8577(2)
GiaGa Observatory (203)	0.36-m SCT f/5.8	Moravian G2-3200	C	66251(2)
Balzaretto Observatory (A81)	0.20-m SCT f/5.0	SBIG ST7-XME	C	1394(2)
HOB Astronomical Observatory (L63)	0.20-m SCT f/6.0	ATIK 383L+	C	8577(1)

Table II. Observing Instrumentations. RCT: Ritchey-Chretien, SCT: Schmidt-Cassegrain.

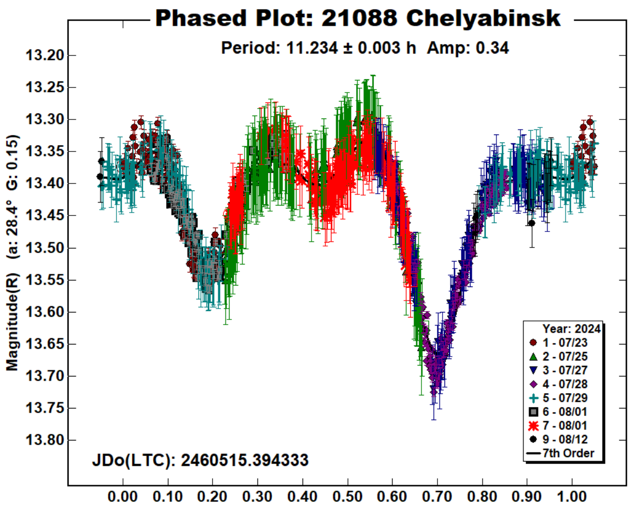

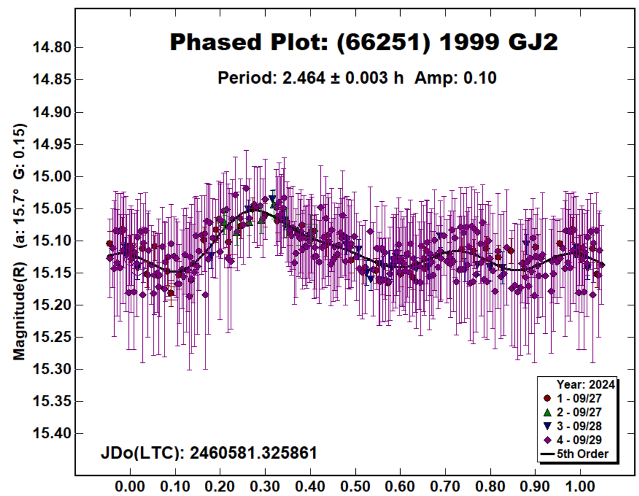

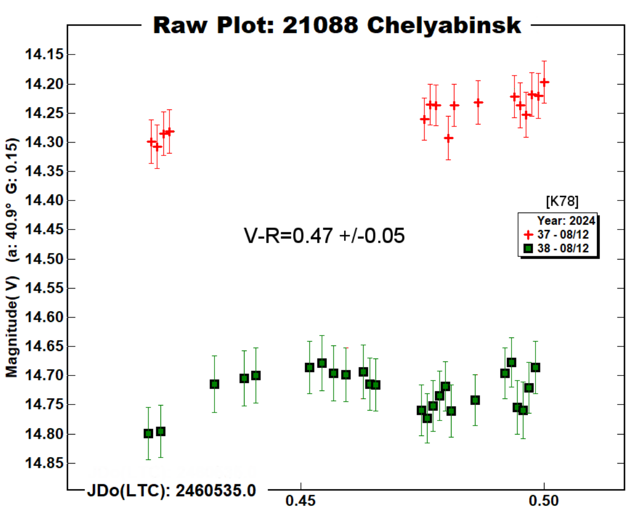

(66251) 1999 GJ2 is an Amor Near-Earth asteroid. Collaborative observations were made over two nights. The period analysis shows a synodic period of $P = 2.464 \pm 0.003$ h with an amplitude $A = 0.10 \pm 0.03$ mag. The period is close to the previously published results in the LCDB.

References

Harris, A.W.; Young, J.W.; Scaltriti, F.; Zappala, V. (1984). "Lightcurves and phase relations of the asteroids 82 Alkmene and 444 Gyptis." *Icarus* **57**, 251-258.

Shevchenko V.G.; Lupishko D.F. (1998). "Optical properties of Asteroids from Photometric Data." *Solar System Research* **32**, 220-232.

UAI (2024). "Unione Astrofili Italiani" web site. *https://www.uai.it*

Warner, B.D.; Harris, A.W.; Pravec, P. (2009) "The asteroid lightcurve database." *Icarus* **202**, 134-146. Updated 2024 Oct. *https://minplanobs.org/alcdef/index.php*

Warner, B.D. (2023). MPO Software, MPO Canopus v10.8.6.20. Bdw Publishing. *http://minorplanetobserver.com*

LIGHTCURVE AND ROTATION PERIOD ANALYSIS FOR FOUR MINOR PLANETS

Mike Wiles
Chiricahua Skies Observatory
4126 N. Twilight Cir.
Mesa, AZ 85207
mikewilesaz@gmail.com

(Received: 2024 October 11)

Photometric measurements of CCD observations on four main-belt asteroids were made from 2024 September through 2024 October. Phased lightcurves were created for each one. All the data have been submitted to the ALCDEF database.

Photometric CCD observations of three main-belt asteroids were performed at Chiricahua Skies Observatory (MPC V43) near Sunizona, AZ. Images were taken using a 0.35m f/4.69 Corrected Dall-Kirkham telescope and Teledyne CCD47-10 sensor yielding an image scale of 1.61”/pixel. Table I shows observing circumstances and results. All images for these observations were obtained between 2024 September and 2024 October.

Data reduction and period analysis were done using *Tycho* (Parrott, 2023). The asteroid and five or more comparison stars were measured. Comparison stars were selected with colors within the range of 0.5 < B-V < 0.95 to correspond with color ranges of asteroids.

Comparison star magnitudes were obtained from the ATLAS catalog (Tonry et al., 2018), which is incorporated directly into Tycho. A measuring aperture equal to 4× FWHM of the target was used for asteroids and comp stars. This was typically a radius of 5 pixels on the measuring aperture. Interference from field stars resulted in the exclusion of affected observations. Period determination was done using Tycho.

Asteroids were selected from the CALL website (Warner, 2011), either for having uncertain periods or no reported period at all. In this set of observations, all three asteroids had previously reported periods. The Asteroid Lightcurve Database (LCDB) Warner et al. (2009) was consulted to locate previously published results. All new data for these asteroids has been submitted to the ALCDEF database.

2042 Sitarski was observed on five nights in an eight-day period near opposition during its 2024 apparition. 356 observations were used to determine the rotation period of the asteroid. Searching the LCDB one previous period of 2.63 ± 0.01 hours has been reported by Warell (2017). The author calculated a period of 8.37 ± 0.01 hours, disagreeing with Warell. The amplitude of the light curve is 0.165 ± 0.19 magnitude.

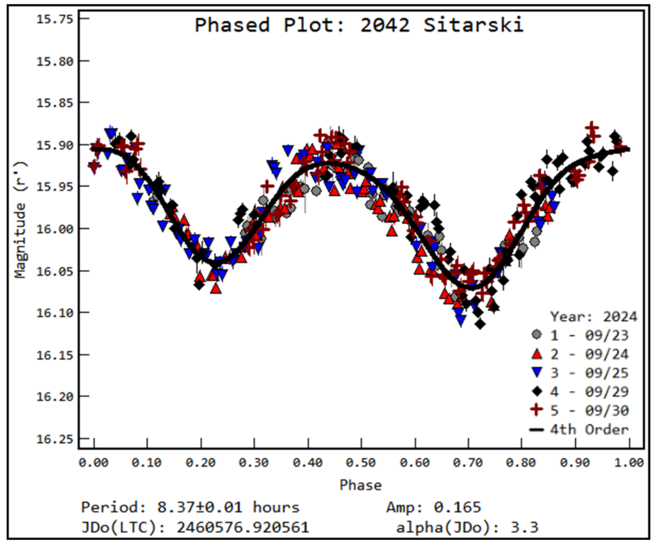

3026 Sarastro has a single reported period in the LCDB. Chang et al. (2016) reported a period of 7.87 ± 0.13 hours and assigned a quality code U=2 indicating some ambiguity. The referenced period was derived from data that did not cover a complete period. The author observed the minor planet over twelve nights in 2024 September and 2024 October and calculated a period of 11.82 ± 0.01 hours, disagreeing with Chang’s result.

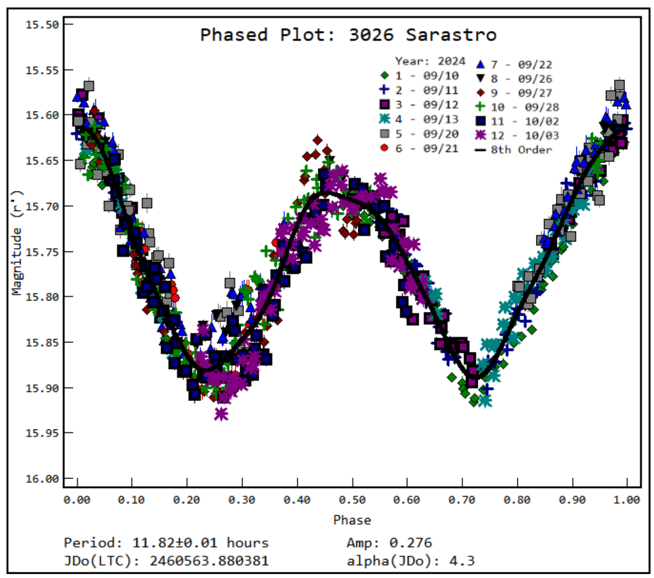

Number	Name	yyyy mm/dd	Phase	L_{PAB}	B_{PAB}	Period(h)	P.E.	Amp	A.E.	Grp
2042	Sitarski	2023/09/23-09/30	0.6, 3.5	7	0	8.37	0.01	0.165	0.019	Merxia
3026	Sarastro	2024/09/10-10/03	4.2,10.7	343	9	11.82	0.01	0.276	0.023	MB-O
6094	Hisako	2024/09/10-09/28	5.3, 8.4	1	11	75.13	0.03	0.663	0.027	Eunomia
8606	1971 UG	2024/10/06-10/10	9.1,10.7	38	1	2.658	0.001	0.306	0.019	MB-O

Table I. Observing circumstances and results. The phase angle is given for the first and last date. If preceded by an asterisk, the phase angle reached an extrema during the period. L_{PAB} and B_{PAB} are the approximate phase angle bisector longitude/latitude at mid-date range (see Harris et al., 1984). Grp is the asteroid family/group (Warner et al., 2009).

6094 Hisako was observed in a dense dataset of 884 observations on eleven nights in an eighteen-night period in 2024 September. Two previously reported periods were found in the LCDB. Behrend (2015web) reported a period of 16.4 ± 0.1 h and Klinglesmith III et al. (2016) reported a period of 4.05 ± 0.002 h. In the report Klinglesmith noted low confidence in the result because of the large scatter in the data. The author computed a period of 75.13 ± 0.03 h and an amplitude of 0.663 ± 0.027 magnitude. This disagrees with the two previously reported period solutions.

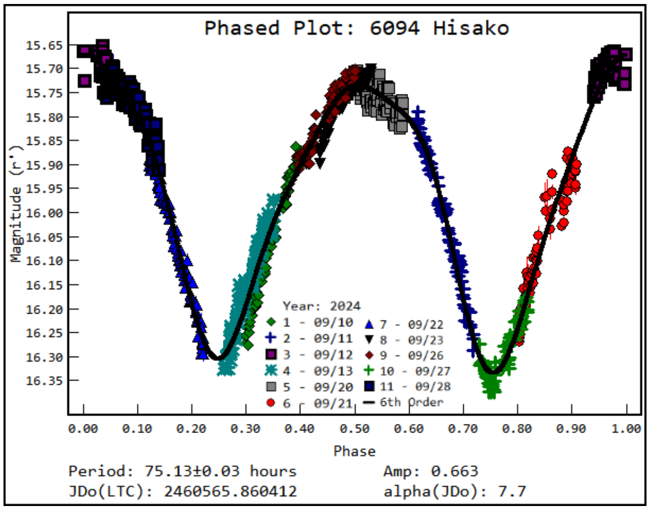

8606 1971 UG was observed over five consecutive nights in 2024 October. This outer main-belt asteroid has a low eccentricity orbit inclined 11.8º to that of the orbital plane of the solar system. No previous periods have been reported in the LCDB for this target. From a total of 192 observations a period of 2.658 ± 0.001 hours was determined with an amplitude of 0.306 ± 0.019 magnitude.

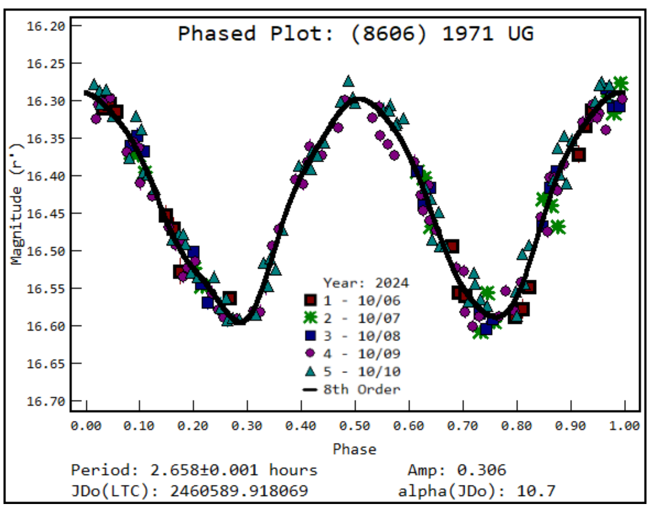

Acknowledgements

The author would like to thank Tom Polakis for his many years of encouragement and mentorship. Thanks also go out to Daniel Parrott for his responsive support of questions regarding the *Tycho* software package.

References

Behrend, R. (2015web). Observatoire de Geneve web site. *http://obswww.unige.ch/~behrend/page5cou.html*

Chang, C.; Lin, H.; Ip, W.; Prince, T.; Kulkarni, S.R.; Levitan, D.; Laher, R.; Surace, J. (2016). "Large Super-fast Rotator Hunting Using the Intermediate Palomar Transient Factory." *Astrophys. J.* **227**, 20C.

Harris, A.W.; Young, J.W.; Scaltriti, F.; Zappala, V. (1984). "Lightcurves and phase relations of the asteroids 82 Alkmene and 444 Gyptis." *Icarus* **57**, 251-258.

JPL (2023). Small Body Database Lookup. *https://ssd.jpl.nasa.gov/tools/sbdb_lookup.html*

Klinglesmith III, D.; Hendrickx, S.; Madden, K.; Montgomery, S.; (2016). "Asteroid Light Curves from Estcorn Observatory." *Minor Planet Bull.* **43**, 234.

Parrot, D. (2023). Tycho software. *https://www.tycho-tracker.com*

Tonry, J.L.; Denneau, L.; Flewelling, H.; Heinze, A.N.; Onken, C.A.; Smartt, S.J.; Stalder, B.; Weiland, H.J.; Wolf, C. (2018). "The ATLAS All-Sky Stellar Reference Catalog." *Astrophys. J.* **867**, A105.

Warell, J. (2017). "Lightcurve Observations of Nine Main-belt Asteroids." *Minor Planet Bull.* **44**, 304.

Warner, B.D.; Harris, A.W.; Pravec, P. (2009) "The asteroid lightcurve database." *Icarus* **202**, 134-146. Updated 2024 Oct. *https://minplanobs.org/alcdef/index.php*

Warner, B.D. (2011). Collaborative Asteroid Lightcurve Link website. *http://www.minorplanet.info/call.html*

LIGHTCURVES AND ROTATION PERIODS OF 209 DIDO, 268 ADOREA, 2732 WITT, AND 2836 SOBOLEV, WITH A NOTE ON 1402 ERI

Frederick Pilcher
Organ Mesa Observatory (G50)
4438 Organ Mesa Loop
Las Cruces, NM 88011 USA
fpilcher35@gmail.com

(Received: 2024 October 8)

Synodic rotation periods and amplitudes are found for 209 Dido 5.7356 ± 0.0001 hours, 0.11 ± 0.01 magnitudes; 268 Adorea 7.7982 ± 0.0002 hours, 0.11 ± 0.01 magnitudes; 2732 Witt 12.6244 ± 0.0003 hours, 0.55 ± 0.03 magnitudes; and 2836 Sobolev 4.7548 ± 0.0001 hours, amplitude 0.75 ± 0.05 magnitudes. A 4-hour lightcurve of 1402 Eri showed no perceptible variation.

The new observations to produce the results reported in this paper were made at the Organ Mesa Observatory with a Meade 35-cm LX200 GPS Schmidt-Cassegrain, SBIG STL-1001E CCD, 60 second exposures for 209 Dido and 268 Adorea, and 120 second exposures for 1402 Eri, 2732 Witt, and 2836 Sobolev, unguided, clear filter. Image measurement and lightcurve construction were with *MPO Canopus* software with calibration star magnitudes for solar colored stars from the CMC15 catalog reduced to the Cousins R band. Zero-point adjustments of a few × 0.01 magnitude were made for best fit. To reduce the number of data points on the lightcurves and make them easier to read, data points have been binned in sets of 3 with maximum time difference 5 minutes.

209 Dido. Eight previously published periods are listed in "The Asteroid Lightcurve Database" (Warner et al., 2009, updated 2023 October), seven of them in the range from 5.7351 hours to 5.745 hours. New observations on six nights 2024 Sept. 11 - Oct. 8 provide an excellent fit to an asymmetric bimodal lightcurve with period 5.7356 ± 0.0001 hours, amplitude 0.11 ± 0.01 magnitudes. The agreement with previously published periods is excellent.

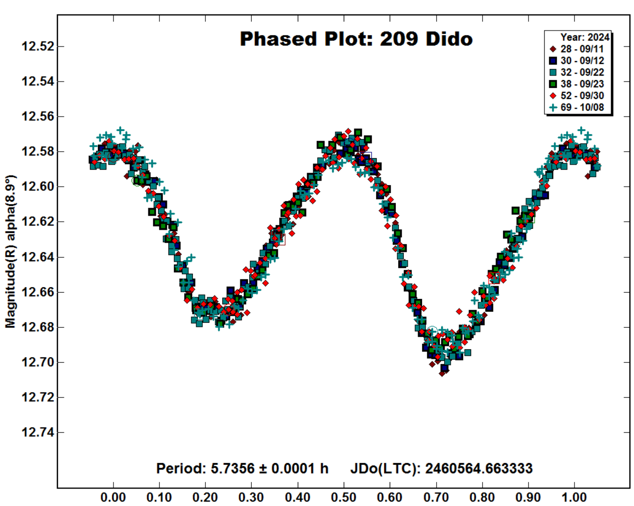

268 Adorea. Previously published periods are by Tedesco (1979), 6.1 hours; Holliday (1995), 9.44 hours; Behrend (2005web), 15.595 hours; Stephens (2006), 7.8 hours; and Hawley (2023), 7.7952 hours. New observations on nine nights 2024 July 8 - Aug. 8 provide a good fit to an asymmetric bimodal lightcurve with period 7.7982 ± 0.0002 hours, amplitude 0.11 ± 0.01 magnitudes. This value is consistent with the periods published by Stephens (2006) and Hawley (2023). The earlier periods by Tedesco (1979), Holliday (1995) and Behrend (2005web) can now be rejected.

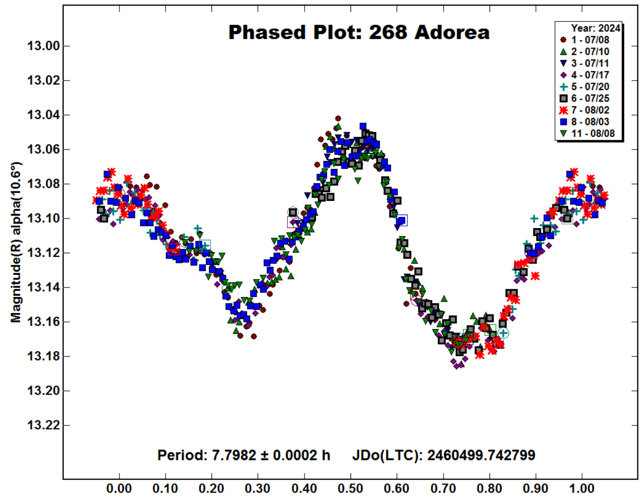

1402 Eri. This object is one of the faintest lower numbered minor planets, fainter than magnitude 17 at most oppositions. For this reason, no previous lightcurves have been published in the Lightcurve Database (Warner et al., 2009, updated 2023 October). At its 2024 opposition its magnitude brightened to 16. If the period had been short and the amplitude large, they could have been found with a 35-centimeter telescope. However, these parameters were not observed. A four-hour lightcurve on 2024 June 11 showed a 0.1 magnitude scatter of data points and variation of no more than 0.02 magnitudes. It was apparent that a reliable period could not be found with the available equipment, especially during the local cloudy/rainy season and at southerly declination. No more sessions were obtained.

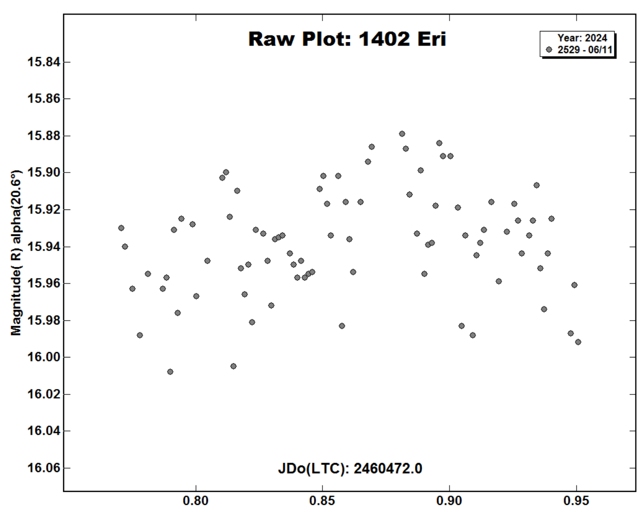

Number	Name	yyyy/mm/dd	Phase		L_{PAB}	B_{PAB}	Period(h)	P.E	Amp	A.E.
209	Dido	2024/09/11-2024/10/08	8.9 -	0.9	13	2	5.7356	0.0001	0.11	0.01
268	Adorea	2024/07/08-2024/08/08	10.5 -	0.5	317	-1	7.7982	0.0002	0.11	0.01
1402	Eri	2024/06/11-2024/06/11	20.6 -	20.5	302	8	---	---	---	---
2732	Witt	2024/08/10-2024/09/12	*6.0 -	7.9	331	-1	12.6244	0.0003	0.55	0.03
2836	Sobolev	2024/09/01-2024/09/28	10.4 -	1.6	4	3	4.7548	0.0001	0.70	0.05

Table I. Observing circumstances and results. The phase angle is given for the first and last date, unless a minimum (second value) was reached. L_{PAB} and B_{PAB} are the approximate phase angle bisector longitude and latitude at mid-date range (see Harris et al., 1984).

2732 Witt. The only previously published rotation period is by Behrend (2018web), 12.622 hours. New observations on ten nights 2024 Aug 10 - Sept. 12 provide a good fit to a period of 12.6244 ± 0.0003 hours, amplitude 0.55 ± 0.03 magnitudes. This value is in good agreement with Behrend (2018web).

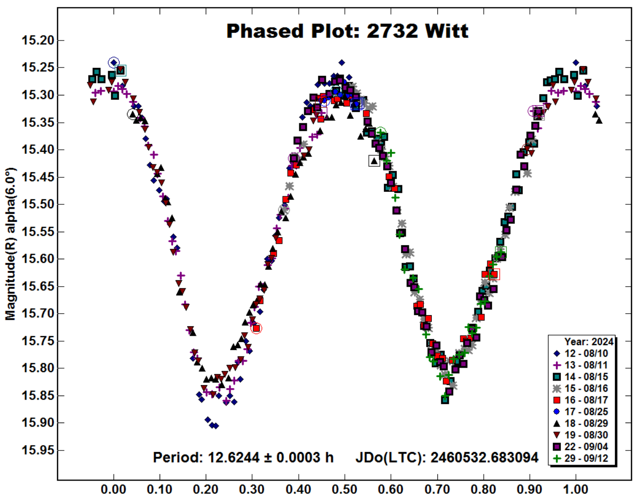

2836 Sobolev. The Lightcurve Database (Warner et. al, 2009) lists no previously published lightcurves. However, Durech et al. (2016) present a sidereal period of 4.754883 hours based on lightcurve inversion of multiyear sparse data from the Lowell photometric database. New dense lightcurves on four nights 2024 Sept. 1-28 provide a good fit to a synodic period of 4.7548 ± 0.0001 hours, amplitude 0.75 ± 0.05 magnitudes. This value is in excellent agreement with Durech et al. (2016).

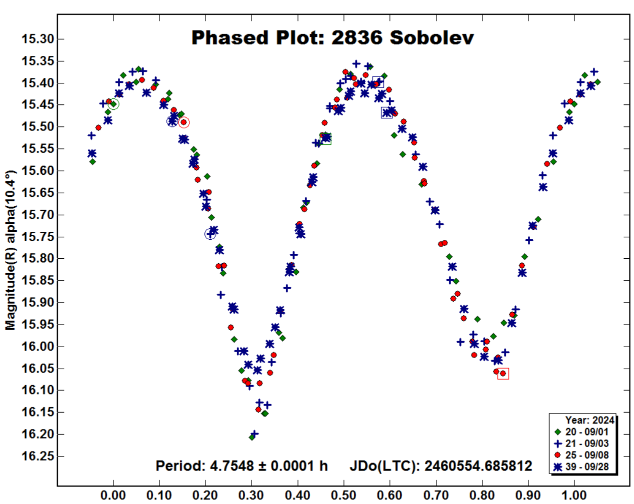

References

Behrend, R. (2005web, 2018web). Observatoire de Geneve web site. *http://obswww.unige.ch/~behrend/page_cou.html*

Durech, J.; Hanus, J.; Oszkiewicz, D.; Vanco, R. (2016). “Asteroid models from the Lowell photometric data base.” *Astron. Astrophys.* **587**, A98.

Harris, A.W.; Young, J.W.; Scaltriti, F.; Zappala, V. (1984). “Lightcurves and phase relations of the asteroids 82 Alkmene and 444 Gyptis.” *Icarus* **57**, 251-258.

Hawley, W. (2023). “The lightcurve and rotation period for 268 Adorea and (16735) 1996 JJ.” *Minor Planet Bull.* **50**, 247-248.

Holliday, B. (1995). “Lightcurve observations of minor planet 268 Adorea.” *Minor Planet Bull.* **22**, 33.

Stephens, R.D. (2006). “Asteroid lightcurve photometry from Santana and GMARS Observatories - winter and spring 2006.” *Minor Planet Bull.* **33**, 100-101.

Tedesco, E.F. (1979). PhD Dissertation, New Mexico State University.

Warner, B.D.; Harris, A.W.; Pravec, P. (2009). “The Asteroid Lightcurve Database.” *Icarus* **202**, 134-146. Updated 2023 October. *https://minplanobs.org/MPInfo/php/lcdb.php*

ASTEROID PHOTOMETRY: LIGHTCURVE RESULTS FOR SIX TARGETS

Milagros Colazo
Astronomical Observatory Institute,
Faculty of Physics, Adam Mickiewicz University,
ul. Słoneczna 36, 60-286 Poznań, POLAND
Grupo de Observadores de Rotaciones de Asteroides (GORA),
ARGENTINA
https://aoacm.com.ar/gora/index.php
milirita.colazovinovo@gmail.com

Raúl Melia
Observatorio de Raúl Melia Carlos Paz (GORA RMC)
Carlos Paz (Córdoba- ARGENTINA)

Néstor Suárez
Observatorio Antares (MPC X39)
Pilar (Buenos Aires- ARGENTINA)

Víctor Amelotti
Observatorio Astronómico Naos (GORA NAO)
Alta Gracia (Córdoba- ARGENTINA)

Ariel Stechina
Observatorio de Ariel Stechina 1 (GORA OAS)
Reconquista (Santa Fe- ARGENTINA)

Paolo Aldinucci
Osservatorio Astronomico di Orciatico (MPC D41)
Lajatico (Pisa-ITALIA)

Bruno Monteleone
Osservatorio Astronomico "La Macchina del Tempo" (MPC M24)
Ardore Marina (Reggio Calabria-ITALIA)

Mario Morales
Observatorio de Sencelles (MPC K14)
Sencelles (Mallorca-Islas Baleares-ESPAÑA)

Marcos Anzola
Observatorio Astronómico Vuelta por el Universo (GORA OMA)
Córdoba (Córdoba- ARGENTINA)

Aldo Wilberger
Observatorio Los Cabezones (MPC X12)
Santa Rosa (La Pampa- ARGENTINA)

Tiago Speranza
Observatorio Astronómico Municipal Reconquista (GORA OMR)
Reconquista (Santa Fe- ARGENTINA)

Francisco Santos
Observatorio Astronómico Giordano Bruno (MPC G05)
Piconcillo (Córdoba-ESPAÑA)

Damián Scotta
Observatorio de Damián Scotta 1 (GORA ODS)
San Carlos Centro (Santa Fe- ARGENTINA)

Giuseppe Ciancia
Specola "Giuseppe Pustorino 1" (GORA GC1)
Palizzi Marina (Reggio Calabria-ITALIA)

Carlos Colazo
Observatorio Astronómico El Gato Gris (MPC I19)
Tanti (Córdoba- ARGENTINA)

(Received: 2024 October 13 Revised: 2024 November 18)

Synodic rotation periods and amplitudes are reported for: 494 Virtus, 866 Fatme, 1075 Helina, 1279 Uganda, 1424 Sundmania, 1593 Fagnes, (5977) 1992 TH1, (58143) 1983 VD7.

The periods and amplitudes of asteroid lightcurves presented in this paper are the product of collaborative work by the GORA (Grupo de Observadores de Rotaciones de Asteroides) group. In all the studies, we have applied relative photometry assigning V magnitudes to the calibration stars.

The image acquisition was performed without filters and with exposure times of a few minutes. All images used were corrected using dark frames and, in some cases, bias and flat-field corrections were also used. Photometry measurements were performed using *FotoDif* software and for the analysis, we employed *Períodos* software (Mazzone, 2012).

Below, we present the results for each asteroid studied. The lightcurve figures contain the following information: the estimated period and period error and the estimated amplitude and amplitude error. In the reference boxes, the columns represent, respectively, the marker, observatory MPC code, or - failing that - the GORA internal code, session date, session offset, and several data points.

Targets were selected based on the following criteria: 1) those asteroids with magnitudes accessible to the equipment of all participants, 2) those with favorable observation conditions from Argentina or Spain or Italy, i.e. with negative or positive declinations δ, respectively, and 3) objects with few periods reported in the literature and/or with Lightcurve Database (LCDB) (Warner et al., 2009) quality codes (U) of less than 3.

In this work, we present measurements of periods corresponding to asteroids previously analyzed by our team. These lightcurves display improved results and are part of a new long-term project that we are initiating.

494 Virtus. It is a C-type asteroid, discovered in 1902 by M. Wolf (NASA, 2024). Several periods were measured for this asteroid with the following results: *P* = 4.9903 h (Behrend, 2008web), *P* = 5.570 h ± 0.003 h (Hamanowa and Hamanowa, 2009), and more recently *P* = 40.431 ± 0.004 h (Dose, 2022). We have determined a 40.47 ± 0.03 h period, which is consistent with the one proposed by Dose.

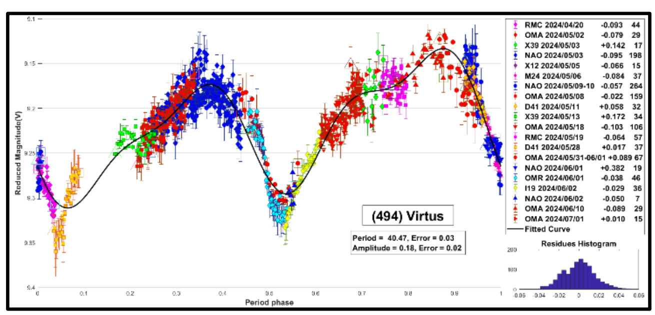

866 Fatme. It was discovered in 1917 by M. Wolf (NASA, 2024). Several periods were measured for this asteroid with the following results: *P* = 20.03 h ± 0.01 h (Stephens, 2002), *P* = 9.36 h ± 0.05 h (Behrend, 2012web), and *P* = 11.600 ± 0.001 h (Dose, 2021). The results we obtained, *P* = 22.798 ± 0.022 h with *Δm* = 0.24 ± 0.03 mag, are consistent with the longer period proposed by Stephens.

Number	Name	yy/ mm/dd- yy/ mm/dd	Phase	L_{PAB}	B_{PAB}	Period(h)	P.E.	Amp	A.E.	Grp
494	Virtus	24/04/20-24/07/01	*2.1,19.9	215	-1	40.47	0.03	0.18	0.02	MB-O
866	Fatme	24/07/02-24/08/05	*4.7,08.3	292	-4	22.798	0.022	0.24	0.03	MB-O
1075	Helina	24/05/28-24/07/14	5.0,16.9	238	8	44.75	0.05	0.62	0.04	EOS
1279	Uganda	24/05/18-24/07/03	16.7,30.5	216	-7	11.172	0.043	0.21	0.06	MB-I
1424	Sundmania	24/05/09-24/07/05	*3.5,16.2	237	4	93.3	0.2	0.44	0.02	MB-O
1593	Fagnes	24/05/25-24/07/13	10.3,29.1	247	12	25.310	0.015	0.45	0.02	MARS
5977	1992 TH1	24/06/30-24/07/11	12.2,08.0	302	9	42.5	0.2	0.63	0.03	MAR
58143	1983 VD7	24/07/07-24/08/06	*16.0,04.6	303	-18	79.1	0.2	0.57	0.03	MB-I

Table I. Observing circumstances and results. The phase angle is given for the first and last date. If preceded by an asterisk, the phase angle reached an extremum during the period. L_{PAB} and B_{PAB} are the approximate phase angle bisector longitude/latitude at mid-date range (see Harris et al., 1984). Grp is the asteroid family/group (Warner et al., 2009). MB-I: main-belt inner; MAR: 170 Maria; MB-O: main-belt outer; MARS: Mars-crosser; EOS: 221 Eos.

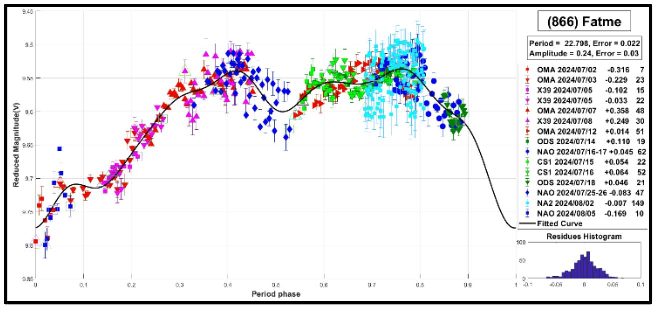

1075 Helina. It was discovered in 1926 by G. Neujmin (NASA, 2024). The more recent period published in the literature corresponds to P = 44.9 h (Martikainen et al., 2021). Our period P = 44.75 ± 0.05 h agrees with the one measured by Martikainen et al.

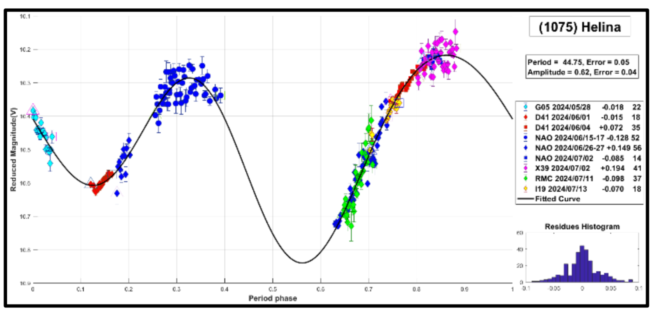

1279 Uganda. It was discovered in 1933 by C. Jackson (NASA, 2024). In the literature, we found only one period reported for this asteroid: P = 11.6 h (Binzel, 1987). Our study supports the aforementioned period and yielded the following data: P = 11.172 ± 0.043 h with Δm = 0.21 ± 0.06 mag. The previously reported period, derived from fragmentary lightcurves, may be subject to significant uncertainty, according to JPL.

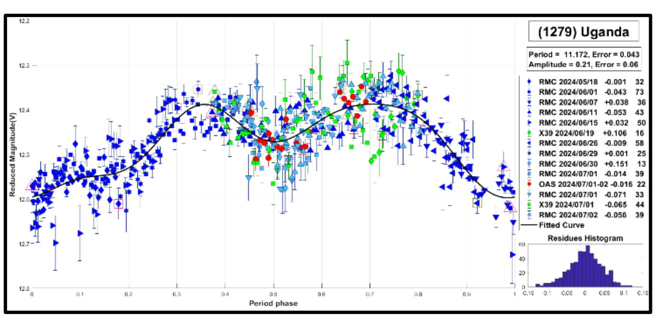

1424 Sundmania. It was discovered in 1937 by Y. Vaisala (NASA, 2024). The more recent period published in the literature corresponds to P = 93.73 h (Martikainen et al., 2021). The results we obtained are P = 93.3 ± 0.2 h and Δm = 0.44 ± 0.02 mag. Our period agrees well with the one measured by Martikainen et al.

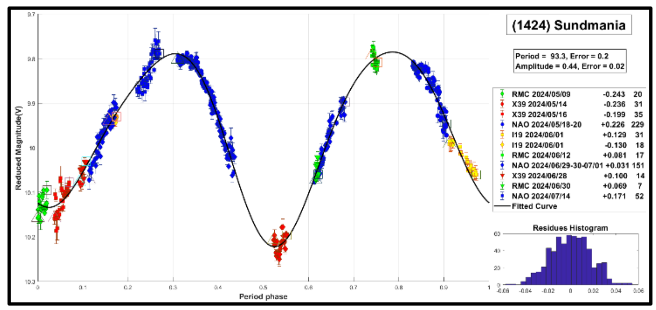

1593 Fagnes. It was discovered in 1951 by S. Arend (NASA, 2024). We found in the literature two rather different periods calculated for this object: P = 16.45 ± 0.03 h (Harris et al., 1992), and P = 25.25 h (Behrend, 2021web). The results we obtained are P = 25.310 ± 0.015 h. Our period well agrees with the one measured by Behrend.

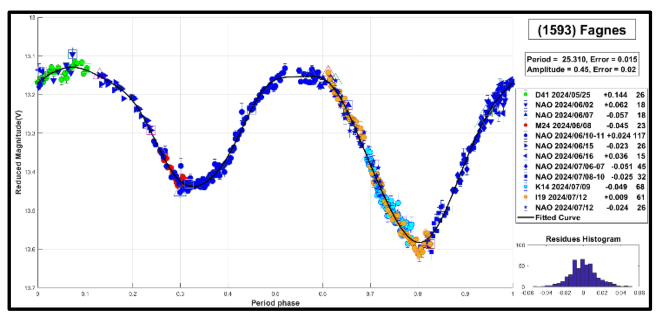

(5977) 1992 TH1. It was discovered in 1992 by H.E. Holt (NASA, 2024). Interestingly, we couldn't find a reported period for this object in the literature. According to our observations and after a thorough analysis, we propose a period of P = 42.5 ± 0.2 h and Δm = 0.63 ± 0.03 mag.

Observatory	Telescope	Camera
D41 Osservatorio Astronomico di Orciatico	SCT (D=355mm; f=7.4)	CCD SBIG ST10XME
G05 Obs.Astr.Giordano Bruno	SCT (D=203mm; f=6.3)	CCD Atik 420 m
I19 Obs.Astr.El Gato Gris	SCT (D=355mm; f=10.6)	CCD SBIG STF-8300M
K14 Obs.Astr.de Sencelles	Newtonian (D=250mm; f=4.0)	CCD SBIG ST-7XME
M24 Oss.Astr.La Macchina del Tempo	RCT (D250mm; f=8.0)	CMOS ZWO ASI 1600MM
X12 Obs.Astr.Los Cabezones	Newtonian (D=200mm; f=5.0)	CMOS QHY 174M
X39 Obs.Astr.Antares	Newtonian (D=250mm; f=4.72)	CCD QHY9 Mono
NAO Obs.Astr.Naos	Newtonian (D=250mm; f=4.0)	CMOS QHY 163M
OAS Obs.Astr.de Ariel Stechina 1	Newtonian (D=254mm; f=4.7)	CCD SBIG STF-402
OMA Obs.Astr.Vuelta por el Universo	Newtonian (D=150mm; f=5.0)	CMOS POA Neptune-M
OMR Obs.Astr.Municipal Reconquista	Newtonian (D=254mm; f=4.0)	Player One Ceres-M
RMC Obs.Astr.de Raúl Melia Carlos Paz	Newtonian (D=254mm; f=4.7)	CMOS QHY 174M

Table II. List of observatories and equipment.

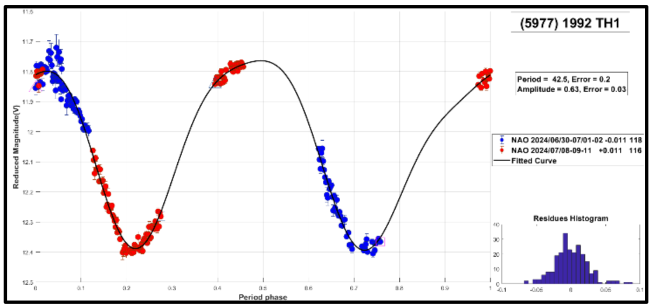

(58143) 1983 VD7. It was discovered in 1983 by Cavriana (NASA, 2024). For this asteroid, we could not find published periods in the literature either. In this work, we propose a period of $P = 79.1 \pm 0.2$ h with $\Delta m = 0.57 \pm 0.03$ mag.

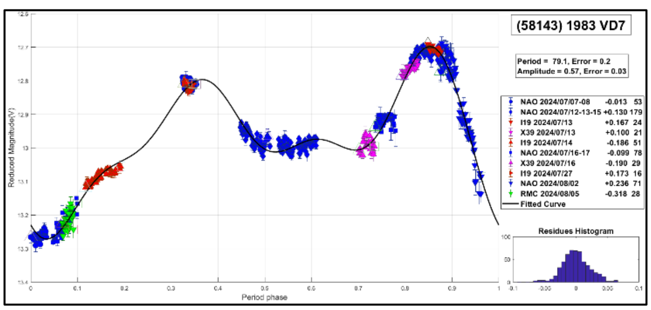

Acknowledgements

We want to thank Julio Castellano as we used his *FotoDif* program for preliminary analyses, Fernando Mazzone for his *Períodos* program, which was used in final analyses, and Matías Martini for his CalculadorMDE_v0.2 used for generating ephemerides used in the planning stage of the observations. This research has made use of the Small Bodies Data Ferret (*https://sbnapps.psi.edu/ferret/*), supported by the NASA Planetary System. This research has made use of data and/or services provided by the International Astronomical Union's Minor Planet Center.

References

Behrend, R. (2008web, 2012web, 2021web). Observatoire de Geneve website. *http://obswww.unige.ch/~behrend/page_cou.html*

Binzel, R.P. (1987). “A photoelectric survey of 130 asteroids.” *Icarus* **72**, 135-208.

Dose, E.V. (2021). “Lightcurves of Eighteen Asteroids.” *Minor Planet Bulletin* **48**, 125-132.

Dose, E.V. (2022). “Lightcurves of Seventeen Asteroids.” *Minor Planet Bulletin* **49**, 141-148.

Hamanowa, H., Hamanowa, H. (2009). “Lightcurves of 494 Virtus, 556 Phyllis, 624 Hektor 657 Gunlod, 111 Reinmuthia, 1188 Gothlandia, and 1376 Michelle.” *Minor Planet Bulletin* **36**, 87-88.

Harris, A.W.; Young, J.W.; Scaltriti, F.; Zappala, V. (1984). “Lightcurves and phase relations of the asteroids 82 Alkmene and 444 Gyptis.” *Icarus* **57**, 251-258.

Harris, A.W.; Young, J.W.; Dockweiler, T.; Gibson, J.; Poutanen, Á.; Bowell, E. (1992). “Asteroid lightcurve observations from 1981.” *Icarus* **95**, 115-147.

Martikainen, J.; Muinonen, K.; Penttilä, A.; Cellino, A.; Wang, X.B. (2021). “Asteroid absolute magnitudes and phase curve parameters from Gaia photometry.” *Astronomy & Astrophysics* **649**, A98.

Mazzone, F.D. (2012). Períodos software, version 1.0. *http://www.astrosurf.com/salvador/Programas.html*

NASA Planetary Data System Small Bodies Data Ferret (2024). *https://sbnapps.psi.edu/ferret/*

Stephens, R.D. (2002). “Photometry of 866 Fatme, 894 Erda, 1108 Demeter, and 3443 Letsungdao.” *The Minor Planet Bulletin* **29**, 2-3.

Warner, B.D.; Harris, A.W.; Pravec, P. (2009). “The Asteroid Lightcurve Database.” *Icarus* **202**, 134-146. *http://www.minorplanet.info/lightcurvedatabase.html*

PHOTOMETRIC OBSERVATIONS AND ANALYSIS OF SEVEN ASTEROIDS

Charles Galdies
Znith Observatory
31, Armonie, E. Bradford Street,
Naxxar NXR 2217, MALTA
charles.galdies@um.edu.mt

Stephen M. Brincat
Flarestar Observatory (MPC: 171)
Fl.5 George Tayar Street,
San Gwann SGN 3160, MALTA

Marek Bucek
Luckystar Observatory (MPC: M55)
Dr. Lučanského 547, Važec, 032 61, SLOVAKIA

(Received: 2024 September 24)

We report the results of our photometric observations of seven main-belt asteroids from three observatories in Malta, and Slovakia. We obtained the lightcurves for the following asteroids, which can facilitate future analysis at different oppositions: (4798) Mercator; (4958) Wellnitz; (13042) 1990 QE; (15127) 2000 EN45; (16591) 1999 SY17; (28746) 2000 GB148; and (108522) 2001 LQ.

We report on photometric observations of seven main-belt asteroids from two observatories located in Malta, and one at Važec, Slovakia. Through these observatories listed in Table I, we have observed the following asteroids: (4798) Mercator; (4958) Wellnitz; (13042) 1990 QE; (15127) 2000 EN45; (16591) 1999 SY17; (28746) 2000 GB148; and (108522) 2001 LQ. We employed a clear filter (unfiltered) with SR (Sloan R) zero point for all other images and calibrated all of our images using dark and flat-field subtraction frames.

We remotely controlled all our equipment over the internet or from a nearby location for each telescope. We used *Sequence Generator Pro* (Binary Star Software) for image acquisition by all Maltese Observatories. Luckystar Observatory used the *NINA* image acquisition software (Berg, 2023). We used *MPO Canopus* software (Warner, 2017) for our image analysis, to obtain differential aperture photometry and to construct light curves. Table I displays the details of the instrumentation and Observation Runs for each target. We selected near-solar color comparison stars using the Comparison Star Selector (CSS) feature of *MPO Canopus*. We based all brightness measurements on the Asteroid Terrestrial-impact Last Alert System (ATLAS) catalogue (Tonry et al., 2018).

Observatory/ Country	Scope and Type	Camera	Observed Asteroids (#Nights)
Flarestar Obs. (MPC: 171)/ MALTA	0.25-m SCT	Moravian G2-1600	#16591 (4) #28746 (4) #108522 (4)
Luckystar Obs. (MPC: M55)/ SLOVAKIA	0.25-m SCT	Atik 460EX	#4958 (8) #13042 (2) #15127 (7)
Znith Astronomy Obs./ MALTA	0.2-m SCT	Moravian G2-1600	#4798 (4)

Table I – Instrumentation and Observation Runs. SCT: Schmidt-Cassegrain Telescope.

(4798) Mercator is a main-belt asteroid discovered on 1989 September 26 by E.W. Elst at La Silla Observatory (Chile). The estimated diameter of Mercator is 5.02 ± 0.138 km (Masiero et al., 2011) and has an absolute magnitude *H* of 13.64 and orbits with a semi-major axis of 2.197 AU with an eccentricity of 0.110. Mercator takes 3.26 years to complete an orbit around the sun (JPL, 2024).

This asteroid was observed from Znith Observatory on 4 nights, namely on 2024 April 05 and May 02, 05 and 12. Our results yielded a synodic period of 3.453 ± 0.001 h with an amplitude of 0.15 ± 0.05 mag. The LCDB database does not show any published period for (4798) Mercator.

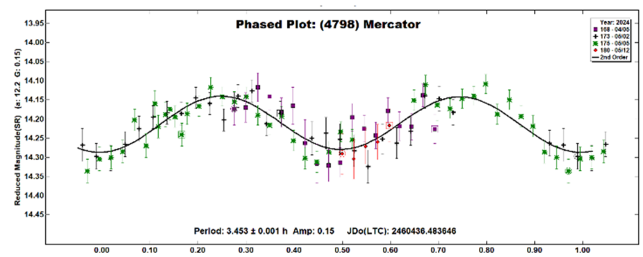

(4958) Wellnitz is a main-belt asteroid that was discovered on July 13, 1991 by H.E. Holt at Palomar (USA) (JPL, 2024). Its estimated diameter is 16.358 ± 0.244 km (Masiero et al., 2014). It orbits the sun with a semi-major axis of 3.0145 AU and has an eccentricity of 0.077 and an absolute magnitude H of 11.76. The asteroid completes one orbit around the sun every 5.23 years (JPL, 2024).

We have observed asteroid Wellnitz from Luckystar Observatory over eight nights, namely on 2023 Sep 20 and Oct 4, 5, 10, 11, 15, 16 and 17. Based on these observations, we determined the synodic period to be 5.118 ± 0.001 hours, with an amplitude of 0.11 ± 0.04 mag. The LCDB database does not show any published period for (4958) Wellnitz.

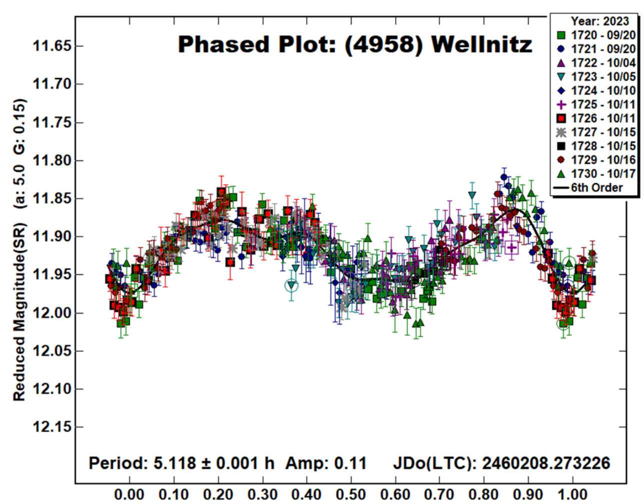

(13042) 1990 QE is also a main-belt asteroid. This asteroid was first discovered on 1990 Aug 18 by E.F. Helin at Palomar (USA). The asteroid has an estimated diameter of 7.367 ± 0.276 km (Masiero et al., 2012), an absolute magnitude *H* of 13.95 and orbits the sun at a semi-major axis of 2.567 AU. Its orbit has an eccentricity of 0.240, and orbits the sun every 4.11 years (JPL, 2024).

(13042) 1990 QE was observed from Luckystar Observatory over 2 nights on 2023 September 10 and 12 from which we derived the synodic period to be 3.32 ± 0.01 h with an amplitude of 0.39 ± 0.04 mag. The LCDB database does not show any published period for (13042) 1990 QE.

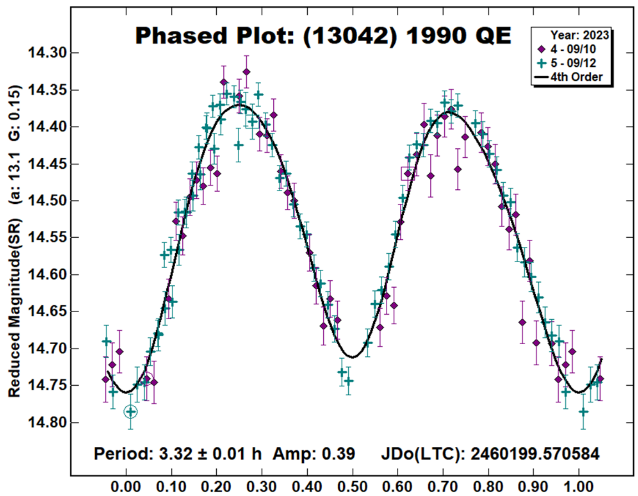

(15127) 2000 EN45 is main-belt asteroid that was discovered on March 09, 2000 by LINEAR. It has an estimated diameter of 19.323 ± 0.204 km diameter, based on *H* of 12.29. It orbits the sun with a semi-major axis of 2.999 AU with an eccentricity of 0.28 and orbital period of 5.19 years (JPL, 2024).

Luckystar Observatory observed this target for a period of 6 nights starting from 2023 October 17, 18, 22 and November 1, 4, and 6. Our results of (15127 2000 EN45 show a derived synodic period of 12.8512 ± 0.0137 h with an amplitude of 0.26 ± 0.04 mag. The LCDB database does not show any published period for (15127) 2000 EN45.

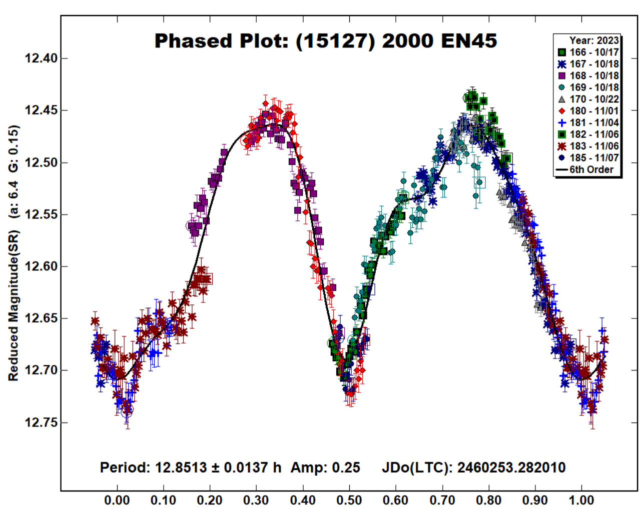

(16591) 1999 SY17 is a main-belt asteroid and was discovered on 1992 September 30 by H.E. Holt at Palomar Observatory, USA (JPL, 2024). The absolute magnitude *H* is 14.43. The semi-major axis of this asteroid is 2.29 AU and its orbit has an eccentricity of 0.281. It orbits the sun every 3.47 years (JPL, 2024).

(16591) 1992 SY17 was observed on 4 nights from Flarestar Observatory on 2023 July 13, 18, 19 and 22. Our data shows the rotation period to be 2.737 ± 0.0003 h, with an amplitude of 0.23 ± 0.10 mag. Warner et al. (2009) reports a value of 2.737 h based on an incomplete phase plot produced in 2013 by Pál et al. (2020).

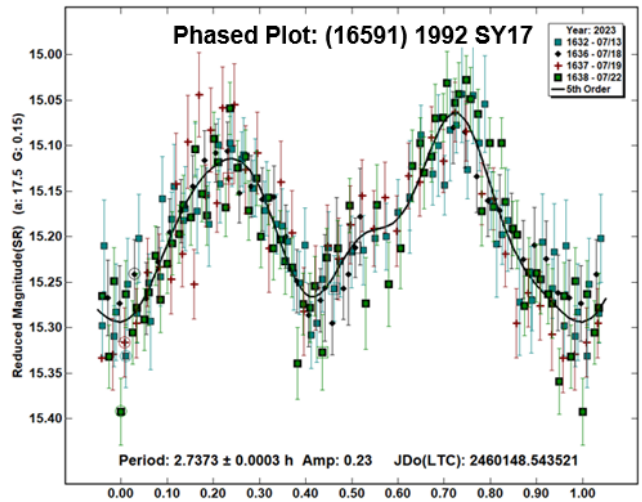

(28746) 2000 GB148 is another main-belt asteroid that was discovered by LINEAR on 2000 Apr 05 at Socorro. Its absolute magnitude *H* of 15.82. This minor planet orbits the sun with a semi-major axis of 2.373 AU and its orbit has an eccentricity of 0.217, and a period of 3.66 years (JPL, 2024). Observations from Flarestar Observatory were acquired over 4 nights on 2023 August 09, 10, 11 and 13. We derived a synodic period of 6.977 ± 0.008 h with an amplitude of 0.32 ± 0.1 mag. The LCDB database does not show any published period for (28746) 2000 GB148.

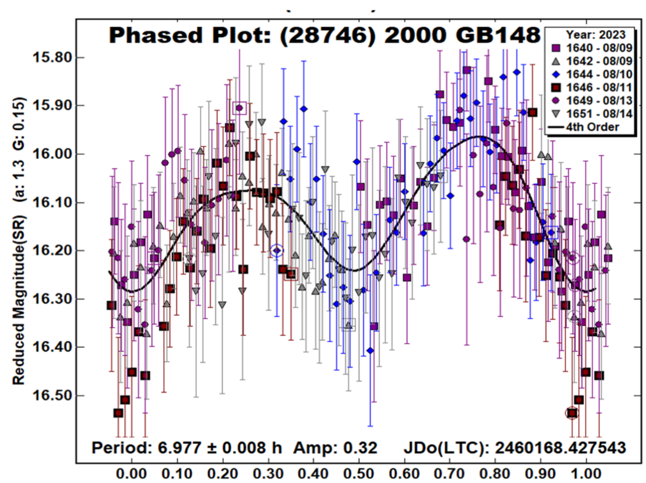

(108522) 2001 LQ is a Mars-crossing asteroid that was discovered on 2001 June 14, by LEONOS at Anderson Mesa (JPL, 2024). The estimated diameter of 6.963 ± 1.95 km (Nugent et al., 2016). The asteroid orbits the sun with a semi-major axis of 2.597 AU and has an eccentricity of 0.389. It has an absolute magnitude *H* of 13.96 and completes one orbit around the sun every 4.18 years (JPL, 2024).

The asteroid (108522) was observed by Flarestar Observatory on the nights of 2023 November 14, 16, 20 and 30. Based on these observations, the synodic period was determined to be 8.963 ± 0.001 hours, with an amplitude of 1.04 ± 0.10 mag. Warner et al., (2009) revised its orbital period as 8.359 h based on an incomplete phase plot (P; U quality 2) produced in 2015 (Waszczak et al., 2015).

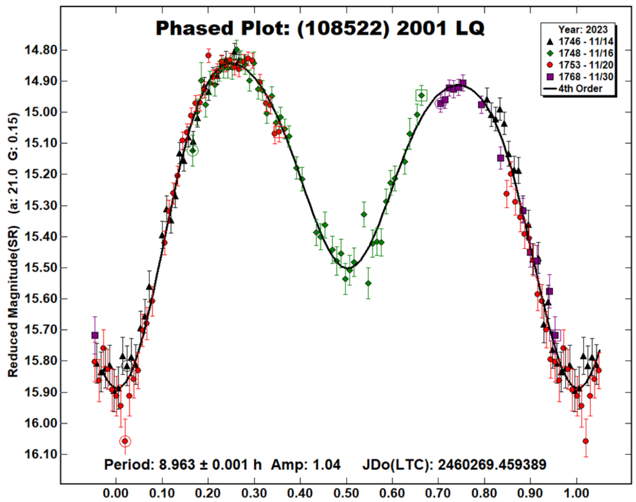

Acknowledgements

We would like to thank Brian Warner for his work in the development of *MPO Canopus* and for his efforts in maintaining the CALL website (Warner, 2016; 2021). This research has made use of the JPL's Small-Body Database (JPL, 2024).

References

Berg, S. (2023). Nightime Imaging 'N' Astronomy (NINA) website. *https://nighttime-imaging.eu/*. Last accessed 2024 September 4.

Harris, A.W.; Young, J.W.; Scaltriti, F.; Zappala, V. (1984). "Lightcurves and phase relations of the asteroids 82 Alkmene and 444 Gyptis." *Icarus* **57**, 251-258.

JPL, (2024). Small-Body Database Browser - JPL Solar System Dynamics web site. *http://ssd.jpl.nasa.gov/sbdb.cgi*. Last accessed: 2024 January 6.

Masiero, J.R.; Mainzer, A.K.; Grav, T.; Bauer, J.M.; Cutri, R.M.; Dailey, J.; Eisenhardt, P.R.M..; McMillan, R.S.; Spahr, T.B.; Skrutskie, M.F.; Tholen, D.; Walker, R.G.; Wright, E.-L.; DeBaun, E.; Elsbury, D.; Gautier, T.; Gomillion, S.; Wilkins, A. (2011). "Main Belt Asteroids with WISE/NEOWISE. I. Preliminary Albedos and Diameters." *The Astrophysical Journal* **741(68)**, 20pp. *https://iopscience.iop.org/article/10.1088/0004-637X/741/2/68/pdf*

Masiero, J.R.; Grav, T.; Mainzer, A.K.; Nugent, C.R.; Bauer, J.M.; Stevenson, R.; Sonnett, S. (2014). "Main-Belt Asteroids With WISE/NEOWISE: Near-Infrared Albedos." *The Astrophysical Journal* **791(2)**, 121.

Nugent, C.R.; Mainzer, A.; Bauer, J.; Cutri, R.M.; Kramer, E.A.; Grav, T.; Masiero, J.; Sonnett, S.; Wright, E. L. (2016). "NEOWISE Reactivation Mission Year Two: Asteroid Diameters and Albedos." *The Astronomical Journal* **152(63)**, 12pp. DOI: 10.3847/0004-6256/152/3/63.

Pál, A.; Szakáts, R.; Kiss, C.; Bódi, A.; Bognár, Z.; Kalup, C.; Kiss, L.L.; Marton, G.; Molnár, L.; Plachy, E.; Sárneczky, K.; Szabó, G.M.; Szabó, R. (2020). "Solar System Objects Observed with TESS - First Data Release: Bright Main-belt and Trojan Asteroids from the Southern Survey." *Ap. J. Suppl Ser*. **247**, id. 26-34.

Tonry, J.L.; Denneau, L.; Flewelling, H.; Heinze, A.N.; Onken, C.A.; Smartt, S.J.; Stalder, B.; Weiland, H.J.; Wolf, C. (2018). "The ATLAS All-Sky Stellar Reference Catalog." *Astrophys. J.* **867**, A105.

Warner, B.D.; Harris, A.W.; Pravec, P. (2009). "The Asteroid Lightcurve Database." *Icarus* **202**, 134-146. Updated 2024 June 2. *http://www.minorplanet.info/lightcurvedatabase.html*

Warner, B.D. (2016). Collaborative Asteroid Lightcurve Link website. *http://www.minorplanet.info/call.html*. Last accessed: 2024 September 4.

Warner, B.D. (2017). MPO Software, MPO Canopus version. 10.7.10.0. Bdw Publishing. *http://www.minorplanetobserver.com/*

Warner, B.D. (2021). Asteroid Lightcurve Photometry Database (ALCDEF) at *https://minplanobs.org/alcdef/index.php*

Waszczak, A.; Chang, C.-K.; Ofeck, E.O.; Laher, F.; Masci, F.; Levitan, D.; Surace, J.; Cheng, Y-C.; Ip, W-H.; Kinoshita, D.; Helou, G.; Prince, T.A.; Kulkarni, S. (2015). "Asteroid light curves from the Palomar transient factory survey: rotation periods and phase functions from sparse photometry." *The Astonomical Journal* **150(3)**, 75pp. *https://dx.doi.org/10.1088/0004-6256/150/3/75*

Number	Name	yyyy mm/dd	Phase	L_{PAB}	B_{PAB}	Period(h)	P.E.	Amp	A.E.	Grp
4798	Mercator	2024 04/05-05/12	12.3,10.3	216.3	4.6	3.453	0.001	0.15	0.05	9104*
4958	Wellnitz	2023 09/20-10/17	5.0, 8.3	4.3	10.4	5.118	0.001	0.11	0.04	606
13042	1990 QE	2023 09/10-09/12	13.1,12.9	355.4	18.1	3.32	0.01	0.39	0.04	2007
15127	2000 EN45	2023 10/17-11/06	6.4,13.7	21.5	12.0	12.858	0.002	0.26	0.04	9106*
16591	1992 SY17	2023 07/13-07/22	17.4,14.3	308.1	13.1	2.737	0.0003	0.23	0.1	9103
28746	2000 GB148	2023 08/09-08/13	1.6, 3.9	315.1	1.5	6.967	0.0099	0.34	0.3	2004
108522	2001 LQ	2023 11/14-11/30	21.4,16.3	62.9	-24.6	8.963	0.001	1.04	0.1	9103

Table II. Observing circumstances and results. The phase angle is given for the first and last date. If preceded by an asterisk, the phase angle reached an extrema during the period. L_{PAB} and B_{PAB} are the approximate phase angle bisector longitude/latitude at mid-date range (see Harris et al., 1984). Grp is the asteroid family/group (Warner et al., 2009).

LIGHTCURVES OF EIGHT ASTEROIDS

Eric V. Dose
3167 San Mateo Blvd NE #329
Albuquerque, NM 87110
mp@ericdose.com

(Received: 2024 October 14)

We present lightcurves and synodic rotation periods for eight asteroids including the family parent asteroid (1128) Astrid.

We present asteroid lightcurves obtained via the workflow process described by Dose (2020) and later improved (Dose, 2021). This workflow applies to each image an ensemble of typically 25-80 nearby comparison ("comp") stars selected from the ATLAS refcat2 catalog (Tonry, 2018). This abundance of comp stars and our custom diagnostic plots allow for rapid identification and removal of outlier, variable, and poorly measured comp stars.

The product of this custom workflow is one night's time series of absolute Sloan r' (SR) magnitudes for one target asteroid. These absolute magnitudes are corrected for instrument transforms, sky extinction, and image-to-image ("cirrus") fluctuations, and thus they represent absolute magnitudes at the top of earth's atmosphere. These magnitudes are imported directly into *MPO Canopus* software (Warner, 2021) where they are adjusted for distance and phase-angle dependence, then fit by Fourier analysis including identifying any aliases, and plotted.

Phase-angle corrections are made by applying a *H-G* model and finding the *G* value that minimizes best-fit RMS error across all nights' data for that apparition. When we cannot estimate *G*, usually due to a narrow range of phase angles, we apply the Minor Planet Center's default value of 0.15. No nightly zero-point adjustments (Delta Comps in *MPO Canopus*) were made to any session, other than by estimating *G*.

Lightcurve Results

Eight asteroids were observed from New Mexico Skies observatory at 2210 meters elevation in southern New Mexico. Images were acquired with: a 0.50-m PlaneWave OTA on a PlaneWave L-500 mount and equatorial wedge, and a SBIG AC4040M CMOS camera cooled to -15°C and fitted with a Schott GG495 light yellow filter.

This equipment was operated remotely via *ACP* software (DC-3 Dreams), running one-night plan files generated by python scripts (Dose, 2020). Exposure times targeted 2-5 millimagnitudes uncertainty in asteroid instrumental magnitude, subject to a minimum exposure of 90 seconds to ensure suitable comp-star photometry, and to a maximum of 480 seconds.

FITS images were calibrated using temperature-matched, exposure-matched, median-averaged dark images and recent flat images of a flux-adjustable light panel. Calibrated images were plate-solved by *TheSkyX* (Software Bisque), and target asteroids were identified in *Astrometrica* (Herbert Raab). All photometric images were visually inspected; the author excluded images with inadequate tracking or seeing quality, excessive interference by cloud or moon, or having stars, satellite tracks, cosmic ray artifacts, residual image artifacts, or other apparent light sources within 12 arcseconds of the target asteroid's signal centroid. Images passing these screens were submitted to the workflow.

The GG495 light-yellow filter used here requires only modest first-order transforms to yield magnitudes in the standard Sloan r' (SR) passband. In our hands, using this filter (rather than a clear filter or no filter) improves transform linearity and night-to-night magnitude reproducibility to a degree outweighing the minor loss of signal-to-noise ratio caused by ~15% loss of measured flux.

Our workflow employs as comp stars all ATLAS refcat2 entries with: distance of at least 15 arcseconds from image boundaries and from other catalogued flux sources, no catalog VARIABLE flag, SR magnitude within [-2, +1] of the target asteroid's SR magnitude on that night (except that very faint asteroids used comp stars with magnitudes in the range 14 to 16), Sloan r'-i' color value within [0.10, 0.34], and absence of variability as seen in session plots of each comp star's instrumental magnitude vs time.

In this report, "period" denotes an asteroid's synodic rotation period, and "mmag" denotes millimagnitudes (0.001 magnitude). In the lightcurves below, *MPO Canopus* v10 shows "SR" for both Pan-STARRS and Sloan r' values.

<u>1128 Astrid</u>. This parent asteroid of the Astrid family was found to have a synodic rotation period of 10.237 ± 0.002 h, in agreement with most (10.228 h, Behrend, 2005web; 10.2 h, Behrend, 2010web; 10.229 h, Waszczak et al., 2015; 10.2340 h, Ďurech et al., 2020; 10.25 h, Polakis, 2021) but not all (14.552 h, Ditteon et al., 2018) previous reports. We find a bimodal lightcurve shape. Our Fourier fit RMS error is 9 mmag, and a H-G model G value of 0.25 gave a markedly improved fit vs the MPC default value of 0.15.

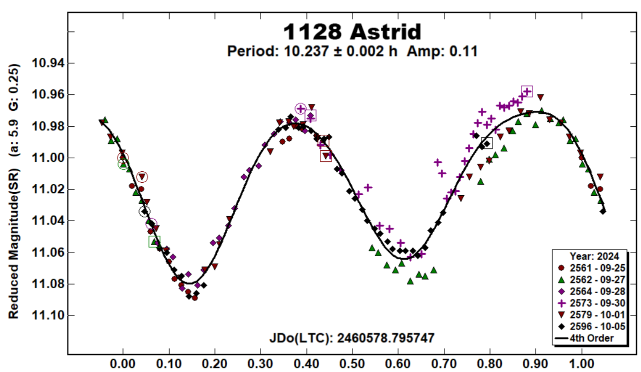

The period spectrum displays aliases at multiples of one-half the bimodal period, but the 10.237 h period estimate on a bimodal basis appears secure.

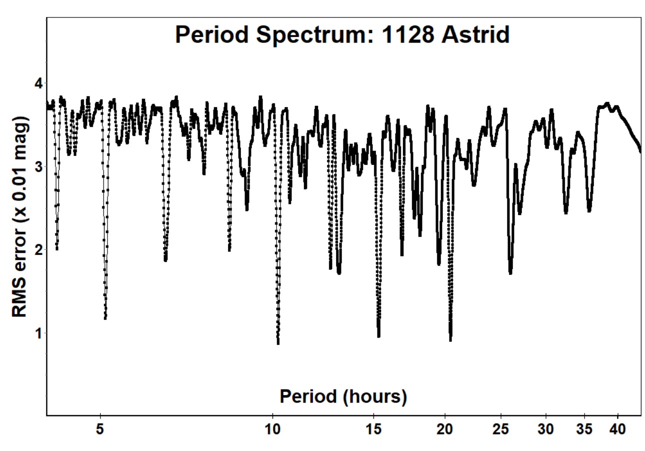

Number	Name	yyyy mm/dd	Phase	L_{PAB}	B_{PAB}	Period(h)	P.E.	Amp	A.E.	Grp
1128	Astrid	2024 09/25-10/05	6.1,1.8	16	-1	10.237	0.002	0.11	0.02	AST
1752	van Herk	2024 09/25-10/13	*10.6, 2.9	17	4	88.466	0.024	0.51	0.04	FLO
1776	Kuiper	2024 05/03-07/31	*8.6,17.8	244	11	103.375	0.055	0.09	0.03	MB-O
1808	Bellerophon	2024 10/04-10/07	15.4,14.2	41	1	4.147	0.002	0.16	0.02	MB-O
2984	Fedynskij	2024 05/28-07/12	*2.3,15.7	247	6	8.140	0.001	0.42	0.04	MB-O
3831	Pettengill	2024 09/26-10/08	26.0,28.8	326	-1	5.431	0.001	0.77	0.05	FLO
4339	Almamater`	2024 10/02-10/14	10.2, 3.3	23	3	109.074	0.084	0.30	0.03	MB-I
6453	1991 NY	2024 09/28-09/30	10.6, 9.4	22	0	2.872	0.002	0.21	0.03	MB-I

Table I. Observing circumstances and results. The phase angle is given for the first and last date. If preceded by an asterisk, the phase angle reached an extrema during the period. L_{PAB} and B_{PAB} are the approximate phase angle bisector longitude/latitude at mid-date range (see Harris et al., 1984). Grp is the asteroid family/group (Warner et al., 2009).

1752 van Herk. From 18 nights' observations of this Flora-family asteroid, we estimate the rotation period to be 88.466 ± 0.024 h, in agreement with one known survey report (88.45 h, Ďurech et al., 2020). Using a G value of 0.28 rather than the MPC default of 0.15 markedly decreased the Fourier fit RMS error, which is 15 mmag.

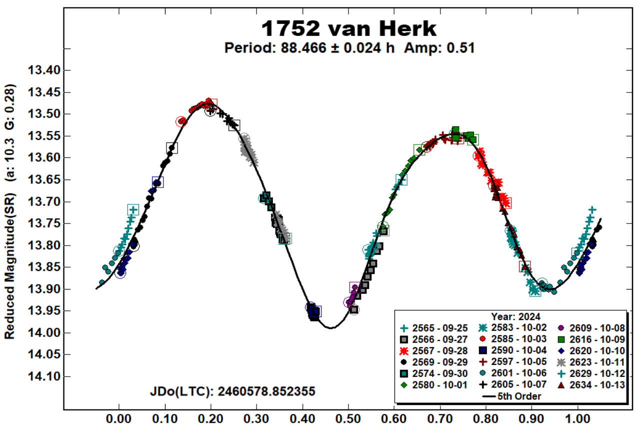

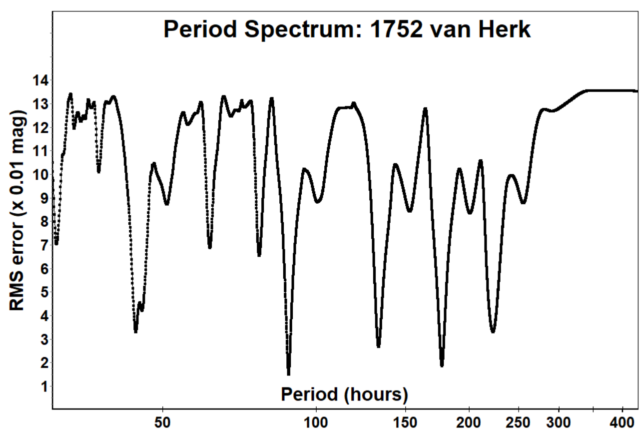

1776 Kuiper. For this bright outer main-belt asteroid, we estimate a period of 103.375 ± 0.055 h from 18 nights of data taken over a span of 20 periods. We found no previous reports of period or lightcurve for this asteroid. The amplitude is modest, and the lightcurve shows significant within-night magnitude trending, consistent with precession ("tumbling"). Our RMS error of 14 mmag includes effects of precession, and a G-value of 0.10 improved the fit.

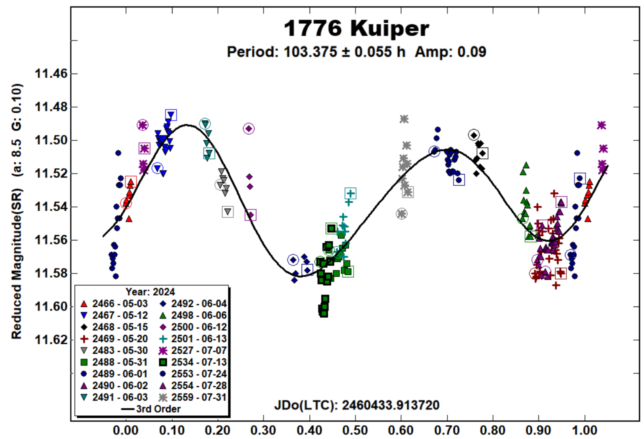

In the period spectrum, precession effects increase the RMS error of the main signals, but the major signals do lie at 0.5, 1, and 1.5 times our proposed period.

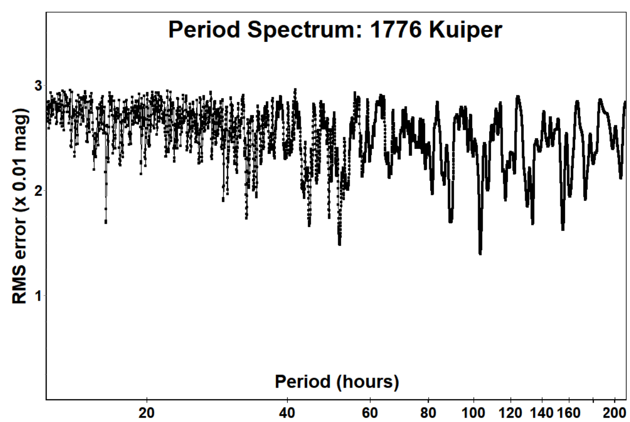

1808 Bellerophon. For this outer main-belt asteroid, we find a period of 4.147 ± 0.002 h, consistent with an early estimate (4 ± 1 h, Harris, 1983) but differing from one known survey result (3.820 h, Waszczak et al., 2015). As the small phase-angle range of our observations precludes G-value estimation, we have applied the MPC default value of 0.15. Our Fourier fit RMS error is 7 mmag.

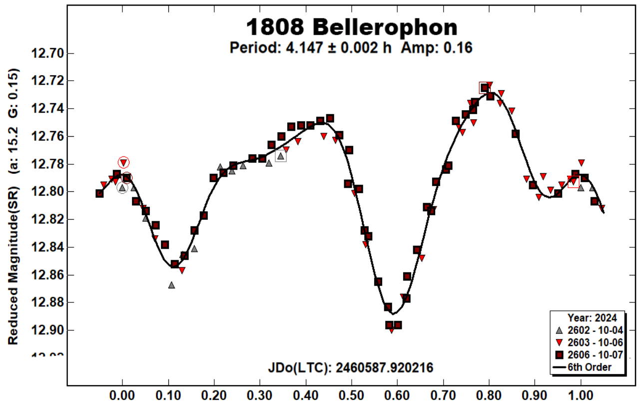

The period spectrum supports our new estimate. No clear signals appear at previous estimates of 3.82 h and 4 h. The 3.82 h estimate is an alias of our result by 1 rotation per day.

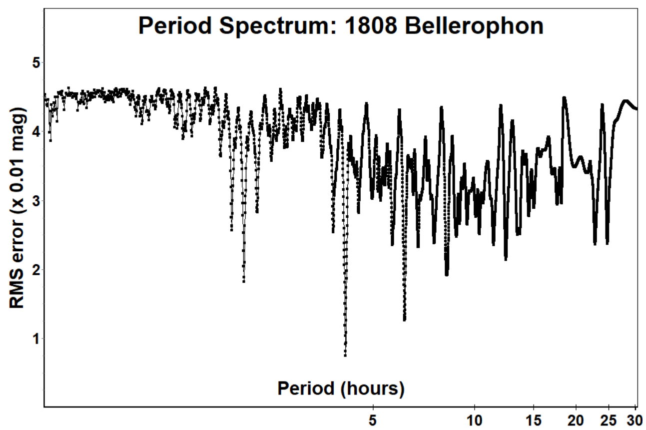

2984 Fedynskij. We find a rotation period of 8.140 ± 0.001 h for this outer main-belt asteroid, in close agreement with one previous survey result of 8.14041 h (Ďurech et al., 2020). The substantial amplitude of 0.42 magnitudes and a persistent difference between the shapes of the bimodal halves persuade us to interpret the lightcurve as bimodal. Our Fourier fit RMS error is 21 mmag.

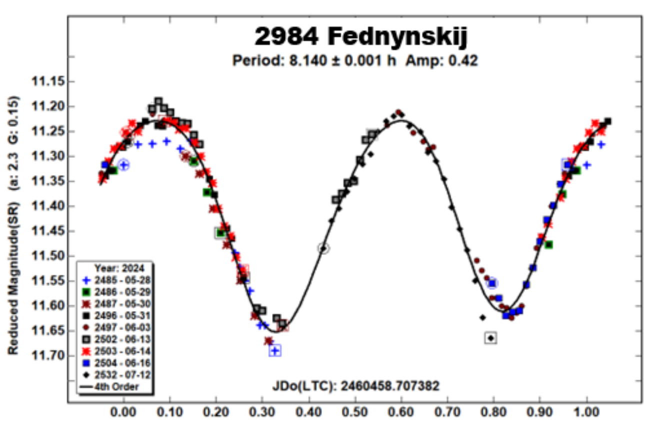

The period spectrum displays numerous alias signals, but all major signals lie at multiples of ½ our proposed period, as expected for a bimodal lightcurve with similar halves.

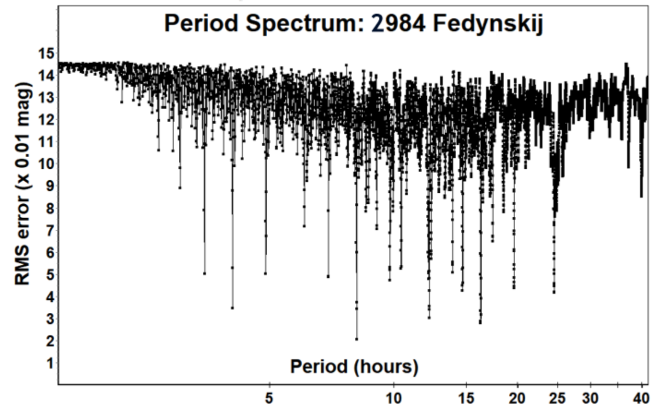

3831 Pettengill. For this Flora-family asteroid, our period estimate of 5.4310 ± 0.0005 h confirms the majority of previous period reports (5.432161 h, Ďurech et al., 2020; 5.431 h, Erasmus et al., 2020; 5.43141 h, Pál et al., 2020) but differs from one other (4.78 h, Behrend, 2011web). The bimodal lightcurve's halves appear as each others' reverse in time. Given the narrow range of phase angles, we adopt the MPC default G value of 0.15, and our fit RMS error is 15 mmag.

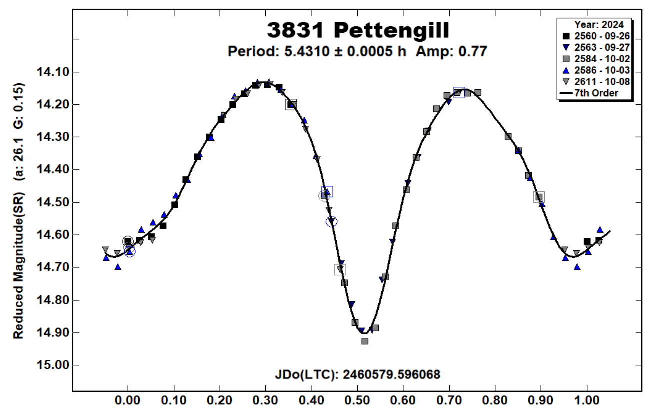

The period spectrum favors our period estimate. Very many signals appear at alias values and at multiples of ½ our period estimate, but the observations' high signal-to-noise ratio might distract from the fact that our estimate's fit RMS error is one-half that of the next best period solution (which itself lies at twice our estimate).

The previously reported estimate of 4.78 h does not appear as a major signal, and we cannot explain it as an alias or simple fractional multiple of the emerging consensus estimate.

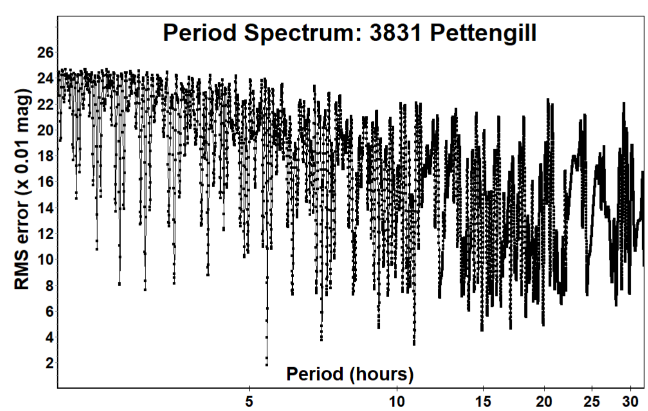

4339 Almamater. We observed this inner main-belt asteroid over 13 consecutive nights (about 3 period durations), yielding a rotation period estimate of 109.074 ± 0.084 h, which differs from the sole known report (30.84 h, Vander Haagen, 2012). The lightcurve is bimodal; the halves are similar except that they differ in minimum brightness. Fourier fit was optimized near G of 0.28, and our RMS error is 12 mmag.

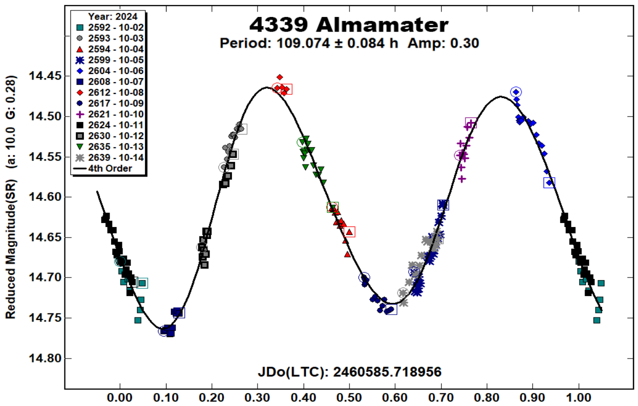

Our period spectrum is dominated by the first four multiples of ½ period, as expected for a bimodal lightcurve with similar halves. No major signal appears near the previously reported estimate of 30.84 h.

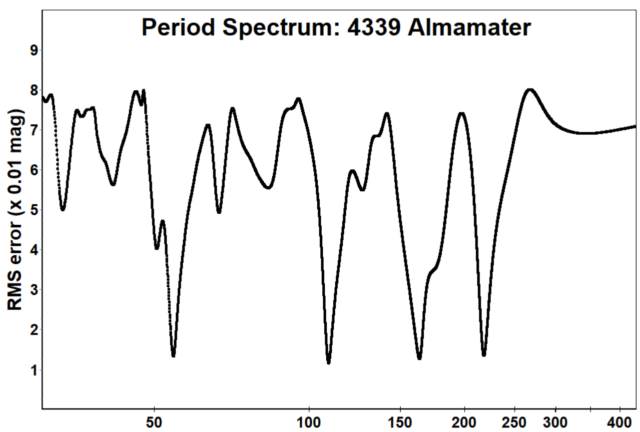

(6453) 1991 NY. Our period estimate of 2.872 ± 0.002 h, generated from three long nights of observation, differs from the sole known period report of 15 h (Pravec et al., 2012web). The lightcurve is clearly bimodal. Our Fourier fit RMS error is 14 mmag.

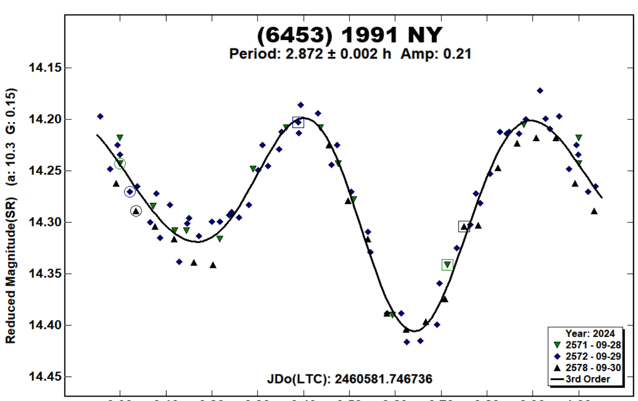

Our period spectrum appears unambiguous; no signal appears at 15 h.

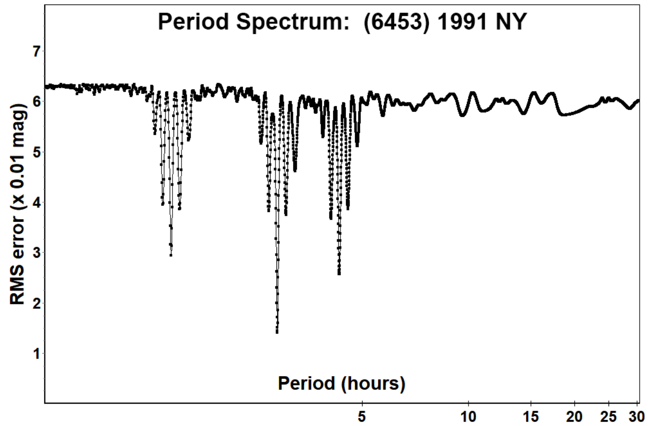

Acknowledgements

The author thanks all contributors to the ATLAS paper (Tonry et al., 2018) for providing openly and without cost the ATLAS refcat2 catalog. Our work also makes extensive use of the python language interpreter and of several supporting packages (notably: astropy, ccdproc, ephem, matplotlib, pandas, photutils, requests, skyfield, and statsmodels), all made available openly and without cost.

References

Behrend, R. (2005web, 2010web, 2011web). Observatoire de Genève web site. *http://obswww.unige.ch/~behrend/page_cou.html*

Ditteon, R.; Adam, A.; Doyel, M.; Gibson, J.; Lee, S.; Linville, D.; Michalik, D.; Turner, R.; Washburn, K. (2018). "Lightcurve Analysis of Minor Planets Observed at the Oakley Southern Sky Observatory: 2016 October - 2017 March." *Minor Planet Bull*. **45**, 13-16.

Dose, E.V. (2020). "A New Photometric Workflow and Lightcurves of Fifteen Asteroids." *Minor Planet Bull*. **47**, 324-330.

Dose, E.V. (2021). "Lightcurves of Nineteen Asteroids." *Minor Planet Bull*. **48**, 69-76.

Ďurech, J.; Tonry, J.; Erasmus, N.; Denneau, L.; Heinze, A.N.; Flewelling, H.; Vančo, R. (2020). "Asteroid models reconstructed from ATLAS photometry." *Astron. Astrophys.* **643**, A59.

Erasmus, N.; Navarro-Meza, S.; McNeill, A.; Sickafoose, A.A.; Denneau, L.; Flewelling, H.; Heinze, A.; Tonry, J.L. (2020). "Investigating Taxonomic Diversity within Asteroid Families through ATLAS Dual-band Photometry." *Astrophys. J. Suppl. Series* **247**, 13.

Harris (1983). As published in the Asteroid Lightcurve Database (LCDB, Warner, 2009).

Harris, A.W.; Young, J.W.; Scaltriti, F.; Zappala, V. (1984). "Lightcurves and phase relations of the asteroids 82 Alkmene and 444 Gyptis." *Icarus* **57**, 251-258.

Pál, A. and 12 colleagues (2020). "Solar System Objects Observed with TESS - First Data Release: Bright Main-belt and Trojan Asteroids from the Southern Survey." *Astrophys. J. Suppl. Series* **247**, 26.

Polakis, T. (2021). "Period Determination for Twenty Minor Planets." *Minor Planet Bull*. **48**, 239-245.

Pravec, P.; Wolf, M.; Sarounova, L. (2012). Ondrejov Asteroid Photometry Project website, Prepublished periods of asteroids page: *https://www.asu.cas.cz/~ppravec/newres.txt*

Tonry, J.L.; Denneau, L.; Flewelling, H.; Heinze, A.N.; Onken, C.A.; Smartt, S.J.; Stalder, B.; Weiland, H.J.; Wolf, C. (2018). "The ATLAS All-Sky Stellar Reference Catalog." *Astrophys. J.* **867**, A105.

Vander Haagen, G.A. (2012). "Lightcurves of 724 Hapag, 2423 Ibarruri, 4274 Karamanov, 4339 Almamater, and 5425 Vojtech." *Minor Planet Bull*. **39**, 48-50.

Warner, B.D.; Harris, A.W.; Pravec, P. (2009). "The asteroid lightcurve database." *Icarus* **202**, 134-146. *https://minplanobs.org/MPInfo/php/lcdb.php*

Warner, B.D. (2021). *MPO Canopus* Software, version 10.8.4.11. BDW Publishing. *http://www.bdwpublishing.com*

Waszczak, A. and 12 colleagues (2015). "Asteroid Light Curves from the Palomar Transient Factory Survey: Rotation Periods and Phase Functions from Sparse Photometry." *Astron. J.*, **150**, 75.

ANALYSIS AND LIGHTCURVES OF ELEVEN ASTEROIDS

Rafael González Farfán (Z55)
Observatorio Uraniborg
Écija, Sevilla, SPAIN
uraniborg16@gmail.com

Faustino García de la Cuesta (J38)
La Vara, Valdés
Asturias, SPAIN

Esteban Reina Lorenz (232)
Masquefa, Can Parellada
Barcelona, SPAIN

Carlos Botana Albá (Y85)
Observatorio en Magalofes
Fene, A Coruña, SPAIN

Javier De Elías Cantalapiedra (L46)
Observatorio en Majadahonda
Madrid, SPAIN

Javier Ruiz Fernández (J96)
Observatorio de Cantabria
Cantabria, SPAIN

Felipe Gómez Pinilla (J36)
Observatorio Diezalaonce
Illana, Guadalajara, SPAIN

Arturo Martín Saura
Observatorio Peñas Blancas
Fuente Álamo, Murcia, SPAIN

José M. Fernández. Andújar (Z77)
Observatorio Inmaculada del Molino
Sevilla, SPAIN

(Received: 2024 July 29)

The analysis, observation, and results of the lightcurves of the eleven asteroids presented here were mostly performed during the months of 2024 March to July, while the others were observed in 2021 and 2023. In some cases, we obtained rotation periods somewhat different from those previously published. For others, we could not find a period in the literature. The eleven asteroids studied and the derived rotation periods were: 236 Honoria (12.339 h), 606 Brangane (12.294 h), 737 Arequipa (14.067 h), 1509 Esclangona (3.252 h), 2383 Bradley (5.870 h), 4897 Tomhamilton (18.213 h), 5515 Naderi (5.230 h), 6012 Williammurdoch (2.891 h), 6859 Datemasamune (8.905 h), 7304 Namiki (8.873 h), and 8648 Salix (30.267 h).

We made photometric observations of a total of eleven asteroids, mostly in 2024 but some in 2021 or 2023. In all cases, the images obtained were calibrated in the conventional mode, without photometric filter, and with the application of darks, bias and flats. Data analysis and processing were performed using *FotoDif* (2021), *Tycho Tracker* (2023), and *Periodos* (2020) software. In addition, all data were light-time corrected. Individual lightcurve plots along additional comments as required are presented below.

236 Honoria. The asteroid lightcurve database (LCDB from here on; Warner et al., 2009) gives numerous references to rotation periods of this almost 80-km main-belt asteroid. One of the most recent is due to Colazo et al. (2022). Our independent observations took place two years later, in 2024 April. The analysis confirmed a synodic rotation period $P = 12.339 \pm 0.005$ hours, closely matching Colazo et al. (2022), and lightcurve amplitude of 0.15 ± 0.01 mag.

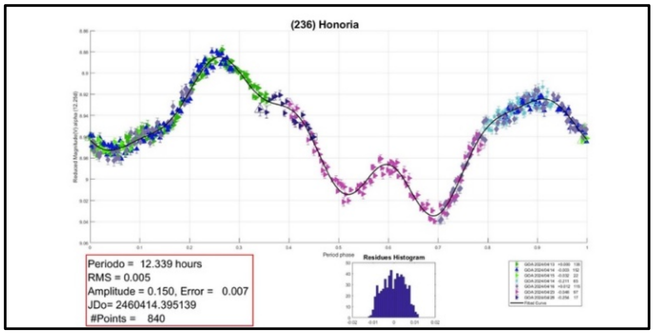

606 Brangane. Behrend (2006web) found a period 12. 2050 hours for Brangane. Hanus et al. (2011) reported a sidereal rotation period 12.29067 h. The results of our observations in 2024 March to May are $P = 12.294 \pm 0.036$ hours and $A = 0.96 \pm 0.05$ mag.

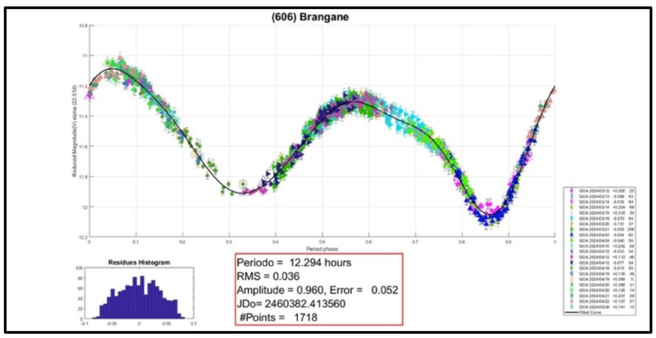

737 Arequipa. The LCDB lists numerous results for this main-belt asteroid that was discovered in 1912. Among those results are from Behrend (2005web; 7.03 h) and Franco et al. (2022; 7.024 h). Many of the previous results report a rotation period of slightly more than 7 hours. Marciniak et al. (2014) reported a period of 14.03 h, but they later revised this to the half-period (Marciniak et al., 2015). Based on our observations in 2024 July, we obtained $P = 14.067 \pm 0.008$ hours and an amplitude $A = 0.19 \pm 0.01$ mag.

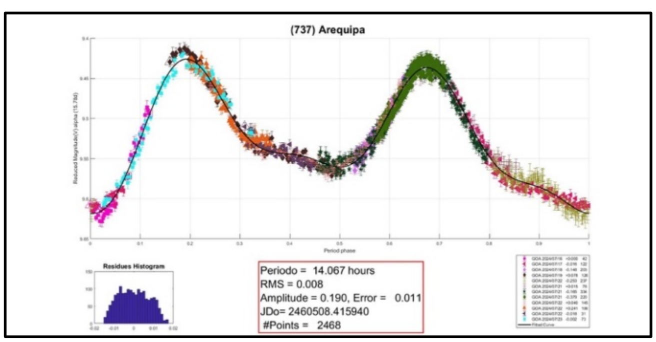

The asymmetry of the lightcurve, non-symmetrical maximums of different amplitudes, and the period spectrum led us to rule out the possibility that our results are a harmonic of the many previous results near 7 hours.

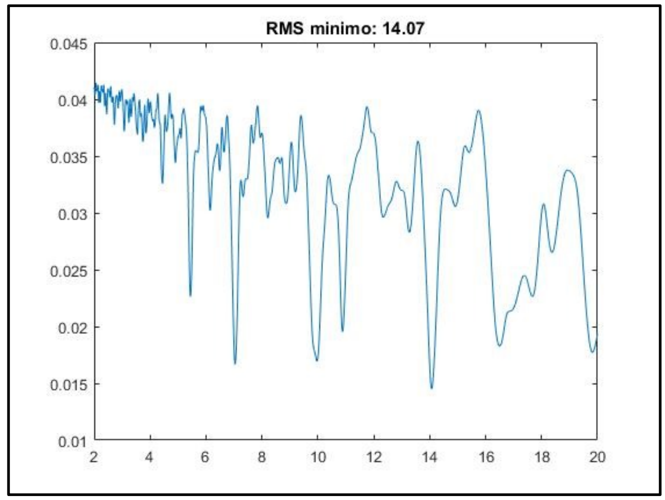

1509 Esclangona. This asteroid is located in the inner part of the main-belt and belongs to the Hungaria group. Warner (2013), reported a synodic rotation period that is in perfect agreement with the one derived from our observations made in 2024 July, $P = 3.252 \pm 0.012$ hours. The lightcurve amplitude is 0.10 ± 0.02 mag.

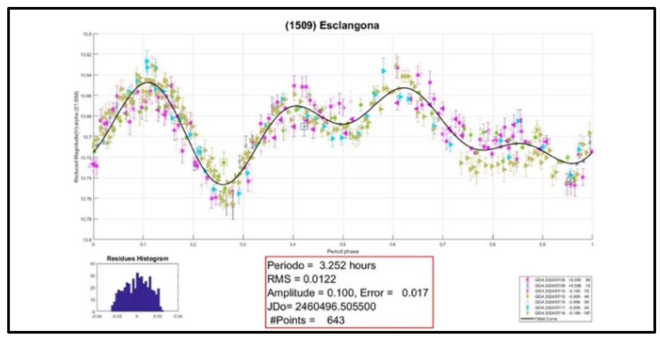

2383 Bradley. The only previous period found in the LCDB was from Warell (2017). The U = 2 rating indicates that the rotation period could be off by 30 %. In the case for Warell, the two sets of observations were separated by almost a month, thus introducing the chance of a rotational alias, i.e., an uncertain number of rotations over the date range of the observations.

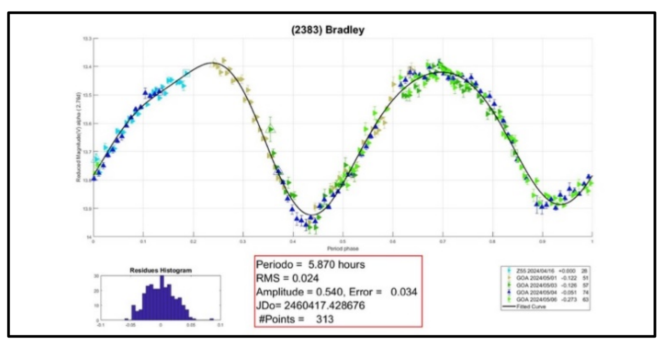

The uncertainty in the period prompted us to observe the asteroid in 2024 April and May. The data set of almost 500 points allowed us to find a period of 5.870 ± 0.024 hours, which is close to the one from Warell (2017). The lightcurve amplitude is $A = 0.54 \pm 0.03$ mag.

4897 Thomhamilton. Behrend (2024web) reported a synodic rotation period of 18.201 h and amplitude of 0.28 mag. Our observations were carried out during 2024 July and provided more than 600 data points._From these, we found a rotation period of P = 18.213 ± 0.012 hours and an amplitude A = 0.31 ± 0.02 mag.

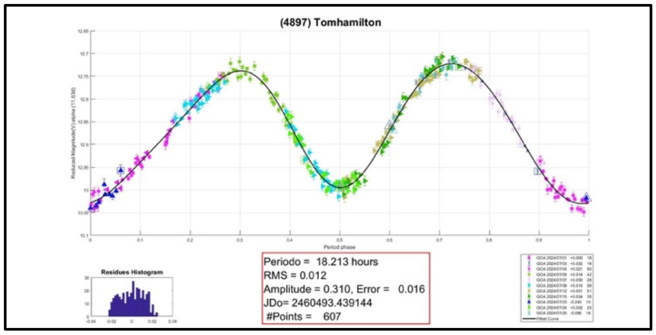

5515 Naderi is a 7-km asteroid (JPL, 2024) that was discovered in 1989. In 2024 April and May, we were able to obtain a lightcurve and determine a rotation period. Pal et al. (2020) reported a period of 5.22997 ± 0.00005 h based on dense data from the TESSS survey. Other periods reported in the LCDB are also close to 5.25 hours. We found P = 5.23 ± 0.02 hours and a lightcurve amplitude of A = 0.46 ± 0.03. The period is in good agreement with previous results.

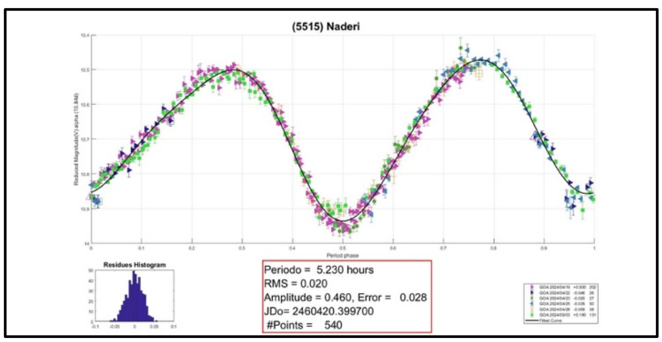

6012 Williammurdoch. Skiff et al. (2019) reported a period of 2.890 hours based on data obtained in 2011. There were no other periods reported in the LCDB. Our team worked on this asteroid during 2024 April and was able to obtain a lightcurve of about 160 points. This allowed us to deduce a rotation period P = 2.891 ± 0.026 hours, in agreement with Skiff et al. (2019), and lightcurve amplitude A = 0.20 ± 0.04 mag.

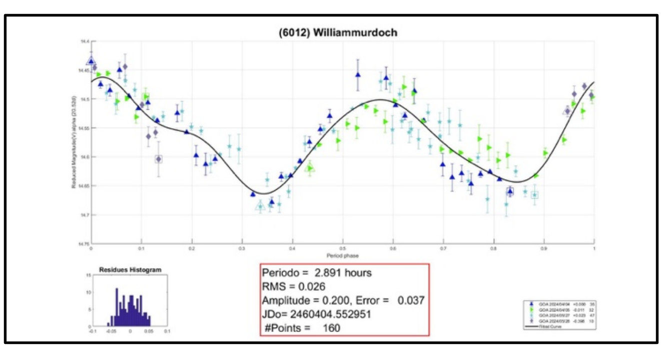

6859 Datemasamune. Stephens et al. (2021) reported a period of 5.94 hours. Many other results in the LCDB for this main-belt asteroid are in close agreement. However, all are rated U = 2, or worse, indicating a need of additional observations to verify and refine the period.

The lightcurve amplitude has never been reported to be more than 0.12 mag. With low amplitudes, despite dense data sets, there can be ambiguities in the solution since it is not safe to assume that the lightcurve is monomodal or bimodal (Harris et al., 2014).

Our group worked on this asteroid in 2024 July, obtaining a large data set of almost 1,000 points. The deduced rotation period was P = 8.905 ± 0.01 hours with an amplitude A = 0.08 ± 0.02 mag. The periodogram we obtained seems to favor clearly our result.

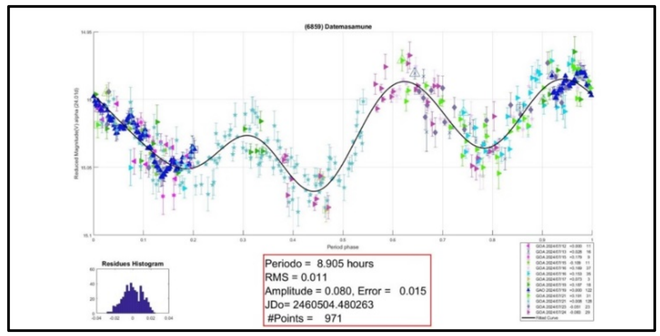

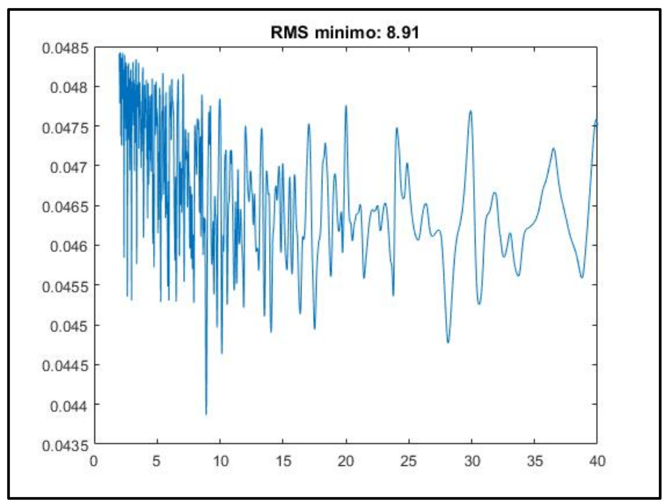

7304 Namiki. Durech et al. (2018) reported a sidereal period of 8.87383 h for this Mars-crosser discovered in 1994 (JPL, 2024). Numerous other synodic periods found in the LCDB are in close agreement at about 8.87 hours.

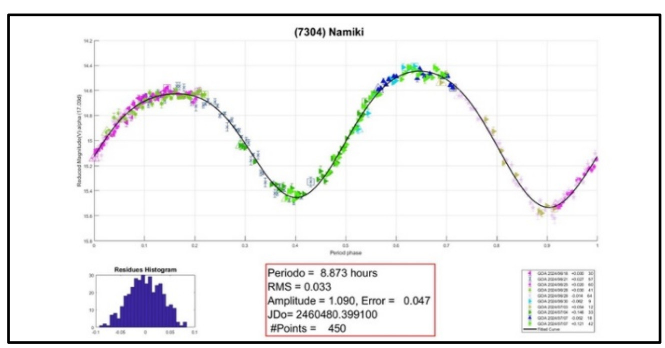

Number	Asteroid	20yy mm/dd	Phase	Period(h)	P.E.	Amp	A.E.
236	Honoria	24/04/13-24/04/28	12.2-15.2	12.339	0.005	0.150	0.007
606	Brangane	24/03/13-24/05/08	22.5-17.0	12.294	0.036	0.960	0.052
737	Arequipa	24/07/16-24/07/23	15.9-13.4	14.067	0.008	0.190	0.011
1509	Esclangona	24/07/04-24/07/14	21.8-18.0	3.252	0.012	0.100	0.017
2383	Bradley	24/04/16-24/05/08	2.8-15.2	5.870	0.024	0.540	0.030
4897	Tomhamilton	24/07/01-24/07/24	11.7- 6.1	18.213	0.012	0.310	0.016
5515	Naderi	24/04/21-24/01/27	10.4- 9.5	5.230	0.020	0.460	0.028
6012	Williammurdoch	24/04/03-24/04/05	20.6-20.2	2.891	0.026	0.200	0.037
6859	Datemasamune	24/07/13-24/07/25	23.8-17.8	8.905	0.011	0.080	0.015
7304	Namiki	24/06/21-24/07/07	18.1-23.7	8.873	0.009	1.090	0.047
8648	Salix	21/01/02-21/02/16	6.7-20.9	30.267	0.023	0.410	0.033

Table I. Observing circumstances and results. Phase is the solar phase angle given at the start and end of the date range. If preceded by an asterisk, the phase angle reached an extrema during the period.

Our group observed this asteroid in 2024 June and July. The analysis of our data lead to P = 8.873 ± 0.033 hours, in good agreement with previous results, and a lightcurve amplitude A = 1.09 ± 0.05 mag.

8648 Salix. The LCDB listed no rotation periods for Salix. There is one night of observations for 2011 March 13 submitted by Skiff reported in the ALCDEF database (*https://alcdef.org*). Analysis of our data, obtained in 2021 January and February, led to a lightcurve that fit a period of P = 30.267 ± 0.023 hours with an A = 0.41 ± 0.03 mag.

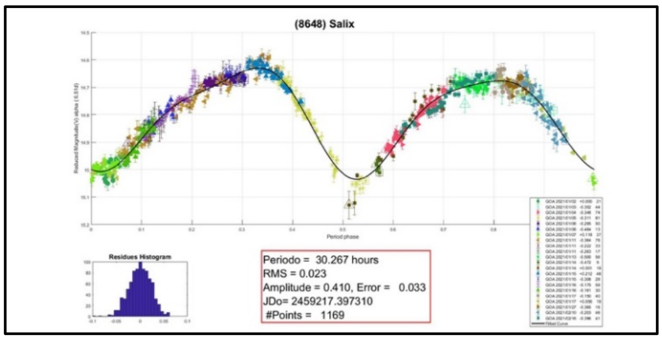

References

Behrend, R. (2005web; 2006web; 2024web) Observatoire de Geneve web site.
htttp://obswww.unige.ch/~behrend/page_cou.html

Colazo, M.; Morales, M.; Fornari, C.; Chapman, A.; and 20 co-authors. (2022). "Photometry and Light Curve Analysis of Eight Asteroids by GORA'S Observatories." *Minor Planet Bull.* **49**, 48-51.

Durech, J.; Hanus, J.; Ali-Lagoa, V. (2018). "Asteroid models reconstructed from the Lowell Photometric Database and WISE data." *Astron. Astrophys.* **617**, A57.

FotoDif (2021). Photometry software.
http://astrosurf.com/orodeno/fotodif/index.htm

Franco, L.; Marchini, A.; Papini, R.; Iozzi, M.; and 16 co-authors (2022). "Collaborative Asteroid Photometry from UAI: 2023 April-June." *Minor Planet Bull.* **49**, 228-232.

Hanus, J.; Durech, J.; Broz, M.; Warner, B.D.; and 11 co-authors (2011). "A study of asteroid pole-latitude distribution based on an extended set of shape models derived by the lightcurve inversion method." *Astron. Astrophys.* **530**, A134.

Harris, A.W.; Pravec, P.; Galad, A.; Skiff, B.A.; Warner, B.D.; Vilagi, J.; Gajdos, S.; Carbognani, A.; Hornoch, K.; Kusnirak, P.; Cooney, W.R.; Gross, J.; Terrell, D.; Higgins, D.; Bowell, E.; Koehn, B.W. (2014). "On the maximum amplitude of harmonics on an asteroid lightcurve." *Icarus* **235**, 55-59.

JPL (2024). Small-Body Database Lookup.
https://ssd.jpl.nasa.gov/tools/sbdb_lookup.html#/?sstr=2383
https://ssd.jpl.nasa.gov/tools/sbdb_lookup.html#/?sstr=6012

Marciniak, A.; Pilcher, F.; Santana-Ros, T.; Oszkiewicz; Kankiewicz, P. (2014). "Against the bias in physics of asteroids: Photometric survey of long-period and low-amplitude asteroids." *Asteroids, Comets, and Meteors conference*, Poster 57.

Marciniak, A.; Pilcher, F.; Oszkiewicz, D.; Bartczak, P.; and 20 co-authors. (2015). "Against the bias in physics of asteroids: Photometric survey of long-period and low-amplitude asteroids." *Plan. Space Sci* **118**, 256-266.

Pal, A.; Szakáts, R.; Kiss, C.; Bódi, A.; Bognár, Z.; Kalup, C.; Kiss, L.L.; Marton, G.; Molnár, L.; Plachy, E.; Sárneczky, K.; Szabó, G.M.; Szabó, R. (2020). "Solar System Objects Observed with TESS - First Data Release: Bright Main-belt and Trojan Asteroids from the Southern Survey." *Ap. J. Suppl Ser.* **247**, id. 26.

Períodos (2020). Period analysis software.
http://www.astrosurf.com/salvador/Programas.html

Skiff, B.A.; McLelland, K.P.; Sanborn, J.; Pravec, P.; Koehn, B.W. (2019). "Lowell Observatory Near-Earth Asteroid Photometric Survey (NEAPS): Paper 4." *Minor Planet Bull.* **46**, 458-503.

Stephens, R.D.; Coley, D.R.; Warner, B.D. (2021). "Main-belt Asteroids Observed from CS3: 2021 January to March." *Minor Planet Bull.* **48**, 246-267.

Tycho Tracker (2023). Astronomy software.
https://www.tycho-tracker.com

Warell, J. (2017). Lightcurve Observations of Nine Main-belt Asteroids." *Minor Planet Bull.* **44**, 304-305.

Warner, B.D.; Harris, A.W.; Pravec, P. (2009). "The asteroid lightcurve database." *Icarus* **202**, 134-146. Updated 2023 October.
https://www.minorplanet.info/php/lcdb.php

Warner, B.D. (2013). "Asteroid Lightcurve Analysis at the Palmer Divide Observatory: 2013 January - March." *Minor Planet Bull.* **40**, 137-145.

ANALYSIS AND REVIEW OF ROTATION CURVES AND PERIODS OF 12 ASTEROIDS

Rafael González Farfán (Z55)
Observatorio Uraniborg
Écija, Sevilla, SPAIN
uraniborg16@gmail.com

Faustino García de la Cuesta (J38)
La Vara, Valdés
Asturias, SPAIN

Esteban Reina Lorenz (232)
Masquefa, Can Parellada
Barcelona, SPAIN

Carlos Botana Albá (Y85)
Observatorio en Magalofes
Fene, A Coruña, SPAIN

Javier De Elías Cantalapiedra (L46)
Observatorio en Majadahonda
Madrid, SPAIN

Javier Ruiz Fernández (J96)
Observatorio de Cantabria
Cantabria, SPAIN

Fernando Limón Martínez (Z50)
Observatorio Mazariegos
Mazariegos, Palencia, SPAIN

Felipe Gómez Pinilla (J36)
Observatorio Diezalaonce
Illana, Guadalajara, SPAIN

José M. Fernández Andújar (Z77)
Observatorio Inmaculada del Molino
Sevilla, SPAIN

(Received: 2024 July 29)

The twelve asteroids presented here were observed from 2024 May to September. Analysis of the resulting data lead to generating lightcurves, finding rotation periods, and drawing some conclusions from the results. The asteroids studied and the derived periods are: 114 Kassandra (10.734 h), 901 Brunsia (3.136 h), 924 Toni (19.436 h), 1065 Amundsenia (7.758 h), 2168 Swope (7.354 h), 2555 Thomas (2.858 h), 2801 Huygens (4.378 h), 2994 Flynn (9.750 h), 3735 Trebon (8.472 h), 5749 Urduja (2.813 h), 21088 Chelyabinsk (11.272 h), and (66251) 1999 GJ2 (2.463 h). In some cases, the results were almost identical to those previously published but there were several for which we found no previously reported lightcurves or periods.

Observations of twelve asteroids were made by the authors between 2024 May and September. In all cases, the images obtained were calibrated in the conventional mode, without photometric filter, and with the application of darks, bias and flats. Data analysis and processing were performed using *FotoDif* (2021), *Tycho Tracker* (2023), and *Períodos* (2020) software. In addition, all data were light-time corrected. Individual lightcurve plots along with additional comments as required are presented below.

114 Kassandra. Part of the main asteroid belt and discovered in July 1871, we had the opportunity to observe this asteroid (incompletely) in September 2020 and February 2023. However, it was not until July and August 2024 that we were able to plot a complete and updated lightcurve. This allowed us to obtain a rotation period of 10.743 ± 0.023 hours and an amplitude of 0.240 ± 0.032 mag.

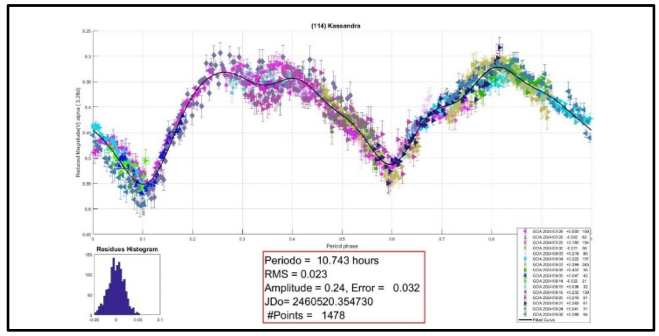

901 Brunsia. We were able to observe this asteroid in early 2024 August. Out lightcurve allowed us to deduce a rotation period of 3.136 ± 0.005 hours and an amplitude of 0.12 ± 0.01 mag. The period is in good agreement with Franco et al. (2022).

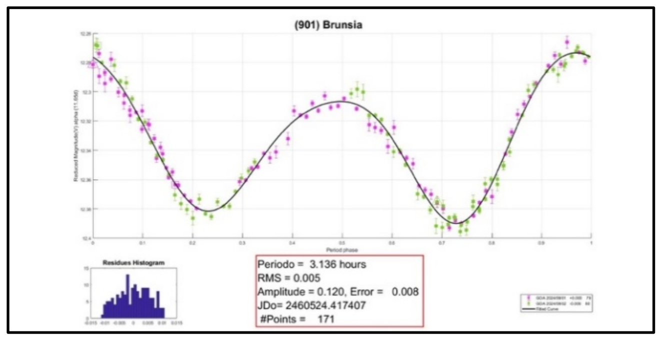

924 Toni. Several periods have been reported since 1998. For example, Behrend (2006web; 2007web) reported a period near 21 hours. However, our data obtained in 2024 July to September allowed us to propose a result of 19.436 ± 0.016 hours and an amplitude of 0.26 ± 0.02 mag, which seems to be more in line with those published by Pilcher (2015).

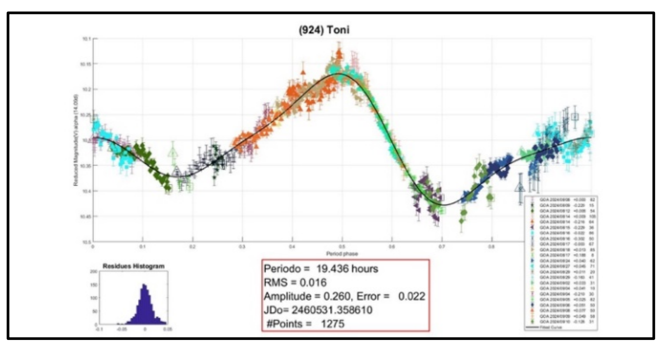

1065 Amundsenia. There are subtle differences in the results for the rotation period in the literature. For example, Pravec et al. (2006web) published a result of 7.759 h while Stephens (2018) found 7.790 h, and Behrend (2020web) reported 7.740h. The amplitudes varied between 0.08 and 0.16 mag. Our work for this asteroid, carried out in 2024 September, led to a rotation period of 7.758 ± 0.012 hours and an amplitude of 0.10 ± 0.02 mag.

Number	Asteroid	2024 mm/dd	Phase	Period(h)	P.E.	Amp	A.E.
114	Kassandra	07/25-24/08/04	2.4,12.3	10.743	0.023	0.24	0.03
901	Brunsia	08/01-24/08/02	11.7,12.3	3.136	0.005	0.12	0.01
924	Toni	07/08-24/09/10	4.5,13.4	19.436	0.016	0.26	0.02
1065	Amundsenia	09/05-24/09/11	10.5, 7.3	7.758	0.012	0.10	0.02
2168	Swope	08/04-24/08/07	18.1,16.8	7.354	0.024	0.91	0.03
2555	Thomas	09/23-24/09/28	0.6, 2.6	2.858	0.017	0.25	0.02
2801	Huygens	08/11-24/09/15	21.6, 9.5	4.378	0.026	0.08	0.03
2994	Flynn	08/13-24/08/28	17.5, 9.3	9.750	0.029	0.38	0.04
3735	Trebon	05/27-24/06/13	12.5,17.4	8.472	0.033	0.68	0.05
5749	Urduja	08/19-24/08/26	5.0, 4.9	2.813	0.046	0.10	0.07
21088	Chelyabinsk	07/27-24/08/04	30.0,35.3	11.272	0.017	0.31	0.02
66251	1999 GJ2	08/08-24/08/11	39.0,38.0	2.463	0.018	0.10	0.03

Table I. Observing circumstances and results. Phase is the solar phase angle given at the start and end of the date range.

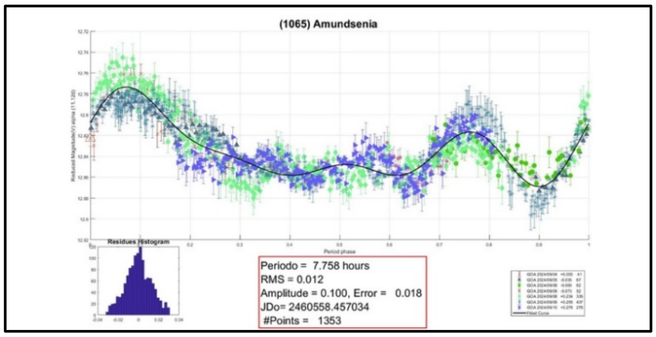

2168 Swope. The only previous result we found was a 3D model in DAMIT (Durech et al., 2023) that gave a sidereal rotation period of 7.352 hours. Our observations, carried out in 2024 August, allowed us to plot a lightcurve with an amplitude of 0.91 ± 0.03 mag and a similar period of 7.354 ± 0.024 hours.

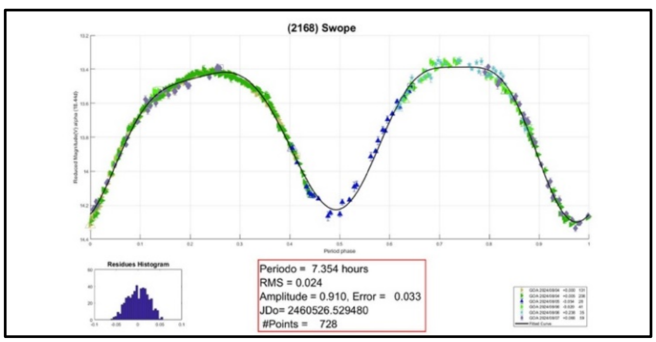

2555 Thomas. During 2024 September, we made observations of this asteroid, which allowed us to plot a lightcurve of more than 700 points and then deduce a rotation period of 2.858 ± 0.017 hours with an amplitude of 0.25 ± 0.03 mag.

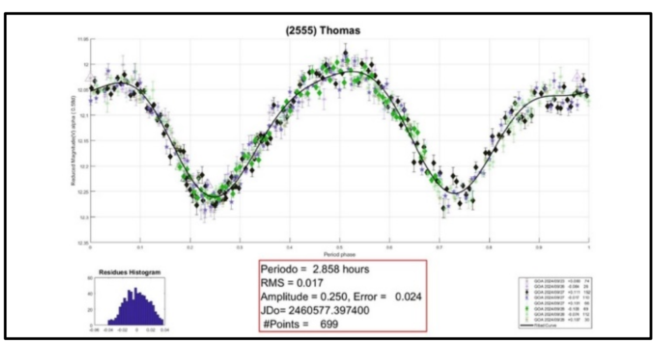

2801 Huygens. We did not find any lightcurves or rotation periods in the literature. Analysis of the data from our observations made in 2024 August and September led to a lightcurve with a small amplitude of 0.08 ± 0.03 mag that was fit to a rotation period of 4.378 ± 0.026 hours. Given the low amplitude, we recommend more observations at future apparitions to confirm our results.

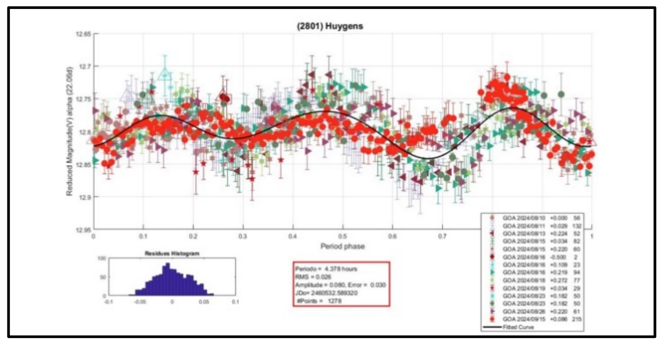

2994 Flynn. The rotational period published by JPL (2024) for this asteroid is 9.747 hours, although JPL points out that this is based on very few observations. This is almost a 3:2 ratio with the period found by Erasmus et al. (2020), suggesting that the two periods are harmonically related. Our observations from 2024 August are more in line with the first result. We obtained a lightcurve with more than 660 points. This allowed us to deduce a rotation period of 9.750 ± 0.029 hours and an amplitude of 0.38 ± 0.04 mag.

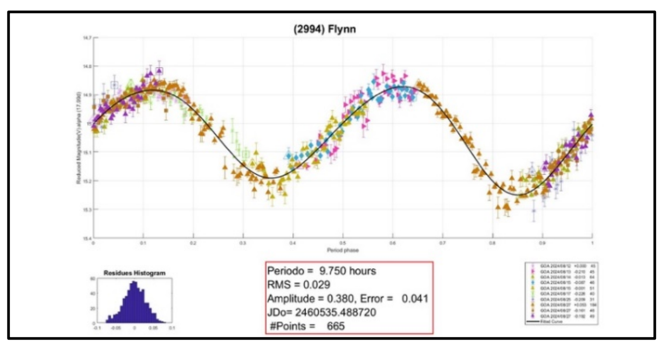

3735 Trebon. The ALCDEF database (*https://alcdef.org*) has observations going back to 2010. The rotation period given in the LCDB (Warner et al., 2009) is 8.471 hours. Data from our observations carried out in 2024 May and June allowed us to plot a lightcurve that fit a period of 8.472 ± 0.033 hours, close to the LCDB value, and an amplitude of 0.68 ± 0.05 mag.

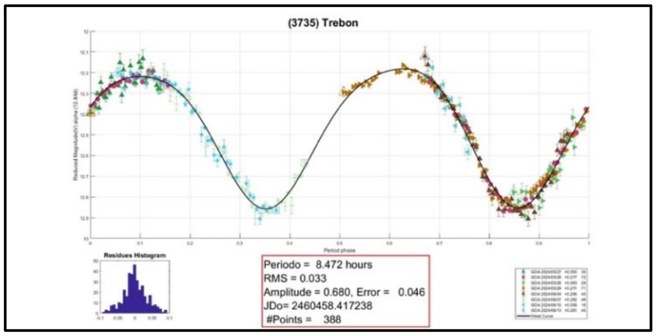

5749 Urduja (1991 FV). We found no published lightcurve or rotation period for this asteroid in the literature, so we decided that it would be a good target for study. The observations took place during 2024 June and allowed us to plot a curve of more than 700 points. From this, we were able to deduce a rotation period of 2.813 ± 0.046 hours and an amplitude of 0.10 ± 0.07 mag.

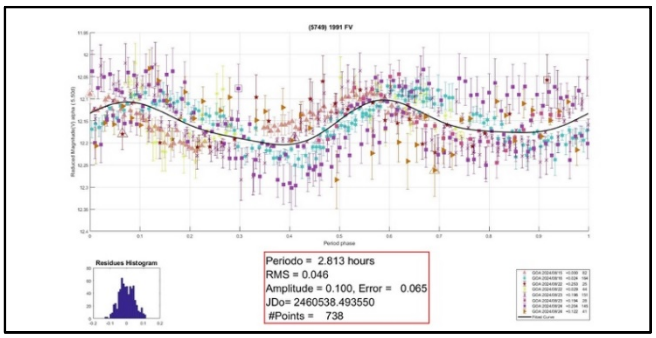

21088 Chelyabinsk. The data obtained by our team allowed us to deduce a rotation period very similar to that of Warner and Stephens (2021; 11.23 hours). Our lightcurve, with more than 3800 points, best fits a period $P = 11.272 \pm 0.017$ hours and has an amplitude of 0.31 ± 0.03 mag.

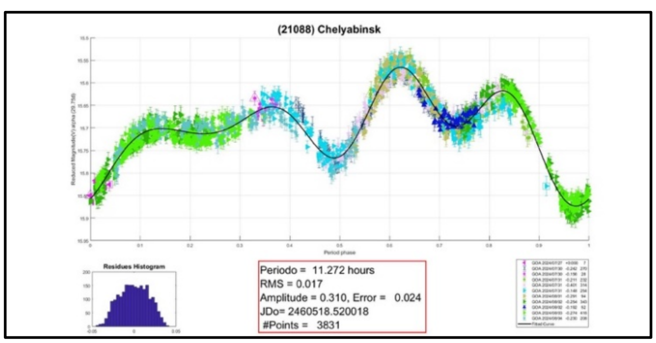

(66251) 1999 GJ2. There are numerous observations of this asteroid uploaded to the ALCDEF site since 2005. Most of them suggest a rotation period of about 2.5 hours. During the month of 2024 August, we were able to construct a lightcurve of more than 700 points. The synodic rotation period was found to be $P = 2.463 \pm 0.018$ hours and an amplitude of 0.10 ± 0.03 mag. The period is in agreement with previously published results.

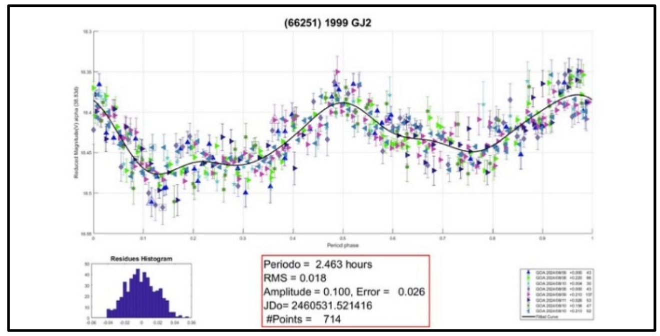

References

Behrend, R. (2006web; 2007web; 2020web) Observatoire de Geneve web site. *http://obswww.unige.ch/~behrend/page_cou.html*

Durech, J. (2023). DAMIT website. *https://astro.troja.mff.cuni.cz/projects/damit/?q=2168*

Durech, J.; Tonry, J.; Erasmus, N.; Denneau, L.; Heinze, A.N.; Flewelling, H.; Vanco, R. (2020). "Asteroid models reconstructed from ATLAS photometry." *Astron. Astrophys.* **643**, A59.

Erasmus, N.; Navarro-Meza, S.; McNeill, A.; Trilling, D.E.; Sickafoose, A.A.; Denneau, L.; Flewelling, H.; Heinze, A.; Tonry, J.L. (2020). "Investigating Taxonomic Diversity within Asteroid Families through ATLAS Dual-band Photometry." *Ap. J. Suppl. Ser.* **247**, A13.

FotoDif (2021) software. *http://astrosurf.com/orodeno/fotodif/index.htm*

Franco, L.; Marchini, A.; Papini, R.; Iozzi, M.; Bacci, P.; Maestripieri, M.; Baj, G.; Galli, G.; Mortari, F; Gabellini, D; Ruocco, N.; Tinelli, L.; Montigiani, N.; Mannucci, M.; Scarfi, G.; Salvaggio, F. (2022). "Collaborative Asteroid Photometry from UAI: 2021 October-December." *Minor Planet Bull*. **49**, 128-130.

JPL (2024). Small-Body Database Lookup *https://ssd.jpl.nasa.gov/tools/sbdb_lookup.html#/?sstr=2383* *https://ssd.jpl.nasa.gov/tools/sbdb_lookup.html#/?sstr=2994*

Períodos (2020) software. *http://www.astrosurf.com/salvador/Programas.html*

Pilcher, F. (2015). "Rotation Period Determinations for 275 Sapientia, 309 Fraternitas, and 924 Toni." *Minor Planet Bull*. **42**, 38-39.

Pravec, P.; Wolf, M.; Sarounova, L. (2006). *http://www.asu.cas.cz/~ppravec/neo.htm*

Stephens, R.D. (2018). "Asteroids Observed from CS3: 2017 October - December." *Minor Planet Bull*. **45**, 135-137.

Tycho Tracker (2023) software. *https://www.tycho-tracker.com*

Warner, B.D.; Harris, A.W.; Pravec, P. (2009). "The Asteroid Lightcurve Database." *Icarus* **202**, 134-146. Updated 2023 Oct. *https://www.minorplanet.info/php/lcdb.php*

Warner, B.D.; Stephens, R.D. (2021). "Near-Earth Asteroid Lightcurve Analysis at the Center for Solar System Studies: 2020 September to 2021 January." *Minor Planet Bull.* **48**, 170-179.

LIGHTCURVE ANALYSIS FOR THIRTEEN MAIN-BELT AND THREE NEAR EARTH ASTEROIDS

Gonzalo Fornas, AVA - J57
CAAT - Centro Astronómico del Alto Turia, SPAIN
gon@iicv.es

Álvaro Fornas AVA - J57
CAAT - Centro Astronómico del Alto Turia, SPAIN

Fernando Huet, AVA - Z93
Enrique Rathmann, AVA - Y78
Tros Alt Observatory

Enrique Arce, AVA - J67
Rafael Barberá, AVA - J57
CAAT - Centro Astronómico del Alto Turia, SPAIN

Vicente Mas, AVA - J57
CAAT - Centro Astronómico del Alto Turia, SPAIN

(Received: 2024 October 18)

Photometric observations for thirteen main-belt, and three near-Earth asteroids. We derived synodic periods for 838 Seraphina, 1762 Rusell, 2047 Smetana, 2383 Bradley, 2692 Chkalov, 3895 Earhart, (23512) 1992 PC3, (23880) Tongil, (25330) 1999 KV4, (31545) 1999 DN6, (32459) 2000 SK87, (39489) 1981 EU6, (42449) 3496 T-3, (84833) 2003 AF9, (96720) 1999 LP, (352143) 1999 LP. In addition, we found sidereal periods for 838 Seraphina, 1762 Rusell, 2047 Smetana, 2383 Bradley, 2692 Chkalov, and 3895 Earhart.

We report on the photometric analysis for results thirteen main-belt and three near-earth asteroids by Asociación Valenciana de Astronomía (AVA). The data were obtained during the third quarter of 2024. We present graphic results of data analysis, mainly lightcurves, with the plot phased to a given period. We managed to obtain several accurate and complete lightcurves and calculating as accurately as possible their rotation periods.

Observatory	Telescope	CCD
C.A.A.T. J57	43 cm DK	QHY- 600
C.A.A.T. J57	250 mm NW	ZWO ASI 1600
Z93	0.20 m SC	SBIG ST8300
J67	0.25 m SC	SBIG ST7
Tros Alt Y78	0.20 m SC	ZWO ASI 294 MM PRO

Table I. List of instruments used for the observations.

We focused on asteroids with no reported period and those where the reported period was poorly established and needed confirmation. The targets were selected from the Collaborative Asteroid Lightcurve website (*https://minorplanet.info/php/call.php*), the Minor Planet Center (*https://www.minorplanetcenter.net/*), and Warner et at. (2024). The Asteroid Lightcurve Database (LCDB; Warner et al., 2009) was consulted to locate previously published results.

Images were measured using *MPO Canopus* (Bdw Publishing) with a differential photometry technique. The comparison stars were restricted to near solar-color to minimize color dependencies, especially at larger air masses. The lightcurves show the synodic rotation period. The amplitude (peak-to-peak) that is shown is that for the Fourier model curve and not necessarily the true amplitude.

If we found sufficient data in the ALCDEF database (*https://alcdef.org*) in addition to our own data, we used *LCInvert (*Bdw Publishing) to try to model the asteroid. The program uses the inversion method described by Kaasalainen and Torppa (2001) written by J. Durech based on the original FORTRAN code by Kaasalainen. The method allows using *dense* data such as we obtained together with *sparse* data from all-sky programs such as Catalina, USNO, Atlas, Palomar, etc. We use weighting coefficients to account for the density of the data. We usually assign a value of 1 to *dense* data and 0.3 to *sparse* data.

This is an iterative method that, based on an initial estimate of the period given by the lightcurve, finds the local minimum of χ^2 and gives the corresponding solution. The procedure starts with six initial poles for each trial period and selects the period that gives the lowest χ^2. If there is a clear minimum in χ^2 when plotted as a function of the period, we can assume it as a correct solution. Not always we get a clear solution. We have referenced only those asteroids with an unambiguous calculation.

Error estimates for the inversion method are not obvious. The smallest separation of local minima (Kaasalainen, 2001; Kaasalainen et al., 2001), in the period parameter space is roughly given by

$$\Delta P \approx 0.5 * P^2/\Delta t$$

Where Δt is the full epoch range of the dataset. This derives from the fact that the maxima and minima of a double sinusoidal lightcurve for periods P and $P \pm \Delta P$ are at the same epochs after Δt time. As we can read at Kaasalainen et al. (2001), "The period error is mostly governed by the epochs of the lightcurves. If the best local χ^2minimum of the period spectrum is clearly lower than the others, one can obtain an error estimate of, say, a hundredth part of the smallest minimum width ΔP since the edge of a local minimum ravine always lies much higher than its bottom."

Durech proposes an estimate of error of

$$\Delta P \approx (1/10 * 0.5)\ P^2/\Delta t$$

The factor 1/10 means that the period accuracy is 1/10 of the difference between local minima in the periodogram.

<u>838 Seraphina</u>. This outer main-belt asteroid was discovered on 1916 September 24 at Heidelberg by M.F. Wolf.

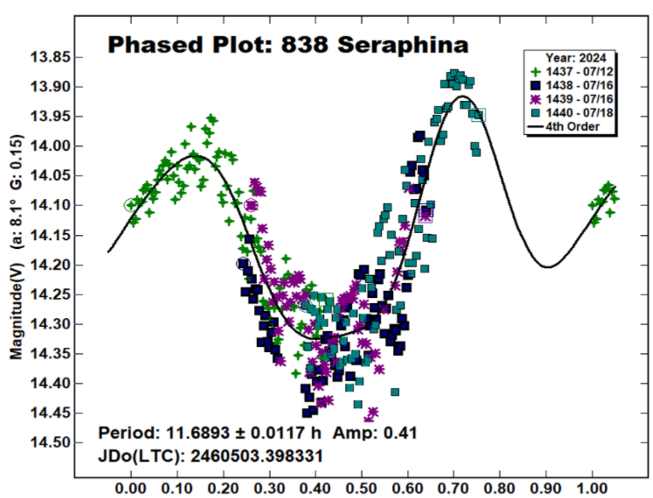

We used our dense data obtained from 2015 November 4-17 and sparse data from ATLAS (887 pts; 2017/9/29-2024/7/9), Catalina (502 pts; 2005/9/30-2024/7/9), LONEOS (24 pts; 2000/9/8-2007/1/16), Palomar (149 pts; 2019/8/23-2022/5/15), and USNO (191 pts; 1998/2/26-2014/5/17) to find a sidereal rotation period of 11.72437 ± 0.00005 h, the error being based on data from 2015-2024. Durech and Hanus (2018) found a sidereal period of 11.7245 h and refined this (Durech et al., 2019) to 11.72446 h. The graph shows the χ^2 value as a function of the period. The large number of points below the 10% error (green line) would make any shape model suspect.

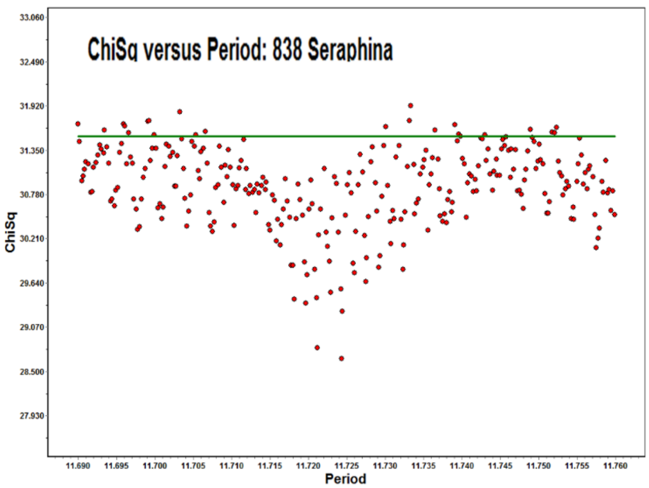

For modeling, we used our *dense* data and those from Klinglesmith (2014/3/23-2014/5/5) found on the ALCDEF site and *sparse* data from ATLAS (1215 pts; 2017/10/19-2024/7/5), Catalina (297 pts; 2003/10/26-2022/1/28), LONEOS (57 pts; 1998/10/12-2007/12/5), Palomar (80 pts; 2019/4/2-2022/8/16), and USNO (107 pts; 1997/9/23-2011/11/1) to determine a sidereal rotation period of 12.793707 ± 0.00005 h. The error estimated error is based on a data ranging from 2004-2024. The plot shows the convergence of the results and only one or two periods meeting the 10% rule. Durech and Hanus (2018) and Durech et al. (2018b) found sidereal periods of 12.79374 h and 12.7933 h, respectively.

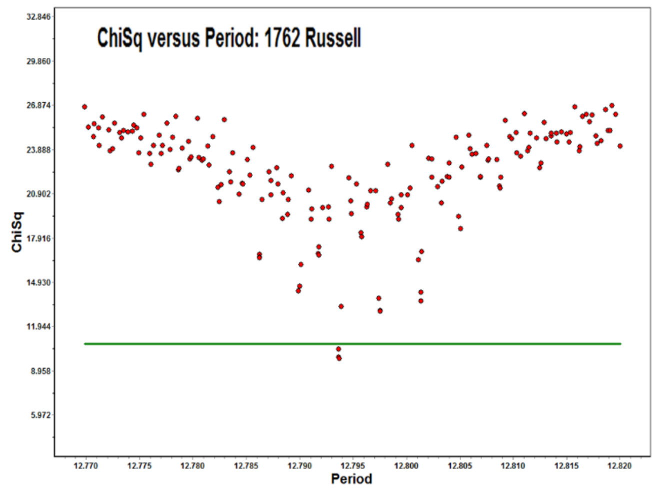

<u>1762 Russell</u>. This outer main-belt asteroid of the Koronis family was discovered on 1953 October 8 at Brooklyn Observatory, Indiana University. We made observations from 2024 April 15 to June 4. Our analysis found a synodic period of 12.7942 ± 0.0006 h with an amplitude of 0.45 mag. Cooney Jr. et al. (2015) found 12.797 h. Slivan et al. (2022) found 12.7946 h, which is consistent with our calculations.

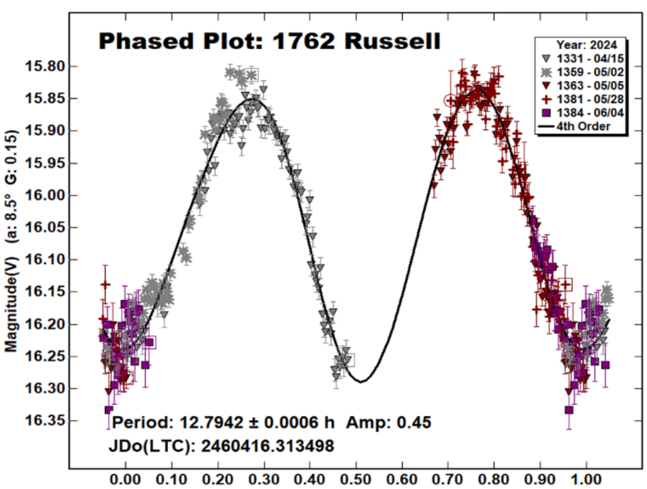

<u>2047 Smetana</u>. We made observations of this Hungaria group member in 2024 April 15-18. From our data, found a synodic rotation period of 2.4954 ± 0.0016 h with an amplitude of 0.14 mag. There were several entries from Warner (2006; 2.4969 h), (2011; 2.4801 h), (2013; 2.4970 h), (2016; 2.498 h). All of these are within the error of our result. This asteroid is a binary (Warner, 2013), but our data do not allow us to verify this.

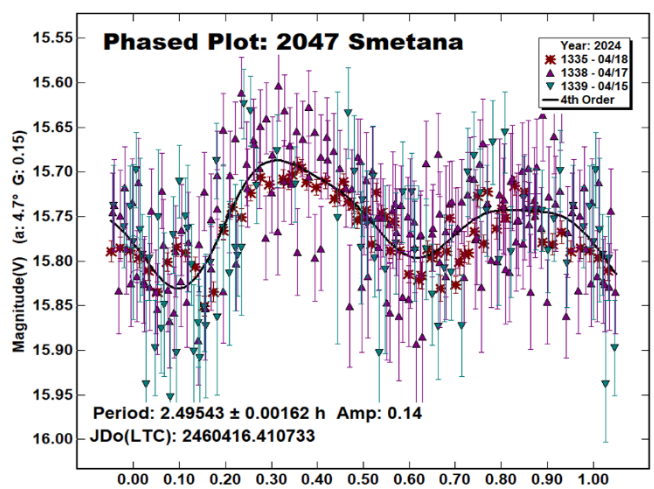

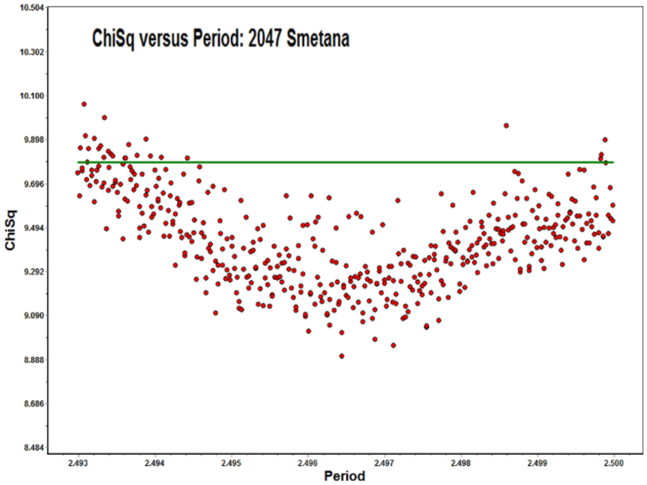

We use our *dense* data those from Warner that were in the ALCDEF database along with *sparse* data from ATLAS (708 pts; 2017/8/3-2024/6/1), Catalina (603 pts; 2005/13/27-2024/5/14), and Palomar (156 pts; 2018/11/21-2022/12/19) to find a sidereal rotation period.

The period with the lowest χ^2 value is 2.4927947 ± 0.000001 h; the error is based on data over the interval between 2006-2024. We think that the binary character of the asteroid prevents a clear convergence. There are not previous data about the sidereal period of this asteroid.

<u>2383 Bradley</u>. This inner main-belt asteroid was discovered on 1981April 5 at Aderson Mesa by E. Bowell. We made observations from 2024 April 4 to May 7. From our data we derived a rotation period of 5.871 ± 0.001 h and an amplitude of 0.53 mag. Warell (2017) found a period of 5.823 h.

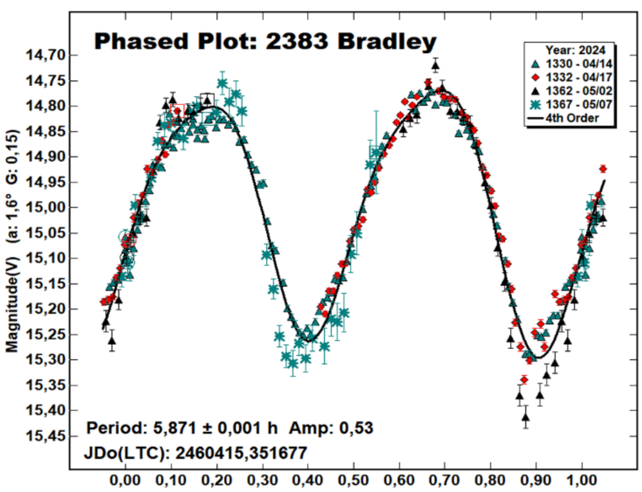

Dense data found in the ALCDEF database were obtained by Farfan, Elias, and Botana from 2024/4/16 to 2024/5/9 were combined with our data and *sparse* data from ATLAS (842 pts; 2018/3/6-2024/7/11), Catalina (444 pts; 2003/12/5-2023/12/31), and Palomar (57 p pts; 2019/1/7-2020/12/21). These led to a sidereal rotation period of 5.8703 ± 0.0002 h, the error being based on the interval 2024 April 16 to September 5. The graph shows a very limited number of results below the 10% line, adding some confidence to our finding. We found no previously reported sidereal periods.

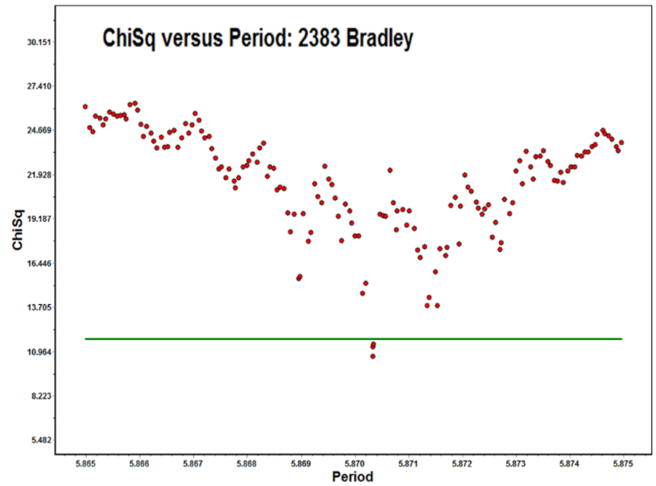

<u>2692 Chkalov</u>. This outer main-belt asteroid was discovered on 1976 December 16 by L.I. Chernykh at Nauchnyj. We made observations from 2024 Jul 12-28. From our data, we derived a rotation period of 6.5914 ± 0.0019 h and an amplitude of 0.13 mag. Garcerán et al. (2016) reported a period of 6.11 h while Pal et al. (2020) determined a sidereal period of 13.1901 h with ATLAS dual band photometry.

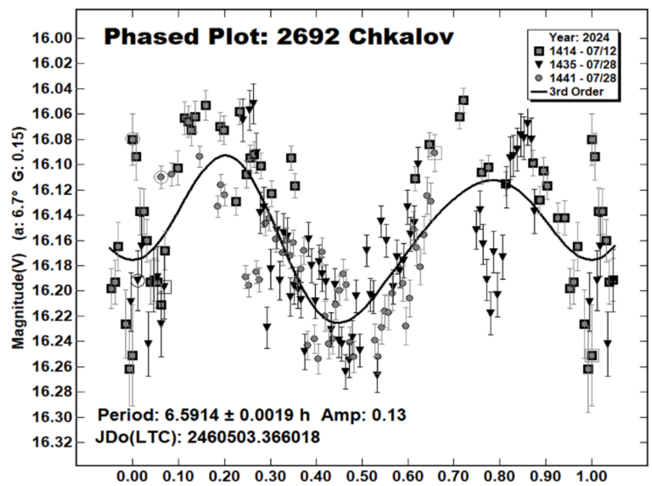

Our *dense* data from 2024 and 2015/7/30-2015/5/8, and those in ALCDEF from Pal et al. (2029/3/2-20219/3/25) were combined with *sparse* data from ATLAS (1038 pts; 2017/8/24-2024/7/11), Catalina (492 pts; 2008/7/21-2023/7/21), and Palomar (75 pts; 2013/12/2-2021/11/24). The inversion method found a sidereal rotation period of 6.587720 ± 0.000002 h. The error is based on data from 2015 September to 2024 June. Note that all of the data points are below the 10% line (found at the very top of the plot). The best that can be said is that at least the sidereal and synodic periods are similar and not aliases of one another.

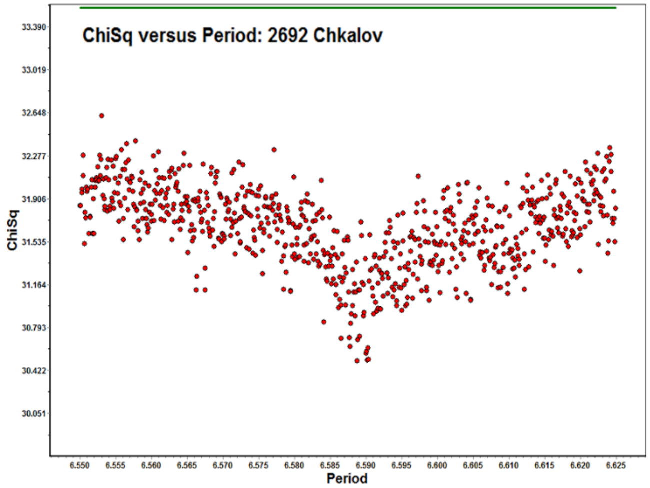

Our *dense* data from 2024 and 2023 1/25 to 4/7 and those in ALCDEF from Warner (2009/4/20-21) and Stephens and Warner (2020/7/26- 29) and *sparse* data from ATLAS (1268 pts; 2017/6/23-2024/7/11), Catalina (485 pts; 2003/12/28-2023/5/8), and Palomar (68 pts; 2018/9/10-2022/2/15) were used in the inversion method to find a sidereal rotation period of 3.56461854 ± 0.000002 h with the error based on data in the interval between 2009 May and 2024 Aug. The plot shows a good convergence by having only two data points below the 10% line. Durech et al. (2020) found a sidereal period of 3.564614 h.

3895 Earhart. This inner main-belt asteroid of the Phocaea family was discovered on 1987 February 23 by C.S. Shoemaker at Palomar. We made observations from 2024 July 9 to August 11. From our data, we derived a synodic rotation period of 3.564716 ± 0.000044 h and an amplitude of 0.54 mag. Behrend (2009web; 2016web; 2020web) found a period of 3.56451 h, 3.56445 h and 3.56501 h, respectively. Skiff (2016web) found 3.5645 h. Other results are Warner (2009, 3.564 h), Aznar Macias et al. (2016, 3.556 h), Stephens and Warner (2021, 3.567 h), and Benishek (2021, 3.5646 h).

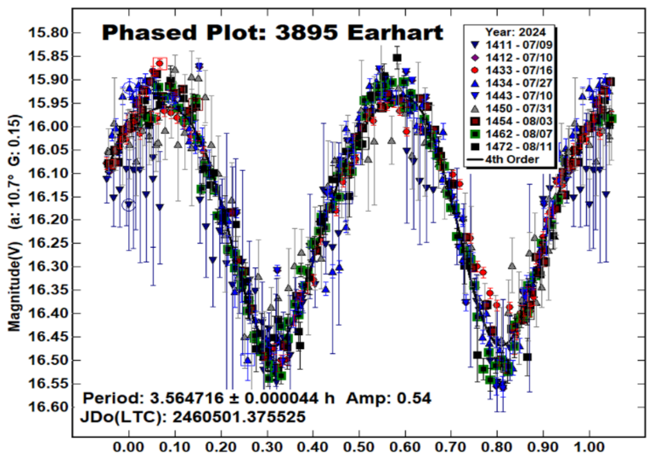

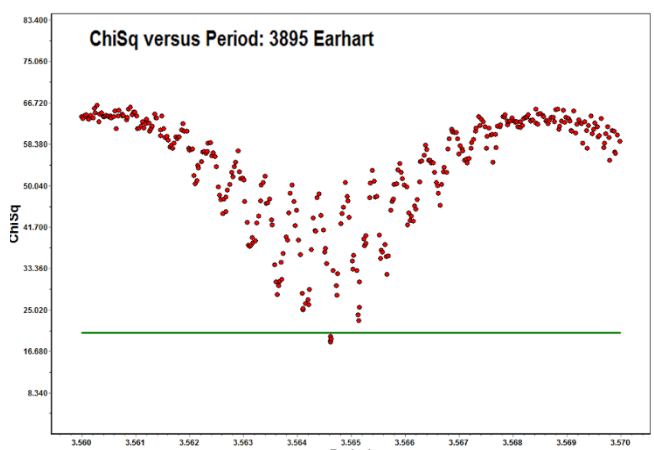

(23512) 1992 PC3. This outer main belt asteroid was discovered on 1992 August 6 at Palomar by H.E. Holt.

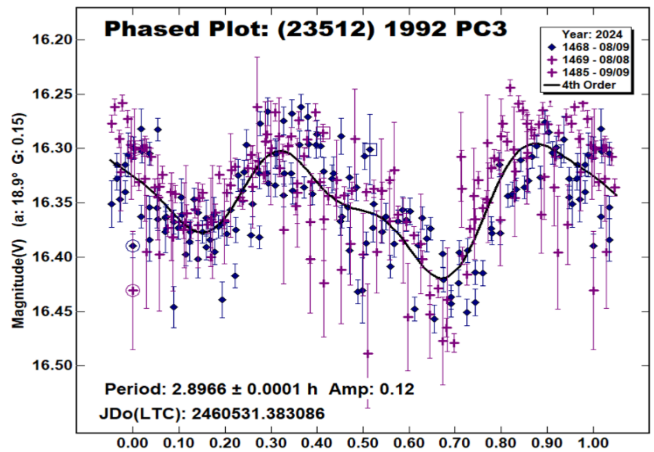

We made observations on 2024 August 9 to September 9. From our data we derive a rotation period of 2.8966 ± 0.0001 h and an amplitude of 0.12 mag. We have not previous information about its rotation period.

(23880) Tongil. This middle main-belt asteroid was discovered on 1998 September 18 at Younchun by T.H. Lee. Our observations from 2024 August 3 to September 4 led to a period of 3.35217 ± 0.00017 h and an amplitude of 0.21mag. We found no other reported rotation period.

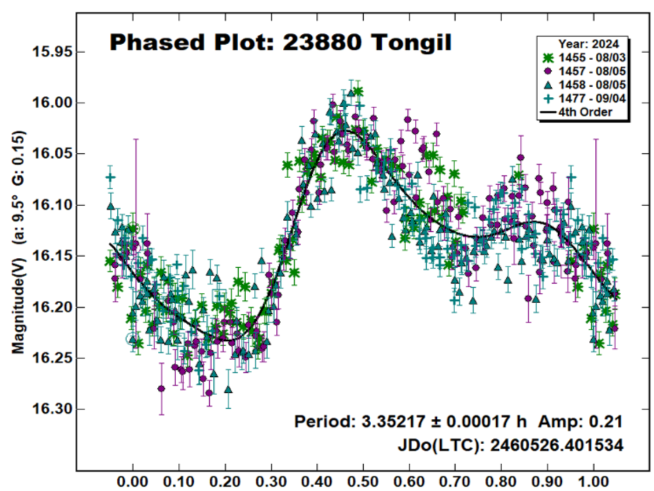

(25330) 1999 KV4. This near-Earth Apollo asteroid was discovered on 1999 May 17 at Catalina. Analysis of observations from 2024 April 12 to May 11 found a period of 4.89998 ± 0.00003 h and an amplitude of 0.06 mag. Pravec et al. (2002web) reported 4.919 h.

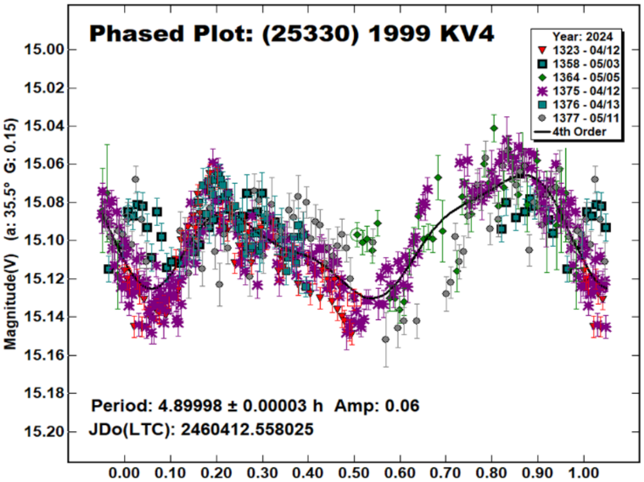

(31545) 1999 DN6. This middle main-belt asteroid was discovered on 1999 February 20 at Socorro by LINEAR. We made observations on 2024 April 13 to May 8. From our data we derived a rotation period of 5.2241 ± 0.0005 h and an amplitude of 0.10 mag. We did not find any previous information about its rotation period.

The large scatter in the low amplitude lightcurve reduces confidence in the solution, despite the asymmetrical shape. As noted by Harris et al. (2014), very low amplitude lightcurves at relatively small phase angles cannot be assumed to be bimodal. There is a *small* possibility that shape really is more symmetrical and that the variations are due to a satellite. A higher quality data set, both noise and more consecutive observing sessions are needed.

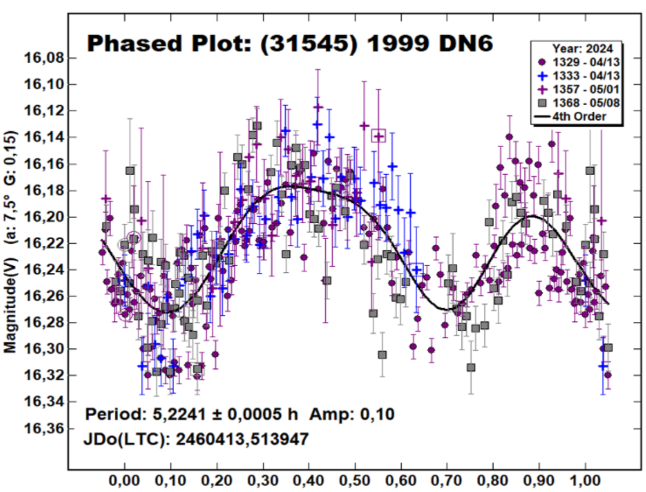

(32459) 2000 SK87 is a middle main-belt asteroid that we observed from 2024 April 10 to May 4. Data analysis a period of 8.3562 ± 0.0008 h with an amplitude of 0.15 mag. A double period of 16.7 h is also a possibility. This appears to be the first period to be reported.

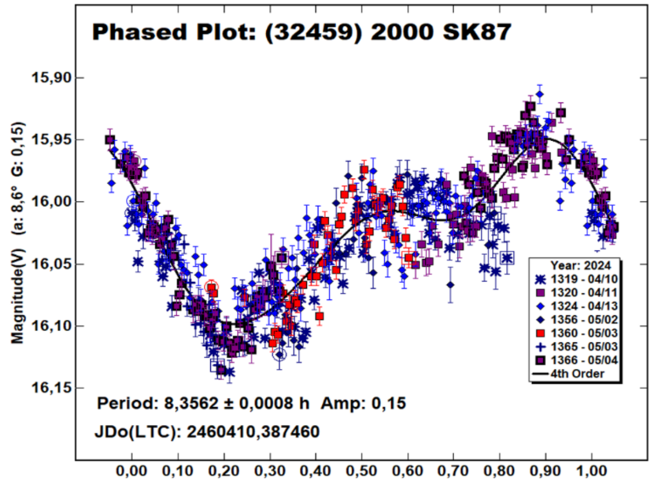

(39489) 1981 EU6. This near-Earth asteroid was discovered in 1981 March at Siding Spring by S.J. Bus. Our observations from 2024 August 1-9 led to a rotation period of 2.41151 ± 0.00028 h and an amplitude of 0.08 mag. Waszczak et al. (2015) found 2.258 h.

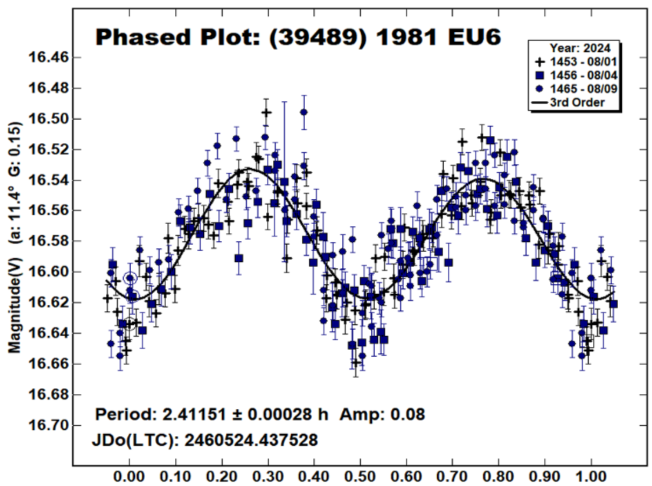

(42449) 3496 T-3. This middle main belt asteroid was discovered in 1977 at Palomar by C.J. van Houten. Analysis of observations made from 2024 September 14-29 determined a period 6.7450 ± 0.0012 h and an amplitude of 0.24 mag. This may be the first period reported.

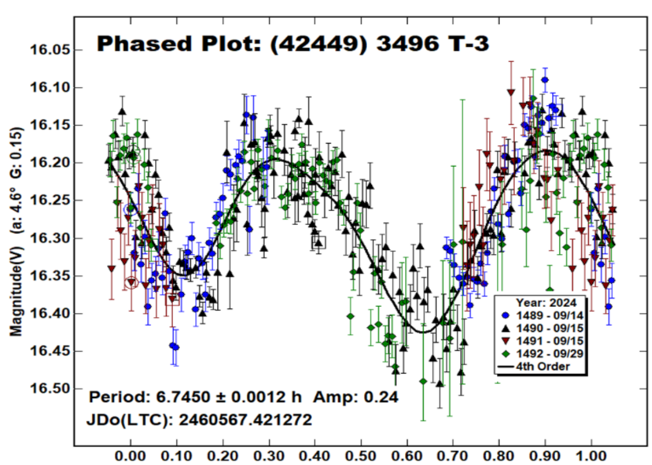

(84833) 2003 AF9. We made observations of this inner main-belt asteroid from 2024 August 7 to September 28 and found a period of 11.9055 ± 0.0005 h and an amplitude of 0.62 mag. We have not previous information about its rotation period.

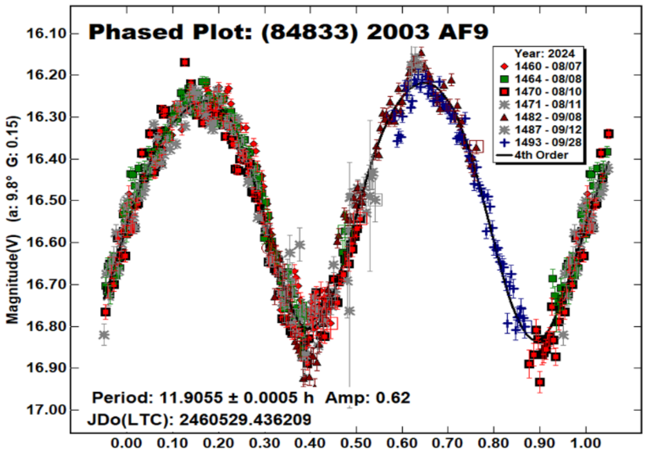

(96720) 1999 LP. This inner main belt asteroid was discovered on 1999 June 4 by LINEAR at Socorro.

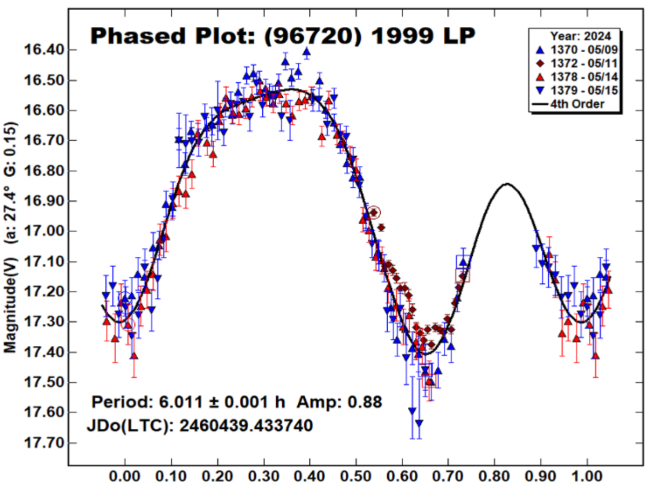

We made observations on 2024 May 9 to 15. From our data we derive a rotation period of 6.011 ± 0.001 h and an amplitude of 0.88 mag. We have not previous information about its rotation period.

(352143) 2007 LR32. This near-Earth asteroid was discovered on 2007 June 15 by LINEAR at Socorro. We made observations on 2024 September 9 to October 1. From our data we derived a rotation period of 2.4175 ± 0.0001 h and an amplitude of 0.11 mag. Behrend (2007web) reported a period of 2.4162 h.

Number	Name	Sidereal Period (h)	P. Error
838	Seraphina	11.724370	0.00005
1762	Rusell	12.793707	0.00005
2047	Smetana	2.4927947	0.000001
2383	Bradley	5.8703	0.0002
2692	Chkalov	6.587720	0.000002
3895	Earhart	3.56461854	0.000002

Table II. Sidereal rotation period obtained from LCINVERT, when available.

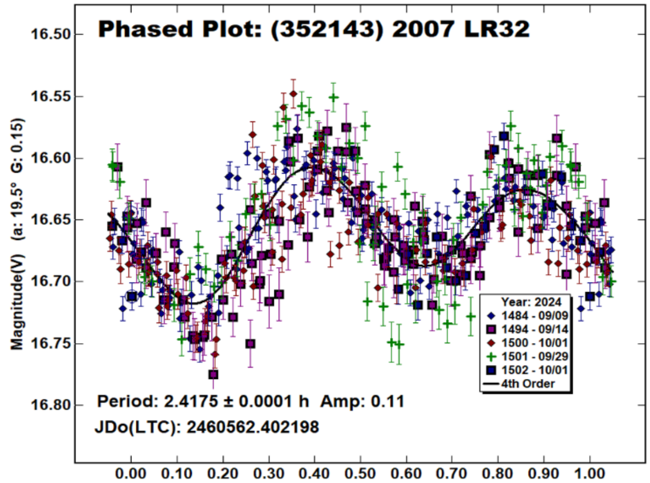

Acknowledgements

We would like to express our gratitude to Brian Warner for supporting the CALL web site and his suggestions.

References

Aznar Macias, A.; Carreno Garceran, A.; Arce Masego, E.; Brines Rodriques, P.; Lozano de Haro, J.; Fornas Silva, A.; Fornas Silva, G.; Mas Martinez, V.; Rodrigo Chiner, O.; Herrero Porta, D. (2016). "Twenty-one Asteroid Lightcurves at Group Observadores de Asteroides (OBAS): Late 2015 to Early 2016." *Minor Planet Bull*. **43**, 257-263.

Behrend, R. (2007web; 2009web; 2016web; 2020web). Observatoire de Geneve web site. *http://obswww.unige.ch/~behrend/page_cou.html*

Benishek, V. (2021). "Photometry of 30 Asteroids at Sopot Astronomical Observatory: 2020 February - October." *Minor Planet Bull*. **48**, 77-83.

Cooney Jr., W.R.; Gross, J.; Terrell, D.; Klinglesmith III, D.A.; Hanowell, J. (2015). "Rotation Period and Lightcurve of 1762 Russell." *Minor Planet Bull*. **42**, 66-67.

Durech, J.; Hanus, J. (2018). "Reconstruction of asteroid spin states from Gaia DR2 photometry." *Astron. Astrophys*. **620**, A91.

Durech, J.; Hanus, J.; Ali-Lagoa, V. (2018). "Asteroid models reconstructed from the Lowell Photometric Database and WISE data." *Astron. Astrophys*. **617**, A57.

Durech, J.; Hanus, J.; Vanco, R. (2019). "Inversion of asteroid photometry from Gaia DR2 and the Lowell Observatory photometric database." *Astron. Astrophys.* **631**, A2.

Durech, J.; Tonry, J.; Erasmus, N.; Denneau, L.; Heinze, A.N.; Flewelling, H.; Vanco, R. (2020). "Asteroid models reconstructed from ATLAS photometry." *Astron. Astrophys*. **643**, A59.

Garceran, A.C.; Aznar, A.; Mansego, E.A.; Rodriguez, P.B.; de Haro, J.L.; Solva, A.F.; Silva, G.F.; Martinez, V.M.; Chiner, O.R. (2016). "Nineteen Asteroids Lightcurves at Asteroids Observers (OBAS) - MPPD: 2015 April - September." *Minor Planet Bull*. **43**, 92-97.

Number	Name	2024/mm/dd	Phase	L_{PAB}	B_{PAB}	Period(h)	P.E.	Amp	A.E.	Grp
838	Seraphina	07/12-07/18	18.1, 6.5	303	12	11.6893	0.0117	0.41	0.05	MB-O
1762	Rusell	04/15-06/04	8.1,18.6	184	1	12.7942	0.0006	0.45	0.05	MB-O
2047	Smetana	04/15-04/18	7.5, 4.7	214	42	2.4954	0.0016	0.14	0.02	MB-M
2383	Bradley	04/14-05/07	1.0,14.2	204	-1	5.871	0.001	0.53	0.05	MB-I
2692	Chkalov	07/12-07/28	6.3, 5.2	300	11	6.5914	0.0019	0.13	0.02	MB-O
3895	Earhart	07/09-08/11	11.0, 8.8	304	15	3.564716	0.00004	0.54	0.05	MB-I
23512	1992 PC3	08/09-09/09	8.5, 9.4	331	13	2.8966	0.0001	0.12	0.02	MB-O
23880	Tongil	08/03-09/04	9.4,10.6	324	11	3.35217	0.00017	0.21	0.02	MB-M
25330	1999 KV4	04/12-05/11	35.7,17.4	213	17	4.89998	0.00003	0.06	0.01	NEA
31545	1999 DN6	04/13-05/08	7.4,14.7	210	13	5.2241	0.0005	0.10	0.01	MB-M
32459	2000 SK87	04/10-05/04	8.5,17.2	196	11	8.3562	0.0008	0.15	0.02	MB-M
39489	1981 EU6	08/01-08/09	19.2,15.9	328	13	2.41151	0.00028	0.08	0.01	NEA
42449	3496 T-3	09/14-09/29	4.1, 6.9	355	4	6.7450	0.0012	0.24	0.05	MB-M
84833	2003 AF9	08/07-09/28	9.5,26.9	325	16	11.9055	0.0005	0.62	0.05	MB-I
96720	1999 LP	05/09-05/15	27.2,26.3	239	35	6.011	0.001	0.88	0.05	MB-I
352143	2007 LR32	09/09-10/01	32.0,28.2	356	22	2.4175	0.0001	0.11	0.02	NEA

Table III. Synodic Periods. Observing circumstances and results. The phase angle values are for the first and last date. L_{PAB} and B_{PAB} are the approximate phase angle bisector longitude and latitude at mid-date range (see Harris et al., 1984). Grp is the asteroid family/group (Warner et al., 2009). MB-I/O: Main-belt inner/outer; NEA: Near Earth Asteroid; MC: Mars-Crosser.

Harris, A.W.; Young, J.W.; Scaltriti, F.; Zappala, V. (1984). “Lightcurves and phase relations of the asteroids 82 Alkmene and 444 Gyptis.” *Icarus* **57**, 251-258.

Harris, A.W.; Pravec, P.; Galad, A.; Skiff, B.A.; Warner, B.D.; Vilagi, J.; Gajdos, S.; Carbognani, A.; Hornoch, K.; Kusnirak, P.; Cooney, W.R.; Gross, J.; Terrell, D.; Higgins, D.; Bowell, E.; Koehn, B.W. (2014). “On the maximum amplitude of harmonics on an asteroid lightcurve.” *Icarus* **235**, 55-59.

Kaasalainen, M. (2001). “Interpretation of lightcurves of precessing Asteroids.” *Astron. Astrophys.* **376**, 302–309. doi:10.1051/0004-6361:20010935.

Kaasalainen, M.; Torppa, J. (2001). “Optimization Methods for Asteroid Lightcurve Inversion. I Shape detemination.” *Icarus* **143**, 24-36.

Kaasalainen, M.; Torppa, J.; Muinonen, K. (2001). “Optimization Methods for Asteroid Lightcurve Inversion. II The complete Inversion Problem.” *Icarus* **153**, 37-51.

Pal, A.; Szakáts, R.; Kiss, C.; Bódi, A.; Bognár, Z.; Kalup, C.; Kiss, L.L.; Marton, G.; Molnár, L.; Plachy, E.; Sárneczky, K.; Szabó, G.M.; Szabó, R. (2020). “Solar System Objects Observed with TESS - First Data Release: Bright Main-belt and Trojan Asteroids from the Southern Survey.” *Ap. J. Suppl Ser*. **247**, id. 26.

Pravec, P.; Wolf, M.; Sarounova, L. (2002web). *http://www.asu.cas.cz/~ppravec/neo.htm*

Skiff, B.A. (2016). Posting on CALL web site. *https://minorplanet.info/php/call.php*

Slivan, S.M.; Colclasure, A.; Escobedo, I.; Henopp, A.; Knight, R.; Mitchell, A.; Wilkin, F (2022). “Synodic and Sidereal Rotation Periods of Koronis Family Member (1762) Russell.” *Minor Planet Bull*. **49**, 71-73.

Stephens, R.D.; Warner, B.D. (2021). “Main-belt Asteroids Observed from CS3: 2020 July to September.” *Minor Planet Bull.* **48**, 56-69.

Warner, B.D. (2006). “Asteroid lightcurve analysis at the Palmer Divide Observatory - March - June 2006.” *Minor Planet Bull*. **33**, 85-88.

Warner, B.D. (2009). “Asteroid Lightcurve Analysis at the Palmer Divide Observatory: 2009 March-June.” *Minor Planet Bull*. **36**, 172-176.

Warner, B.D. (2011). “Asteroid Lightcurve Analysis at the Palmer Divide Observatory: 2010 December - 2011 March.” *Minor Planet Bull*. **38**, 142-149.

Warner, B.D. (2013). “Seeing Double Old and New: Observations and Lightcurve Analysis at the Palmer Divide Observatory of Six Binary Asteroids.” *Minor Planet Bull*. **40**, 94-98.

Warner, B.D. (2016). “Asteroid Lightcurve Analysis at CS3-Palmer Divide Station: 2016 April - July.” *Minor Planet Bull*. **43**, 300-304.

Warner, B.D.; Harris, A.W.; Pravec, P. (2009). “The Asteroid Lightcurve Database.” *Icarus* **202**, 134-146. Updated 2023 April. *https://minorplanet.info/php/lcdb.php*

Warner, B.D.; Harris, A.W.; Durech J.; Lance A.M. (2024). “Lightcurve Photometry Opportunities: 2024 July - September.” *Minor Planet Bull*. **51**, 293-296.

Warell, J. (2017). “Lightcurve Observations of Nine Main-belt Asteroids.” *Minor Planet Bull.* **44**, 304-305.

Waszczak, A.; Chang, C.-K.; Ofek, E.O.; Laher, R.; Masci, F.; Levitan, D.; Surace, J.; Cheng, Y.-C.; Ip, W.-H.; Kinoshita, D.; Helou, G.; Prince, T.A.; Kulkarni, S. (2015). “Asteroid Light Curves from the Palomar Transient Factory Survey: Rotation Periods and Phase Functions from Sparse Photometry.” *Astron. J.* **150**, A75.

PHOTOMETRY OF 24 ASTEROIDS FROM SOPOT ASTRONOMICAL OBSERVATORY: 2024 MARCH - OCTOBER

Vladimir Benishek
Belgrade Astronomical Observatory
Volgina 7, 11060 Belgrade 38, SERBIA
vlaben@yahoo.com

(Received: 2024 October 15)

Lightcurves and synodic rotation periods for 24 asteroids are derived from photometric data obtained at Sopot Astronomical Observatory during 2024 March - October.

Photometric observations of 24 asteroids were conducted at Sopot Astronomical Observatory (SAO) from 2024 March through October in order to determine the asteroids' synodic rotation periods. For this purpose, two 0.35-m *f*/6.3 Meade LX200GPS Schmidt-Cassegrain telescopes were employed. The telescopes are equipped with a SBIG ST-8 XME and a SBIG ST-10 XME CCD cameras. The exposures were unfiltered and unguided for all targets. Both cameras were operated in 2×2 binning mode, which produces image scales of 1.66 arcsec/pixel and 1.25 arcsec/pixel for ST-8 XME and ST-10 XME cameras, respectively. Prior to measurements, all images were corrected using dark and flat field frames.

Photometric reduction was conducted using *MPO Canopus* (Warner, 2018). Differential photometry with up to five comparison stars of near solar color ($0.5 \leq B\text{-}V \leq 0.9$) was performed using the Comparison Star Selector (CSS) utility. This helped ensure a satisfactory quality level of night-to-night zero-point calibrations and correlation of the measurements within the standard magnitude framework. Field comparison stars were calibrated using standard Cousins R magnitudes derived from the Carlsberg Meridian Catalog 15 (VizieR, 2024) Sloan r' magnitudes using the formula: $R = r' - 0.22$ in all cases presented in this paper. In some instances, small zero-point adjustments were necessary in order to achieve the best match between individual data sets in terms of achieving the most favorable statistical indicators of Fourier fit goodness.

Lightcurve construction and period analysis was performed using *Perfindia* custom-made software developed in the R statistical programming language (R Core Team, 2020) by the author of this paper. The essence of its algorithm is reflected in finding the most favorable solution for rotation period by minimizing the *residual standard error* of the lightcurve Fourier fit.

The lightcurve plots presented in this paper show so-called 2% error for rotation periods, i.e. an error that would cause the last data point in a combined data set by date order to be shifted by 2% (Warner, 2012) and represented by the following formula:

$$\Delta P = (0.02 \cdot P^2) / T$$

where P and T are the rotation period and the total time span of observations, respectively. Both of these quantities must be expressed in the same units. Table I gives the observing circumstances and results.

Observations and results

<u>1739 Meyermann</u>. A bimodal solution for a rotational period of $P = 2.821 \pm 0.006$ h, obtained from observations performed on two consecutive nights in 2024 August, statistically matches virtually all previously found period results present in the Asteroid Lightcurve Database (LCDB; Warner et al., 2009). Some of those previous period results are as follows: 2.8219 h (Pravec, 2007web), 2.82146 h (Behrend, 2020web), 2.821 h (Pravec, 2021web).

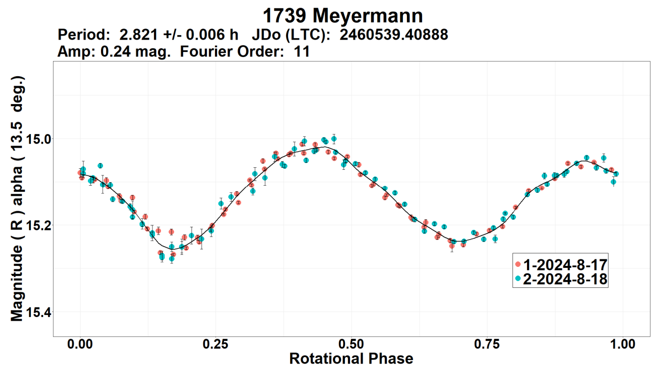

<u>1740 Paavo Nurmi</u>. According to the LCDB records, there were no rotation period determinations for this asteroid previously. Photometric observations carried out over three consecutive nights in early 2024 August show a period of $P = 4.649 \pm 0.009$ h.

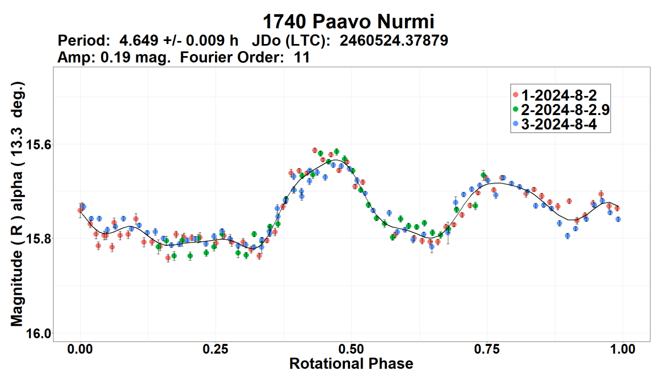

<u>1779 Parana</u>. No records on previous rotation period results for this asteroid were found. A period of $P = 3.9210 \pm 0.0007$ h associated with a low-amplitude lightcurve ($A = 0.08$ mag.) and obtained from the five-night 2024 July dataset, emerges as a statistically most favorable solution in the period analysis. More thorough observations of this asteroid in future apparitions would be expressly desired for the sake of verification of this currently only rotation period result.

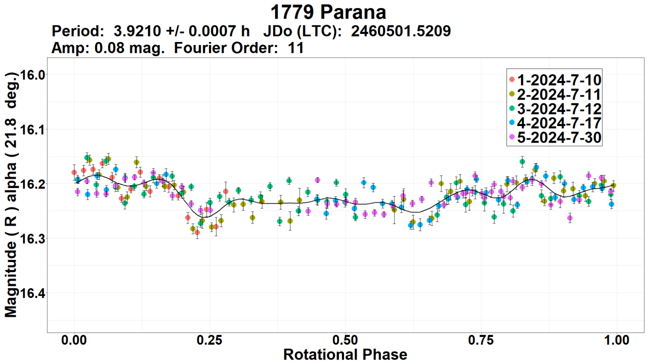

1842 Hynek. Period of $P = 3.998 \pm 0.002$ h obtained from the SAO observations conducted over three nights in 2024 April-May, although sufficiently close to the most of the previous results in the LCDB ranged between 3.94 h and 3.943 h still shows some deviation from them, which is most likely a consequence of the shortness of two of the three individual datasets, as well as partially fragmentary data and the lack of repeated data coverage of the entire rotational cycle due to bad weather conditions and the inability to focus exclusively on this target.

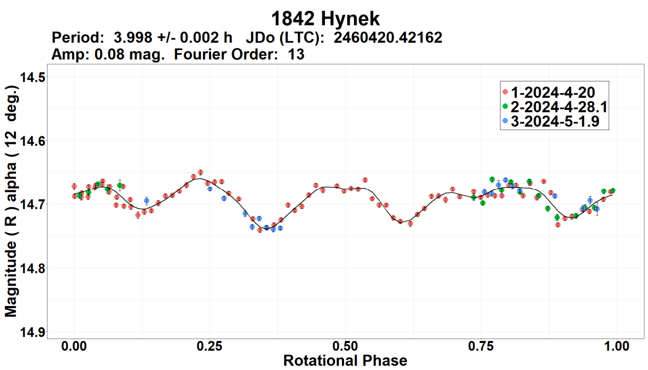

2680 Mateo. Another asteroid with no known rotation period. Period analysis of dense photometric data obtained on three nights in 2024 September-October strongly suggests as the most likely solution a trimodal lightcurve with a period of $P = 3.3130 \pm 0.0005$ h.

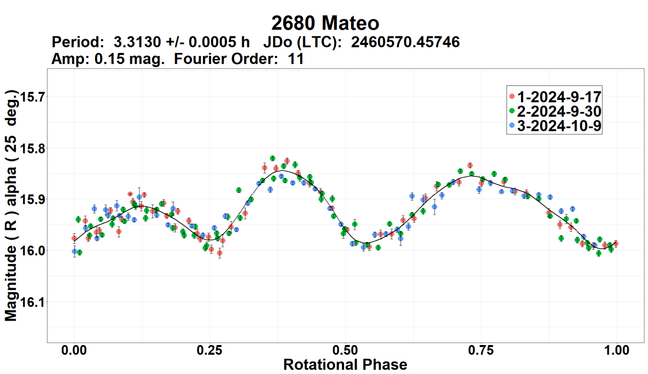

3429 Chuvaev. A bimodal solution for a period of $P = 3.365 \pm 0.002$ h matches exactly the only previously found period result of 3.365 h by Waszczak et al. (2015).

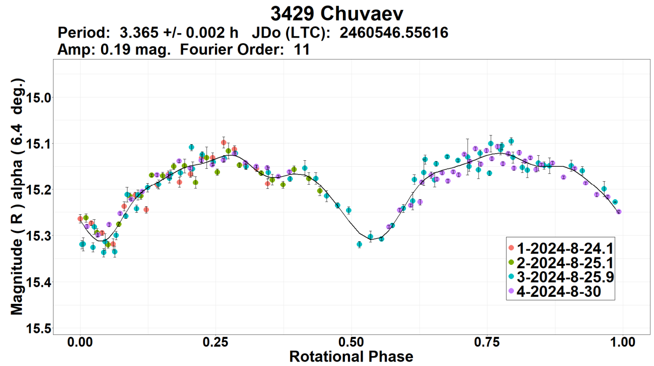

3654 AAS. According to the LCDB records this is the first rotation period determination for this asteroid. Period analysis conducted upon the data acquired on three nights in 2024 September-October yielded a bimodal period solution of $P = 3.548 \pm 0.002$ h.

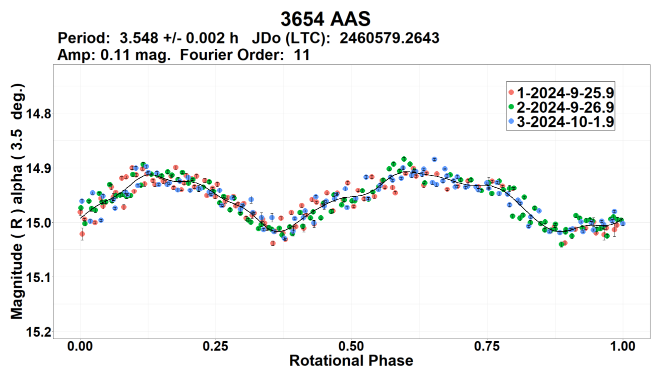

4189 Sayany. Pal et al. (2020) found the only previous rotation period result of 2.76132 h, which matches the value of $P = 2.7604 \pm 0.0006$ found from the 2024 June data.

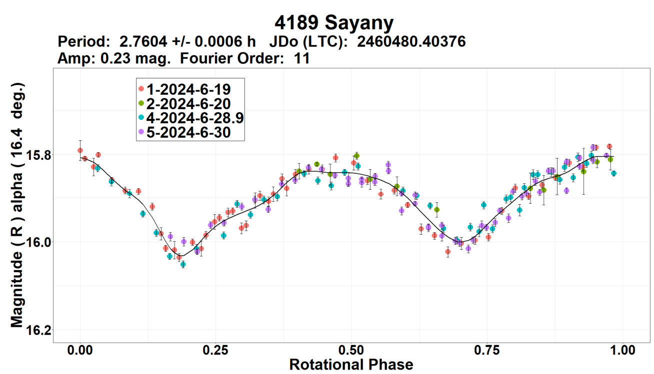

4228 Nemiro. Data obtained over six nights in 2024 July-August revealed a very low amplitude lightcurve ($A = 0.04$ mag.) and a period of $P = 2.7868 \pm 0.0005$ h. The result found is largely consistent with the only previous period result of 2.772 ± 0.003 h by Pravec (2007web).

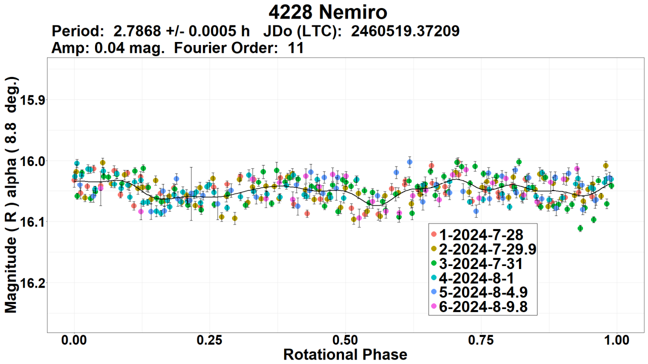

5181 SURF. Observations from two consecutive nights in early 2024 October show a bimodal solution and a period of $P = 6.11 \pm 0.03$ h, which is highly consistent with two previously found rotation periods of 6.111 h (Hayes-Gehrke et al., 2015) and 6.1097 h (Pravec, 2015web).

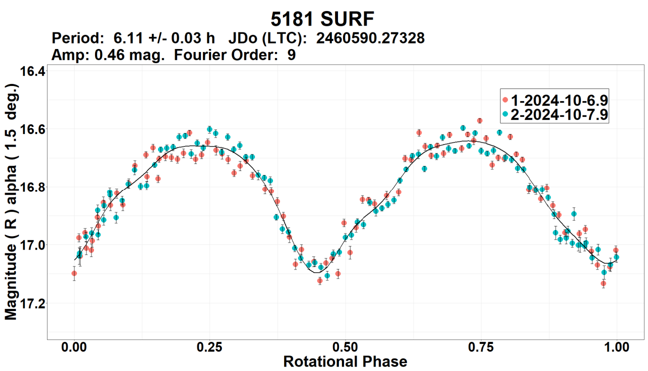

6922 Yasushi. Erasmus et al. (2020) found a rotation period of 3.434 h, identical to that derived from the SAO observations from two nights in the first half of 2024 March: $P = 3.434 \pm 0.003$ h.

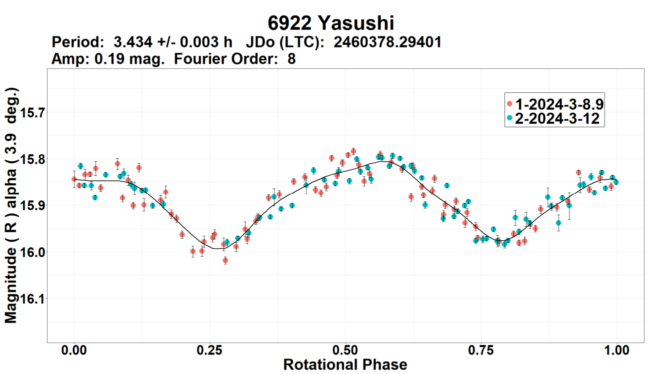

7159 Bobjoseph. Prior to this rotation period determination, there were no period results reported. Dense photometric data acquired in 2024 September-October indicate a bimodal period solution of $P = 4.113 \pm 0.002$ h.

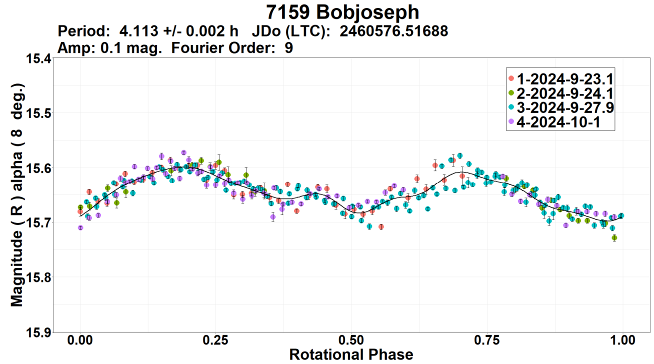

(8162) 1990 SK11. A low-amplitude lightcurve ($A = 0.08$ mag.) phased to a period of $P = 4.550 \pm 0.006$ h was found to be the most favorable solution in period analysis conducted on the data obtained on three nights in 2024 October.

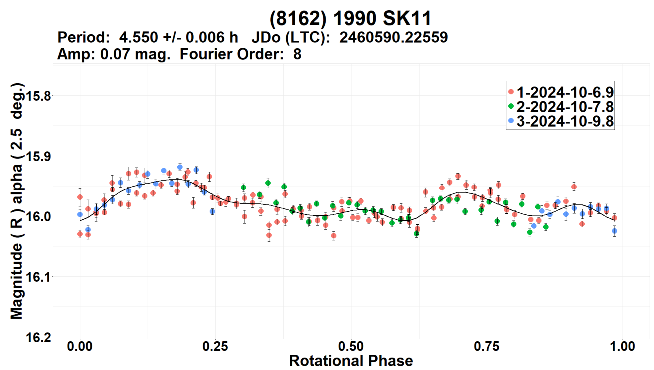

8577 Choseikomori. A bimodal period of $P = 5.573 \pm 0.006$ h derived from the 2024 June SAO observations statistically matches the only previously determined period by Pal et al. (2020, 5.57121 h).

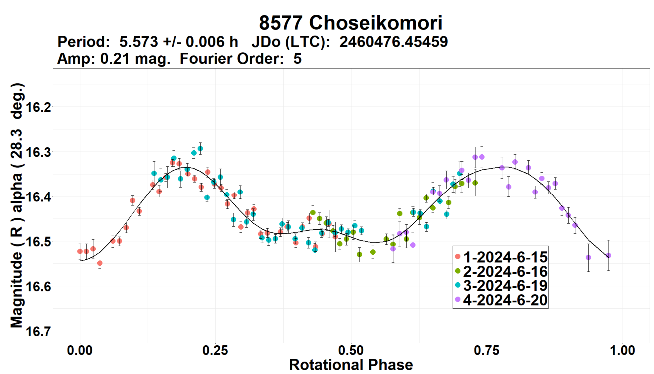

(8692) 1992 WH. A bimodal period value ($P = 4.69 \pm 0.02$ h) found using the 2024 August SAO data collected on two consecutive nights is in good agreement with two previous results by Waszczak et al. (2015, 4.698 h) and by Pal et al. (2020, 4.68562 h).

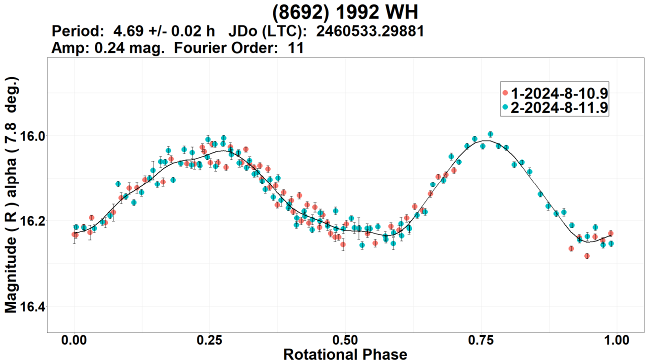

(9302) 1985 TB3. A bimodal rotation period of P = 3.059 ± 0.001 h derived from a dense photometric dataset taken in 2024 September is identical to the only previously reported result by Waszczak et al. (2015, 3.059 h).

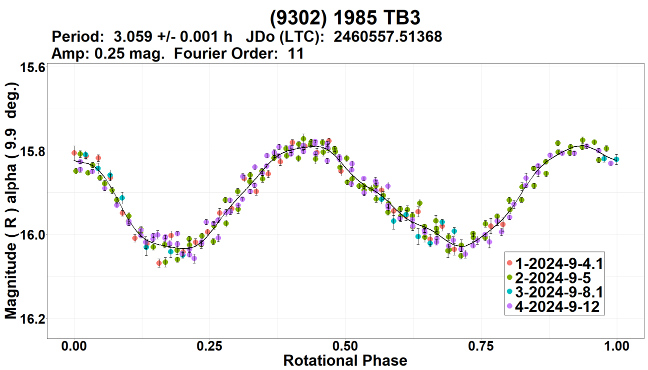

10332 Defi. Dense photometry performed over six nights in 2024 late June - early July unambiguously indicates a period of P = 2.8403 ± 0.0007 h as the most favorable solution. The only previously reported solution derived from sparse photometry by Pal et al. (2020, 20.5142 h) shows a significant discrepancy with the newly established value.

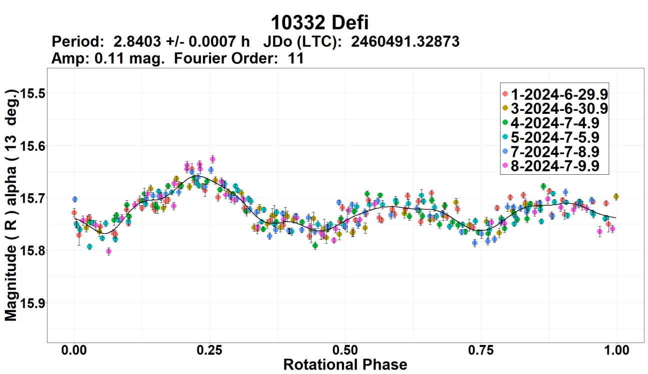

(15254) 1990 QM4. Waszczak et al. (2015) found a period of 2.318 h. A bimodal period of P = 4.632 ± 0.003 h was derived as a solution from the SAO observations in 2024 April-May, which is exactly twice the value found by Wasczak et al. The lightcurve corresponding to a longer period is characterized by two distinctive maxima, different in shape and intensity, and the splitting of the lightcurve into two equal halves indicates their apparent mismatch. The maximum difference in the intensity of the two halves of the lightcurve reaches ~ 0.05 mag., which is not negligible and cannot be the result of noise, which is certainly well below this level. These facts are in favor of a longer period of 4.632 h over the previously derived half-shorter period of 2.318 h. Certainly, it would be very desirable to continue observing this asteroid in the future apparitions in order to definitively resolve period ambiguity.

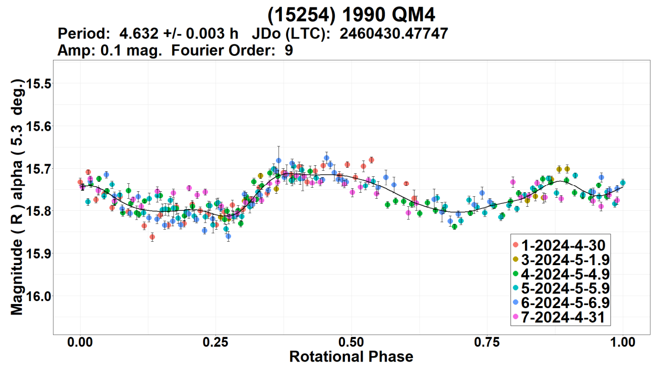

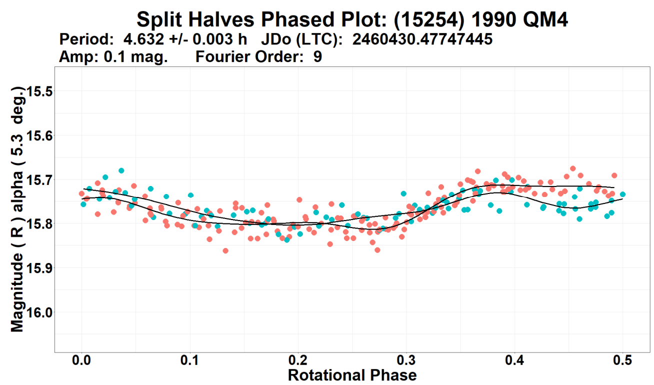

(16161) 2000 AC68. No previous rotation period determinations were found in the LCDB. Photometric data from 2024 June show a bimodal period solution of P = 3.970 ± 0.003 h.

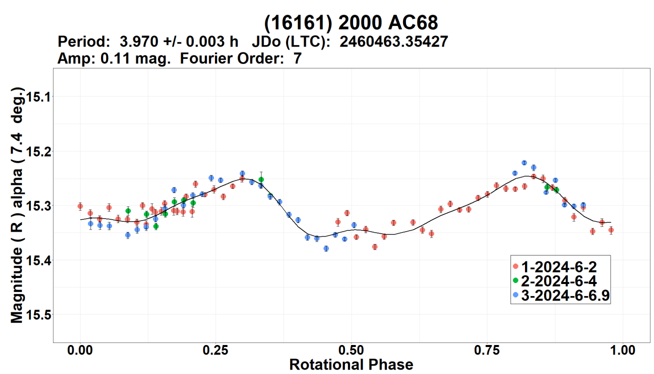

(25330) 1999 KV4. Although the 2024 April 2024 SAO data obtained over two consecutive nights did not cover a large portion of the rotation cycle twice, the result for the period (P = 4.93 ± 0.02 h) derived from such a combined dataset shows very good agreement with the only previously found rotation period by Pravec (2002web, 4.919 h).

Number	Name	20yy/mm/dd	Phase	L_{PAB}	B_{PAB}	Period (h)	P.E.	Amp	A.E.	Grp
1739	Meyermann	24/08/16-24/08/18	13.5,12.9	346	3	2.821	0.006	0.24	0.03	MB-I
1740	Paavo Nurmi	24/08/01-24/08/04	13.3,12.3	332	1	4.649	0.009	0.19	0.02	MB-I
1779	Parana	24/07/10-24/07/30	21.8,11.6	322	1	3.9210	0.0007	0.08	0.03	MB-I
1842	Hynek	24/04/19-24/05/01	12.0, 6.7	227	8	3.998	0.002	0.08	0.01	MB-I
2680	Mateo	24/09/16-24/10/09	25.0,16.2	41	2	3.3130	0.0005	0.15	0.02	HER
3429	Chuvaev	24/08/24-24/08/30	6.4, 2.7	340	1	3.365	0.002	0.19	0.03	MB-I
3654	AAS	24/09/25-24/10/02	*3.5, 1.0	8	1	3.548	0.002	0.11	0.02	MB-I
4189	Sayany	24/06/18-24/06/30	16.4,11.4	294	8	2.7604	0.0006	0.23	0.03	V
4228	Nemiro	24/07/27-24/08/09	*8.8, 5.4	316	8	2.7868	0.0005	0.04	0.03	MB-I
5181	SURF	24/10/06-24/10/08	1.5, 1.7	13	-3	6.11	0.03	0.46	0.03	HER
6922	Yasushi	24/03/08-24/03/12	3.9, 2.9	173	4	3.434	0.003	0.19	0.03	FLOR
7159	Bobjoseph	24/09/23-24/10/01	8, 3.2	11	3	4.113	0.002	0.10	0.02	MB-I
8162	1990 SK11	24/10/06-24/10/09	2.5, 3.6	12	4	4.550	0.006	0.07	0.02	MB-I
8577	Choseikomori	24/06/14-24/06/20	28.3,27.2	312	9	5.573	0.006	0.21	0.04	MB-I
8692	1992 WH	24/08/10-24/08/12	7.8, 7.2	328	8	4.69	0.02	0.24	0.03	V
9302	1985 TB3	24/09/04-24/09/12	9.9, 4.9	356	0	3.059	0.001	0.25	0.02	MB-I
10332	Defi	24/06/09-24/07/10	*13.0,12.4	285	21	2.8403	0.0007	0.11	0.02	MB-I
15254	1990 QM4	24/04/29-24/05/07	*5.3, 5.9	222	8	4.632	0.003	0.10	0.03	MB-I
16161	2000 AC68	24/06/01-24/06/06	*7.4, 7.6	252	11	3.970	0.003	0.11	0.02	MB-I
25330	1999 KV4	24/04/25-24/04/27	17.5,16.6	213	12	4.93	0.02	0.12	0.03	NEA
45375	2000 AZ115	24/08/10-24/08/12	14.8,14.3	330	15	3.182	0.005	0.35	0.03	MB-I
66251	1999 GJ2	24/08/20-24/08/24	34.3,32.7	343	22	2.461	0.002	0.11	0.02	NEA
67976	2000 XA7	24/07/26-24/08/07	11.9, 8.7	319	12	6.306	0.003	0.18	0.03	MB-I
70410	1999 SE3	24/06/28-24/07/16	28.9,26.3	317	30	2.5890	0.0004	0.14	0.03	PHO

Table I. Observing circumstances and results. Phase is the solar phase angle given at the start and end of the date range. If preceded by an asterisk, the phase angle reached an extrema during the period. L_{PAB} and B_{PAB} are the average phase angle bisector longitude and latitude at the mid-date range (see Harris et al., 1984). Grp is the asteroid family/group (Warner et al., 2009): MB-I = main-belt inner, NEA = near-Earth asteroid, V = Vestoid, PHO = Phocaea, HER = Hertha, FLOR = Flora.

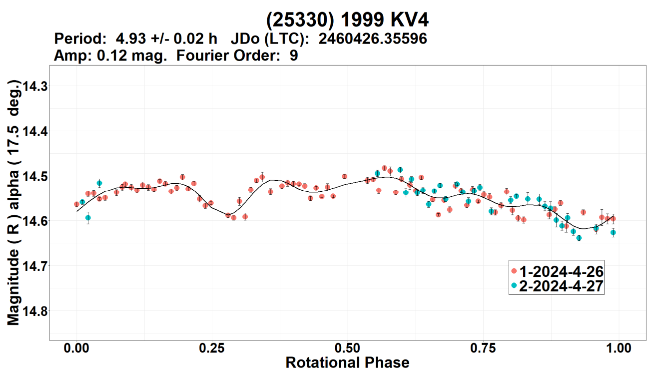

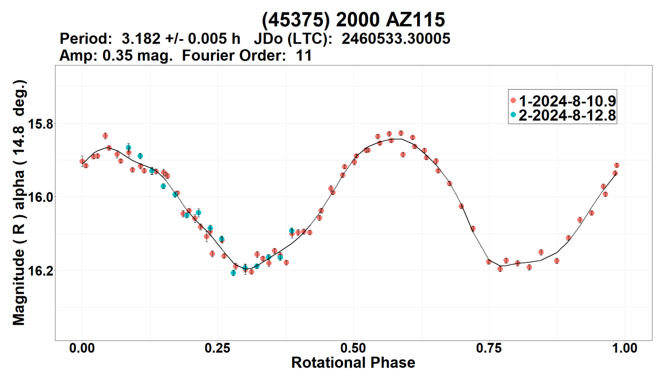

(45375) 2000 AZ115. Another main-belt asteroid with no previously known rotation period. Dense photometry from two nights in 2024 August points to a bimodal period solution of $P = 3.182 \pm 0.005$ h and a fairly large lightcurve amplitude of 0.35 mag., at a relatively low solar phase angles. Nevertheless, despite the dense photometric data, it should be noted that a large part of the rotation cycle for the obtained period is covered by observations only once, so this period result should be treated with a certain degree of caution. Refinement of the period result obtained in the 2024 apparition would be highly desirable in the future.

(66251) 1999 GJ2. Previously established rotation period results by Pravec (2005web, 2.4621 h; 2022web, 2.4614 h and 2.4629 h) for this near-Earth asteroid are in good agreement with the period value ($P = 2.461 \pm 0.002$ h) found from dense photometric data collected at SAO during two nights in late 2024 August. The 2024 result is somewhat different from the value found by Warner and Stephens (2022, 2.573 h) from the observations done in 2022 June.

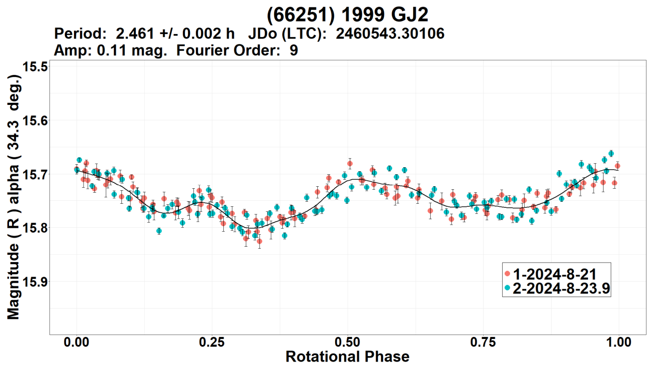

(67976) 2000 XA7. The only previous rotation period is from Pal et al. (2020, 26.4765 h), derived from sparse photometric data. Dense photometric observations at SAO in 2024 July - August indicate the complete incorrectness of the previous result, yielding an unequivocal bimodal period solution of $P = 6.306 \pm 0.003$ h.

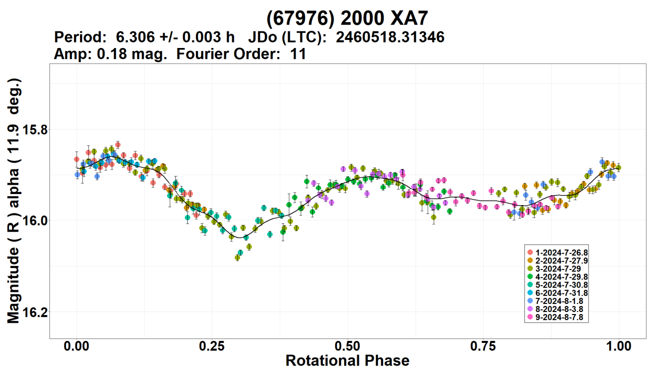

(70410) 1999 SE3. The newly established value for the rotation period ($P = 2.5890 \pm 0.0004$ h) from dense photometric data accumulated over as many as 15 nights in 2024 June-July confirms the earlier results by Stephens (2014, 2.5895 h) and by Waszczak et al. (2015, 2.590 h).

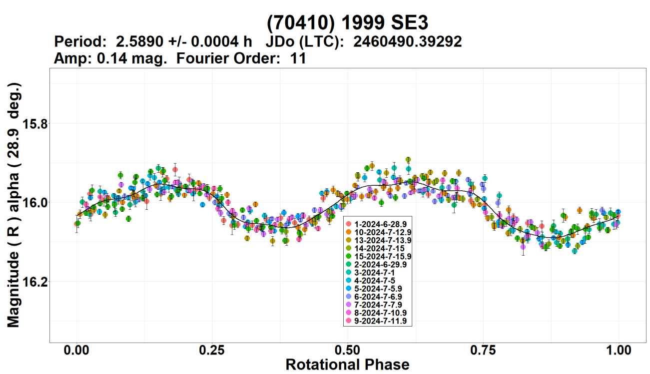

Acknowledgements

Observational work at Sopot Astronomical Observatory is generously supported by Gene Shoemaker NEO Grants awarded by the Planetary Society in 2018 and 2022.

References

Behrend, R. (2020web). Observatoire de Geneve web site. *http://obswww.unige.ch/~behrend/page_cou.html*

Erasmus, N.; Navarro-Meza, S.; McNeill, A.; Trilling, D.E.; Sickafoose, A.A.; Denneau, L.; Flewelling, H.; Heinze, A.; Tonry, J.L. (2020). "Investigating Taxonomic Diversity within Asteroid Families through ATLAS Dual-band Photometry." *Astrophys. J. Suppl. Ser.* **247**, A13.

Harris, A.W.; Young, J.W.; Scaltriti, F.; Zappala, V. (1984). "Lightcurves and phase relations of the asteroids 82 Alkmene and 444 Gyptis." *Icarus* **57**, 251-258.

Hayes-Gehrke, M.N.; Afe, A.; Cha, D.; Cotton, A.; Diedrick, J.; Liu, K.; Livas, M.; Melone, K.; Mistry, S.; Murphy, J.; Ren, X.; Romano, P.; Scearce, M.; Smith, A.; Summers, B. (2015). "Lightcurve Analysis of 5181 SURF." *Minor Planet Bull.* **42**, 245.

Pal, A.; Szakáts, R.; Kiss, C.; Bódi, A.; Bognár, Z.; Kalup, C.; Kiss, L.L.; Marton, G.; Molnár, L.; Plachy, E.; Sárneczky, K.; Szabó, G.M.; Szabó, R. (2020). "Solar System Objects Observed with TESS - First Data Release: Bright Main-belt and Trojan Asteroids from the Southern Survey." *Ap. J. Supl. Ser.* **247**, 26-34.

Pravec, P. (2002web, 2005web, 2007web, 2015web, 2021web, 2022web). Photometric Survey for Asynchronous Binary Asteroids web site. *http://www.asu.cas.cz/~ppravec/newres.txt*

R Core Team (2020). R: A language and environment for statistical computing. R Foundation for Statistical Computing. Vienna, Austria. *https://www.R-project.org/*

Stephens, R.D. (2014). "Asteroids Observed from CS3: 2014 April - June." *Minor Planet Bull.* **41**, 226-230.

VizieR (2024). *http://vizier.u-strasbg.fr/viz-bin/VizieR*

Warner, B.D.; Harris, A.W.; Pravec, P. (2009). "The Asteroid Lightcurve Database." *Icarus* **202**, 134-146. Updated 2023 Oct. *http://www.minorplanet.info/lightcurvedatabase.html*

Warner, B.D. (2012). The MPO Users Guide: A Companion Guide to the MPO Canopus/PhotoRed Reference Manuals. BDW Publishing, Eaton, CO.

Warner, B.D. (2018). MPO Canopus software, version 10.7.11.3. *http://www.bdwpublishing.com*

Warner, B.D.; Stephens, R.D. (2022). "Near-Earth Asteroid Lightcurve Analysis at the Center for Solar System Studies: 2022 March - June." *Minor Planet Bull.* **49**, 274-279.

Waszczak, A.; Chang, C.-K.; Ofek, E.O.; Laher, R.; Masci, F.; Levitan, D.; Surace, J.; Cheng, Y.-C.; Ip, W.-H.; Kinoshita, D.; Helou, G.; Prince, T.A.; Kulkarni, S. (2015). "Asteroid Light Curves from the Palomar Transient Factory Survey: Rotation Periods and Phase Functions from Sparse Photometry." *Astron. J.* **150**, A75.

LIGHTCURVES OF TWENTY-TWO ASTEROIDS

Geoffrey Stone
Dimension Point Observatory (V42)
14 Galaxy Point, Mayhill, NM 88339
geoff@first-light-systems.com

(Received: 2024 October 14 Revised: 2024 November 19)

We present lightcurves and synodic rotation periods for twenty-two asteroids.

Photometric observation of these minor planets was conducted from 2023 October through 2024 October at Dimension Point Observatory (MPC V42) located near Mayhill, NM.

Images were acquired using PlaneWave Instruments 0.43-m *f*/6.8 and 0.61-m *f*/6.5 Corrected Dall-Kirkham telescopes on PlaneWave Instruments L-500 and L-600 mounts. Image acquisition was with a Finger Lakes Instrumentation Kepler KL400 back-illuminated CMOS camera. The equipment was operated remotely using *ACP Expert* (Denny, 2024) and *MaximDL* (George, 2021).

Target selection and planning was performed using the authors own Python scripts. Orbital elements, ephemeris and other information were obtained from the Minor Planet Center (MPC) (*http://www.minorplanet.net),* the JPL Solar System Dynamics (*http://ssd.jpl.nasa.gov*) and the Lowell Observatory Minor Planet Services (*http://asteroid.lowell.edu*) websites and the LCDB database (Warner et al., 2009).

Images were made unguided in HDR mode, either unfiltered or with a yellow long-pass blue-blocking filter, utilizing camera internal stacking every 30 seconds. Exposure duration varied based on the target brightness and apparent motion but was typically 120 seconds.

Image calibration, plate solving, measurement and period analysis were performed using *Tycho-Tracker* V11 (Parrott, 2024). Comparison stars of near solar color were chosen from the ATLAS refcat2 star catalog using Sloan r´ magnitudes (Tonry et al., 2018) using the comparison star selection feature of *Tycho-Tracker*.

2042 Sitarski is a middle main-belt asteroid that is a member of the Merxia dynamical family. It was discovered in 1960 by van Houten and van Houten-Groeneveld at Palomar on plates taken by T. Gehrels. It is named in honor of Grzegorz Sitarski, an astronomer at the Polish Academy of Sciences. We observed Sitarski on four nights in 2024 September and October resulting in a total of 393 total observations.

We found one prior rotation period report from Warell (2017) of 2.63 hours. Analysis of our data resulted in a best-fit period of 8.377 ± 0.004 hours with an amplitude of 0.1727 ± 0.0123 mag resulting in a typical bimodal lightcurve, disagreeing with Warell.

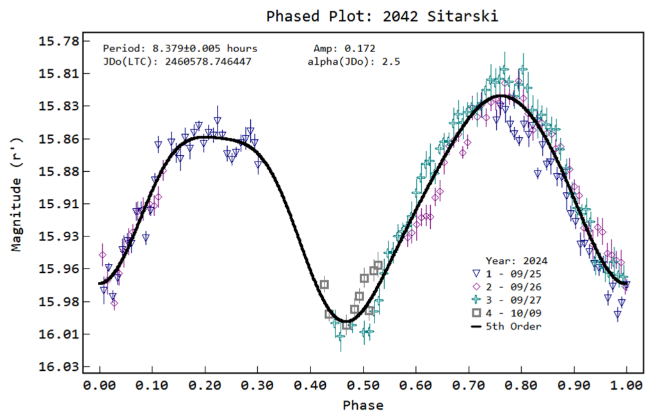

Number	Name	yyyy mm/dd	Phase	L_{PAB}	B_{PAB}	Period(h)	P.E.	Amp	A.E.	Grp
2042	Sitarski	2024 09/25-10/09	*1.6, 4.3	7	0	8.377	0.004	0.17	0.01	MERXIA
2460	Mitlincoln	2024 09/12-09/12	4.2, 4.4	358	0	2.992	0.011	0.17	0.02	MB-I
2935	Naerum	2024 04/30-07/11	9.5,24.1	231	17	450.8	0.2	0.55	0.02	MB-M
3654	AAS	2024 09/09-09/10	12.9,13.6	5	1	3.545	0.002	0.15	0.02	MB-I
3869	Norton	2024 08/15-08/19	8.9,10.8	340	6	7.606	0.003	0.15	0.02	MB-I
3895	Earhart	2024 07/12-07/16	8.8,10.0	305	16	3.565	0.002	0.51	0.03	MB-I
4222	Nancita	2023 11/15-11/17	10.0, 8.7	64	-2	3.873	0.002	0.56	0.03	MC
4706	Dennisreuter	2024 09/25-09/28	4.6, 6.1	13	-1	3.685	0.003	0.10	0.02	MB-M
5725	Nordlingen	2024 04/29-05/09	4.9, 7.4	216	9	3.412	0.002	0.15	0.02	MB-I
6026	Xenophanes	2024 09/09-09/11	7.4, 8.2	8	1	4.106	0.002	0.44	0.03	MB-O
7079	Baghdad	2024 07/17-08/21	*6.7,13.2	312	7	2.860	0.003	0.06	0.01	MC
8356	Wadhwa	2023 09/24-10/15	7.6,20.7	351	1	3.080	0.002	0.29	0.02	MB-I
9436	Shudo	2024 04/26-05/02	11.7,14.5	197	5	3.779	0.002	0.14	0.01	NYSA
13713	1998 QN30	2024 10/05-10/11	8.5, 4.8	25	-1	6.312	0.004	0.87	0.03	MB-I
16693	Moseley	2024 09/08-10/14	*12.3,12.8	2	16	71.72	0.07	1.06	0.5	EUNOMIA
17133	1999 JC81	2024 06/06-06/10	11.8,10.9	261	19	6.694	0.002	0.27	0.02	MB-M
22074	2000 AB113	2024 10/13-10/14	8.5, 8.8	37	-13	3.806	0.004	0.37	0.03	EOS
37163	Huachucaclub	2024 08/20-09/07	9.5,16.9	314	6	6.811	0.007	1.01	0.05	MB-I
37187	2000 WP60	2024 05/07-06/30	*7.0,21.5	249	11	580.1	1.0	0.23	0.03	MB-M
69894	1998 SD125	2024 10/05-10/10	3.6, 5.6	26	-1	3.725	0.002	0.52	0.05	EOS
86608	2000 EK85	2024 05/08-05/13	13.2,13.9	234	15	3.534	0.007	0.10	0.01	MC
93636	2000 UF81	2024 03/30-06/03	8.5,23.7	189	16	12.791	0.004	0.32	0.02	MB-M

Table I. Observing circumstances and results. The phase angle is given for the first and last date. If preceded by an asterisk, the phase angle reached an extrema during the period. L_{PAB} and B_{PAB} are the approximate phase angle bisector longitude/latitude at mid-date range (see Harris et al., 1984). Grp is the asteroid family/group (Warner et al., 2009).

2460 Mitlincoln is an inner main-belt asteroid discovered in 1980 by L.G. Taff and D. Beatty at Socorro. It is named after the MIT Lincoln Laboratory. We observed it on one night in 2024 September resulting in a total of 252 observations.

A search of the LCDB showed six prior reported periods: 2.77 h by Warner (2002), 3.009 by Behrend (2004web), 2.667 by Warner (2011), 2.8277 by Kryszczynska et al. (2012), 3.0068 by Benishek (2019) and 3.0052 by Mannucci (2020). Analysis of our data resulted in a bimodal lightcurve with a best fit of 2.992 ± 0.011 hours and an amplitude of 0.1653 ± 0.0153 mag, in close agreement with Benishek and Mannucci.

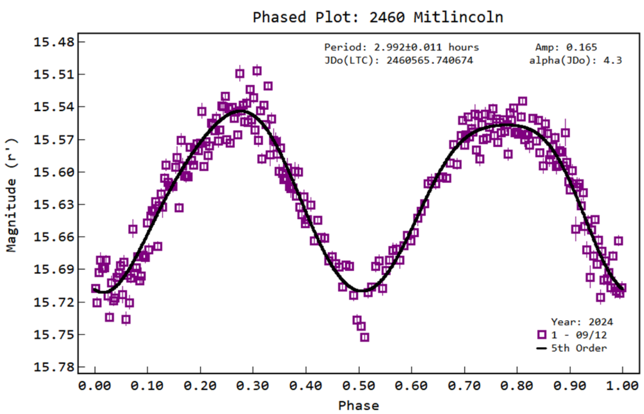

2935 Naerum is a middle main-belt asteroid discovered in 1976 by R.M. West at La Silla. We observed it on 22 nights in 2024 April through July resulting in a total of 708 observations.

No prior period reports were found in the LCDB. Analysis of our data resulted in a best fit of 450.8 ± 0.2 hours with an amplitude of 0.555 ± 0.023 mag. The period spectrum shows spikes at 225 and 450 hours. We adopted the latter value which gave a bimodal result. Coverage is incomplete so this result could be wrong.

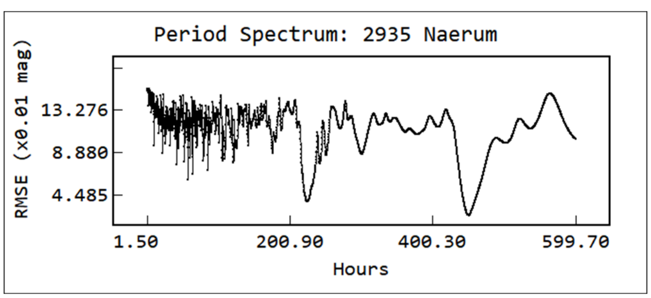

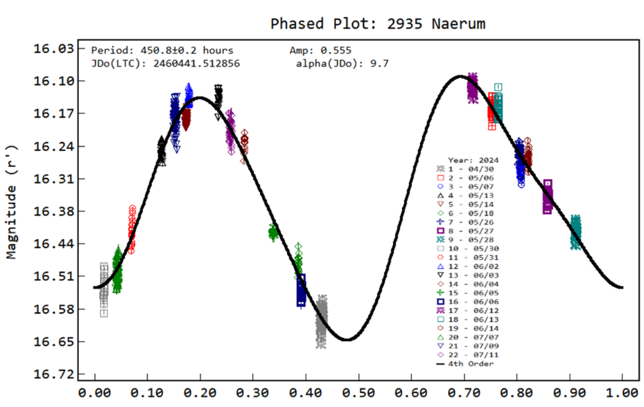

3654 AAS is a main-belt asteroid discovered in 1949 by Goethe Link Observatory in Brooklyn. We observed it on two nights in 2024 September resulting in 235 observations.

We found no prior reports of a rotation period. Analysis of our data resulted in a best fit period of 3.545 ± 0.002 h with an amplitude of 0.1445 ± 0.0146 mag.

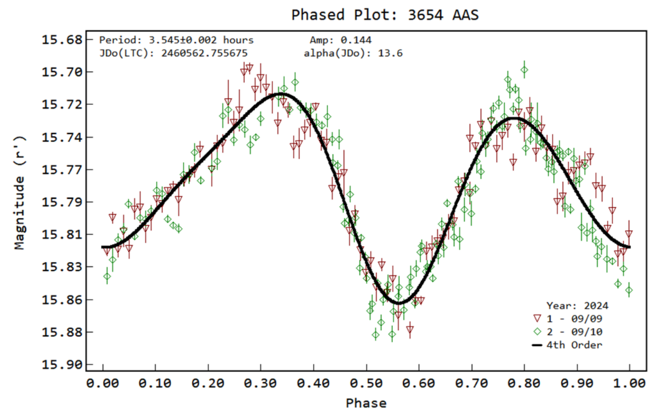

3869 Norton is a main-belt asteroid discovered in 1981 by Bowell at Flagstaff. We observed Norton on five nights in 2024 August resulting in a total of 875 observations.

We found two prior reports. Pál et. al. (2020) reported 17.0957 h and Benishek (2022) reported 7.605 h. Analysis of our data resulted in a best fit of 7.606 ± 0.003 h with an amplitude of 0.1489 ± 0.0161 mag, in agreement with Benishek.

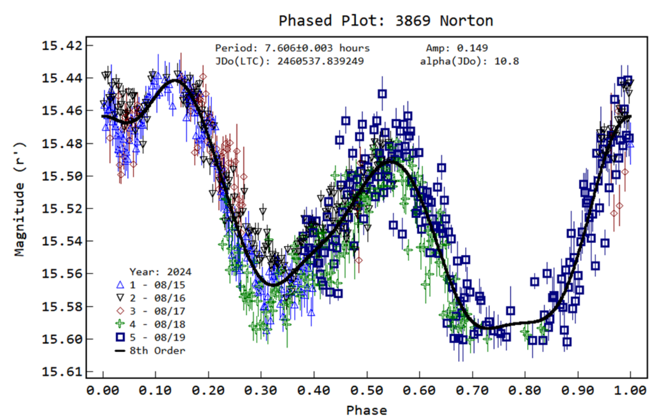

3895 Earhart is an inner main-belt asteroid discovered in 1987 by C. Shoemaker at Palomar. The LCDB shows ten prior rotation period reports and an uncertainty score U of 3 with period 3.5645 hours. We observed it on five nights in 2024 July resulting in a total of 229 observations.

Analysis of our data resulted in a best fit period of 3.565 ± 0.002 h with an amplitude of 0.513 ± 0.029 mag, in close agreement with prior reports.

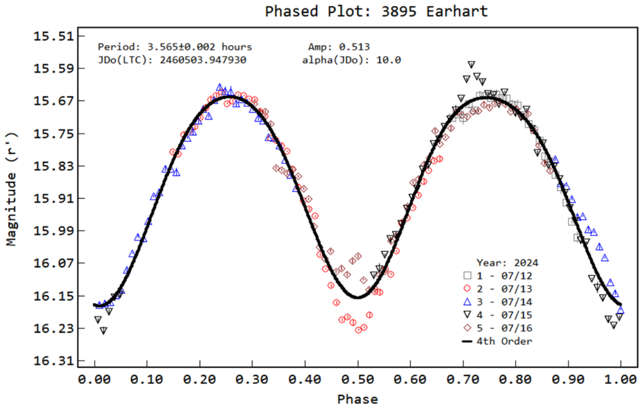

4222 Nancita is a Mars-crossing asteroid discovered in 1988 by E. Helin at Palomar. There were two prior reports in the LCDB of 3.8732±0.0003 by Higgins et al. (2006) and 3.872921±0.000002 by Ďurech et al. (2018). We observed on three nights in 2023 November resulting in a total of 177 observations.

Analysis of the data resulted in a best fit of 3.8730±0.002 hours with an amplitude of 0.557 ± 0.03 mag in close agreement with the prior reports.

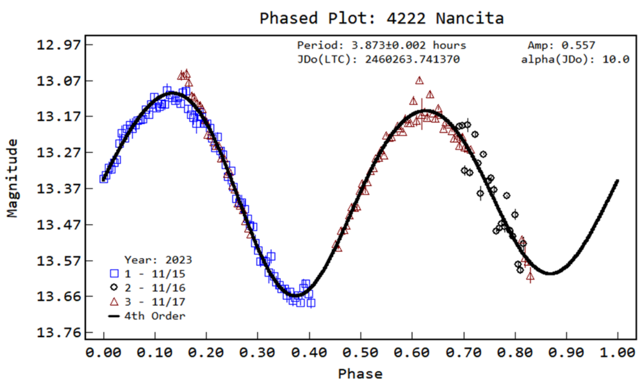

4706 Dennisreuter is an inner main-belt asteroid discovered by R. Rajamohan at Kavalur in 1988. It is named for Dennis C. Reuter, a physical chemist at the Goddard Space Flight Center, who developed instrumentation and techniques to measure the spectra of comets and planetary bodies. We observed it on four nights in 2024 September resulting in a total of 319 observations.

The LCDB shows a period of 2.578 with a uncertainty score U of 1. Waszczak et. al. (2015) reported 2.578 h and Fornas et al. (2022) reported 3.690 h. A fifth order Fourier fit of our data resulted a period of 3.685 ± 0.003 h with an amplitude of 0.1 ± 0.02 mag, in close agreement with Fornas.

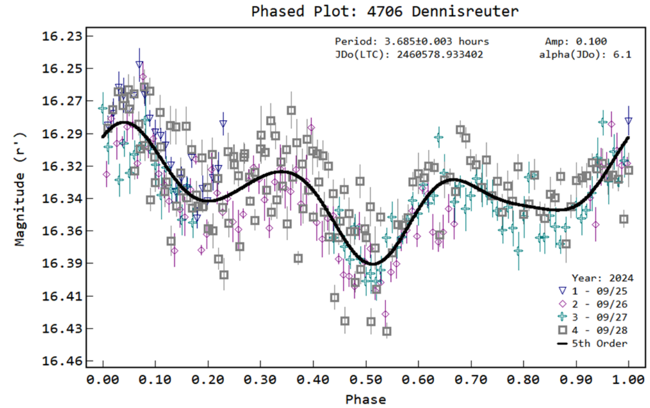

5725 Nordlingen is an inner main-belt asteroid discovered in 1988 by C. Shoemaker at Palomar. We observed it on seven nights in 2024 April and May resulting in a total of 263 observations.

We were unable to find any prior period reports. Analysis of our data resulted in a best fit of 3.412 ± 0.002 hours with an amplitude of 0.15 ± 0.02 mag.

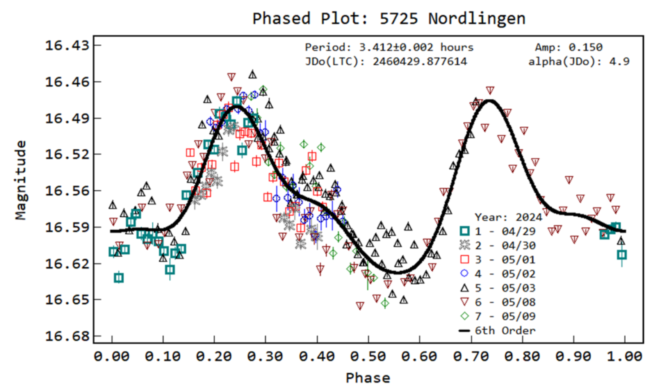

6026 Xenophanes is an inner main-belt asteroid discovered in 1993 by E.W. Elst at La Silla. We observed it on two nights in 2024 September for a total of 206 observations.

We found three prior reports in the LCDB. Two by Waszczak et al. (2015) of 4.490 h and 4.109 h along with one from Hanuš et al. (2016) of 3.7817. The LCDB quality score U was 2. Analysis of our data resulted in a clear bimodal lightcurve with best fit period of 4.106 ± 0.002 h with an amplitude of 0.4424 ± 0.0249 mag, close to the second report from Waszczak et al.

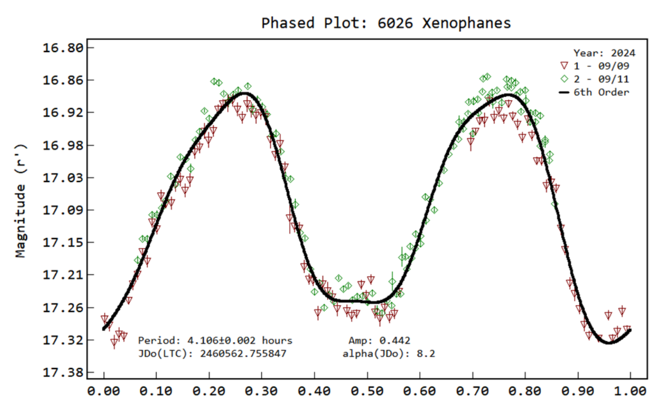

7079 Baghdad is a Mars-crosser discovered in 1986 by E. Elst and V. Ivanova at Smolyan. We observed is on six nights in 2024 July and August resulting in a total of 256 observations.

We were unable to find any prior rotation period reports. Analysis of our data resulted in a best fit of 2.86 ± 0.003 h with an amplitude of 0.06 ± 0.012 mag.

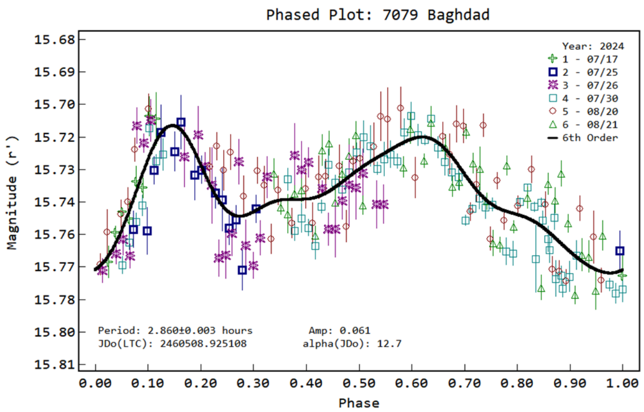

8356 Wadhwa is an inner main-belt asteroid discovered in 1989 by C. Shoemaker and E. Shoemaker at Palomar. It is named in honor of Dr. Meenakshi Wadhwa, who is currently the director of the Arizona State University School of Earth and Space Exploration. We observed Wadhwa on two nights in 2023 September and October resulting in a total of 296 observations.

We found three prior reports for Wadhwa, 3.04303±0.00004 by Pravec et al. (2008web), 3.04±0.01 by Buchheim (2009) and 3.0411±0.0001 by Pravec et al. (2019web). Analysis of our data resulted in a best fit of 3.080 ± 0.002 hours with an amplitude of 0.29 ± 0.02 mag, slightly longer than the prior reports.

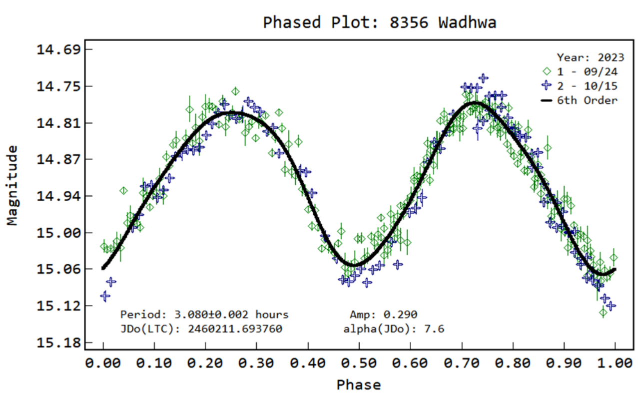

9436 Shudo is an inner main belt asteroid discovered in 1997 by T. Kobayashi at Oizumi. It is a member of the Nysa family. It is named for a private boys' junior and senior high school in Hiroshima, Japan. We observed it on six nights in 2024 April and May resulting in a total of 475 observations.

A search of the LCDB did not reveal any reports of a synodic period. Analysis of our data resulted in a best fit of 3.779 ± 0.002 hours with an amplitude of 0.14 ± 0.01 mag. Due to the relatively short period several nights covered complete or nearly cycles. The period spectrum is unambiguous, with no other meaningful signals.

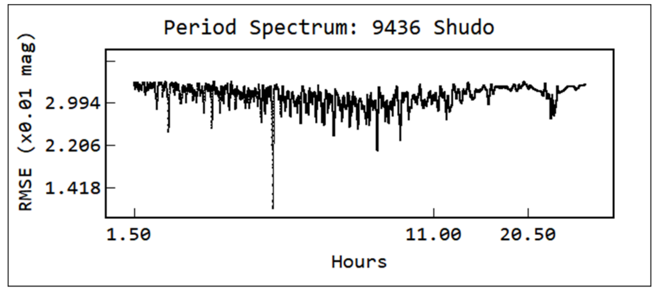

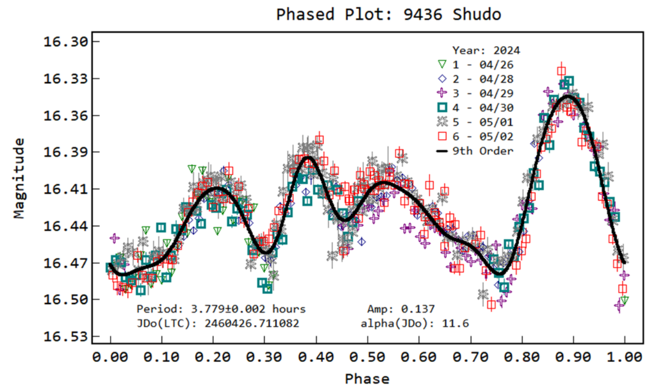

13713 1998 QN30 is an inner main-belt asteroid. We observed it on six nights in 2024 October resulting in a total of 346 observations.

We found one prior report by Waszczak et al. (2015) of 6.338 hours. The LCDB lists the quality score U as 2. Analysis of our data resulted in a best fit period of 6.312 ± 0.0004 hours with an amplitude of 0.868 ± 0.0331 mag, in close agreement with Waszczak et al. The small gap at phase 0.2 was caused by data points removed due to contamination by a background star. If not for that, the coverage would be complete.

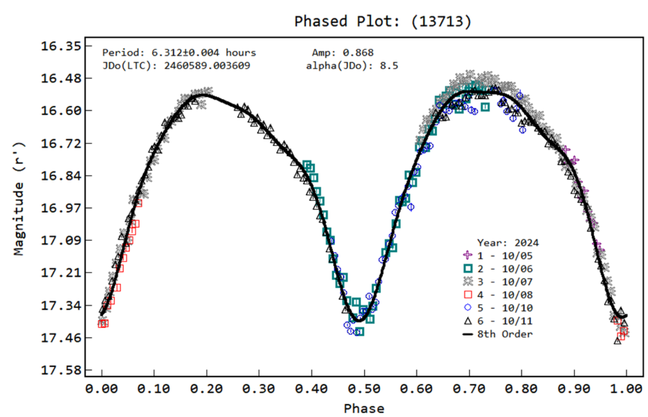

16693 Moseley is a middle main-belt asteroid of the Eunomia family. It was discovered in 1994 by D.J. Asher at Siding Spring. It is named for Terence J.C.A. Moseley, editor of Stardust, and a founding member of the Irish Federation of Astronomical Societies. We observed Moseley on seventeen nights in 2024 September and October resulting in a total of 979 observations.

We found no prior rotation period reports. Analysis of our data resulted in a best fit of 71.71 ± 0.07 hours. Since we were unable to observe a clear minimum, the amplitude is uncertain, but appears to exceed 1 magnitude and is likely between 1 and 1.5 magnitude. Coverage is incomplete so this result could be wrong. Further observations are needed.

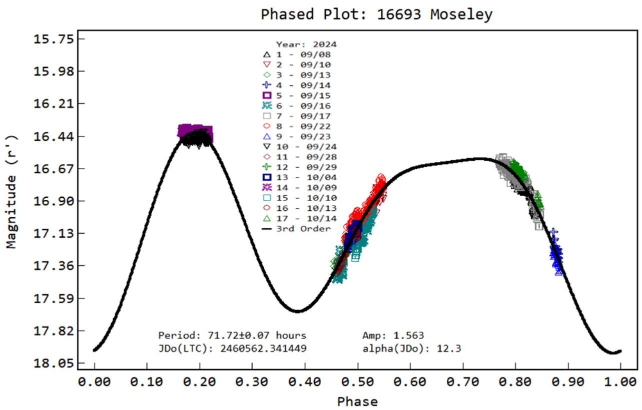

17133 1999 JC81 is a middle main-belt asteroid discovered by LINEAR at Socorro. We observed it on eight nights in 2024 June, resulting in a total of 269 observations.

A search of the ALCDEF revealed one report by Pál et al. (2020) of 48.1942 ± 0.0005 hours with an amplitude of 0.14 ± 0.03 magnitude based on data extracted from TESS observations. Analysis of our data resulting in a best fit of 6.694 ± 0.002 hours with an amplitude of 0.268 ± 0.015 mag, disagreeing with Pál et al.

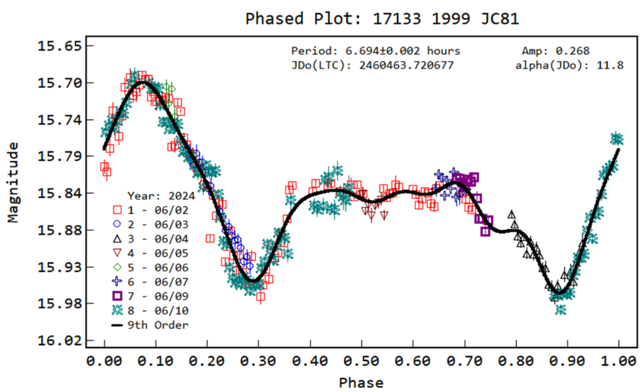

Pál et al. provided data to the ALCDEF database which we downloaded and analyzed to try to understand the discrepancies with our results.

There are a small number of significant outliers in the Pál et al. data as shown in the plots below. Including these outliers results in a spectrum with several peaks, one peak is near the reported 48.19 hours. Suppressing these outliers results in a spectrum with a peak at 6.69 hours, in close agreement with our result, but with a much lower amplitude. The lightcurve shape is also different from our result. We are unable to explain these discrepancies.

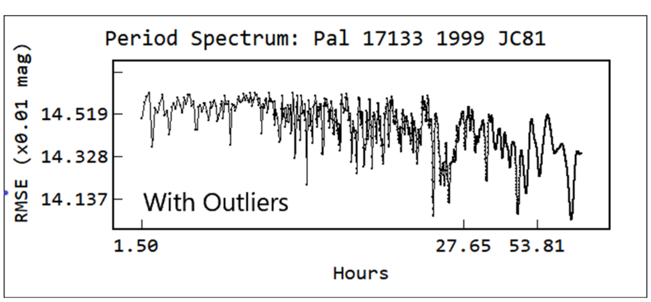

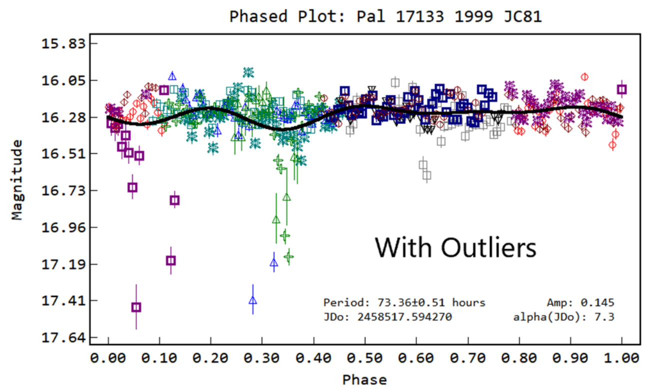

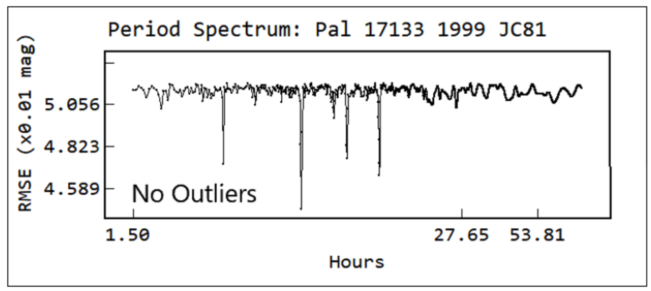

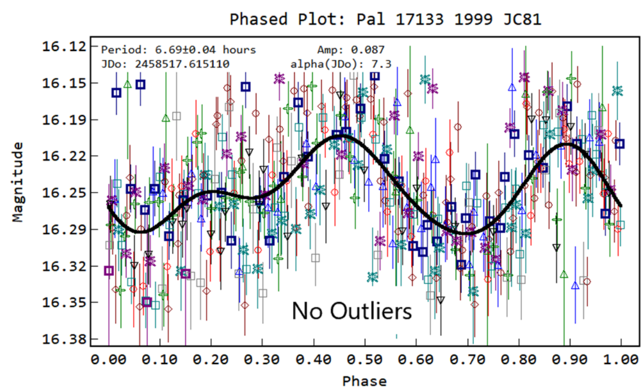

22074 2000 AB113 is an outer main-belt asteroid that is a member of the Eos family. It was discovered in 2000 by LINEAR at Socorro. We observed it on two nights in 2024 October for a total of 129 observations.

We found one prior report from Ďurech et al. (2020) of 3.801 hours with a quality score U of 2. Analysis of our data resulted in a best fit of 3.806 ± 0.004 hours with an amplitude of 0.369 ± 0.0314 mag, in close agreement with Ďurech et al.

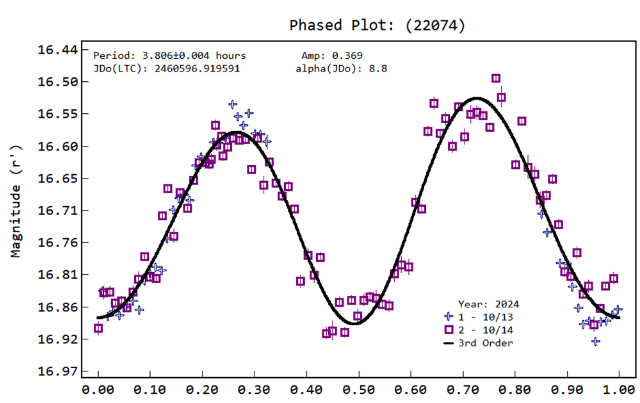

37163 Huachucaclub, an inner main-belt asteroid, was discovered by Medkeff and Healy at Junk Bond Observatory in 2000. It is named after the Huachuca Astronomy Club of Sierra Vista, AZ. We observed it on 10 nights in 2024 August and September resulting in a total of 454 observations.

Waszczak et. al. (2015) reported a period of 5.967 hours and an amplitude of 0.8 mag. The LCDB shows a quality score of 2. Analysis of our observations resulted in a best fit of 6.811 ± 0.007 hours with an amplitude of 1.01 ± 0.05 mag, longer than the Waszczack et al. report.

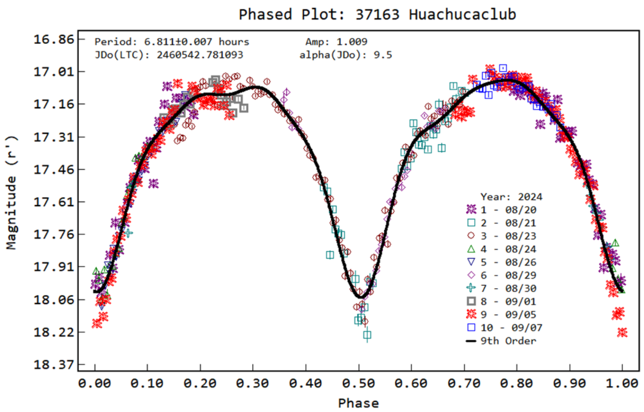

37187 2000 WP60 is a middle main-belt asteroid discovered in 2000 by LINEAR at Socorro. We observed it on 26 nights in 2024 May through July resulting in a total of 1017 observations.

We were unable to find any prior rotation period reports. Analysis of our data resulted in a best fit of 580.1 ± 1.0 hours with an amplitude of 0.225 ± 0.028 mag. The lightcurve shows signs indicating it may be tumbling.

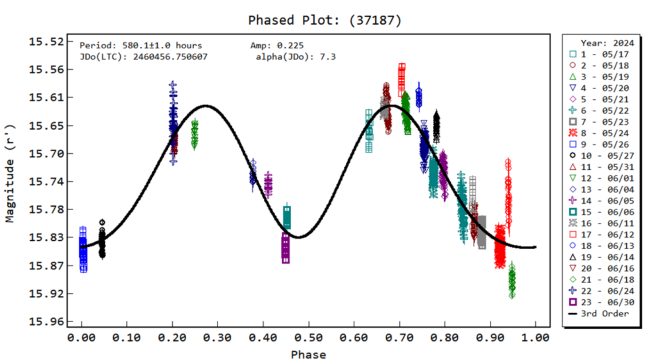

69894 1998 SD125 is an outer main-belt asteroid that is a member of the Eos family. It was discovered in 1998 by LINEAR at Socorro. We observed it on six nights in 2024 October resulting in a total of 223 observations.

We found no prior rotation period reports. Analysis of our data resulting in a best fit period of 3.725 ± 0.002 hours with an amplitude of 0.521 ± 0.047 mag.

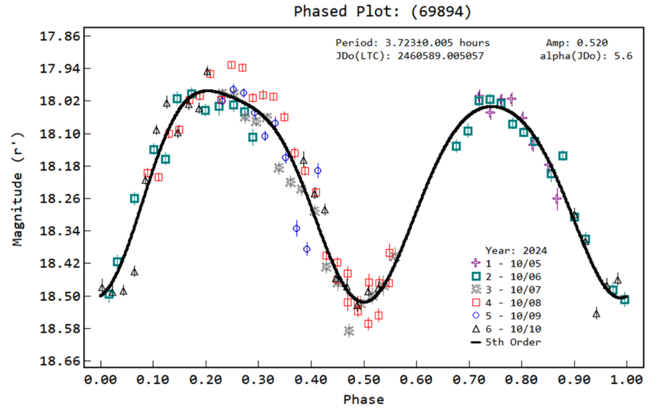

86608 2000 EK85 is a Mars crossing asteroid discovered by LINEAR at Socorro. We observed it on four nights in 2024 May resulting in a total of 197 observations.

We found no prior rotation period reports. Analysis of our data resulted in a best fit of 3.534 ± 0.007 hours with an amplitude of 0.097 ± 0.02 mag.

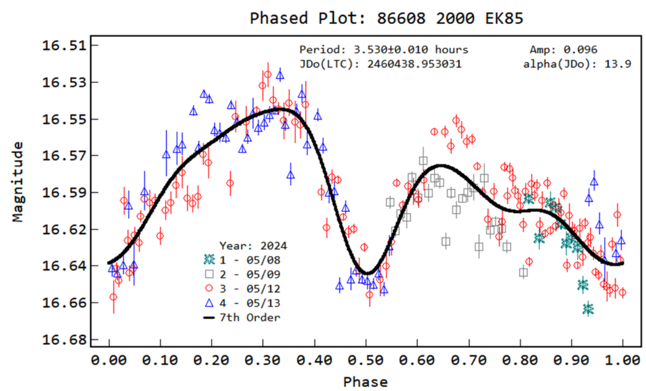

93636 2000 UF81 is a middle main-belt asteroid discovered by LINEAR at Socorro. We observed it on twelve nights in 2024 March, April and May resulting in a total of 625 observations.

We found no prior rotation period reports. Analysis of our data resulted in a best fit period of 12.791 ± 0.004 hours with an amplitude of 0.32 ± 0.03 mag.

The period spectrum contains aliases at one-half the proposed period. While there is a small gap in the lightcurve, given the large number of cycles covered, and the relatively poor fit for the aliases, we are confident that this bimodal lightcurve is the correct period.

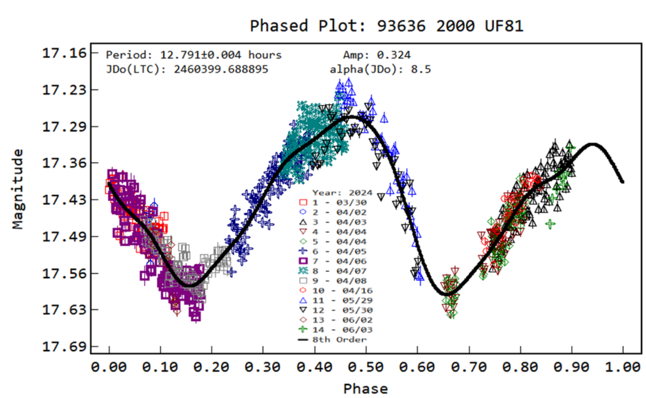

Acknowledgements

The author gratefully acknowledges the generosity of Dr. Richard Post for ongoing use of one of his domes to house the author's telescope.

The author thanks Brian Warner, Tom Polakis, Mike Wiles and Eric Dose for their advice and guidance that has improved the results of this research.

This research used data from the Asteroid Terrestrial-impact Last Alert System (ATLAS) project, funded through NASA grants NN12AR55G, 80NSSC18K0284, and 80NSSC18K1575. The ATLAS science products have been made possible through the contributions of the University of Hawaii Institute for Astronomy, the Queen's University Belfast, the Space Telescope Science Institute, and the South African Astronomical Observatory.

Funding for PDS observations, analysis, and publication was provided by NASA grant NNX13AP56G.

Work on the asteroid lightcurve database (LCDB) was funded in part by National Science Foundation grants AST-1210099 and AST-1507535.

Data from the MPC's database is made freely available to the public. Funding for this data and the MPC's operations comes from a NASA PDCO grant (80NSSC22M0024), administered via a University of Maryland - SAO subaward (106075-Z6415201). The MPC's computing equipment is funded in part by the above award, and in part by funding from the Tamkin Foundation.

This research used data found on the JPL Solar System Dynamics Website. The JPL Solar System Dynamic group's ephemeris development, maintenance, and improvement test are part of NASA's Advanced Multi-Mission Operations System, which is funded by NASA's Science Mission Directorate, Planetary Science Division.

References

Behrend, R. (2004web). Observatoire de Geneve web site. *http://obswww.unige.ch/~behrend/page_cou.html*

Benishek, V. (2019). "Lightcurves and Synodic Rotation Periods for Seven Asteroids: 2019 April-July." *Minor Planet Bull.* **46**, 506-508.

Benishek, V. (2022). "CCD Photometry of 29 Asteroids at Sospot Astronomical Observatory: 2020 July-2021 September." *Minor Planet Bull.* **49**, 38-44.

Buchheim, R. (2009). "Lightcurves of Asteroids 358 Apollonia, 734 Benda and 8356 Wadhwa." *Minor Planet Bull.* **36**, 84-85.

Denny, R. (2024). *ACP Expert* software, version 9.1. DC-3 Dreams. *https://acpx.dc3.com*

Ďurech, J.; Hanuš, J.; Ali-Lagoa, V. (2018). "Asteroid models reconstructed from the Lowell Photometric Database and WISE data." *Astron. Astrophys.* **617**, id. A57.

Ďurech, J.; Tonry, J.; Erasmus, N.; Denneau, L.; Heinze, A.N.; Flewelling, H.; Vančo, R. (2020). "Asteroid models reconstructed from ATLAS photometry." *Astro. Astrophys.* **643**, id. A59.

Fornas, G.; Fornas, A.; Mas, V. (2022). "Nine Main Belt Asteroids, One Near Earth, and Two Potentially Hazardous Asteroid Lightcurves." *Minor Planet Bull.* **49**, 196-199.

George, D.; Sharratt, G.; Benson, E.; Browne, H.; Browne, P.; Creery, C.; Boltwood, P.; Mussar, R.; Waring, J.; Lawrence, O.; Robichaud, A. (2021). *Maxim DL* software v6.28. *https://diffractionlimited.com/*

Hanuš, J.; Ďurech, J.; Oszkiewicz, D.A.; Behrend, R.; Carry, B.; Delbo, B.; Adam, O.; Afonina, V.; Anquetin, R.; Antonini, P.; Audejean, M.; Aurard, P.; Bachschmidt, M.; Baduel, B.; Barbotin, E.; Barroy, P.; Baudouin, P.; Berard, L.; Berger, N.; and 149 colleagues (2016). "New and Updated Convex Shape Models of Asteroids Based on Optical Data from a Large Collaboration Network." *Astronomy & Astrophysics* **586**, A108.

Harris, A.W.; Young, J.W.; Scaltriti, F.; Zappala, V. (1984). "Lightcurves and phase relations of the asteroids 82 Alkmene and 444 Gyptis." *Icarus* **57**, 251-258.

Higgins, D.; Pravec, P.; Kusnirak, P.; Reddy, V.; Dyvig, R. (2006). "Asteroid lightcurve analysis at Hunters Hill Observatory and collaborating stations - summer 2005/6." *Minor Planet Bull.* **33**, 64-66.

Kryszczynska, A.; Colas, F.; Hirsch, R.; Ivanova, V.; Apostolovska, G.; Bilkina, B.; Velichko, F.P.; Kwiatkowski, T.; Kankiewicz, P.; Vachier, F.; Umlenski, V.; Michalowski, T.; Marciniak, A.; Maury, A.; Kaminski, K.; Fagas, M.; Dimitrov, W.; Borczyk, W.; Sobkowiak, L. (2012) "Do Slivan states exist in the Flora family? I. Photometric survey of the Flora region." *Astron. Astrophys.* **546**, id. A72.

Mannucci, M. (2020). "Rotational Period Determination for Asteroids 2460 Mitlincoln 3070 Aitken and (11116) 1996 EK." *Minor Planet Bull.* **47**, 5-6.

Pál, A.; Sazkáta, R.; Kiss, C.; Bódi, A.; Bognár, Z.; Kalup, C.; Kiss, L.; Marton, G.; Molnár, L.; Plachy, E.; Sárneczky, K.; Szabó, G.; Szabó, R. (2020). "Solar System Objects Observed with TESS - First Data Release: Bright Main-belt and Trojan Asteroids from the Southern Survey." *Ap. J. Suppl. Ser.* **247**, id. 26. *axXiv:2001.05822*

Parrott, D. (2024). Tycho-Tracker software v11.5. *http://www.tycho-tracker.com*

Pravec, P.; Wolf, M.; Sarounova, L. (2008web, 2019web). *http://www.asu.cas.cz/~ppravec/neo.htm*

Tonry, J.; Denneau, L.; Flewelling, H.; Heinze, A.; Onken, C.; Smartt, S.; Stalder, B.; Weiland, H.; Wolf, C. (2018). "The ATLAS All-Sky Stellar Reference Catalog." *Ap. J.* **867**, id. 105.

Warell, J. (2017). "Lightcurve Observations of Nine Main-belt Asteroids. *Minor Planet Bull.* **44**, 304-305.

Warner, B.D. (2002). "Asteroid Photometry at the Palmer Divide Observatory: Results for 1333 Cevenola and 2460 Mitlincoln." *Minor Planet Bull.* **29**, 74-75.

Warner, B.D.; Harris, A.W.; Pravec, P. (2009). "The asteroid lightcurve database." *Icarus* **202**, 134-146. Updated 2023 April 24. *https://minorplanet.info/php/lcdb.php*

Warner, B.D. (2011). "Upon Further Review: VI. An Examination of Previous Lightcurve Analysis from the Palmer Divide Observatory." *Minor Planet Bull.* **38**, 96-101.

Waszczak, A.; Chang, C.-K.; Ofek, E.O.; Laher, R.; Masci, F.; Levitan, D.; Surace, J.; Cheng, Y.-C.; Ip, W.-H.; Kinoshita, D.; Helou, G.; Prince, T.A.; Kulkarni, S. (2015). "Asteroid Light Curves from the Palomar Transient Factory Survey: Rotation Periods and Phase Functions from Sparse Photometry." *Astron. J.* **150**, A75.

A NEW SATELLITE OF (172376) 2002 YE25 DETECTED BY STELLAR OCCULTATION

David Gault
22 Booker Road
Hawkesbury Heights, 2777 AUSTRALIA
djgault57@gmail.com

Peter Nosworthy, Dave Herald
Trans-Tasman Occultation Alliance (TTOA)

(Received: 2024 August 17)

Two observers in Australia, at two separate sites, observed (172376) 2002 YE25 occult TYC 6854-1090, an 11th magnitude star, on 2022 May 16.447 UT. The minor planet was nine magnitudes fainter than the star. An occultation at both sites was not expected to be observed due to the small diameter of the asteroid and the cross-path spacing of the two sites being much larger than the asteroid. However, both sites detected a clear occultation that reached the limit of 3 magnitudes fainter than the star for both recordings. We observed chord lengths across one body of 3.8 km and the second body of 3.3 km, with a mid-chord separation of 15.3 km. We rule out the possibility that the two occultations were caused by a double star, or a highly elongate object like 433 Eros or 216 Kleopatra.

D. Gault and P. Nosworthy observed (172376) 2002 YE25 occult TYC 6854-01090-1. An occultation at both sites was not expected due to the 5.7 km diameter of the asteroid and the 15.52 km cross-path spacing of the two sites being much larger than the asteroid. They observed from their home observatories located in The City of The Blue Mountains, west of Sydney, Australia, at Hawkesbury Heights and Hazelbrook. The sites are equipped with 28 and 30 cm Schmidt-Cassegrain telescopes, Watec 910BD video cameras, and IOTA-VTIs (2024), which inserted an accurate GPS-derived time stamp into the video stream. The occultation occurred at an altitude of 19 degrees. Observation circumstances and timings are shown in Table I and lightcurves of the target and a comparison star are shown in Figure. 1.

For this event, the recordings were closely analyzed to determine the limiting magnitude of the recording, noting that during the occultation events, the lightcurve dropped to zero light-level. The occulted star had a Gaia G-band magnitude of 11.0; stars fainter than 13.9 were visible on the recording. The equivalent magnitude drops of at least 3.0 magnitudes for both events in each recording is much larger than the 0.75 mag drop that would occur if the star was a double star of equal magnitude – thereby excluding a double star as being an explanation for the event.

Observer	Longitude	Latitude	Altitude	Event	Time UT	
Gault	150 38 27.9	-33 39 51.90	286m	D	10:43:31.52	+/-0.02
				R	10:43:31.96	+/-0.02
Nosworthy	150 27 06.5	-33 42 26.60	648m	D	10:43:30.07	+/-0.02
				R	10:43:30.46	+/-0.02

Table I. Observation circumstances and disappearance and reappearance times UTC of the 2022 May 16 occultations. The sites were separated by 15.52 km across the occultation path.

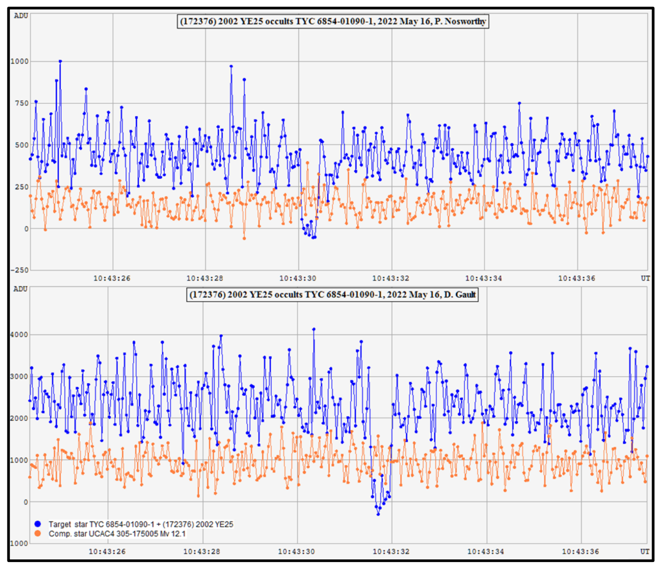

Fig. 1. Lightcurves by Gault and Nosworthy of the 2022 May 16 occultations of the MG 11.0 target star by the asteroid main body and satellite. Light values of the MG 12.1 comparison star are also shown.

Reduction of the Observations

Event times and observation circumstances were entered into *Occult* (Herald, 2024) and reduced for each observation. The sky-plane plots are shown on Figure 2.

The NEOWISE diameter of 2002 YE25, as determined at two epochs in 2010, is 5.7 ± 0.6 km, giving an equivalent cross-sectional area of between 20 and 31 sq km. The two occultation chords were of lengths 3.8 and 3.3 km, with a mid-chord separation of 15.3 km. Assuming a highly elongate cylindrical object similar to that of minor planets 433 Eros or 216 Kleopatra, the minimal apparent cross-sectional area would be greater than 55 sq km (i.e., much larger than that expected from the NEOWISE diameter).

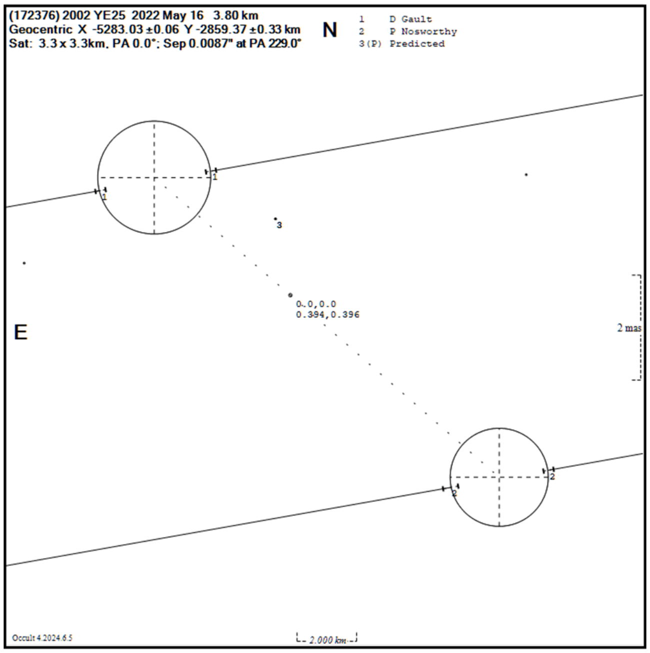

Figure 2. Reduction sky-plane plots of the 2022 May 16 occultation events for 2002 YE25.

However, if the two occultation chords were caused by spherical bodies 10 percent larger than the respective chords, the combined cross-sectional area of those bodies would be 24 sq km, fully consistent with that expected from the NEOWISE diameter. Accordingly, the observation is fully consistent with 2002 YE25 being a binary system.

Using a circular fit, we determined the chords for the two bodies:

Main body	3.8 ± 0.6 km
Satellite	3.3 ± 1.5 km

These diameters were then used to derive a separation of 8.7 ± 1.0 mas between the two with the satellite at position angle 229 ± 1 deg relative to the primary.

We are not aware of any lightcurve measurements of this asteroid. The observations of 2022 May 16 were the subject of *CBET* 5151.

References

IOTA-VTI (2024). GPS-disciplined video time inserter. *https://videotimers.com/home.html*

Herald, D. (2024). *OCCULT* software. *http://www.lunar-occultations.com/iota/occult4.htm*

LIGHTCURVE ANALYSIS FOR FOUR NEAR-EARTH ASTEROIDS OBSERVED JULY-SEPTEMBER 2024

Peter Birtwhistle
Great Shefford Observatory
Phlox Cottage, Wantage Road
Great Shefford, Berkshire, RG17 7DA
United Kingdom
peter@birtwhistle.org.uk

(Received: 2024 October 13 Revised: 2024 October 31)

Lightcurves and amplitudes for four near-Earth asteroids observed from Great Shefford Observatory during close approaches between July and September 2024 are reported. All are small objects with rotation periods shorter than 5 minutes and one is identified as having tumbling rotation.

Photometric observations of near-Earth asteroids during close approaches to Earth between July - September 2024 were made at Great Shefford Observatory using a 0.40-m Schmidt-Cassegrain and Apogee Alta U47+ CCD camera. All observations were made unfiltered and with the telescope operating with a focal reducer at f/6. The 1K×1K, 13-micron CCD was binned 2×2 resulting in an image scale of 2.16 arc seconds/pixel. All the images were calibrated with dark and flat frames and *Astrometrica* (Raab, 2024) was used to measure photometry using APASS Johnson V band data from the UCAC4 catalogue (Zacharias et al., 2013) and G band data from the Gaia DR 2 catalogue (Brown et al., 2018). *MPO Canopus* (Warner, 2023), incorporating the Fourier algorithm developed by Harris (Harris et al., 1989) was used for lightcurve analysis.

No previously reported results have been found in the Asteroid Lightcurve Database (LCDB) (Warner et al., 2009), from searches via the Astrophysics Data System (ADS, 2024) or from wider searches unless otherwise noted. All size estimates are calculated using H values from the Small-Body Database Lookup (JPL, 2024b), using an assumed albedo for NEAs of 0.2 (LCDB readme.pdf file) and are therefore uncertain and offered for relative comparison only.

2024 NM3. The ATLAS facility at Rio Hurtado, Chile discovered this Aten (*H = 25.2, D ~28 m*) on 2024 Jul 14.3 UTC. It passed Earth at 2.0 Lunar Distances (L.D.) on 2024 Jul 17.6 UTC (Dupouy et al., 2024) and was observed on three consecutive nights, 2024 Jul 17.0, 18.0 and 19.0 UTC. Average apparent magnitude and speed (arcsec/min) over the three nights were 16.7, 16.7, 17.6 and 100, 113, 53 respectively, resulting in the least scatter being achieved in the first night's measurements. Independent period spectra from the three nights produced very similar results, combined here in one diagram separated vertically. It can be seen that all the significant minima in the last two dates correspond with minima in the plot for Jul 17.0 UTC. The best fit in all three dates is for a rotation period of 0.047 h and all the other significant minima are integer multiples of 1/4, 1/3 or 1/2 of that period. *MPO Canopus* was configured to plot phased lightcurve diagrams for the three dates with the lightcurve maximum positioned at phase = 0.00 (= phase 1.00). The best-defined period, from Jul 17.0, of 0.046654 ± 0.000003 h (~2.8 min) was then used to propagate likely errors forwards to the other two dates to estimate whether the maximum in the first date matched the maxima in the following two dates and therefore whether the lightcurve shapes were directly comparable. The likely error in number of rotations ΔN between two dates was derived from eq. (3) in Kwiatkowski et al. (2010):

$$\Delta N \approx \Delta t\, \Delta P / P^2$$

where Δt is the time interval separating two lightcurves, P is the period from one of the individual solutions and ΔP is the maximum period uncertainty, with Δt, ΔP and P expressed in the same units.

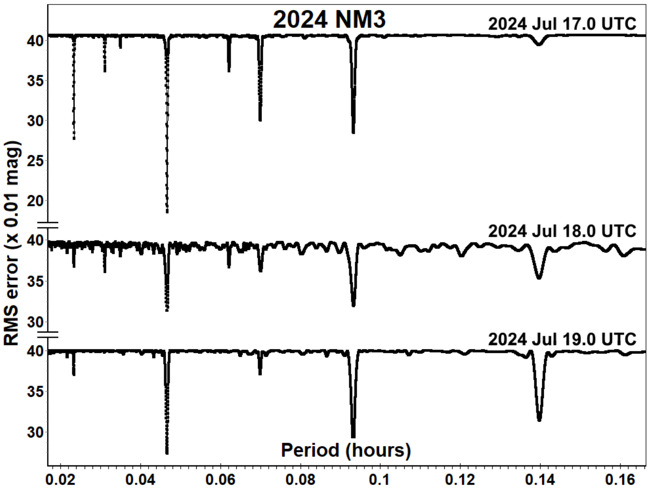

Propagating the period and its likely error from Jul 17.0 to Jul 18.0 predicts that maximum would occur at phase 0.89 ± 0.03 on the Jul 18.0 plot after 450 rotations had completed. Similarly propagating from Jul 17.0 to Jul 19.0 predicts that maximum would occur at phase 0.80 ± 0.07 on the Jul 19.0 plot after 992 rotations had completed. These predicted ranges of maxima are shown on the last two lightcurves as horizontal grey bars towards the top right and indicate that corresponding features in each are indeed likely to be comparable at similar phase values but also suggest the real error in the period used for Jul 17.0 is probably several times larger than stated. Matching features can be identified in each plot, including the deepest minima occurring at phase ~0.75. The trimodal lightcurve apparent in Jul 17.0 and Jul 18.0 becomes less defined by Jul 19.0. Being at close range throughout and traversing 76° of sky, it is likely the aspect angle of 2024 NM3 (Earth → asteroid → asteroid spin axis) changed dramatically over the three nights, causing rapid changes to the surface features presented to Earth and probably accounting for the reducing amplitude with increasing phase angle and the observed changes in lightcurve shape.

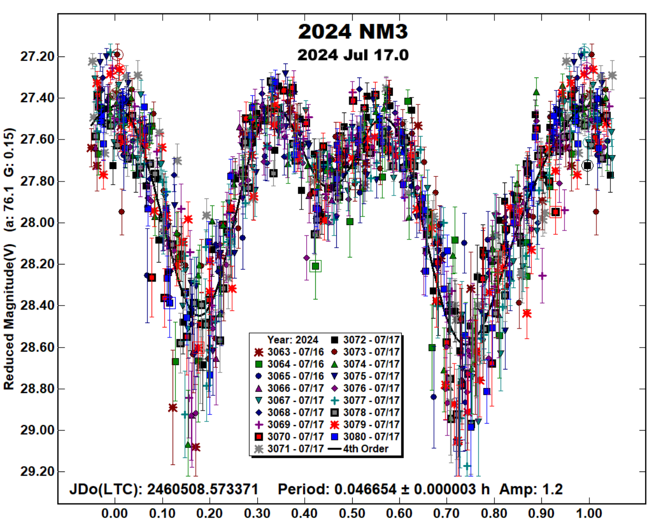

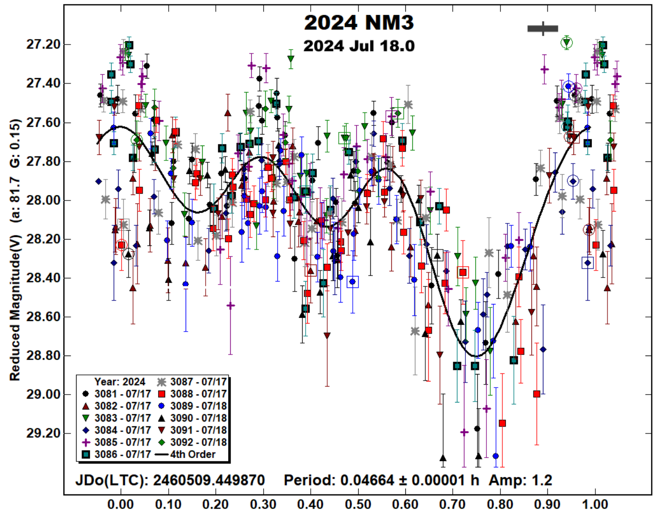

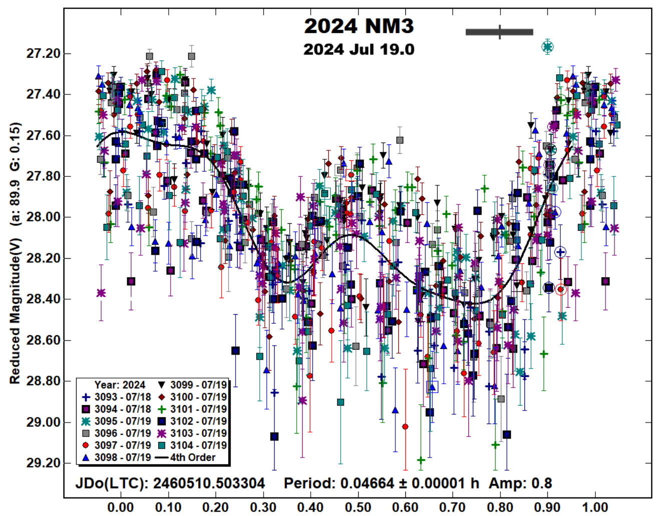

While under observation on Jul 17.0, 18.0 and 19.0, 2024 NM3 completed 60, 46 and 63 rotations respectively.

<u>2024 OM1</u>. Discovered from the Moonbase South Observatory in Namibia on 2024 Jul 29.0 UTC this Apollo (*H = 24.3, D ~41 m*) passed Earth at 3.6 L.D. on 2024 Aug 6.9 UTC (Herman et al., 2024). It was observed over a period of 2.3 h starting at 2024 Aug 7.03 UTC and, with an apparent speed of 105 arcsec/min exposures were kept to 5.6 seconds to keep trailing within the measurement annulus of *Astrometrica*. 691 measurements were obtained for the photometric analysis.

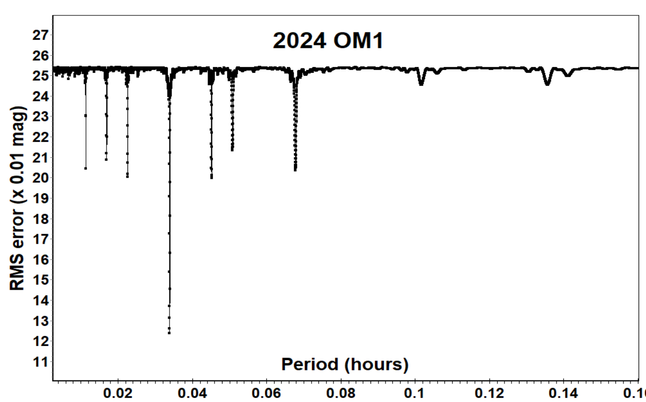

A period spectrum shows the best fit period to be 0.0339 h (~2.0 min) and the resulting lightcurve is apparently tri-modal, with an amplitude of 0.9. The next eight strongest minima in the period spectrum give significantly worse fits and are all integer multiples of half or a third of the best-fit period. During the period under observation 2024 OM1 completed 68 revolutions.

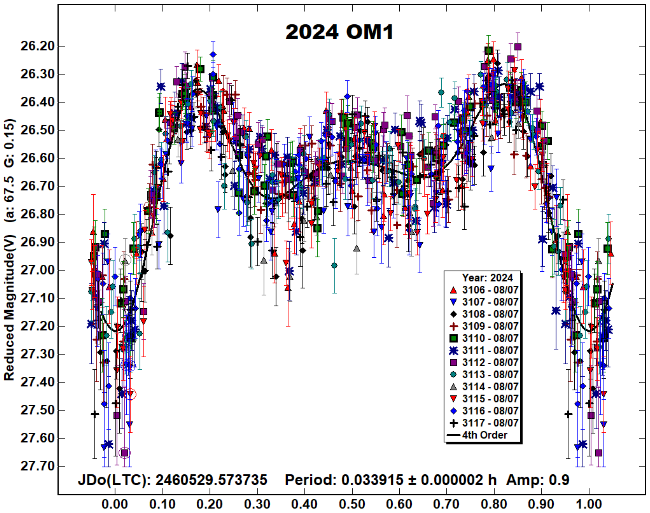

2024 RJ12. This Apollo (*H = 27.7, D ~8 m*) was a ZTF team discovery from Mt. Palomar on 2024 Sep 10.2 UTC, passing closest to Earth at 1.7 Lunar Distances (LD) about 90 min later (Bacci et al., 2024). It was actively observed for 67 min over a period of 3.7 h starting at 2024 Sep 10.88 UTC and with an apparent speed of 80 arcsec/min exposures were kept to shorter than 8 s to limit image trailing. The phase angle reduced to 3.9° by the end of the period of observation, with 2024 RJ12 reaching opposition 2 h later.

The analysis indicates that with phase effects being minimal it has a relatively low 0.2 mag amplitude and a bimodal lightcurve with period 2.4 min. During the 67 min 2024 RJ12 was being observed it completed 28 rotations.

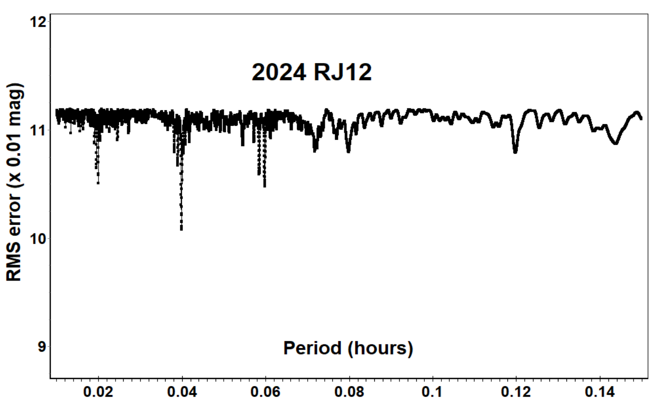

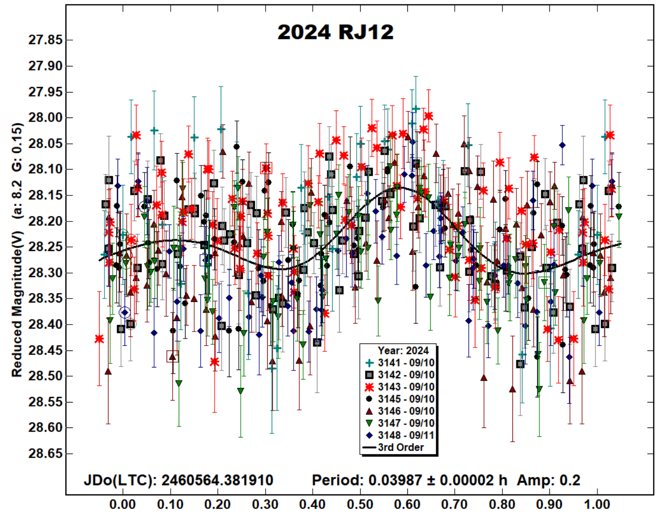

2024 SQ. The Mt. Lemmon Survey discovered this Apollo (*H = 25.8, D ~20 m*) on 2024 Sep 24.3 UTC, 4 days before an approach to within 3 LD from Earth on 2024 Sep 28.3 UTC (Gilmore et al., 2024). It is listed by both the SENTRY (JPL, 2024a) and NEODyS (NEODyS, 2024) systems as a virtual impactor with a number of low-probability potential impacts starting in 2084. It was actively observed for 1.3 hours over a period of 2.1 hours starting on 2024 Sep 28.04 UTC when its apparent speed was 120 arcsec/min. Exposures were kept to 5.4 seconds or shorter to limit image trailing. Large magnitude variations were obvious within 1 minute and at occasional minima 2024 SQ was too faint to record. A period spectrum shows the best-fit solution to be at 0.0744 h (~4.5 min) but a lightcurve, marked PAR shows a large amount of scatter especially between phases 0.6 - 0.8 and non-principal axis rotation (NPAR) or tumbling was suspected.

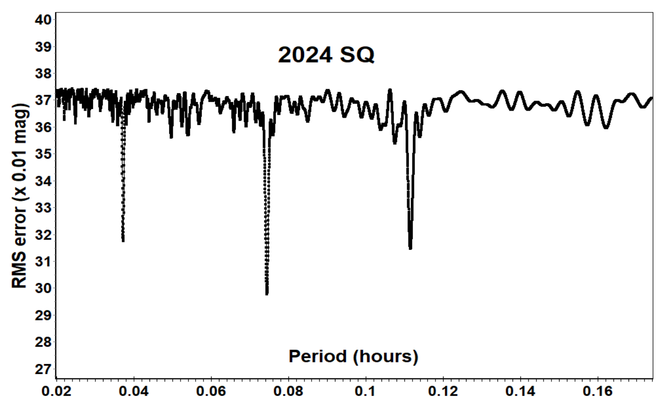

Several possible secondary periods were identified using the Dual Period Search function of *MPO Canopus* with the strongest of those at 0.1078 ± 0.0001 h (~6.5 min), the resulting pair of NPAR lightcurves are labelled P1 and P2. However, it is not clear whether P2, or one of the other possible secondary solutions may be real and not just an alias of the real secondary period, for instance another apparent solution P3 at 0.0627 h is related to the P1 and P2 periods, where 1/P1 + 2/P2 = 2/P3. Nevertheless, it is expected that 2024 SQ may be rated as PAR = -3 (NPA rotation reliably detected with the two periods resolved. An ambiguity of the periods solution may be tolerated provided the resulting spectrum of frequencies with significant signal is the same for the different solutions). (Petr Pravec, personal communication).

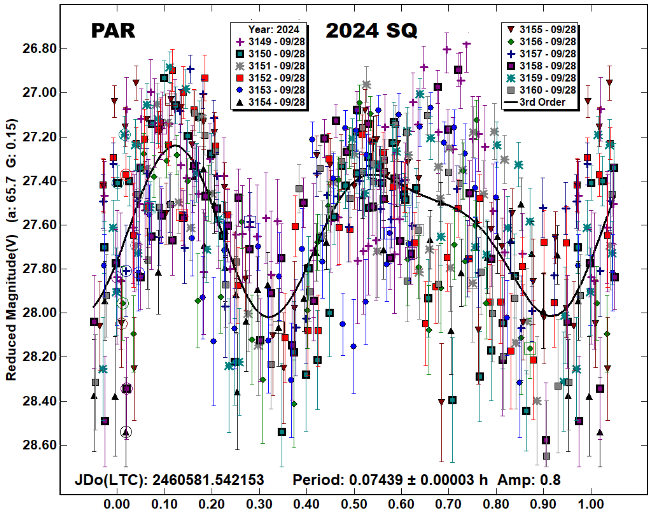

Due to 2024 SQ being occasionally too faint to record at its faintest minima, the amplitude and consequently the calculated minimum elongation of the asteroid (Min a/b in Table I) are likely to be underestimated in this analysis. 2024 SQ completed 17 rotations of the dominant 0.0744 h period during the 1.3 h of active observation.

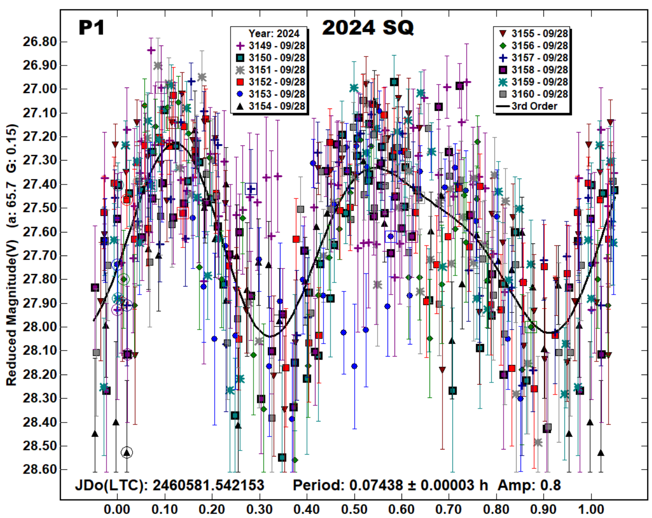

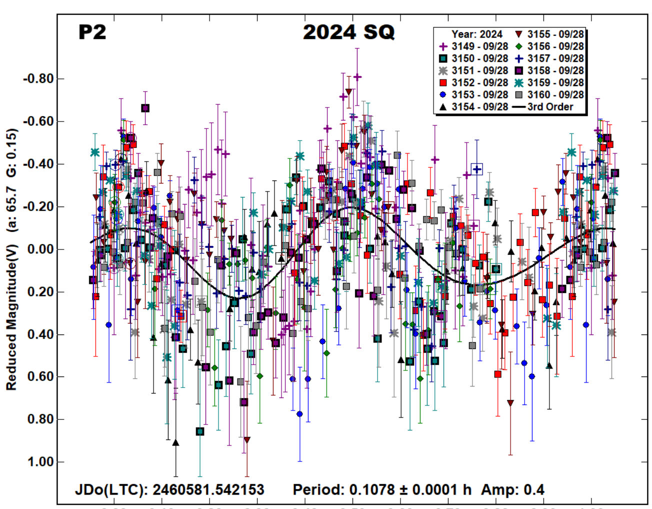

Number	Name	Integration times	Max intg/Pd	Min a/b	Pts	Flds
	2024 NM3	5.1-12.9	0.077	1.4*	1836	42
	2024 OM1	5.5,5.6	0.046	1.3*	691	12
	2024 RJ12	6.5-7.6	0.053	1.1	424	7
	2024 SQ	2.0-5.4	0.020	1.5*	472	12

Table I. Ancillary information, listing the integration times used (seconds), the fraction of the period represented by the longest integration time (Pravec et al., 2000), the calculated minimum elongation of the asteroid (Zappala et al., 1990), the number of data points used in the analysis and the number of times the telescope was repositioned to different fields. Note: * = Value uncertain, based on phase angle > 40°.

Acknowledgements

The author wishes to thank Dr. Petr Pravec, Astronomical Institute, Czech Republic for his continued help with the analysis of tumbling asteroids. The author also gratefully acknowledges a Gene Shoemaker NEO Grant from the Planetary Society (2005) and a Ridley Grant from the British Astronomical Association (2005), both of which facilitated upgrades to observatory equipment used in this study.

References

ADS (2024). Astrophysics Data System. *https://ui.adsabs.harvard.edu/*

Bacci, P.; Maestripieri, M.; Tesi, L.; Fagioli, G.; Sannino, L.; Mancuso, A.; Mercanti, S.; Gentile, C.; Buzzi, L.; Wagh, Y.; Ye, Q.-Z.; Z.T.F. Collaboration; Duev, D.A.; Helou, G.; Lin, H.-W. and 19 colleagues (2024). “2024 RJ12.” MPEC 2024-R253. *https://minorplanetcenter.net/mpec/K24/K24RP3.html*

Brown, A.G.A. and The Gaia Ccollaboration (2018). “Gaia Data Release 2: Summary of the contents and survey properties.” *Astronomy & Astrophysics* **616**, A1.

Dupouy, P.; Laborde, J.; Jaeger, M.; Prosperi, E.; Dankov, K.; Korlevic, K.; Poropat, L.; Husar, D.; Junius, M.; Demetz, L.; Ditz, P.; Hellot, R.; Steinbach, T.; Denneau, L.; Siverd, R. and 11 colleagues (2024). “2024 NM3.” MPEC 2024-O02. *https://minorplanetcenter.net/mpec/K24/K24O02.html*

Gilmore, A.C.; Kilmartin, P.M.; Leonard, G.J.; Gray, B.; Rankin, D.; Shelly, F.C.; Dupouy, P.; de Vanssay, J.B.; Kechin, Y.; Lipunov, V.; Gorbovskoy, E.; Tiurina, N.; Balanutsa, P.; Felber, T.; Carvajal, V.F. and 20 colleagues (2024). “2024 SQ.” MPEC 2024-S51. *https://minorplanetcenter.net/mpec/K24/K24S51.html*

Harris, A.W.; Young, J.W.; Scaltriti, F.; Zappala, V. (1984). “Lightcurves and phase relations of the asteroids 82 Alkmene and 444 Gyptis.” *Icarus* **57**, 251-258.

Harris, A.W.; Young, J.W.; Bowell, E.; Martin, L.J.; Millis, R.L.; Poutanen, M.; Scaltriti, F.; Zappala, V.; Schober, H.J.; Debehogne, H.; Zeigler, K. (1989). “Photoelectric Observations of Asteroids 3, 24, 60, 261, and 863.” *Icarus* **77**, 171-186.

Herman, J.; Lowe, T.; Minguez, P.; Schultz, A.; Smith, I.; Chambers, K.; de Boer, T.; Fairlamb, J.; Gao, H.; Huber, M.; Lin, C.-C.; Magnier, E.; Ramanjooloo, Y.; Wainscoat, R.; Weryk, R. and 10 colleagues (2024). “2024 OM1.” MPEC 2024-O111. *https://minorplanetcenter.net/mpec/K24/K24OB1.html*

Number	Name	yyyy mm/dd	Phase	L_{PAB}	B_{PAB}	Period(h)	P.E.	Amp	A.E	PAR	H
	2024 NM3	2024 07/16-07/17	76.1-76.3	-28	12	0.046654	0.000003	1.2	0.3		25.2
		2024 07/17-07/18	81.8-82.6	-41	35	0.04664	0.00001	1.2	0.4		
		2024 07/18-07/19	90.0-90.6	-66	46	0.04664	0.00001	0.8	0.4		
	2024 OM1	2024 08/07-08/07	67.5-71.1	-10	-3	0.033915	0.000002	0.9	0.2		24.3
	2024 RJ12	2024 09/10-09/11	7.7-3.9	-11	3	0.03987	0.00002	0.2	0.1		27.7
	2024 SQ	2024 09/28-09/28	65.8-70.0	39	-3	0.07438	0.00003	0.8	0.4	-3	25.8
						0.1078	0.0001	0.4	0.4		

Table II. Observing circumstances and results. The phase angle is given for the first and last date. If preceded by an asterisk, the phase angle reached an extrema during the period. L_{PAB} and B_{PAB} are the approximate phase angle bisector longitude/latitude at mid-date range (see Harris et al., 1984). Amplitude error (A.E.) is calculated as √2 × (lightcurve RMS residual). PAR is the expected Principal Axis Rotation quality detection code (Pravec et al., 2005) and H is the absolute magnitude at 1 au from Sun and Earth taken from the Small-Body Database Lookup (JPL, 2024b).

JPL (2024a). Sentry: Earth Impact Monitoring. *https://cneos.jpl.nasa.gov/sentry/*

JPL (2024b). Small-Body Database Lookup. *https://ssd.jpl.nasa.gov/tools/sbdb_lookup.html*

Kwiatkowski, T.; Buckley, D.A.H.; O'Donoghue, D.; Crause, L.; Crawford, S.; Hashimoto, Y.; Kniazev, A.; Loaring, N.; Romero Colmenero, E.; Sefako, R.; Still, M.; Vaisanen, P. (2010). "Photometric survey of the very small near-Earth asteroids with the SALT telescope - I. Lightcurves and periods for 14 objects." *Astronomy & Astrophysics* **509**, A94.

NEODyS (2024). Near Earth Objects Dynamic Site. *https://newton.spacedys.com/neodys*

Pravec, P.; Hergenrother, C.; Whiteley, R.; Sarounova, L.; Kusnirak, P.; Wolf, M. (2000). "Fast Rotating Asteroids 1999 TY2, 1999 SF10, and 1998 WB2." *Icarus* **147**, 477-486.

Pravec, P.; Harris, A.W.; Scheirich, P.; Kušnirák, P.; Šarounová, L.; Hergenrother, C.W.; Mottola, S.; Hicks, M.D.; Masi, G.; Krugly, Yu.N.; Shevchenko, V.G.; Nolan, M.C.; Howell, E.S.; Kaasalainen, M.; Galád, A. and 5 colleagues. (2005). "Tumbling Asteroids." *Icarus* **173**, 108-131.

Raab, H. (2024). Astrometrica software, version 4.15.0.455. *http://www.astrometrica.at/*

Warner, B.D.; Harris, A.W.; Pravec, P. (2009). "The Asteroid Lightcurve Database." *Icarus* **202**, 134-146. Updated 2023 Oct. *https://www.minorplanet.info/php/lcdb.php*

Warner, B.D. (2023). MPO Software, Canopus version 10.8.6.20, Bdw Publishing, Colorado Springs, CO.

Zacharias, N.; Finch, C.T.; Girard, T.M.; Henden, A.; Bartlett, J.L.; Monet, D.G.; Zacharias, M.I. (2013). "The Fourth US Naval Observatory CCD Astrograph Catalog (UCAC4)." *The Astronomical Journal* **145**, 44-57.

Zappala, V.; Cellini, A.; Barucci, A.M.; Fulchignoni, M.; Lupishko, D.E. (1990). "An analysis of the amplitude-phase relationship among asteroids." *Astron. Astrophys*. **231**, 548-560.

CCD PHOTOMETRIC OBSERVATIONS OF 617 PATROCLUS-MENOETIUS MUTUAL EVENTS

Brian D. Warner
Center for Solar System Studies (CS3 - U82)
446 Sycamore Ave.
Eaton, CO 80615, USA
brian@MinPlanObs.org

Russ Durkee
Shed of Science Observatory (V61)
Minneapolis, MN, USA

Michael Fauerbach
Roque de los Muchachos Observatory (950)
Cerro Tololo Inter-American Observatory (807)
Florida Gulf Coast University
Fort Myers, FL, USA

John Gebauer, William Cloutier
McCarthy Observatory (932)
New Milford, CT, USA

Alessandro Nastasi
Galhassin Robotic Telescope (L34)
Wide-field Mufara Telescope (M57)
GAL Hassin - Centro Internazionale per le Scienze Astronomiche
Isnello, ITALY

Julian Oey
Blue Mountains Observatory (Q68)
Leura, NSW, AUSTRALIA

Robert D. Stephens
Center for Solar System Studies (CS3 - U81)
Rancho Cucamonga, CA, USA

Daniel Guimaraes Tedesco
Carlos Henrique de Oliveira Barreto
Remote Observatory of Campos dos Goytacazes (ROCG; Y16)
International University Center
Uninter, BRAZIL

(Received: 2024 October 25   Revised: 2024 November 22)

In response to a call for photometric observations of the Jupiter Trojan binary asteroid, 617 Patroclus-Menoetius, we formed a collaboration of observers in the United States, Italy, Brazil, and Australia. The observations were to coincide with the 2024-2025 mutual events season, which would allow refining the parameters of the system in preparation for NASA's Lucy fly-by mission in 2033 March. We recorded parts of nine different events from 2024 September 12 through October 23. Analysis found a period of 102.873 ± 0.006 h for the pair when including the events. The period without events was found to be 103.09 ± 0.04 h with an amplitude of 0.12 ± 0.01 mag. While we present analysis of our data for period and event details, we offer no interpretation regarding the parameters of the system beyond the rotation/orbital period. Additional observations will continue for as long as possible.

In 2033 March, NASA's Lucy mission will fly by the Jupiter Trojan 617 Patroclus and its binary companion, Menoetius. Mission planning requires having an accurate determination of the orbital period, the rotation period of the system (slightly different if excluding events from analysis), and the orbital parameters. A call was put out for photometric observations of the system during the mutual events season in mid-2024 to mid-2025 (e.g., Binzel, 2024). The timing, depths, and shapes of the events would provide critical information needed for mission planning.

Brozovic et al. (2024) published a list of predictions for superior and inferior events. The former is when Patroclus is in front of Menoetius and the later when the positions are reversed. We used those predictions to plan observations of events visible from each observatory. Warner observed every clear night between 2024 Sep 13 and Oct 23, except two (it seems that it is important to remember to start the automation script), so that a period could be found when excluding event data. We produced more than 3,800 data points used for analysis.

Lead	Observatory	Tel	MPC	Dates (mm/dd)
Durkee	Shed of Science	0.50	V61	09/30
Fauerbach	Roque de los Muchachos	0.60	950	10/10
	Cerro Tololo Inter-Am.	0.60	807	10/15
Gebauer	McCarthy	0.43	932	10/10
Nastasi	Galhassin Robotic Telescope	0.40	L34	09/12, 09/15 09/24, 10/10
	Wide-field Mufara Telescope	1.0	M57	09/20
Oey	Blue Mountains	0.40	Q68	09/20
Tedesco	Remote Observatory Campos dos Goytacazes	0.28	Y16	09/26-09/28 10/07, 10/08
Stephens	CS3-U81	0.40	U81	09/30
Warner	CS3-U82	0.25	U82	09/13-10/23

Table I. List of observers and dates of contributed data. The "Tel" column gives the telescope aperture, in meters.

Superior Events

PO	Partial Occultation
PE	Partial Eclipse
PO+PE	Partial Occultation and Partial Eclipse with overlap
PO_PE	Partial Occultation and Partial Eclipse without overlap
TO	Total Occultation
TE	Total Eclipse

Inferior Events

PO	Partial Occultation
PE	Partial Eclipse
PO+PE	Partial Occultation and Partial Eclipse with overlap
PO_PE	Partial Occultation and Partial Eclipse without overlap
AO	Annular Occultation
AO+PE	Annular Occultation and Partial Eclipse with overlap
AE	Annular Eclipse

Table II. List of abbreviations for superior and inferior mutual events as defined by Brozovic et al. (2024).

Observing and Reduction Methodology

In order to avoid working with differences among systems as much as possible, all observers used either a clear or Sloan r´ filter in the optical train of the telescope and CCD camera. Differential photometry used ATLAS refcat2 (Tonry et al., 2018) magnitudes of the comp stars. The magnitudes (r´) are on the Pan-STARRS

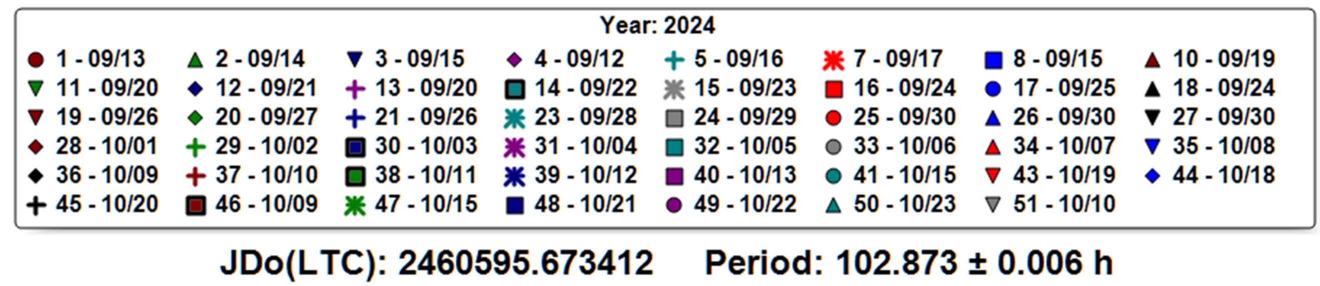

The legend, JD zero-point, and derived period for the phased plot with events included. The plots with excluded events are based on a subset of the full data set and have their own legends, zero-point, and undefined period. Session numbers are mostly, but not always, in date order. A symbol size/color combination can appear more than once due to the limited number of solid colors and symbol shapes.

photometric system, which closely follows the older Sloan (SDSS) system. The two do not have a simple linear conversion between them but, for these purposes, they are "close enough." The response of the CCD cameras favored the red-end of the visible spectrum, and so, by selecting comp stars of near solar/asteroid color, it was possible to merge the data with minimal adjustments to the zero-point. Also helpful was having all images measured by one person using the same software. Only occasional tweaks of < 0.03 mag matched all but two sessions. Those two were provided as pre-measured data using *MPO Canopus* v10 with different filter/catalog settings. Even so, they were easily fitted before analysis began.

Exposures varied from observatory to observatory. Warner, for example, used 2-minute exposures on a 0.3-meter telescope and SBIG STL-1001E (Kodak KAF-1001E 1024×1024×24-micron chip) to get a high SNR (several hundred) for the asteroid and enough for the comps in the field. The asteroid was moving through relatively sparse fields, meaning that there was a limited need to reject images when the asteroid merged with a star, but this also meant not always finding the maximum allowed number of comp stars that met the requirements for color and not being too near saturation or too faint.

In other cases, especially when using modern CMOS or similar cameras, it was harder to keep the asteroid from saturating (going into the non-linear response of the ADU) while using sufficiently long exposures to avoid problems with scintillation noise. Some trial-and-error imaging led to the correct exposure length.

All observers made their original images available to Warner via a cloud account. This included light, flat, dark, and bias frames. Using *MPO Canopus* v12, Warner created a master dark, flat, and bias images when only submasters were available. These *master processing frames* were applied on-the-fly during measuring so that the original images were not altered.

The images were all measured using *MPO Canopus* v12 which allows using the r´ (PR) magnitudes from the ATLAS refcat2 catalog for the up to 15 comp stars used for differential photometry. As noted above, the comp stars were restricted to those of near solar and asteroid color to minimize errors due to color differences.

Period analysis was done with *MPO Canopus* v12 which incorporates the FALC Fourier analysis algorithm written by Alan Harris (Harris et al., 1989). Once events were included in the data set, the period search used 15th-order analysis because of the very deep and sharp minimums. The original period search was confined to 100-106 hours based on the 102.8-hour period on the summary line of the asteroid lightcurve database (LCDB; Warner et al., 2009). With each new data set, the period search range was narrowed to focus on the merging period solution.

Period Analysis with Events

The period spectrum shows the expected minimum near 103 hours. Given the shape of the lightcurve and depth of minimums along with the known nature of the asteroid, no attempt was made to search for shorter or longer alias periods.

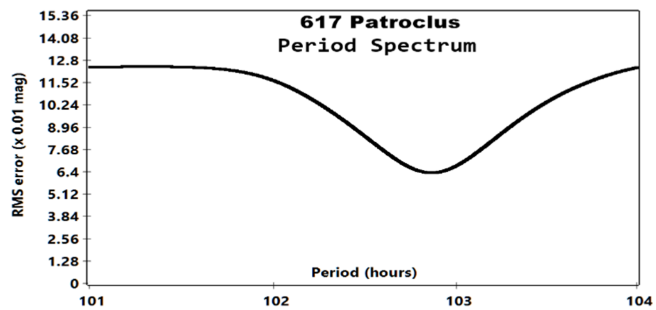

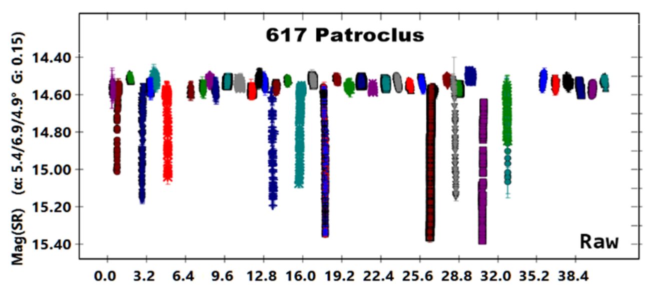

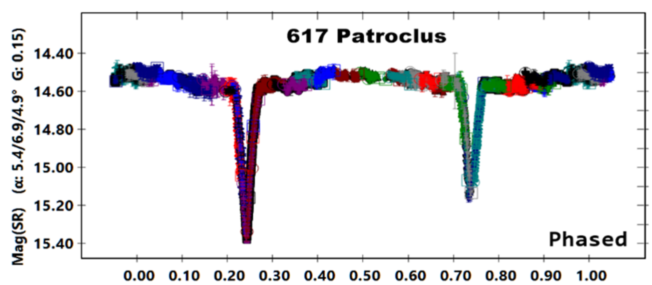

The raw plot shows the individual events and, when expanded, the slow periodic nature of the lightcurve outside events. The phased plot is fit to the adopted period of 102.873 ± 0.006 h. This is the formal error reported by the FALC algorithm. A better estimate is the error in the period that would shift the data from the initial match by 0.01 to 0.10 phase (the latter being the so-called *2% rule*). Using 0.02 phase for the gauge, a more reasonable error is 0.04 h.

*To save space and repetition, the legend, zero-point JD, and period are included in the common plot above, which applies to **all** but the two plots where the period was found when excluding events.*

The Combined Events

Superior Event. The superior event occurs when the secondary, Menoetius, *goes behind the primary*, Patroclus. As an aside, Menoetius was Patroclus' father, so "dad" is taking a back seat in this case. The "Superior" plot shows a close-up the superior event. Zooming in even more shows that the multiple sessions covering the event do not have quite the same shape. This could be due to systematic errors among the data or, possibly, evolution of the mutual events with changing viewing aspect.

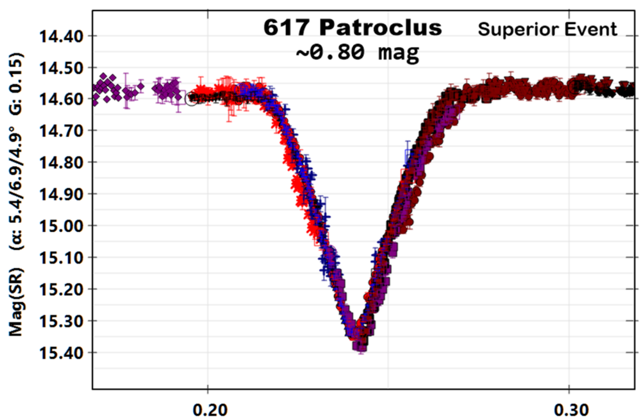

Inferior Event. When Menoetius *passes in front* of Patroclus, this is an inferior event. The depth of about 0.60 mag in the "Inferior" plot leads to an estimated effective diameter ratio between Menoetius and Patroclus of at least 0.86 ± 0.03. This is close to the 0.92 based on the published effective diameters of the two bodies (LCDB; Warner et al, 2009).

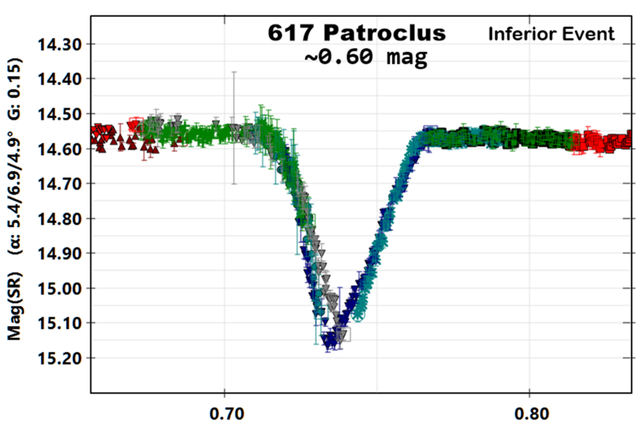

There are much greater differences among the sessions covering the inferior event. Here again, it could be systematic errors or and evolving lightcurve. Detailed modeling will help determine how much of each is a contributor.

The Individual Events

For each event, the date and type are given. Use Table II to interpret the event types. An event in bold text is the one that causes the greatest magnitude drop. Since the full individual events were not observed in their entirety, only some of the mutual circumstances of an event were covered.

It is difficult to determine when the entire event begins and/or ends because there is no sharp shoulder point. In this case, a best guess data point was chosen for the end of the event. For events that were sharply defined on both sides of the minimum, the Time of Minimum/Maximum feature of *MPO Canopus* was used to estimate the time of minimum.

The algorithm is based on the method developed by Hertzsprung (1928) as described by Henden and Kaitchuck (1990). This relies on several data points on either side of the minimum. Each point on one side of the minimum is "connected" to another at about the same amplitude on the other side. An iteration process eventually finds the best estimate for the time of minimum. In our case, about ten pairs were initially used to start the calculations. Since the interval between exposures was usually only a few minutes, this allowed for a fairly precise estimate of the time of minimum.

It's important to note that the values for raw data, not phased to a period nor from a Fourier curve, were used in the analysis. Noise in the data likely had a noticeable effect on our estimated times. Also important is that light-time corrected JD were used in the calculations for minimum. Individual raw data points were in UT. To compare to Brozovic et al. (2024), the times of minimum were adjusted to geocentric UT using a constant of 0.005785 d/au and computing the distance to units of 0.0001 au. This also means that the date/time of points on the plots are light-time corrected and that the correction must be reversed to get the UT value.

The description for computing the error of the estimate was not included in Henden and Kaitchuck. However, the latter provided the necessary details in a private communication.

2024 September 13 (Inferior – **PO** PO+PE, PE). This was observed by Warner (U82). The estimated end of the event was 08:46 UT (0.835 d on the plot). Brozovic et al. (2024) predicted 08:31 UT (0.855 d).

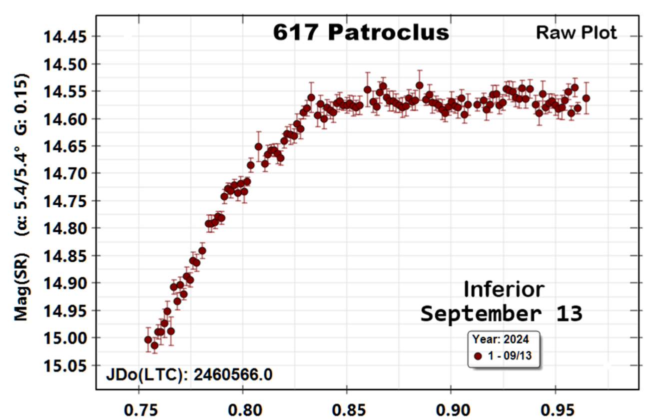

2024 September 15 (Superior – **PO** PO+PE, PE). Observed by Warner at (U82). The estimated time of minimum from our data is 08:09 UT (0.819 d on the plot). Brozovic et al. (2024) predicted 07:56 UT (0.810 d) for the deepest minimum.

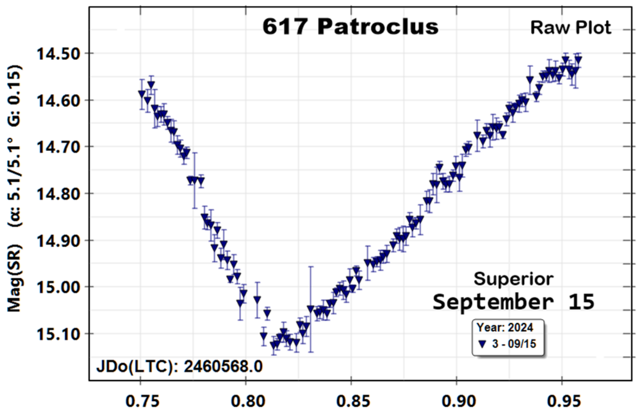

2024 September 17 (Inferior – **PO** PO+PE, PE). Observed by Warner (U82). Based on his data, the estimated time for the start of the event is 09:32 UT (0.877 d on the plot). Brozovic et al. (2024) gave 09:06 UT, or about 0.858 d on the plot.

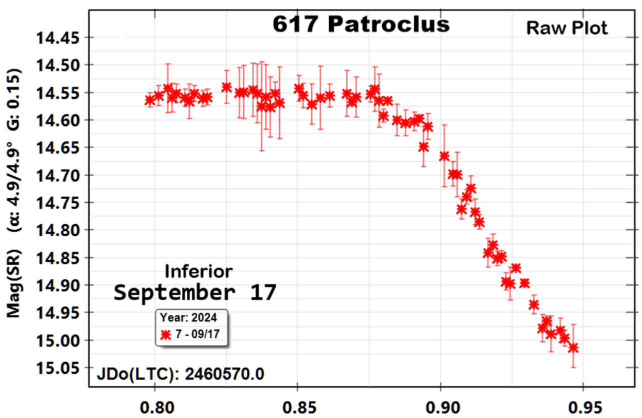

2024 September 26 (Inferior – **PO** PO+PE, PE). Observed by Tedesco (Y16). A very rough estimate for the start of the event is Sep 25 at 23:34 UT (0.461 d on the plot). Brozovic et al. (2024) predicted Sep 25 at 23:02 UT (0.440 d). The left-most data point in the plot is on Sep 25 23:18 UT (0.451 d).

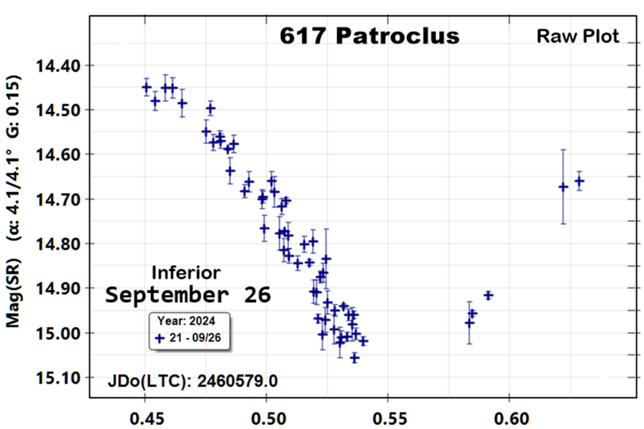

2024 September 28 (Superior – **PO** PO+PE, PE). Observed by Warner (U82). The estimated time for the end of the event is 07:48 UT (0.805 d on the plot). Brozovic et al. (2024) predicted 07:30 (0.793 d).

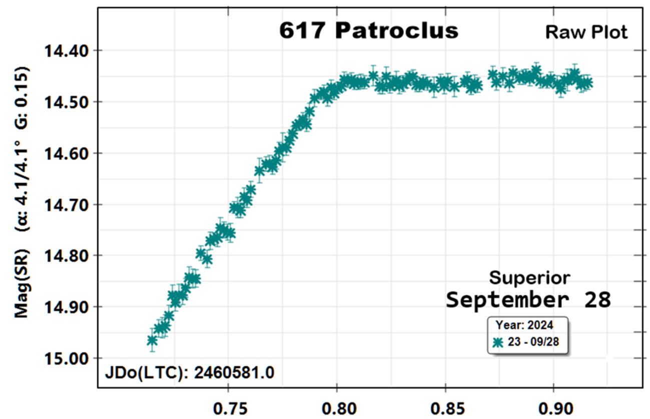

2024 September 30 (Inferior – **PO** PO+PE, AO+PE, PO+PE, PO). Observed by Warner (U82, red circles), Stephens (U81; blue up triangles), and Durkee (V61; black down triangles). The first plot shows how well the data overlapped and, if nothing else, confirmed no significant anomalies in any one data set.

Using Warner's data alone, the estimated time of minimum was 08:47 UT. Stephens' data gave 08:48 UT while Durkee's gave 08:45 UT. Of the three, the Stephens' data gave the strongest signs of a total event (flat bottom), which seems to confirm the annular occultation and partial eclipse with overlap predicted by Brozovic et al. (2024). Their prediction for deepest minimum was at 08:38 UT (0.86 d on the plot).

Start time based on Warner's data was 06:03 UT (0.732 d on the plot), 05:52 UT (0.724 d) from Stephens' data, and 06:14 UT (0.740 d) from Durkee's. Brozovic et al. (2024) predicted 06:00 UT (0.729 d on the plot). The differences are probably mostly due to the uncertainty in estimating the start time.

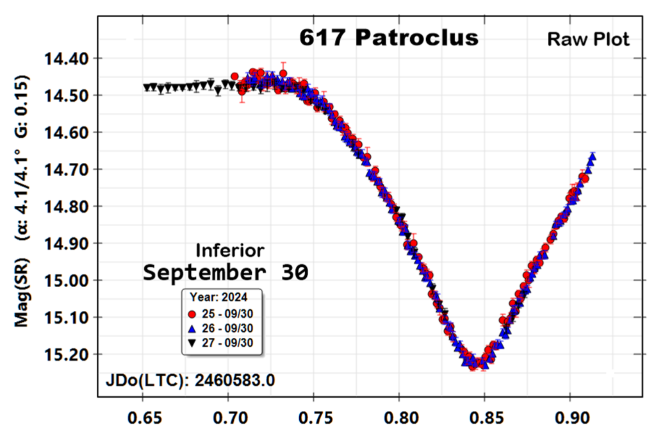

2024 October 9 (Inferior – **PO** PO+PE, AO+PE, PO+PE, PO). Observed by Fauerbach (950), our estimate of event end is 01:16 UT (0.533 d on the plot). Brozovic et al. (2024) predicted end-of-event for 01:05 (0.525 d). The minimum is not fully defined. The earliest data point is on Oct 8 at 22:44 UT (0.425 d on the plot). Brozovic et al. (2024) predicted 22:26 UT (about 0.415 d).

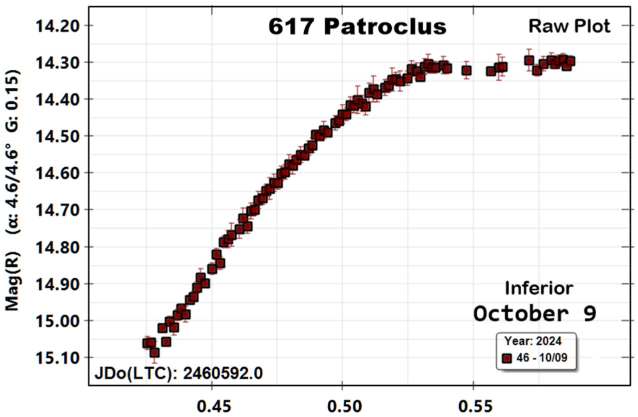

2024 October 10-11 (Superior – **PE** PO+PE, TO, PO+PE, PO). The start and apparent minimum of this event were observed by Nastasi (L34). Because of occasional periods of diminished transparency, the estimate for the start time is more uncertain than in other cases.

Our best estimate is on Oct 10 at 22:50 UT (0.431 d on the plot). Brozovic at al. predicted 23:08 UT (0.442 d). Our estimate for the time of minimum, based on the last data point at the low point, is Oct 11 at 01:47 UT (0.554 d on the plot). Brozovic et al. (2024) predicted 01:45 UT (0.552 d).

The end of the event is not defined, but the data from Warner (U82) around that time indicate approximate symmetry in the minimum point between start and end. The first data point in the Warner subset is at 04:35 UT (0.670 on the plot). Brozovic et al. (2024) predicted 04:08 UT (0.650 d) for event end.

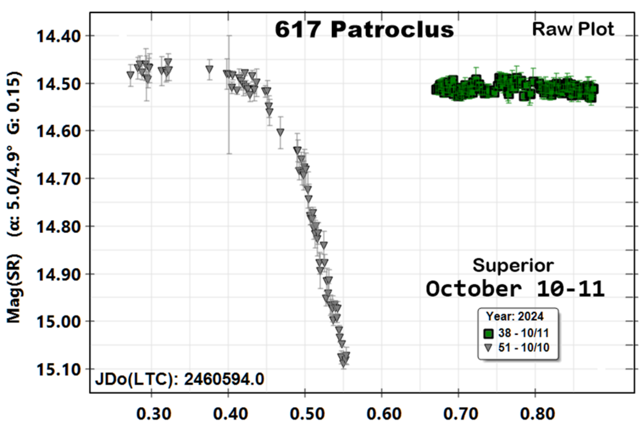

2024 October 13 (Inferior – **PE** PO+PE, PO). Observed by Warner (U82), the estimated time of minimum is 05:37 UT (0.713 d on the plot). Brozovic et al. (2024) listed 05:24 UT (0.704 d) for minimum and 08:03 UT (0.815 d) for end-of-event. Coverage at the end was not complete, but our best estimate is 08:07 UT (0.818 d).

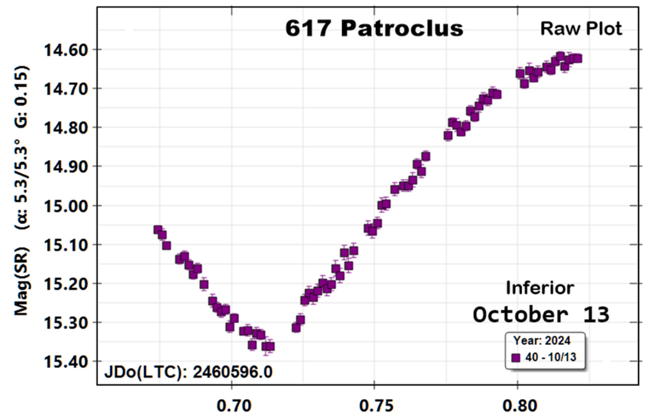

2024 October 15 (Superior – **PE** PO+PE, PO). Observed by Fauerbach (807), whose data started close to the start of the event at 05:52 UT (0.724 d on the plot), which is the same time given by Brozovic et al. (2024). Warner (U82) also observed the same event, with his data starting about 20 minutes earlier. Those data give an estimated event start of 05:47 UT (0.721 d).

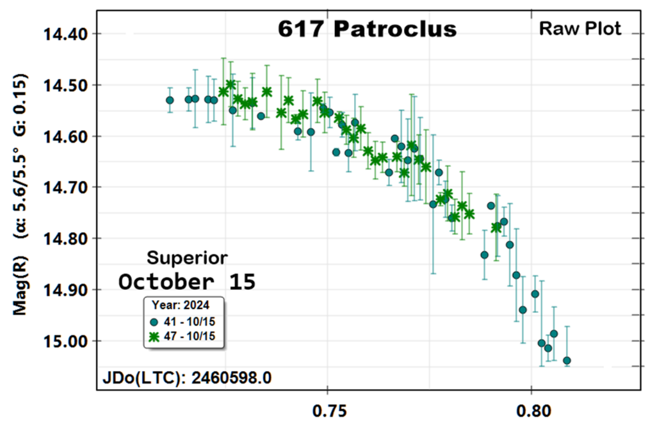

Periods Analysis Sans Events

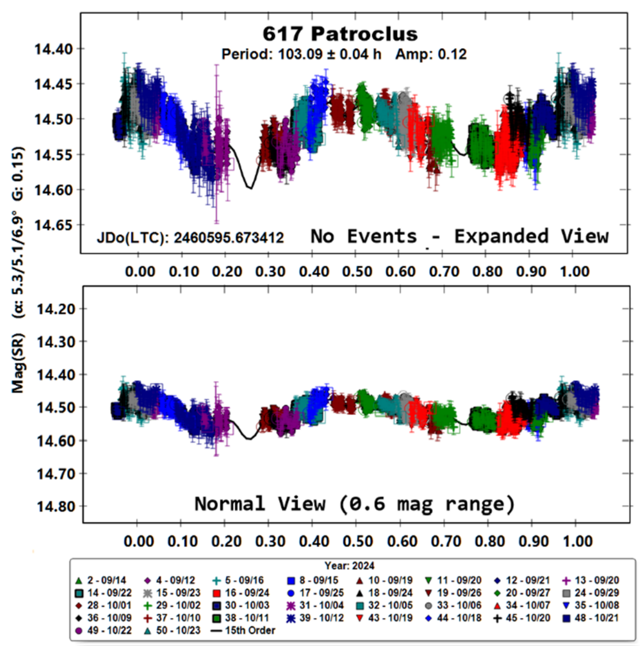

Parameters	This Paper	Brozovic et al.	Difference
Rotational Period with Events (h)	102.873 ± 0.006	102.876 ± 0.005	0.003 h
Rotational Period without Events (h)	103.09 ± 0.04	103.08 ± 0.03	0.01 h
Minimum Depth (Superior, mag)	0.79 ± 0.03	0.76	0.03 mag
Maximum Depth (Inferior, mag)	0.60 ± 0.03	0.61	0.01 mag
Effective Diameter Ratio (Menoetius/Patroclus)	0.86 ± 0.03	0.92	0.06 ± 0.06

Observed Events	This Paper UT	Brozovic et al. UT	UT-Brozovic minutes
Sep 13 – Inferior (end)	08:46	08:31	+15
Sep 15 – Superior (minimum)	08:09	07:56	+14
Sep 17 – Inferior (start)	09:32	09:06	+26
Sep 26 – Inferior (start)	23:34	23:02	+32
Sep 28 – Superior (end)	07:48	07:30	+18
Sep 30 – Inferior (start)	06:14	06:00	+14
(minimum)	08:47	08:38	+9
Oct 09 – Inferior (minimum – Oct 8)	22:44	22:26	+18
(end)	01:16	01:05	+11
Oct 10 – Superior (start)	22:50	23:08	-18
(minimum – Oct 11)	01:47	01:45	+2
(end – Oct 11, earliest time)	04:35	04:08	+27
Oct 13 – Inferior (minimum)	05:37	05:24	+13
(end – ill-defined)	08:07	08:03	+4
Oct 15 – Superior (start – earliest time)	05:47	05:52	-5

Table III. A listing of the observed events, giving the estimated UT from this paper, the UT predicted by Brozovic et al. (2024), and the difference between our estimate and Brozovic et al. (2024). All times in this table are Earth-centric.

It might, maybe even should, be expected that the period derived when using the data with and without the events would be the same or within a couple sigmas. When excluding the events, the period found by *MPO Canopus* was 103.09 ± 0.04 h, making the lower 2-sigma result about 103.01 h. The result using the events was 102.873 ± 0.006 h. If using the more realistic 2-sigma value of 0.08 h, the maximum becomes about 102.879 h. We leave to others to reconcile the differences, which may be to do to with insufficient data outside the events, i.e., not enough overlapping sections of the lightcurve, shadowing effects, lightcurve evolution, or a permutation of the three.

Remarks

We plan additional observations as the mutual event season continues into 2025 mid-January. Most observers will limit their observations to dates and times that can cover some portion of an event. Warner will work the asteroid every possible night until the observing runs are cut too short as the asteroid moves westward across the sky. All the data used in the analysis will be uploaded to the Asteroid Lightcurve Data Exchange Format (ALCDEF) web site at *https://alcdef.org* after publication of the follow-up paper.

Acknowledgements

This research has made use of the Astrophysics Data System, funded by NASA under Cooperative Agreement 80NSSC21M00561. This work has made use of data from the Asteroid Terrestrial-impact Last Alert System (ATLAS) project. ATLAS is primarily funded to search for near earth asteroids through NASA grants NN12AR55G, 80NSSC18K0284, and 80NSSC18K1575; byproducts of the NEO search include images and catalogs from the survey area. The ATLAS science products have been made possible through the contributions of the University of Hawaii Institute for Astronomy, the Queen's University Belfast, the Space Telescope Science Institute, and the South African Astronomical Observatory. We thank *Minor Planet Bulletin* editor, Richard Binzel, and producer, Pedro A. Valdés Sada, for extending the usual submission deadline for this issue so that we could observe and report on as many events as possible. Warner and Stephens thank the Planetary Society for 2007 and 2013 Shoemaker NEO grants which helped purchase some of the equipment used in this effort. In addition, Warner thanks Robert D. ("Bob") Stephens, his long-time observing cohort and occasional on-site maintenance engineer, for his help throughout the years. Tedesco thanks the Wilson Picler Foundation for their support.

References

Binzel, R.P. (2024). "Call for Observations of the Patroclus and Menoetius Mutual Events: Support for the NASA Lucy Mission to the Trojan Asteroids." *Minor Planet Bull.* **51**, 212.

Brozovic, M.; Jacobson, R.A.; Park, R.S.; Descamps, P.; Berthier, J.; Pinilla-Alonso, N.; Popescu, M.; Licandro, J. (2024). "Orbit of Patroclus-Menoetius Binary System and Predictions for the 2024/2025 Mutual Events Season." *Astron. J.* **167**, A104.

Harris, A.W.; Young, J.W.; Bowell, E.; Martin, L.J.; Millis, R.L.; Poutanen, M.; Scaltriti, F.; Zappala, V.; Schober, H.J.; Debehogne, H.; Zeigler, K.W. (1989). "Photoelectric Observations of Asteroids 3, 24, 60, 261, and 863." *Icarus* **77**, 171-186.

Henden, A.A.; Kaitchuck, R.H. (1990). *Astronomical Photometry: A Text of and Handbook for the Advanced Amateur and Professional Astronomer*. pp. 266-270. Willmann-Bell, Richmond, VA, USA.

Hertzsprung, E. (1928). "On the character of the variation of SX Aurigae." *Bull. Astr. Inst. Netherlands* **4**, 178-179. Available from the SAO Astrophysics Data System (ADS): *https://articles.adsabs.harvard.edu/pdf/1928BAN.....4..178H*

Tonry, J.L.; Denneau, L.; Flewelling, H.; Heinze, A.N.; Onken, C.A.; Smartt, S.J.; Stalder, B.; Weiland, H.J.; Wolf, C. (2018). "The ATLAS All-Sky Stellar Reference Catalog." *Astrophys. J.* **867**, A105.

Warner, B.D.; Harris, A.W.; Pravec, P. (2009). "The Asteroid Lightcurve Database." *Icarus* **202**, 134-146. Updated 2024 August. *https://www.minorplanet.info/php/lcdb.php*

617 PATROCLUS-MENOETIUS MUTUAL EVENT LIGHTCURVES

Wayne Hawley
Old Orchard Observatory (Z09)
Fiddington, UK
hawley.wayne@gmail.com

James D. Armstrong, Jameeka Marshall
University of Hawaii Institute for Astronomy
(L09, Q58, Q59, T04, V38, W79, W89, Z17)
34 Ohia Ku Street,
Pukalani, HI 96768, USA

Kent DeGroff
Whiskey Creek Observatory (V19)
New Mexico, USA

Paul C. Leyland
Tacande Observatory (J22)
La Palma, SPAIN

Mohammad Shawkat Odeh
Al Khatim Observatory (M44)
Abu Dhabi, UAE

Julian Oey
Blue Mountains Observatory (Q68)
94 Rawson Pde, Leura, NSW, AUSTRALIA

Alvaro Fornas
AVA (J57)
CAAT Centro Astronómico Alto Turia, SPAIN

Rui Gonçalves
Linhaceira (938)
Tomar, PORTUGAL

Emmanuel Kardasis, Alexia Takoudi
Pelagia-Eleni Observatory (247)
Athens, GREECE

Maxim Usatov
Astrocamp, Nerpio (I79) SPAIN

John Drummond
Possum Observatory (E94)
Gisborne, NEW ZELAND

(Received: 2024 October 17 Revised: 2024 October 31)

We report on photometric observations of the binary Trojan asteroid 617 Patroclus-Menoetius undertaken from July to October 2024.

In response to the paper “Call for Observations of the Patroclus and Menoetius Mutual Events: Support for the NASA Lucy Mission to the Trojan Asteroids” (Binzel, 2024); photometric observations of the binary Trojan asteroid 617 Patroclus-Menoetius were undertaken from 25 July 2024 to 30 October 2024. 617 Patroclus, is a Trojan asteroid discovered 1906-10-17 by A. Kopff at Heidelberg. Its binary pair member, Menoetius was discovered in 2001, with the provisional designation: S/2001 (617) 1.

Here we present mutual event lightcurves derived from photometric images obtained from observatories around the globe. We used the predictions by Brozovic et al. (2024) as a basis for planning our observations. *All lightcurves presented have been light-time corrected accounting for the asteroid's changing distance to Earth.* Several of the co-authors used their own equipment and some used the Las Cumbres Observatory facilities. A full listing of observers and equipment is given in the accompanying table. Photometric reduction was carried out with *TychoTracker Pro* Version 11.7.5. (TT). We archive our data with the Asteroid Lightcurve Database (Warner et al., 2009).

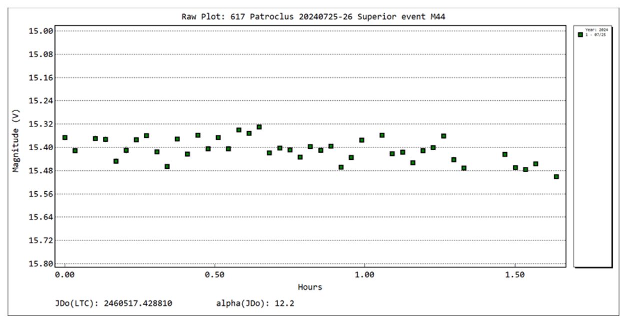

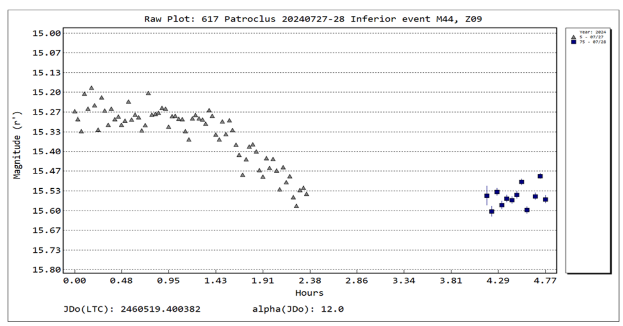

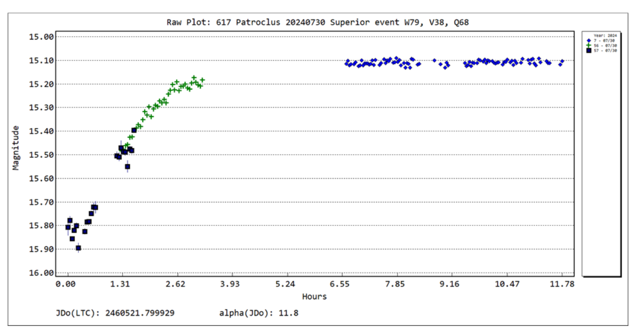

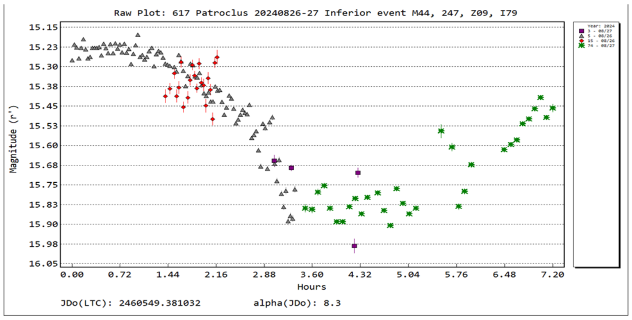
Raw Plot: 617 Patroclus 20240826-27 Inferior event M44, 247, Z09, I79
Magnitude (r')
Hours
JDo(LTC): 2460549.381032
alpha(JDo): 8.3

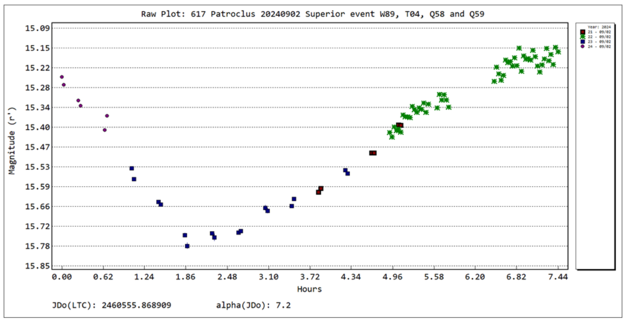
Raw Plot: 617 Patroclus 20240902 Superior event W89, T04, Q58 and Q59
Magnitude (r')
Hours
JDo(LTC): 2460555.868909
alpha(JDo): 7.2

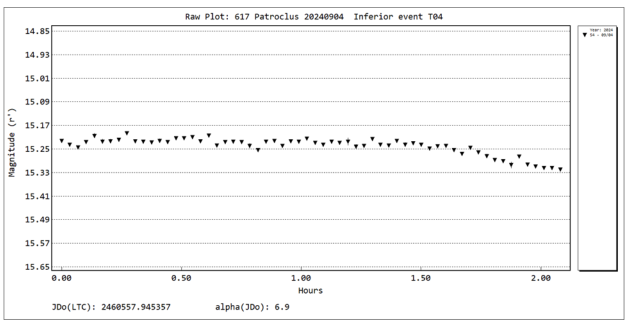
Raw Plot: 617 Patroclus 20240904 Inferior event T04
Magnitude (r')
Hours
JDo(LTC): 2460557.945357
alpha(JDo): 6.9

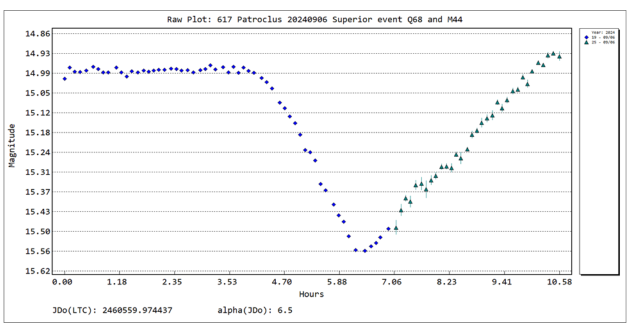
Raw Plot: 617 Patroclus 20240906 Superior event Q68 and M44
Magnitude
Hours
JDo(LTC): 2460559.974437
alpha(JDo): 6.5

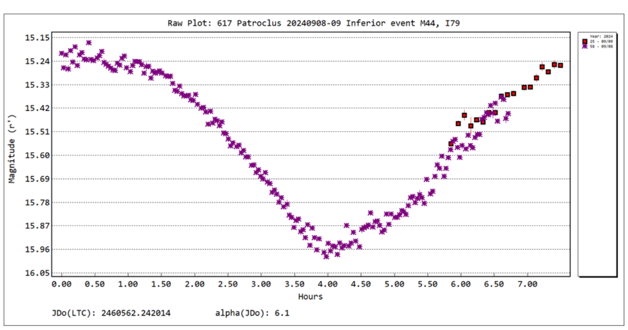
Raw Plot: 617 Patroclus 20240908-09 Inferior event M44, I79
Magnitude (r')
Hours
JDo(LTC): 2460562.242014
alpha(JDo): 6.1

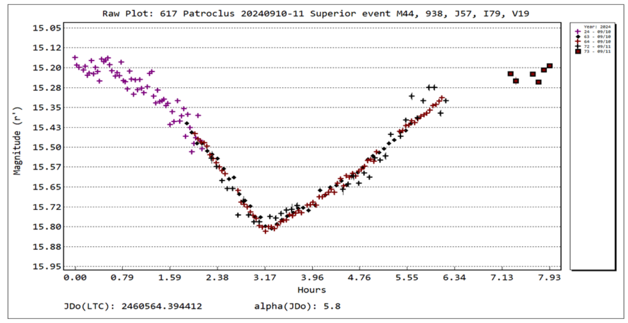
Raw Plot: 617 Patroclus 20240910-11 Superior event M44, 938, J57, I79, V19
Magnitude (r')
Hours
JDo(LTC): 2460564.394412
alpha(JDo): 5.8

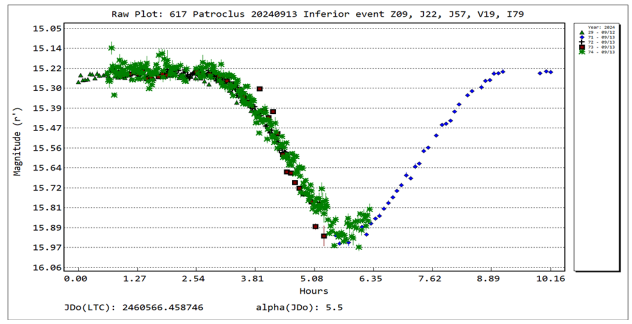
Raw Plot: 617 Patroclus 20240913 Inferior event Z09, J22, J57, V19, I79
Magnitude (r')
Hours
JDo(LTC): 2460566.458746
alpha(JDo): 5.5

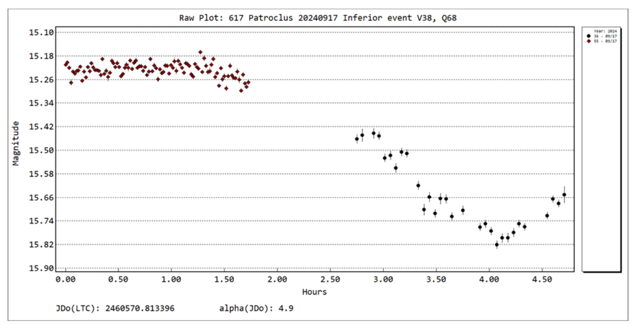
Raw Plot: 617 Patroclus 20240917 Inferior event V38, Q68
Magnitude
Hours
JDo(LTC): 2460570.813396
alpha(JDo): 4.9

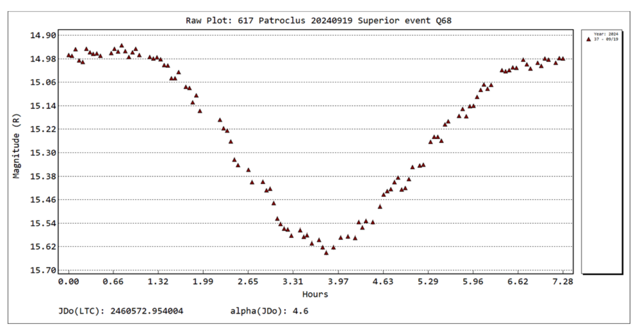
Raw Plot: 617 Patroclus 20240919 Superior event Q68
Magnitude (R)
Hours
JDo(LTC): 2460572.954004
alpha(JDo): 4.6

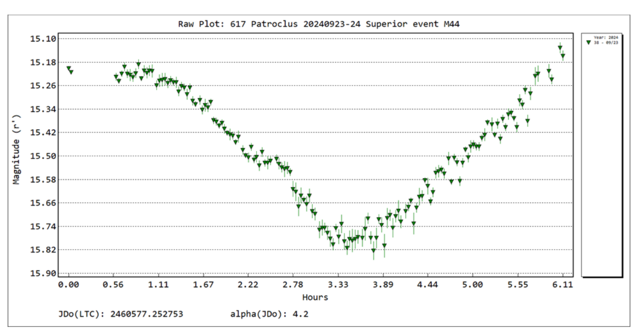
Raw Plot: 617 Patroclus 20240923-24 Superior event M44
Magnitude (r')
Hours
JDo(LTC): 2460577.252753
alpha(JDo): 4.2

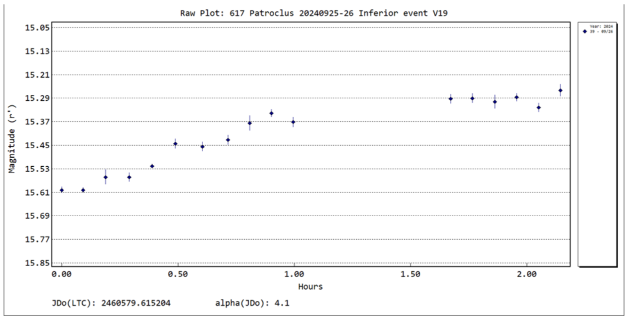

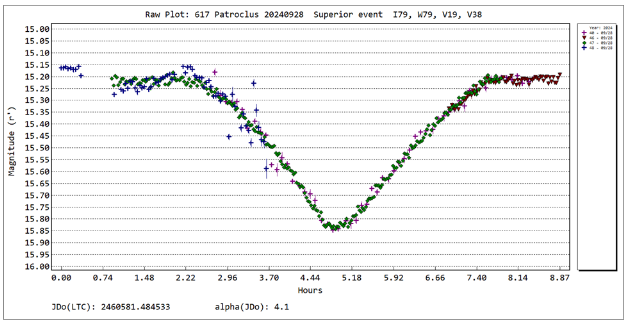

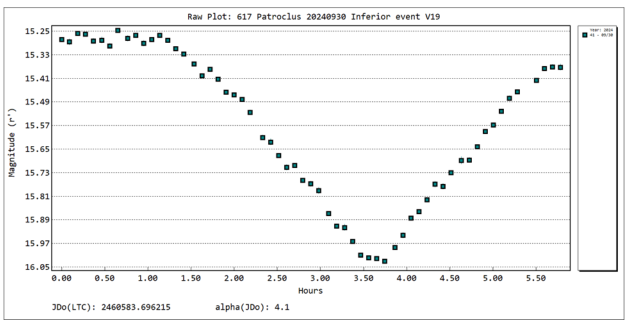

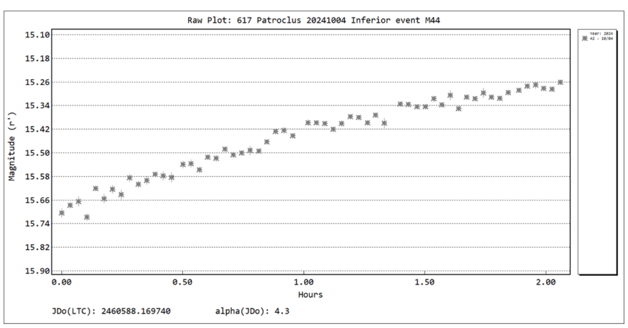

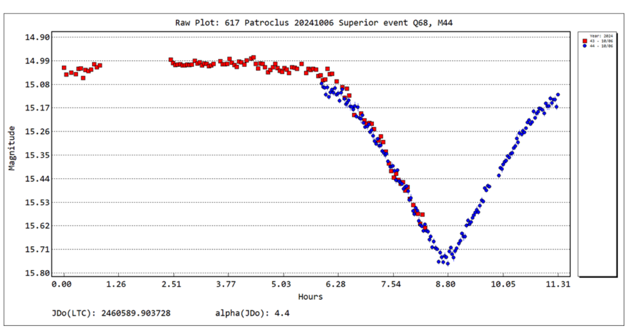

Observatory	Telescope	CCD/CMOS	Filter	Sessions
Old Orchard Observatory (Z09) Hawley	0.35-m SCT f/6.7	SX694 Trius Pro (2×2)	SR	6
Linhaceira Observatory (938) Gonçalves	0.35-m SCT f/5.6	ST-7XME (1×1)	C	2
Al Khatim Observatory (M44) Odeh	0.36-m SCT f/7.7	ASI2600MM Pro	C	10
Sutherland LCO-Aqawan A (L09) Armstrong, Marshall	0.4-m f/8	SBIG STL6303 (1×1)	SR	1
McDonald LCO-Aqawan A (V38) Armstrong, Marshall	0.4-m f/8	SBIG STL6303 (1×1)	SR	3
Tenerife-LCO Aqawan A #2 (Z17) Armstrong, Marshall	0.4-m f/8	SBIG STL6303 (1×1)	SR	2
Possum Observatory (E94) Drummond	0.35-m f/10	SBIG STL11000M (2×2)	C	2
AstroCamp, Nerpio (I79) Usatov	0.4-m f/6.8	Moravian C3-61000 Pro (2×2)	Lum	4
Siding Spring LCO-Clamshell #1 (Q58) Armstrong, Marshall	0.4-m f/8	SBIG STL6303 (1×1)	SR	1
Siding Spring LCO-Clamshell #2 (Q59) Armstrong, Marshall	0.4-m f/8	SBIG STL6303 (1×1)	SR	2
Blue Mountains Observatory (Q68) Oey	0.35-m f5/9	SBI STT-1603 3 (1×1)	C	6
Haleakala-LCO Clamshell #1 (T04) Armstrong, Marshall	0.4-m f/8	SBIG STL6303 (1×1)	SR	3
Cerro Tololo-LCO Aqawan B #1 (W79) Armstrong, Marshall	0.4-m f/8	SBIG STL6303 (1×1)	SR	4
Cerro Tololo-LCO Aqawan A #1 (W89) Armstrong, Marshall	0.4-m f/8	SBIG STL6303 (1×1)	SR	2
Centro Astronómico Alta Turia (J57) Álvaro Fornas Silva	0.43-m f/6.8	QHY600	Lum	2
Tacande Observatory (J22) Leyland	0.4-m Dilworth f/6.5	SX814 Trius Pro (2×2)	V	1
Whiskey Creek Observatory (V19) DeGroff	0.46-m Newt. f/4.2	QHY 268M	V	7
Pelagia-Eleni Observatory (247) Kardasis, Takoudi	0.28-m SCT f/10	ASI 183 Pro	V	2

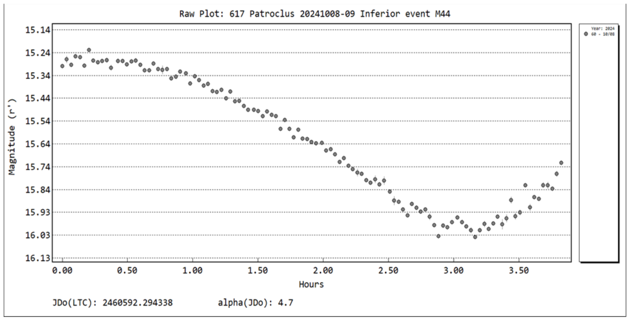

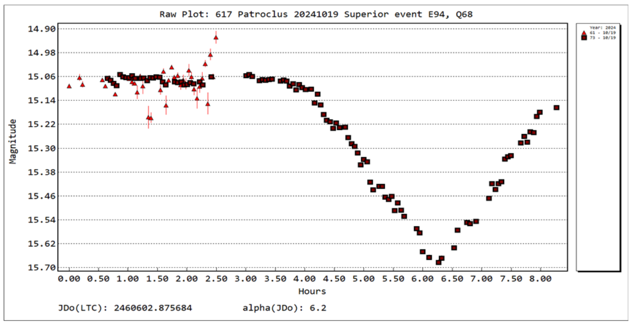

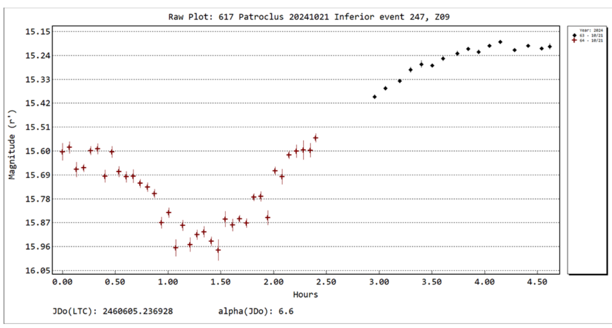

Acknowledgements

Our thanks are extended to Daniel Parrott, author of *TychoTracker Pro*. This work has made use of data from the Asteroid Terrestrial-impact Last Alert System (ATLAS) project (Tonry et al., 2018). ATLAS is primarily funded to search for near earth asteroids through NASA grants NN12AR55G, 80NSSC18K0284, and 80NSSC18K1575; byproducts of the NEO search include images and catalogues from the survey area. The ATLAS science products have been made possible through the contributions of the University of Hawaii Institute for Astronomy, the Queen's University Belfast, the Space Telescope Science Institute, and the South African Astronomical Observatory. The ATLAS Catalog makes use of the formulae to convert Pan-STARRS gri to BVRI. (Kostov and Bonev, 2017). This work makes use of observations from the Las Cumbres Observatory global telescope network. The research work at Blue Mountains Observatory is supported by the 2015 and 2018 Shoemaker NEO grant.

References

Binzel, R.P. (2024). “Call for Observations of the Patroclus and Menoetius mutual events: Support for the Nasa Lucy Mission to the Trojan Asteroids.” *Minor Planet Bulletin* **51**, 212.

Brozovic, M.; Jacobson, R.A.; Park, R.S.; Descamps, P.; Berthier, J.; Pinila-Alonso, N.; Popescu, M.; Licandro, J. (2024). “Orbit of the Patroclus-Menoetius Binary System and Predictions for the 2024/2025 Mutual Events Season.” *Astron. J.* **167**, 104, 12 pp.

JPL (2023). Small-Body Database Lookup. *https://ssd.jpl.nasa.gov/tools/sbdb_lookup.html*

Kostov, A., Bonev, T. (2017) “Transformation of Pan-STARRS1 gri to Stetson BVRI magnitudes. Photometry of small bodies observations.” *Bulgarian Astron. J.* **28**, 3 (ArXiv:1706.06147v2).

Tonry, J.L.; Denneau, L.; Flewelling, H.; Heinze, A.N.; Onken, C.A.; Smartt, S.J.; Stadler, B.; Weiland, H.J.; Wolf, C. (2018). “The ATLAS All-Sky Stellar Reference Catalog.” *Astrophys. J.* **867**, A105.

Warner, B.D.; Harris, A.W.; Pravec, P. (2009). “The Asteroid Lightcurve Database.” *Icarus* **202**, 134-146. Updated 2023 Oct. *https://minorplanet.info/php/lcdb.php*

OBSERVATIONS OF PATROCLUS AND MENOETIUS MUTUAL EVENTS WITH VATICAN ADVANCED TECHNOLOGY TELESCOPE (VATT)

Jean-Baptiste Kikwaya Eluo
Vatican Observatory
V-00120 Vatican City of State
jbkikwaya@arizona.edu; jbkikwaya@gmail.com

Carl W. Hergenrother
Ascending Node Technologies, LLC
Tucson, Arizona, USA

(Received: 2024 October 21)

We report observations of mutual events for the Patroclus and Menoetius binary system. We observed on 7 nights from September 29 to October 6, 2024, UT with the Vatican Advanced Technology Telescope on Mount Graham, Arizona. Two clear mutual events lightcurves were obtained: September 30, 2024, from 06:07:12.0 UT to 09:57:36.0 UT with an amplitude of 0.82 magnitudes and October 02, 2024, from 09:28:48.0 UT to 09:46:04.8 UT with an amplitude of 0.05 magnitudes. On both dates, only part of the mutual event was observed. Three nights (29 Sept 2024 UT, 03 Oct 2024 UT, and 05 Oct 2024) did not show any mutual event as predicted by Brozovic et al. (2024). On two nights, 04 Oct 2024 UT, and 06 Oct 2024 UT, mutual events occurred outside the observing window at the VATT.

The Trojan binary asteroid system formed by (617) Patroclus and (617) I Menoetius is located in the Jupiter L5 Trojan cloud. Its binary nature was discovered in 2001 on Sept 22.6 UT using an adaptive optics system on the 8.1-m Geminid North Telescope on Mauna Kea in the J, H, and K' bands (Merline et al., 2001). The two components are similar in size, with Patroclus having an average diameter of 113 km and Menoetius slightly smaller at 104 km (Binzel, 2024). Buie et al. (2015) reported the two components to be ellipsoids with three-dimensional shape models of 127×117×98 km for Patroclus and 117×108×90 km for Menoetius. These dimensions were refined by Grundy et al. (2018) to be 130.8×126.2×122.8 km for Patroclus and 117.1×110.8×107.8 km for Menoetius. Not only are the two components nearly equal in size, but Mueller et al. (2010) has suggested that they have similar composition and surface properties. The orbital period of the two components while alternatively transiting and occulting each other is estimated to be 4.283 ± 0.004 days by Marchis et al. (2006) and 4.282760 ± 0.000005 days by Grundy et al. (2018).

The Patroclus-Menoetius binary asteroid is a target of the NASA Lucy mission. It is the only currently planned Lucy target in the Jupiter L5 Trojan cloud. After an encounter with the main-belt asteroid (52246) Donaldjohanson on 2025 April 20, Lucy will fly by several objects in Jupiter's L4 Trojan cloud, particularly (3548) Eurybates and its satellite Queta on 2027 August 12, (15094) Polymele on 2027 September 15, (11351) Leucus on 2028 April 2028 and (21900) Orus on 2028 November 11. Then on 2033 Mars 2, Lucy will make a flyby of (617) Patroclus and (617) I Menoetius (Levison et al., 2021).

The orbital plane of the Patroclus-Menoetius binary system crosses the Earth's line-of-sight twice during the course of its 11.89-year orbital period (Binzel, 2024). This favorable geometry occurred during the September 2024 opposition with the binary system having a brightness of 14.6 visual magnitude. It offered the opportunity to produce very precise "mutual event lightcurves" which would help to refine the binary orbit, the sizes and shapes of the two components (Binzel, 2024). These measurements would accurately support the instrument targeting during Lucy flyby to the binary Trojans.

Brozovic et al. (2024) presents precise predictions for mutual occultations and transits of the Patroclus-Menoetius system. Tables 3 and 4 of their work give the times for event start, stop, and mid-event. The work also includes the type of mutual event: PO (Partial Occultation), PE (Partial Eclipse), PO-PE (Partial Occultation and Partial Eclipse with overlap, PO+PE (Partial Occultation and Partial Eclipse without overlap), TO (Total Eclipse), TE (Partial Eclipse), AO (Annular Occultation), and AE (Annular Eclipse).

Observation and reduction

The VATT observation campaign was conducted on 7 nights (between 2024 September 29 UT and 2024 October 06 UT). We used the Vatican Observatory's Vatican Advanced Technology Telescope, an f/1.0 telescope with a primary mirror of 1.8-m in diameter and a 0.38-m f/0.9 secondary mirror (Kikwaya and Hergenrother, 2023). The VATT is located at Mount Graham in southern Arizona with an MPC code of 290.

The VATT4k CCD camera with a 4064×4064 15×15 µm pixel detector was used. To reduce the readout time to 30 seconds, we binned 2×2, resulting in a plate scale of 0.375 arcsec/pixel. VATT4k covers the visible spectrum (300-1000 nm) and has a quantum efficiency that peaks at 450 nm (Kikwaya and Hergenrother, 2024).

For the entire observing run, we collected two hundred bias images and fifteen dome-flat images in the V filter to generate a master bias and a master flat. Several sequences of fifty images were acquired, with the focus being checked at the start and the end of each sequence to ensure the FWHM remained around 2.5 pixels or 1". Observations were limited to elevations higher than 30 degrees.

The *Tycho Tracker* software was used to reduce the data and generate a photometry file containing the time on Julian day, the magnitude of the binary system Patroclus-Menoetius, and the magnitude error. The overall value of the error was around 0.01 magnitude.

All timings reported in this work are for an Earth-based observer. No light-time corrections have been applied.

29 September 2024 UT. We collected 204 images from 06:13:41 UT to 10:06:49 UT. The observation window ended when Patroclus-Menoetius descended to an elevation of less than 30 degrees. There was no mutual event predicted for the night (Brozovic et al., 2024), and our data confirms the lack of a mutual event (Fig. 1).

Date (UT)	Observation		# Images	Mutual Events	
	Start	End		Predicted (Brozovic et al., 2024)	Observed
29 Sep 2024	06:13:41.655	10:06:49.662	204	None predicted	None seen (Fig.1)
30 Sep 2024	04:58:52.942	09:57:51.839	285	PO, PO+PE, AO+PE	PO or PO+PE (Fig.2)
02 Oct 2024	08:21:40.241	09:50:23.478	87	PO, PO+PE, TO	PO or PO+PE (Fig.3)
03 Oct 2024	04:43:32.683	09:42:24.439	285	None predicted	None seen (Fig.4)
04 Oct 2024	06:17:09.119	08:20:59.531	120	PO, PO+PE, AO+PE	None seen (Arizona daytime) (Fig. 5)
05 Oct 2024	06:18:11.866	08:38:03.675	137	None predicted	None seen (Fig.6)
06 Oct 2024	08:12:46.186	09:29:13.267	69	PO, PO+PE, TO	None seen (Arizona daytime) (Fig. 7)

Table I. Observations done during the campaign on mutual events Patroclus-Menoetius from 20 September 2024 UT to 06 October 2024 UT. Starting time, ending time, and number of images obtained during each night are reported. We put side by side the type predicted mutual event predicted by Brozovic et al. (2024) and the mutual event observed. The different types are PO (Partial Occultation), PE (Partial Eclipse), AO (Annular Occultation), TO (total occultation).

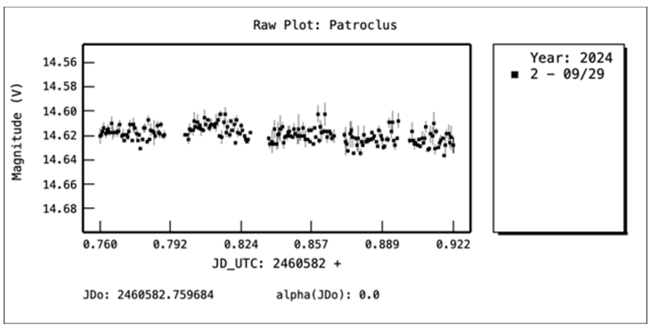

Fig.1. Lightcurve of Patroclus-Menoetius on 29 September 2024. No mutual event was detected, as predicted.

30 September 2024 UT. Two hundred and eighty-five (285) images were collected. The resulting photometry shows a clear mutual event that started at 06:07:12.0 UT and stopped at 09:57:36.0 UT. The mutual event lightcurve was not complete because the target reached the elevation limit of the telescope for our work. Nevertheless, we could estimate the amplitude of the mutual event lightcurve to be 0.82 magnitude. The type of mutual event was predicted to be a PO or PE (Fig. 2).

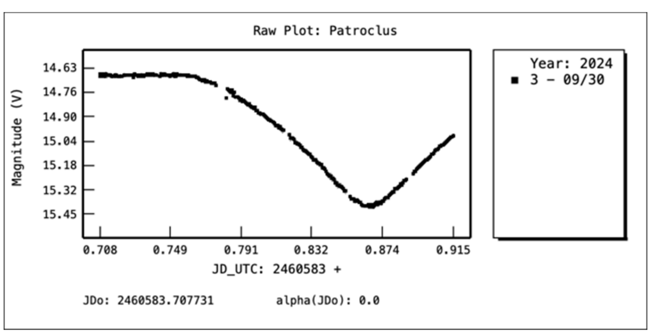

Fig. 2. Inferior mutual event lightcurve of the binary system Patroclus-Menoetius on 30 September 2024 UT.

02 October 2024 UT. We collected 87 images for the night of 03 October 2024. The observations only caught the first 18 minutes of a mutual event from 09:28:48 UT to 09:46:04 UT (Fig. 3). A small amplitude of 0.05 magnitude was estimated for the partially observed event. The elevation of the binary started at around 42 degrees, but dropped quickly below 30 degrees, the limit for our observations.

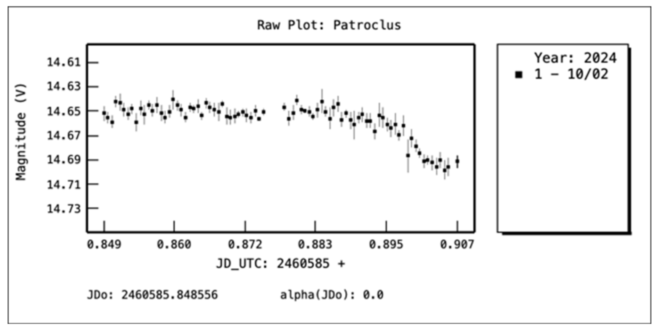

Fig. 3. Superior mutual event lightcurve of binary system Patroclus-Menoetius on 02 October 2024 UT. A drop occurred at the end of our observing window around 09:46:04.8 UT.

03 October 2024 UT. On 03 October 2024 from 04:43:32 to 09:42:24 UT, we collected 285 images. As predicted by Brozovic et al. (2024), no mutual event was observed (Fig. 4).

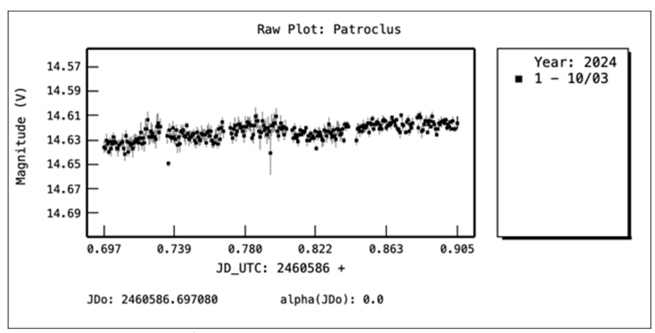

Fig. 4. Lightcurve of binary system Patroclus-Menoetius on 03 October 2024 UT. No signal of mutual even lightcurve is shown as predicted by Brozovic et al. (2024).

04 October 2024 UT. A total of 120 images of the Patroclus-Menoetius system were collected on the night of 04 October 2024 UT. No event was detected as the predicted event for that date occurred outside of the VATT's observing window (Fig. 5).

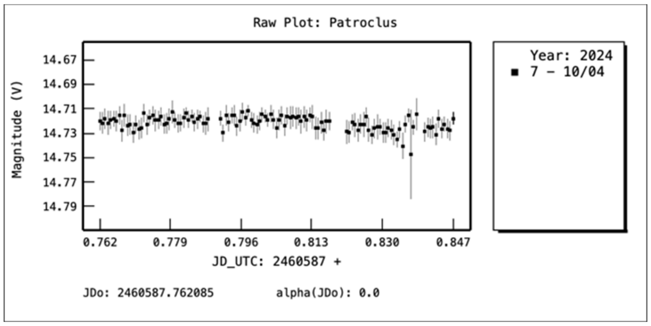

Fig. 5. Lightcurve of binary system Patroclus-Menoetius on the night of 04 October 2024. No mutual event was detected, as predicted.

05 October 2024 UT. On the night of 05 October 2024, 137 images were acquired. We computed the system lightcurve looking for any signal of mutual event (Fig. 6). No signal was detected as predicted by Brozovic et al. (2024).

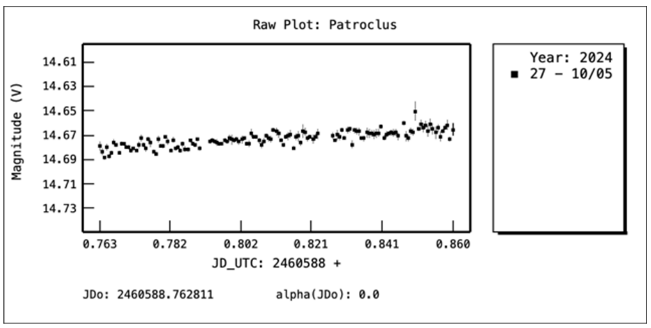

Fig. 6. Lightcurve of binary system Patroclus-Menoetius from the night of 05 October 2024 UT. No mutual event signal detected, as predicted.

06 October 2024 UT. Sixty-nine (69) images were collected on the night of 06 October 2024 UT (Fig. 7). Brozovic et al. (2024) predicted three types of signals: PO (Partial Occultation), PO+PE (Partial Occultation combined with Partial Eclipse), and TO (Total Occultation), but for a period outside of the VATT's observing window.

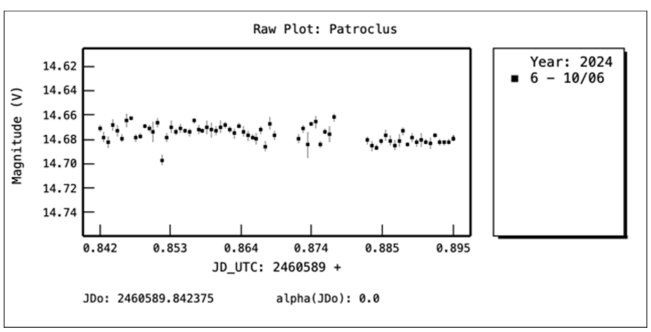

Fig. 7. Lightcurve of binary system Patroclus-Menoetius on the night of 06 October 2024 UT showed no signal of mutual event during this time interval, as predicted.

The Patroclus-Menoetius system photometry presented in this work has been archived with the Asteroid Lightcurve Photometry Database (ALCDEF) (Warner et al., 2011; Stephens and Warner, 2018).

Acknowledgements

We want to thank the Vatican Observatory for allowing us to use VATT. We would also like to express our gratitude to the Vatican Observatory for providing us with funds necessary to complete this research.

References

Binzel, R.P. (2024). "Call for Observations of the Patroclus and Menoetius mutual events: Support for the Nasa Lucy Mission to the Trojan Asteroids." *Minor Planet Bulletin* **51**, 212.

Brozovic, M.; Jacobson, R.A.; Park, R.S.; Descamps, P.; Berthier, J.; Pinila-Alonso, N.; Popescu, M.; Licandro, J. (2024). "Orbit of the Patroclus-Menoetius Binary System and Predictions for the 2024/2025 Mutual Events Season." *Astron. J.* **167**, 104, 12 pp.

Buie, M.W.; Olkin, C.B.; Merline, W.J. and 26 colleagues (2015). "Size and Shape from Stellar Occultation Observations of the double Jupiter Trojan Patroclus and Menoetius." *Astron. J.* **149**, 113.

Grundy, W.M.; Noll, K.S.; Buie, M.W.; Levison, H.F. (2018). "The Upcoming mutual event season for the Patroclus-Menoetius Trojan binary." *Icarus* **305**, 198.

Kikwaya Eluo, J.B.; Hergenrother, C.W. (2023). "Lightcurves and Colors of Four Small Near-Earth Asteroids: 2020 BV14, 2023 HH3, 2023 HT3, 2023 KQ." *Minor Planet Bulletin* **50**, 300-303.

Kikwaya Eluo, J.B.; Hergenrother, C.W. (2024). "Lightcurves and Colors of Seven Small Near-Earth Asteroids: 2023 LQ1, 2023 LT1, 2023 MC, 2023 VQ5, 2023 VE6, 2023 VF6, 2023 VV7." *Minor Planet Bulletin* **51**, 192-196.

Levison, H.F.; Olkin, C.B.; Noll, K.S.; Marchi, S.; Bell, J.F., III; Bierhaus, E.; Binzel, R.; Bottke, W.; Britt, D.; Brown, M.; Buie, M.; Christensen, P.; Emery, J.; Grundy, W.; and 11 colleagues (2021). *Planetary Sci. J.* **2**, 171.

Marchis, F.; Hestroffer, D.; Descamps, P.; Berthier, J.; Bouchez, A.H.; Campbell, R.D.; Chin, J.C.Y.; van Dam, M.A.; Hartman, S.K.; Johansson, E.M.; Lafon, R.E.; Le Mignant, D.; de Pater, I.; Stomski, P.J.; and 4 colleagues (2006). "A low density of 0.8 g cm-3 for the Trojan binary asteroid 617 Patroclus." *Nature* **439**, 565-567.

Merline, W.J.; Close, L.M.; Siegler, N.; Potter, D.; Chapman, C.R.; Dumas, C.; Menard, F.; Slater, D.C.; Baker, A.C.; Edmunds, M.G.; Mathlin, G.; Guyon, O.; Roth, K. (2001). "S/2001 (617) 1" IAU Circular 7741 #2.

Mueller, M.; Marchis, F.; Emery, J.P.; Harris, A.W.; Mottola, S.; Hestroffer, D.; Berthier, J.; di Martino, M. (2010). "Eclipsing binary Trojan asteroid Patroclus: Thermal inertia from Spitzer observations." *Icarus* **205**, 505.

Stephens, R.D.; Warner, B.D. (2018). "The ALCDEF Database and the NASA SBN/PDS: The Perfect Merger." Astronomical Society, DPS Meeting #50, id 417.03.

Warner, B.D.; Stephens, R.D.; Harris, A. H. (2011). "Save the Lightcurves." *Minor Planet Bulletin* **38**, 172-174.

(617) PATROCLUS-MENOETIUS MUTUAL EVENTS OBSERVATIONS FROM OASI OBSERVATORY

Eduardo Rondón-Briceño, Jonatan Michimani, Filipe Monteiro, Weslley Pereira, Plicida Arcoverde, Marçal Evangelista-Santana, Roberto Souza, Teresinha Rodrigues, Daniela Lazzaro
Observatório Nacional, COAST,
Rua Gal José Cristino 77, 20921-400,
Rio de Janeiro, BRASIL
erondon@on.br

(Received: 2024 October 30)

We present the mutual event lightcurves of the (617) Patoclus-Menoetius binary system acquired at the Observatório Astronômico do Sertão de Itaparica (OASI, MPC code Y28) from 2024 September 25 to 2024 October 12.

CCD photometric observations of (617) Patoclus-Menoetius binary system were carried out at the Observatório Astronômico do Sertão de Itaparica (OASI) (MPC code Y28, Nova Itacuruba) of the IMPACTON project, between 2024 September 25 and 2024 October 12. We used the 1.0-m f/8 telescope and a CCD Apo-U47-MB-0, with an array 1024×1024 pixels, set to 2×2 binning and R-Cousins filter. More details on available instrumentation at OASI are given in Rondón et al. (2020).

The data reduction was performed using the *IRAF* package (Tody, 1986) correcting the science image for bias, dark and flat frames. The lightcurves for the mutual events were built using the *MPO Canopus* software (Warner, 2018), computing the differential magnitude.

The asteroid (617) Patroclus-Menoetius, studied in this work, is a Jupiter Trojan binary system in synchronous rotation-orbit, with both components being of similar size (Merline et al., 2001). This object is a target for NASA's Lucy Mission. We observed mutual events for this object between 2024 September 25 AND 2024 October 12. In table I are given the observational dates and observational circumstances. During this period of time, we captured three inferior events, when Menoetius is on the near side to the observer, on the nights of September 25 (Fig. 1, upper panel), October 07 (Fig. 1, first middle panel), October 08 (Fig. 1, second middle panel) and October 12 (Fig. 1, bottom panel). The observed event durations were 3.146, 5.94 and 1.38 hours, respectively.

On the night of October 08 (Fig. 1, second middle panel) we were able to observe the mutual event from its maximum until its possible end, spanning 2.76 hours. The magnitude drop during this event was 0.786, from which we estimated a minimum diameter ratio of 0.717. Data coverage on the night was incomplete due to the object exceeding the telescope's altitude limit.

Figure 2 shows observations from the night of September 27, October 05, 06, and 09, when no mutual events were observed. The magnitude fluctuation seen in these plots are attributed to the rotational variation of each component of the system.

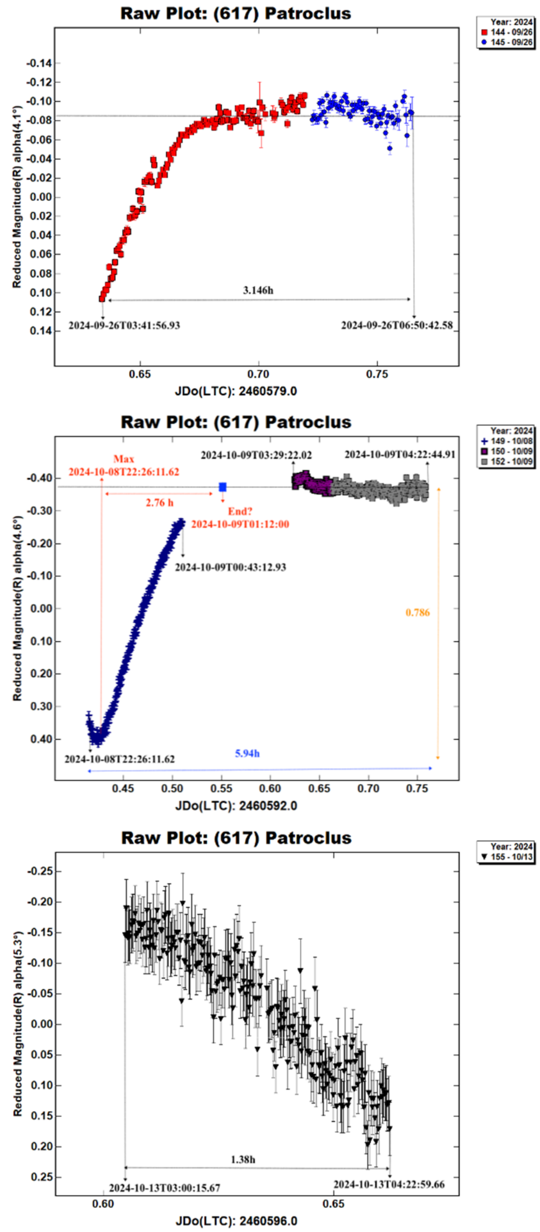

Fig. 1. Mutual events lightcurve observed on the night of September 25 (upper panel), October 07 (first middle panel), October 08 (second middle panel) and October 12 (bottom panel). All events detected were inferior events.

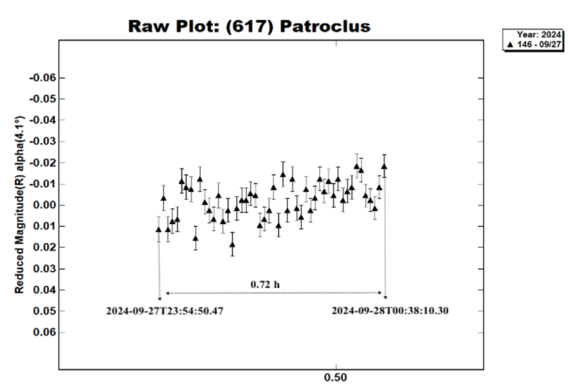

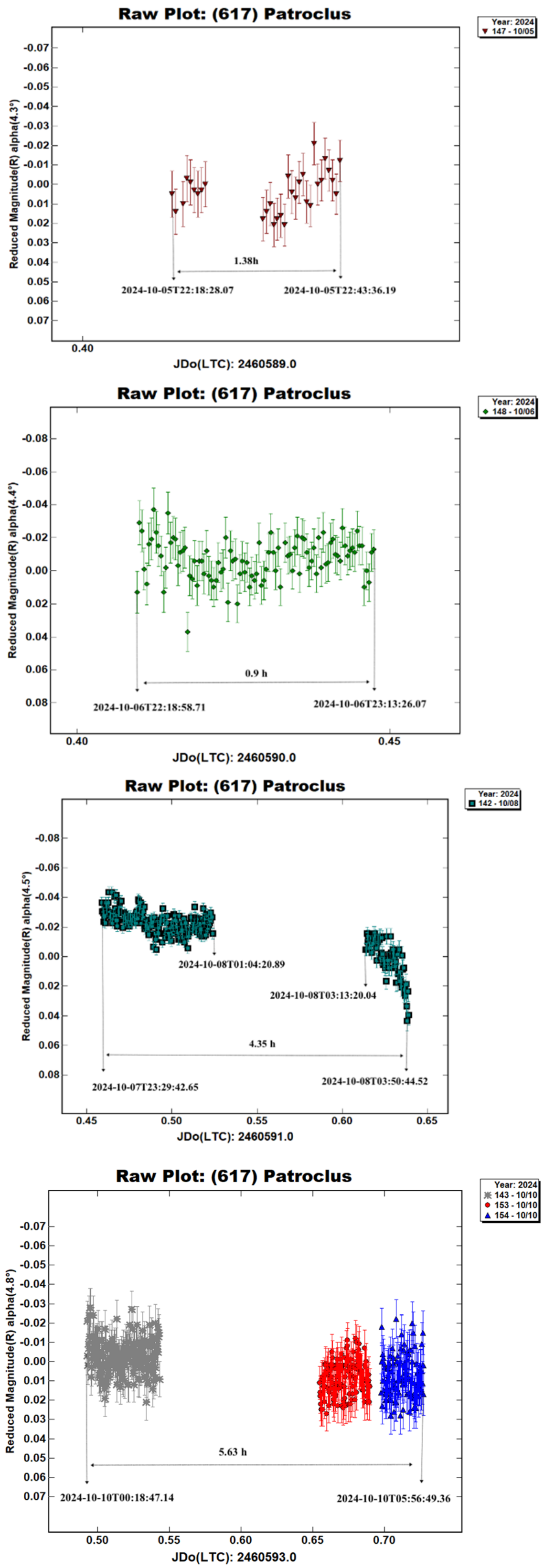

Fig.2. Lightcurve observed at the night of September 27 (upper panel), October 05 (first middle panel), 06 (second middle panel) and 09 (bottom panel). No mutual events were detected in these observation intervals, in agreement with Brozovic et al. (2024) predictions.

Night	Number of images used	Exposure time (s)	Delta (au)	r (au)	alpha(°)
2024-09-25	209	50	3,526	4,487	4.1
2024-09-27	49	50	3.526	4.488	4.1
2024-10-05	32	30	3.537	4.489	4.4
2024-10-06	99	30	3.539	4.489	4.5
2024-10-07	242	30	3.542	4.490	4.6
2024-10-08	600	30	3.546	4.490	4.7
2024-10-09	433	20	3.549	4.490	4.8
2024-10-12	213	20	3.555	4.490	5.0

Table I. Observational nights and observing circumstances, giving the dates, the number of images used, the exposure time, the distance to the Earth (Delta), the distance to the Sun (r), the solar phase angle (alpha).

Acknowledgements

The authors acknowledge CAPES, CNPq and FAPERJ for supporting this work through diverse fellowships and grants, and are grateful to the IMPACTON team, in particular to A. dos Santos and A. Santiago for the technical support at OASI.

References

Brozovic, M.; Jacobson, R.A.; Park, R.S.; Descamps, P.; Berthier, J.; Pinila-Alonso, N.; Popescu, M.; Licandro, J. (2024). "Orbit of the Patroclus-Menoetius Binary System and Predictions for the 2024/2025 Mutual Events Season." *Astron. J.* **167**, 104, 12 pp.

Merline, W.J.; Close, L.M.; Siegler, N.; Potter, D.; Chapman, C.R.; Dumas, C.; Menard, F.; Slater, D.C.; Baker, A.C.; Edmunds, M.G.; Mathlin, G.; Guyon, O.; Roth, K. (2001). "S/2001 (617) 1." IAU Circ. **7741**, #2.

Rondón, E.; Lazzaro, D.; Rodrigues, T.; Carvano, J.M.; Roig, F.; Monteiro, F.; Arcoverde, P.; Medeiros, H.; Silva, J.; Jasmin, F.; de Prá, M.; Hasselmann, P.; Ribeiro, A.; Dávalos, J.; Souza, R. (2020). "OASI: A Brazilian Observatory Dedicated to the Study of the Small Solar System Bodies - Some Results of NEOs Physical Properties." *PASP* **132**, 065001.

Tody, D. (1986). The IRAF data reduction and analysis system. In: Crawford, D.L. (Ed.), Instrumentation in Astronomy VI. p. 733. *http://dx.doi.org/10.1117/12.968154*

Warner, B.D. (2018). MPO Canopus Software, v.10.8.6.3. Bdv publishing. *http://www.bdwpublishing.com*

R-BAND MONITORING OF PATROCLUS AND MENOETIUS MUTUAL EVENTS

Misty C. Bentz
Department of Physics and Astronomy
Georgia State University
25 Park Place, Suite 605
Atlanta, GA 30303 USA
bentz@astro.gsu.edu

Ruel Brown, Sebastian Carrazco-Gaxiola, Akshat S. Chaturvedi, Karina Kimani-Stewart, Ryan Lange, Luke Miles, Mahir Patel, Tamima Saba, Yasmeen Shah, Ben Tipton, Christopher Whyte
Georgia State University
Atlanta, GA USA

(Received: 2024 October 25 Revised: 2024 November 22)

R-band monitoring of 617 Patroclus and its companion Menoetius was conducted over the course of several nights in 2024 September and October. We report the observations of superior and inferior mutual events for this binary asteroid system. Overall, we find reasonable agreement between our observations and the predicted timing of the mutual events, though the observed timing was often discrepant by 5-25 min from the predictions. Event depths were observed to be ΔR = 0.65-0.70 mag. The observations reported here will assist in refining the binary orbit and the asteroid sizes and shapes in preparation for the planned flyby of Patroclus and Menoetius in 2033 by NASA's Lucy mission.

The NASA Lucy mission was launched in 2021 to study the Trojan asteroids of Jupiter. In particular, the binary asteroid pair 617 Patroclus and Menoetius is on the target list for a flyby in 2033 when Lucy reaches the L5 Trojan asteroid cloud (Levison et al., 2021). Patroclus and Menoetius are nearly equal in size, and the orbital period for the binary is 4.28 d (Marchis et al., 2006). However, the detailed shapes, sizes, and orbital parameters of the pair are still relatively uncertain, creating a high level of risk given the detailed planning that is needed for a successful flyby.

To improve the understanding of this binary system, a call for observations was issued for 2024 September-October (Binzel, 2024). Observations of the binary system were recommended during this time to take advantage of the bright visual magnitude of the asteroid pair at opposition as well as the orbital plane of the system crossing the Earth's line of sight, allowing for mutual events between the pair to be readily observed. The timing and duration of several mutual events were predicted by Brozović et al. (2024), and observations were requested to cover the events as well as one or more hours before and after each event, given the imprecise nature of the estimated timing.

In response to the call for observations of the Patroclus-Menoetius binary pair, we conducted broad-band photometric monitoring over the course of several nights between UT dates 2024 September 25 and October 17. Observations were collected by undergraduate, postbaccalaureate, and graduate students at Georgia State University's Hard Labor Creek Observatory in Rutledge, GA. For this program, we employed the Miller Telescope: a 24-inch Planewave f/6.5 Corrected Dall-Kirkham Astrograph equipped with an FLI ProLine CCD. All images were acquired through a Johnson-Cousins R filter, and each image covered a field of view of 26.3 arcmin × 26.3 arcmin with a pixel scale of 0.77 arcsec. Exposure times for individual frames were 300 s. The low declination of the asteroid binary ($\delta \approx -15°$) resulted in observations being acquired at airmasses of 1.5 - 2.5. Weather conditions were mixed across the nights, ranging from clear to partly cloudy.

Images were reduced in IRAF following standard procedures, which included bias and overscan subtraction, dark subtraction, and flat fielding. Aperture photometry was also carried out in IRAF, with measurements of the asteroids and 5-6 field stars acquired from each reduced image. Calibrated R-band measurements of field stars in the Vega system were estimated from Equation 7 of the transformation equations of Jordi et al. (2006) for Population I stars. Sloan g′-r′ colors and Johnson V magnitudes for the field stars were obtained from the AAVSO Photometric All-Sky Survey (Henden et al., 2009).

In the following, we summarize our observations and findings from each night of monitoring. Predictions of the timing of mutual events from Brozović et al. (2024) are indicated in the following lightcurve plots with vertical dotted lines. Julian dates are reported for the midpoint of each observation. All times reported in this discussion and shown in the figures are at Earth. No light-time correction has been applied.

<u>September 25</u>. Observations on this date did not cover any mutual events. Nevertheless, we observed interesting variability in the first half of the night, ΔR = 0.19 ± 0.02 mag between JD-2460578 = 0.73-0.75 d, that is potentially related to the rotation of either Patroclus or Menoetius. Our median precision for the evening was 0.01 mag. The second half of the night was affected by thin clouds, degrading our precision to 0.02 mag. We note that the following night on September 26, when a mutual event was predicted to occur, the first rain bands associated with Hurricane Helene reached northern Georgia, and Helene arrived one day after that.

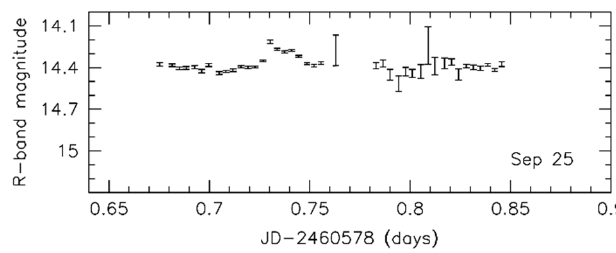

<u>September 28</u>. Observations covered the second half of a predicted superior mutual event with a typical photometric precision of 0.008 mag. The event maximum was predicted to occur at UT 04:50, which is within 5 min of our observed maximum. The event end was predicted to occur at UT 07:30, which is also fairly consistent with our observations. Fitting a smoothly broken power law to the lightcurve, with the break amplitude fixed to the average magnitude after the predicted end of the event, suggests that the end occurs at JD-2406581 = 0.8210 d, or UT 07:42, which is 12 min after the predicted time. The event depth was observed to be ΔR = 0.64 ± 0.02 mag.

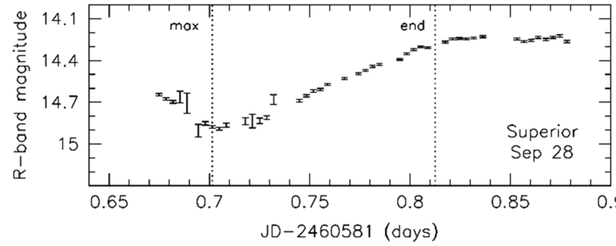

Number	Name	yyyy mm/dd	Phase	L_{PAB}	B_{PAB}	Period(h)	P.E.	Amp	A.E.	Grp
617	Patroclus	2024 09/25-10/17	*4.1,5.8	5	-17	4.282753	0.000023	0.65	0.03	9202

Table I. Observing circumstances and results. The phase angle is given for the first and last date. If preceded by an asterisk, the phase angle reached an extrema during the period. L_{PAB} and B_{PAB} are the approximate phase angle bisector longitude/latitude at mid-date range (see Harris et al., 1984). Grp is the asteroid family/group (Warner et al., 2009). The listed period is for the binary system (Brozović et al., 2024).

September 30. Partly cloudy conditions in the first half of the night prohibited us from observing the start of the predicted inferior mutual event at UT 06:00 and led to a slightly worse photometric precision overall, with a median value of 0.014 mag. Our observations concluded shortly after the predicted event maximum at UT 08:38, however it is difficult to determine from our lightcurve whether we actually observed the event maximum. This could be an artifact of the abrupt end to our time series, or it could indicate that the predicted timing was not accurate to within ~20 min. The asteroid binary varied in brightness by ΔR = 0.65 ± 0.02 mag over the course of our observations, which sets a lower limit for the event depth.

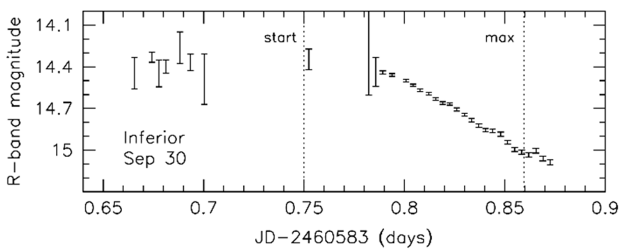

October 2. Mostly clear skies allowed us to observe the asteroid pair for a few hours before the superior event was predicted to begin at UT 09:14. Technical issues arose in the second half of the night, however, which effectively curtailed the observations as the asteroid pair began to set. We did not observe the onset of the superior event. Brightness variations were minimal over the time period covered by our observations, and our typical photometric precision was 0.006 mag.

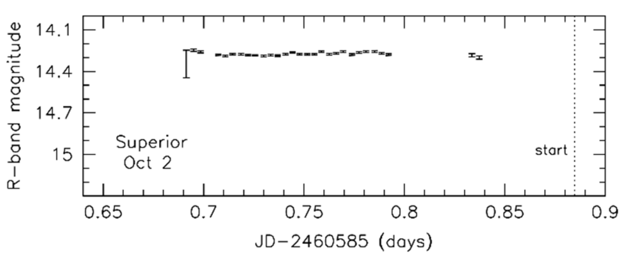

October 11. We observed the end of a superior event, which was predicted to conclude at UT 04:18. This predicted time agrees very well with our lightcurve. Clear skies throughout the night allowed us to achieve a typical precision of 0.008 mag. We detected a change in brightness of ΔR = 0.34 ± 0.02 mag, which is a lower limit to the event depth because our observations did not cover the event maximum.

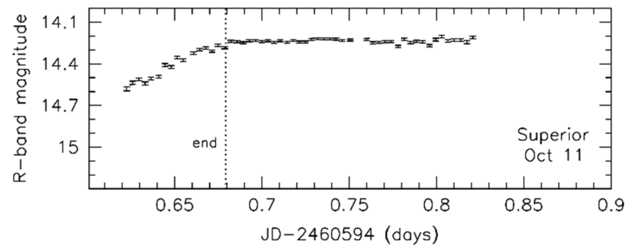

October 13. We observed most of an inferior event, just missing the end as the asteroids set below our window of visibility. Both the start of the mutual event and the maximum were observed to occur after their predicted times. While the predicted start of the event was at UT 02:45, our observations suggest it occurred about 15 min later around JD-2406581 = 0.625 d or UT 03:00. The mutual event maximum was predicted to occur at UT 05:24, and again our observations suggest that it was observed about 10-15 minutes later. The event depth was observed to be ΔR = 0.70 ± 0.03 mag, and we achieved a typical precision 0.014 mag with clear skies but somewhat poor seeing.

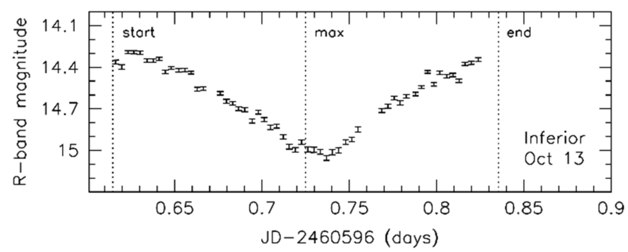

October 15. We observed the onset of a superior mutual event, which was predicted to start at UT 05:52. The precise onset of the mutual event is difficult to determine from simple examination of our lightcurve. Fitting the lightcurve with a smoothly broken power law, with the break amplitude fixed to the average magnitude before the predicted start of the event, suggests that the onset occurs at JD-2406598 = 0.7623 d, or UT 06:18, which is 26 min after the predicted onset. We detected variability of ΔR = 0.35 ± 0.02 mag, which is a lower limit to the event depth because our observations concluded before the event maximum occurred. Clear skies with a waxing gibbous Moon provided reasonable observing conditions but an increased background, leading to a typical precision of 0.015 mag.

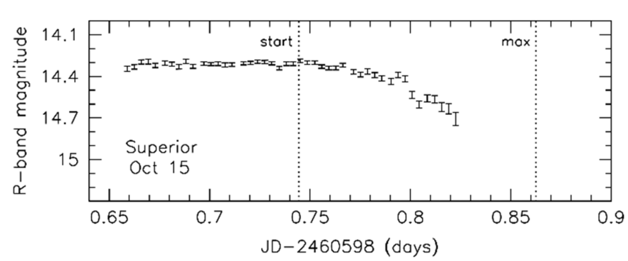

October 17. We monitored the asteroid binary for several hours before the onset of an inferior event, which was predicted to start at UT 09:29. We did not observe any significant variability. Observations were acquired through clear skies with a nearly full moon, leading to a significantly elevated background and a typical precision of 0.025 mag.

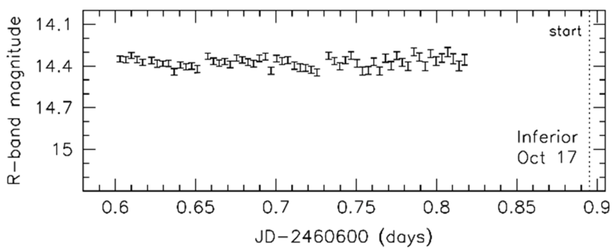

In summary, we acquired observations of superior and inferior mutual events between 617 Patroclus and Menoetius over several nights in 2024 September and October. The low declination of the asteroid binary from our location in north Georgia limited the observing window each night, nevertheless we were able to monitor significant portions of several mutual events. The event timing predictions by Brozović et al. (2024) are in general agreement with our observations, though we find discrepancies in the predicted vs. observed timing of 5-25 min. From those lightcurves that covered more than half of an event, we measured event depths of $\Delta R = 0.65$-0.70 mag, and we provide lower limits on the event depth from lightcurves that covered less than half of an event. Our typical photometric precision varied with the observing conditions and moon phase, ranging from 0.006 mag under excellent conditions to 0.025 mag under a nearly full moon. We expect these observations will assist in a more precise determination of the binary orbit as well as the asteroid sizes and shapes, in preparation for the planned flyby of the system by NASA's Lucy Mission in 2033.

Acknowledgements

NOIRLab IRAF is distributed by the Community Science and Data Center at NSF NOIRLab, which is managed by the Association of Universities for Research in Astronomy (AURA) under a cooperative agreement with the U.S. National Science Foundation. This research was made possible in part based on data from the AAVSO Photometric All-Sky Survey (APASS), funded by the Robert Martin Ayers Sciences Fund and NSF AST-1412587.

References

Binzel, R.P. (2024). "Call for Observations of the Patroclus and Menoetius Mutual Events: Support for the NASA Lucy Mission to the Trojan Asteroids." *Minor Planet Bull.* **51**, 212.

Brozović, M.; Jacobson, R.A.; Park, R.S.; Descamps, P.; Berthier, J., Pinilla-Alonso, N., Popescu, M., Licandro, J. (2024). "Orbit of the Patroclus-Menoetius Binary System and Predictions for the 2024/2025 Mutual Events Season." *Astron. J.* **167**, 104, 12pp.

Harris, A.W.; Young, J.W.; Scaltriti, F.; Zappala, V. (1984). "Lightcurves and phase relations of the asteroids 82 Alkmene and 444 Gyptis." *Icarus* **57**, 251-258.

Henden, A.A.; Terrell, D.; Levine, S.E.; Templeton, M.; Smith, T.C.; Welch, D.L. (2009). "APASS: The AAVSO Photometric All-Sky Survey." *http://www.aavso.org/apass*

Jordi, K.; Grebel, E.K.; Ammon, K. (2006). "Empirical color transformations between SDSS photometry and other photometric systems." *Astron. Astrophys.* **460**, 339-347.

Levison, H.F.; Olkin, C.B.; Noll, K.S.; Marchi, S.; Bell, J.F.; Bierhaus, E.; Binzel, R.; Bottke, W.; Britt, D.; Brown, M.; Buie, M.; Christensen, P.; Emery, J.; Grundy, W.; and 16 colleagues (2021). "Lucy mission to the Trojan asteroids: Science goals." *Planetary Sci. J.* **2(5)**, 13pp.

Marchis, F.; Hestroffer, D.; Descamps, P.; Berthier, J.; Bouchez, A.H.; Campbell, R.D.; Chin, J.C.Y.; van Dam, M.A.; Hartman, S.K.; Johansson, E.M.; Lafon, R.E.; Le Mignant, D.; de Pater, I.; Stomski, P.J.; and 4 colleagues (2006). "A low density of 0.8 g cm^{-3} for the Trojan binary asteroid 617 Patroclus." *Nature* **439**, 565-567.

Warner, B.D.; Harris, A.W.; Pravec, P. (2009). "The Asteroid Lightcurve Database." *Icarus* **202**, 134-146. Updated 2023 Oct 1. *http://www.MinorPlanet.info/php/lcdb.php*

OBSERVATIONS OF MUTUAL EVENTS BETWEEN 617 PATROCLUS AND MENOETIUS ON SEPTEMBER 25, OCTOBER 6, AND OCTOBER 23, 2024

Stephen M. Brincat
Flarestar Observatory (MPC: 171)
Fl.5 George Tayar Street,
San Gwann SGN 3160, MALTA
stephenbrincat@gmail.com

(Received: 2024 September 29 Revised: 2024 November 24)

On September 25, October 6, and October 23, 2024 UT, three photometric observational runs of the Trojan asteroid binary system 617 Patroclus-Menoetius were conducted as part of a coordinated effort to support NASA's Lucy mission, which is set to encounter this pair in March 2033. During these runs, lightcurve measurements were obtained to capture the ingress, egress and mid-eclipse timings of the predicted mutual events between the asteroid Patroclus and its satellite, Menoetius.

This paper presents three photometric observational runs of the Patroclus-Menoetius binary system, conducted from Flarestar Observatory in Malta on September 25, October 6, and October 23, 2024 UT, in support of NASA's Lucy mission. Data from the mutual transits and occultations of this Trojan asteroid were gathered to refine the orbital parameters and physical characteristics of the binary system. These observations were made following a call for contributions by Prof. Richard P. Binzel in the *Minor Planet Bulletin* (Binzel, 2024). The results aim to provide a clearer picture that may assist in mission planning and ensure precise targeting during Lucy's flyby in 2033, ultimately enhancing the scientific return and offering new insights into binary Trojan asteroids; a primary goal for the NASA Lucy mission.

Photometric observations were gathered through a 0.25-m Schmidt-Cassegrain telescope equipped with Moravian CCD using a 1603ME CCD sensor. All images were taken through a clear filter (unfiltered) with Sloan r' zero point and calibrated through dark and flat-field subtraction. Each image covered a field of view of 25.4 arcmin × 17.0 arcmin, with a pixel scale of 0.99 arcsec. The Comparison Star Selector (CSS) feature developed by *MPO Canopus* software (Warner, 2017), was employed to choose near-solar color comparison stars. All brightness measurements were based on the Asteroid Terrestrial-impact Last Alert System (ATLAS) catalogue (Tonry et al., 2018). All data were obtained from Flarestar Observatory in Malta (MPC code:171).

The mutual event data of 2024 September 25-26 of the 617 Patroclus binary system were collected from 21:27 to 01:48 UT, amounting to an observation run of 4 hours and 21 minutes, Observations were taken under good weather conditions. The last quarter moon did not affect the observations, with Patroclus positioned at a moon elongation of 104 degrees. The mutual event was recorded through 60 frames, each with exposure time of 240 s. The same exposure length also applies to all subsequent runs (October 06 and 23). The observatory PC time has been synchronized through *Dimension 4* software (Thinking Man Software, 2024). *All timings refer to JD time or UT times at Earth, where light-time corrections have not been included in any of the presented figures or discussion of event timings.*

The inferior geometry event observed on 25-26 September was scheduled according to the predictions by Brozovic et al. (2024) where the mutual event was predicted to start at 23 h 02 m and end at 04 h 26 m UT with the mid-timing of the 'eclipse' set to occur at 01h 41m UT. (We note that all timing predictions by Brozovic et al. are for an Earth observer.).

From Flarestar Observatory's location at Long. 14.470 East and Lat. 35.905 N (altitude of 110 m), the target at the start of the run (at 21 h 27 m UT) had an airmass of 1.87, culminating at the meridian at airmass of 1.55 at 23 h 32 m UT and ending the run at 01 h 48 m UT at airmass of 1.98.

Provisional results from this run indicate that the predictions set by Brozovic et al. (2024) are in line with the observations obtained; as the last image at average maximum light was recorded at 23h 00m 19s UT (mid-exposure time) coinciding with the start of the eclipse (ingress) at 23h 02m UT. The least brightest data point obtained was also consistent with the predictions made as the faintest data point on the lightcurve was obtained through the image timed at 01h 44m 29s UT. This coincided just after the predicted timing of mid-eclipse set at 01:41 UT. For this run, due to the absence of post mid-eclipse data, the timing results remain uncertain, as the data available is limited and incomplete. The amplitude recorded is of 0.70 ± 0.02 mag.

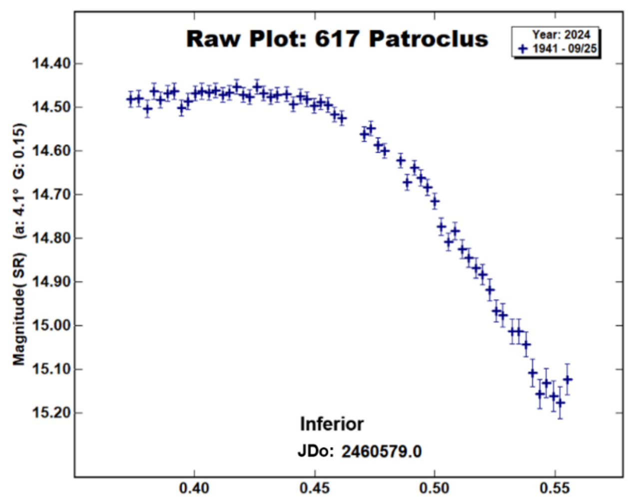

The superior conjunction mutual event predicted on 2024, October 06 provided another opportunity, this time to record the egress of this mutual event. Brozovic et al. (2024) predicted the event to commence at 16 h 12 m UT and end at 21 h 20 m UT with mid-eclipse occurring at 18h 48 m UT.

Number	Name	Family	H	D_{km}	*a (au)*	*e*	*i (deg)*	P(yrs).	Discovered by	yyyy/mm
617	Patroclus	9202*	8.3	140.81	5.21	0.140	22.06	11.08	A. Kopff	1906/10

Table I. Orbital and discovery information. Family is the group or family using the LCDB values. An asterisk indicates a generic group, otherwise, the numbers are from Nesvorny et al. (2015).
Web Sources: JPL: *https://ssd.jpl.nasa.gov/tools/sbdb_lookup.html#/*. MPInfo: *https://minorplanet.info/php/oneasteroidinfo.php*.

The lightcurve obtained from Flarestar Observatory shows a post mid-eclipse phase with the first observation obtained on 19h 31m 18s UT (mid-exposure time) at airmass of 2.56 and ending at 22h 17m 25s UT at airmass of 1.56. The amplitude recorded is that of 0.49 ± 0.02 mag.

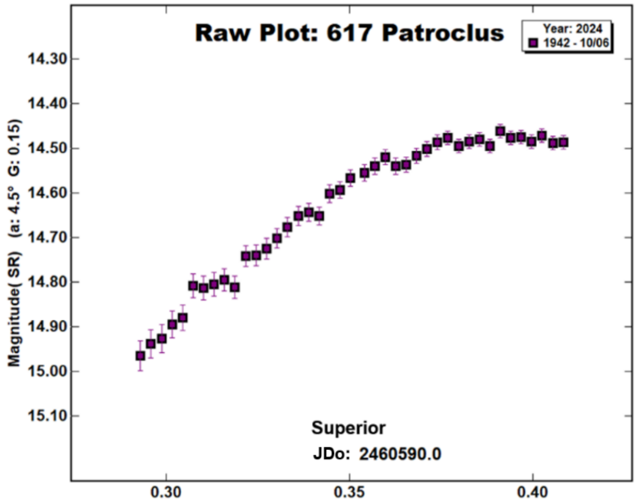

In this instance, mid-eclipse was not recorded as the observation run commenced well after the predicted time of mid-eclipse. Consequently, obtaining a precise minimum time was not possible.

The superior conjunction mutual event on October 23, 2024, was well-documented from Flarestar Observatory, with good coverage of the maximum eclipse phase. For this event, Brozovic et al. (2024) predicted the ingress to start at 19h 22m UT, with the mid-eclipse predicted to occur at 23h 37m UT, and egress at 01h 11m UT.

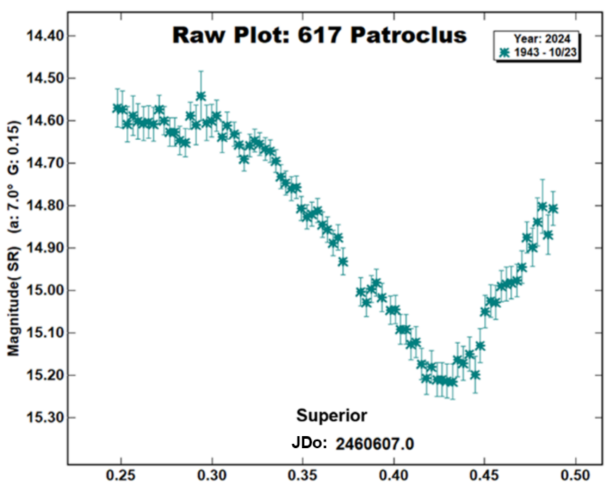

In order to define the time of mid-eclipse with some accuracy, an exercise was carried out where 3 methodologies were adopted to the lightcurve that comprised, a Parabolic fit, a Kwee & van Woerden fit, and a Fourier fit. Results of the derived time of minimum are shown in Table II as derived through the software *Minima* (Version 2.7) by Nelson (2019).

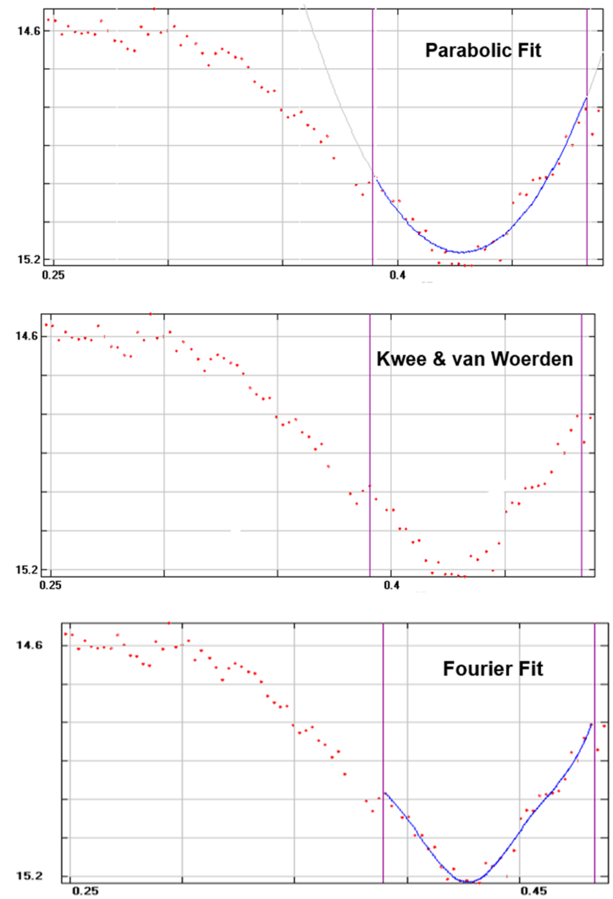

	Time of Minimum (JD)	Error
Parabolic Fit	2460607.42802	0.00125
Kwee & van Woerden	2460607.42713	0.0012
Fourier Fit	2460607.42719	0.00029

Table II.

The simple mean of the Times of Minimum shown in Table II is of JD 2460607.42745 that translates to 2024 October 23 at 22h 15m 31s (UT). The Weighted Mean derived is JD 2460607.42723 with standard error of 0.00027 d. The derived Weighted Mean translates to 2024 October 23 at 22h 15m 12s. The standard deviation of means is of 0.0005 d. Hence the difference of these means is of 0.32m or 19s. The derived time (weighted mean) of maximum eclipse differs by 21m 48s from that predicted time by Brozovic et al. (2024). As noted above, no light-time corrections were applied and hence all timings shown here are terrestrial time in UT.

The predictions by Brozovic and coauthors are quite impressive in consideration of the limitations faced in orbital modeling and component size estimations taken to derive the predictions. Unfavorable weather conditions prevented the observation of additional events that were expected to be visible from Malta.

Acknowledgements

Thanks is directed to Prof Richard Binzel who brought to the attention of these mutual events through his notification at Binzel (2024).

References

Binzel, R.P., (2024). “Call for Observations of the Patroclus and Menoetius Mutual Events: Support for the NASA Lucy Mission to the Trojan Asteroids.” *Minor Planet Bulletin* **51(3)**, 212.

Brozovic, M.; Jacobson, R.A.; Park, R.S.; Descamps, P.; Berthier, J.; Pinilla-Alonso, N.; Popescu, M.; Licandro, J. (2024). “Orbit of the Patroclus-Menoetius Binary System and Predictions for the 2024/2025 Mutual Events Season.” *Astron. J.* **167**, 104, 12 pp. DOI 10.3847/1538-3881/ad1f6e.

Nelson, B. (2019). *Minima (Version 27)*. **Software for photometric data analysis**. Variable Stars South. Available at

https://www.variablestarssouth.org/resources/bob-nelsons-software-tools/software-by-bob-nelson.
Accessed 20 Sept. 2024

Nesvorny, D.; Broz, M.; Carruba, V. (2015). “Identification and Dynamical Properties of Asteroid Families.” In Asteroids IV (P. Michel, F. DeMeo, W.F. Bottke, R. Binzel, Eds.). Univ. of Arizona Press, Tucson, also available on astro-ph.

Thinking Man Software (2024). Dimension 4 Software, version 5.3. Available from *http://www.thinkman.com/dimension4/default.htm.* Accessed 20 Sept. 2024.

Tonry, J.; Denneau, L.; Flewelling, H.; Heinze, A.; Onken, C.; Smartt, S.; Stalder, B.; Weiland, H.; Wolf, C. (2018). “The ATLAS All-Sky Stellar Reference Catalog.” *Ap. J.* **867**, id. 105.

Warner, B.D., (2017). MPO Software, *MPO Canopus*, version 10.7.10.0. Bdw Publishing. *http://www.minorplanetobserver.com/*

PHOTOMETRIC DETECTION OF THE 2024 OCTOBER 23-24 MUTUAL EVENT OF THE PATROCLUS-MENOETIUS BINARY JUPITER TROJAN AT SOPOT ASTRONOMICAL OBSERVATORY

Vladimir Benishek
Belgrade Astronomical Observatory
Volgina 7, 11060 Belgrade 38, SERBIA
vlaben@yahoo.com

(Received: 2024 November 3)

A single lightcurve partially covering the 2024 October 23-24 superior mutual event was obtained for the binary Jupiter Trojan asteroid system 617 Patroclus - Menoetius from Sopot Astronomical Observatory (K90) in Serbia.

During its 11.89-year long heliocentric orbital period, the orbital plane of the binary Jupiter Trojan asteroid system 617 Patroclus - Menoetius (PMS) twice reaches a favorable position in relation to the Earth, allowing observations of mutual eclipses and occultations (mutual events) of the system components. Such a favorable observational geometry of PMS mutual events occurs in the time span 2024 February - 2025 January.

Following the call for observations of PMS mutual events by Binzel (2024) during 2024 September - October, CCD photometric observations of the superior (Patroclus closer to the Sun than Menoetius) mutual event predicted for 2024 October 23-24 (19:22 - 01:11 UT) by Brozovic et al. (2024) were carried out at Sopot Astronomical Observatory (K90) in Serbia. For this purpose, a 0.35-meter (f/6.3) Meade LX200GPS Schmidt-Cassegrain telescope, equipped with a SBIG ST-10 XME CCD camera operating in 2×2 binning mode, was employed. No photometric filters were used. The integration time for individual CCD frames was 180 seconds to achieve satisfactory level of signal-to-noise ratio enabling the required photometric precision of 0.01 mag. or better for individual data points (Binzel, 2024). Aperture photometric reduction with multiple comparison stars of near solar color ($0.5 \leq B\text{-}V \leq 0.9$) was conducted using *MaxIm DL 6* software by Diffraction Limited. Internal calibration of comparison stars was done using the Carlsberg Meridian Catalog 15 (VizieR, 2024) Sloan r’ magnitudes and converted to Cousins R-band magnitudes according to the transformation formula: $R = r' - 0.22$. Prior to photometric reductions, all the images were corrected using master dark and master flat field calibration frames. Time synchronization on the data collection computer was performed using Windows Network Time Protocol (NTP) server (*time.windows.com*).

A total of 95 photometrically usable image frames were acquired in the time interval between ~ 18:42 and ~ 23:50 UT on 2024 October 23. The photometric session termination was determined by the obstruction of the target by local objects on the descending horizon. The weather conditions during the observation time interval are characterized by mostly clear skies with only the occasional appearance of transient thin cirrus clouds. All the frames that were judged to be even slightly affected by weather conditions were removed from the data set.

The obtained data have been uploaded to the Asteroid Lightcurve Data Exchange Format (ALCDEF) database (*https://alcdef.org/*).

The Resulting 2024 October 23-24 Mutual Event Lightcurve

Shown here is the resulting lightcurve constructed from the photometric data with no light-time corrections applied. A smooth cubic spline function with knots at each data point was fitted through the data in order to estimate as accurately as possible the moment of first contact and the maximum of mutual event time, as well as the total intensity drop in magnitudes. Mathematical and statistical procedures were performed in the *R programming language* (R Core Team, 2024) using the *Stats* and *Inflection* libraries for fitting the corresponding functions and finding the inflection points related to the characteristic times of the mutual event.

For the time of the first contact corresponding to the knee of the fitted function, the point of noticeable incurvation with respect to the flat lightcurve continuum (indicated by the green vertical line on the lightcurve plot), the following instant in Julian days was estimated: JD 2460607.33311, which rounded to one minute is: ~ 20:00 UTC, 2024 October 23). The minimum point of the fitted function, taken as the point of minimum light (red vertical line), corresponds to the time instant of JD 2460607.44742 (~ 22:44 UTC, 2024 October 23). The moment of the last contact is not covered by the data.

The maximum brightness (intensity) drop (Δm) is determined as the difference between the intensity of the fit minimum (minimum light) and the mean of the fit of the flat lightcurve continuum up to the first contact time. A value of $\Delta m = 0.61$ magnitudes is estimated for the maximum brightness drop.

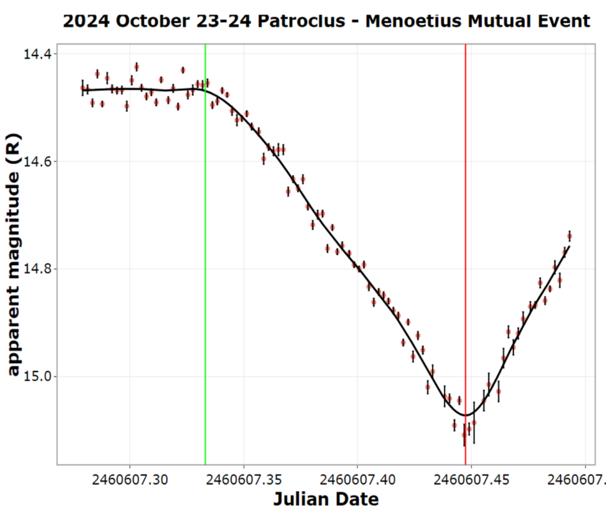

Superior mutual event, with Menoetius in behind of its primary component Patroclus. Timings are Earth-centric; no light-time correction has been applied.

Acknowledgements

Observational work at Sopot Astronomical Observatory is generously supported by Gene Shoemaker NEO Grants awarded by the Planetary Society in 2018 and 2022.

References

ALCDEF (2024). Asteroid Lightcurve Data Exchange Format web site. *https://alcdef.org/*

Binzel, R.P. (2024). "Call for Observations of the Patroclus and Menoetius Mutual Events: Support for the NASA Lucy Mission to the Trojan Asteroids." *Minor Planet Bull.* **51**, 212.

Brozovic, M.; Jacobson, R.A.; Park, R.S.; Descamps, P.; Berthier, J.; Pinilla-Alonso, N.; Popescu, M.; Licandro, J. (2024). "Orbit of the Patroclus-Menoetius Binary System and Predictions for the 2024/2025 Mutual Events Season." *Astron. J.* **167**, 104.12 pp. DOI 10.3847/1538-3881/ad1f6e.

Diffraction Limited MaxIm DL - Astronomy and Scientific Imaging Software. *https://diffractionlimited.com/product/maxim-dl/*

R Core Team (2024). R: A language and environment for statistical computing. R Foundation for Statistical Computing. Vienna, Austria. *https://www.R-project.org/*

VizieR (2024). *http://vizier.u-strasbg.fr/viz-bin/VizieR*

PATROCLUS AND MENOETIUS MUTUAL EVENTS: SUPPORT FOR THE NASA LUCY MISSION TO THE TROJAN ASTEROIDS

Nick Sioulas
NOAK Observatory (L02)
Stavraki Ioannina, GREECE
nsioulas@hotmail.com

(Received: 2024 October 27)

Observations of the Patroclus and Menoetius mutual events are reported in support of the NASA Lucy Mission to the trojan asteroids. This report covers a superior event observed on 2024 October 23 UT.

Following the predictions provided by Brozovic et al. (2024) and a Call for Observations in support of the NASA Lucy Mission (Binzel, 2024), we performed lightcurve measurements of the Patrocolus-Menoetius binary system to detect mutual events between these two components. All observations were performed at the NOAK Observatory, Ioannina Greece (MPC-International Astronomical Union code L02), using a 0.25-m Newtonian Skywatcher optical tube operating at *f*/4.7 at 2024-10-23. The optical tube is mounted on NEQ6 Skywatcher robotic mount and equipped with ATIK 460exm CCD camera. It is a high Quantum Efficiency CCD. No filters used for better signal to noise. Exposure time for all the images was 10 seconds. The camera was binned at 2×2. The image scale after 2×2 binning was 1.57 arcsec/pixel and the field of view 35.9′ × 28.7′. In these fields, the asteroid and five comparison stars were measured for differential photometry.

All images were reduced in the standard manner using nightly flatfield files as well as dark-current and bias images. They were made available to Brian Warner, who was managing a collaboration of observers from around the world. The images were measured using *MPO Canopus* v12 (Waner, 2024) using Pan-STARRS r magnitudes for the comparison stars. After measuring the more than 450 images, the data were placed in 3×5 bins, meaning a maximum of three images per bin with no image more than five minutes apart. The raw plot shows the results of the analysis.

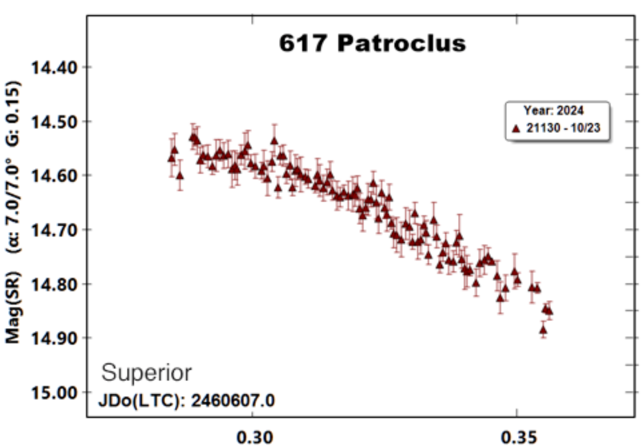

The data were then combined with those from Alessandro Nastasi, another collaborator in Warner's group, who observed on the same date but whose run continued further into the event. In this case, the data were binned 3×1, three per bin no more than 1 minute apart, which avoided making the Nastasi data too sparse. There is close agreement between the two data sets but with a small difference in the descent slope. A more extended data set from NOAK may have shown a better match.

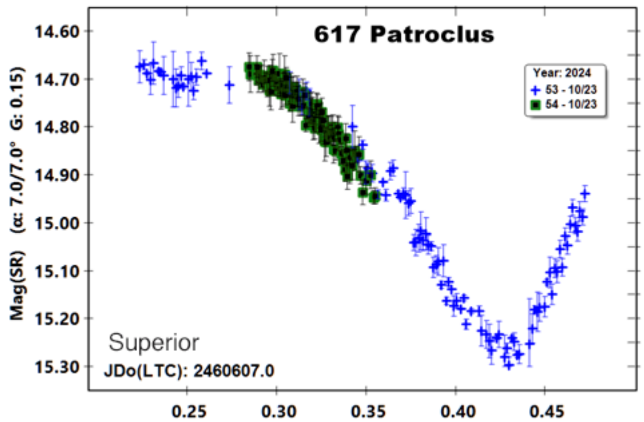

Acknowledgements

Thanks to Brian Warner for measuring the images and producing the plots included here. Acknowledgement is given also to Alessandro Nastasi, Galhassin Robotic Telescope and Wide-field Mufara Telescope, GAL Hassin - Centro Internazionale per le Scienze Astronomiche Isnello, Italy, for the data referenced in this paper.

References

Binzel, R.P. (2024). "Call for Observations of the Patroclus and Menoetius mutual events: Support for the Nasa Lucy Mission to the Trojan Asteroids." *Minor Planet Bulletin* **51**, 212.

Brozovic, M.; Jacobson, R.A.; Park, R.S.; Descamps, P.; Berthier, J.; Pinila-Alonso, N.; Popescu, M.; Licandro, J. (2024). "Orbit of the Patroclus-Menoetius Binary System and Predictions for the 2024/2025 Mutual Events Season." *Astron. J.* **167**, 104. 12 pp.

Warner, B.D. (2024). MPO Software, *MPO Canopus* v12.0.6.1. Bdw Publishing. *https://bdwpublishing.com*

OBSERVATIONS OF (617) PATROCLUS MUTUAL EVENTS IN SUPPORT OF THE LUCY MISSION TO THE TROJAN ASTEROIDS

Francis P. Wilkin, Eduardo Castro,
Abigail Ramsey, Glauk Hizmo
Department of Physics and Astronomy, Union College
807 Union St., Schenectady, NY 12308 USA
wilkinf@union.edu

(Received: 2024 November 1 Revised: 2024 November 22)

We present lightcurves of mutual events of the L5 binary Trojan (617) Patroclus and its companion Menoetius during 2024 Sep-Oct. A total of nine events were observed using four telescopes, with two additional baseline observations.

NASA's Lucy Mission will explore Trojan asteroids in both the L4 and L5 camps in 2027-28 and 2033, respectively. The science goals include determinations of mass, volume, density and surface composition, as well as the search for rings and additional satellites (Levison et al., 2021). The hypothesis that any original Trojan objects have been lost during an early period of planet migration, and later capture of objects from the outer protoplanetary disk repopulated the Trojan swarms will be tested (Morbidelli et al., 2005; Nesvorný et al., 2013). (617) Patroclus and its satellite Menoetius form a binary of similar sizes that exhibit mutual events observable from Earth in two seasons per 12 yr orbital period. Precise orbital predictions for the locations of Patroclus and Menoetius are required for accurate pointing of the camera and other intruments of the Lucy spacecraft when it reaches the pair in March 2033, and our observations were performed in response to the call by Binzel (2024) to assist in this effort. Predicted start, maximum, and end times were made available by Brozović et al. (2024), who provided tables of 8 inferior and 8 superior events which occur in alternation about 2 days apart. For convenience, we have labeled these events I1, S1 through I8, S8 in Table I as well as in our lightcurve legends.

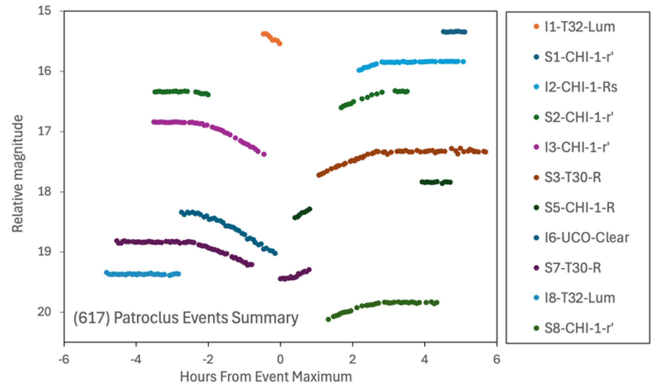

Observations were conducted at remote telescopes on two networks: iTelescope.net and Telescope.Live, as well as at the Union College Observatory. Telescopes and cameras are described in Table II. Filters and telescopes used for individual nights are given in the figure legends. All images were processed for bias, dark, and flat field corrections. We extracted photometric measurements from the images using *AstroImageJ* (Collins et al., 2017).

To visualize the overall coverage at the same time and magnitude scale, we have subtracted the predicted maximum event time for each observation and placed them in a summary figure, using arbitrary vertical offsets for visibility. The timing predictions of Brozović et al. (2024) were given in UTC ("Earth-centric"), so *we have not applied any light-time corrections*. All of our observations are partial due to clouds during reserved full observations. However, for event S2, a gapped full, we obtain an event duration of 5.36 h which exceeds the predicted duration by ~7 minutes. From event S7, an ingress+maximum, we obtain a depth of 0.586 mag. Further analysis of our results will be done in combination with additional observations contributed by other observers to obtain updated solutions for the system physical parameters to assist in Lucy Mission planning (Binzel, 2024).

Event	Start Date (UTC)	Start	Event Max	Stop	Events	Observation coverage
I1	2024 09 21	16:04	18:45	21:48	PO, PO+PE, PE	ITO
S1	2024 09 23	19:17	21:51	24:51	PO, PO+PE, TO, PO+PE, PE	Post-B
I2	2024 09 25	23:02	01:41	04:26	PO, PO+PE, PE	Egr
S2	2024 09 28	02:15	04:50	07:30	PO, PO+PE, TO, PO+PE, PO	Gapped-F
I3	2024 09 30	06:00	08:38	11:09	PO, PO+PE, AO+PE, PO+PE, PO	Ing
S3	2024 10 02	09:14	11:50	14:22	PO, PO+PE, TO, PO+PE, PO	Egr
I4	2024 10 04	12:58	15:30	18:07	PO, PO+PE, AO+PE, PO+PE, PO	-
S4	2024 10 06	16:12	18:48	21:20	PO, PO+PE, TO, PO+PE, PO	-
I5	2024 10 08	19:57	22:26	25:05	PO, PO+PE, AO+PE, PO+PE, PO	-
S5	2024 10 10	23:08	01:45	04:18	PE, PO+PE, TO, PO+PE, PO	ITO+B
I6	2024 10 13	02:45	05:24	08:03	PE, PO+PE, PO	Ing
S6	2024 10 15	05:52	08:42	11:16	PE, PO+PE, PO	-
I7	2024 10 17	09:29	12:22	15:01	PE, PO+PE, PO	-
S7	2024 10 19	12:37	15:40	18:14	PE, PO+PE, PO	Ing+Max
I8	2024 10 21	16:14	19:20	21:58	PE, PO+PE, PO	Pre-B
S8	2024 10 23	19:22	22:37	25:11	PE, PO+PE, PO	Egr

Table I. Mutual Events Season 2024. The first column indicates inferior (I) or superior (S) event and sequence number. Columns 3-5 give the predictions of Brozović et al. (2024). In column 6, possible events include: PO--Partial Occultation, PE--Partial Eclipse, PO+PE--Partial Ocultation and Partial Eclipse with overlap, TO--Total Occultation, AO--Annular Occultation. Column 7 Observation Coverage includes B--Baseline, Ing--Ingress, Egr--Egress, F--Full, ITO--In Transit Only.

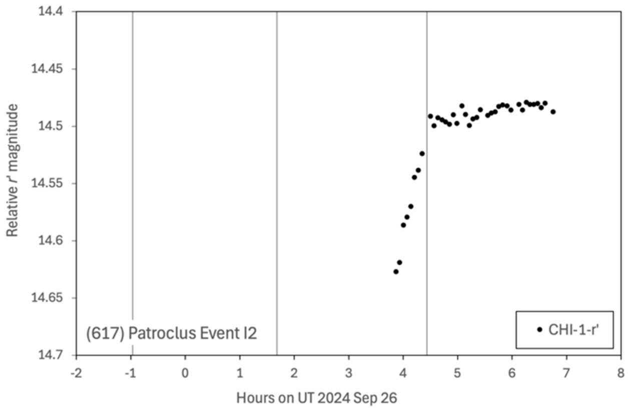
(617) Patroclus Event I2
CHI-1-r'
Relative r' magnitude
Hours on UT 2024 Sep 26

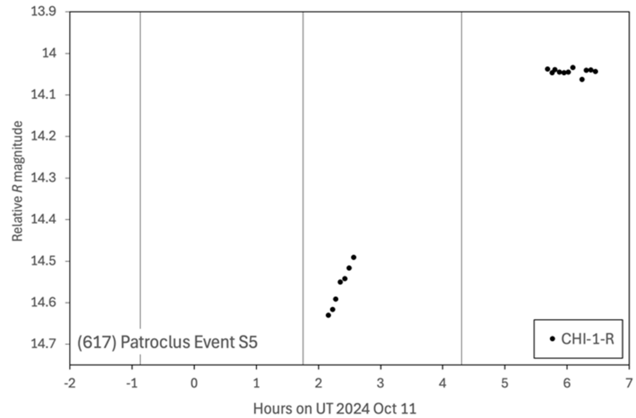
(617) Patroclus Event S5
CHI-1-R
Relative R magnitude
Hours on UT 2024 Oct 11

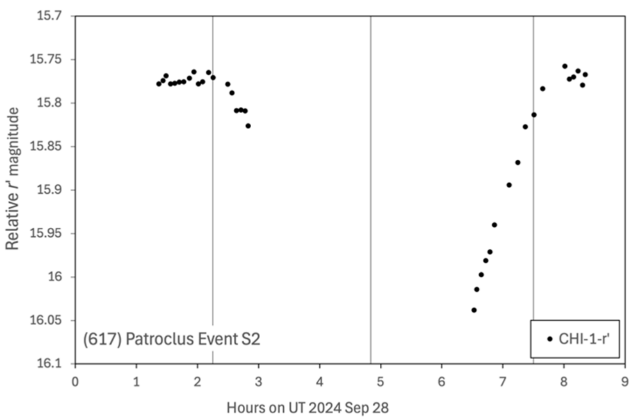
(617) Patroclus Event S2
CHI-1-r'
Relative r' magnitude
Hours on UT 2024 Sep 28

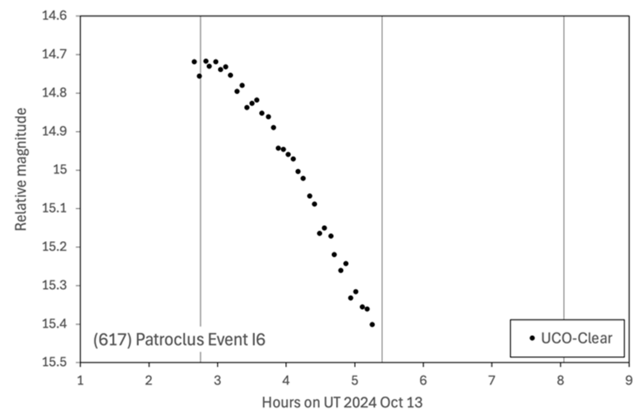
(617) Patroclus Event I6
UCO-Clear
Relative magnitude
Hours on UT 2024 Oct 13

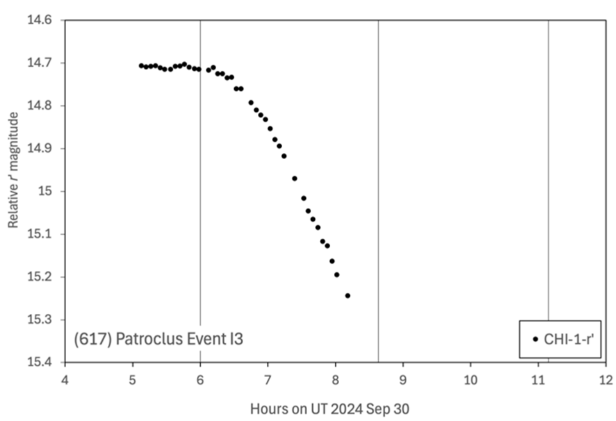
(617) Patroclus Event I3
CHI-1-r'
Relative r' magnitude
Hours on UT 2024 Sep 30

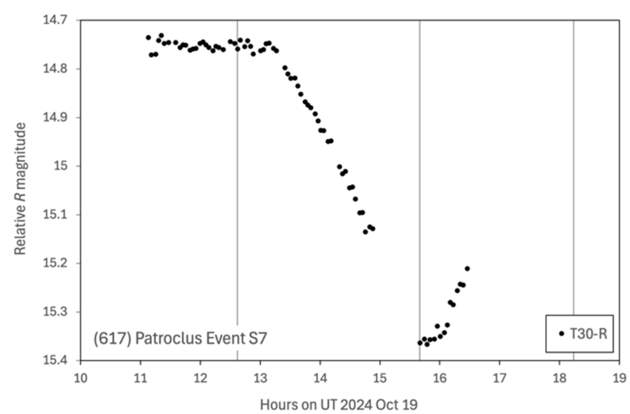
(617) Patroclus Event S7
T30-R
Relative R magnitude
Hours on UT 2024 Oct 19

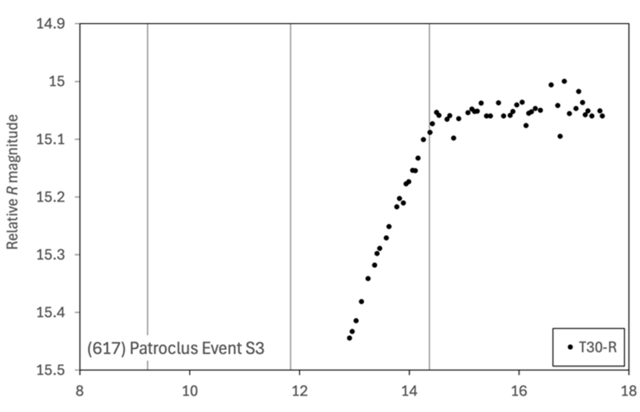
(617) Patroclus Event S3
T30-R
Relative R magnitude
Hours on UT 2024 Oct 2

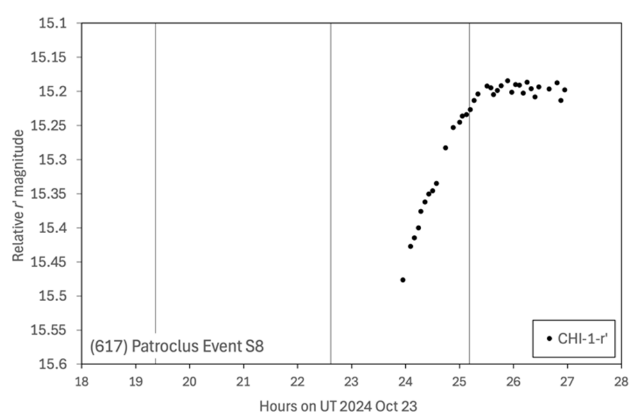
(617) Patroclus Event S8
CHI-1-r'
Relative r' magnitude
Hours on UT 2024 Oct 23

Name	Site	Telescope	Camera	Array	Filter	FOV (′)	Scale (″/pix)
UCO	Schenectady, NY	0.50-m f/8.1	SBIG STXL-11002	2004×1336×9µm	*Clear*	30×20	0.93
T30	Coonabarabran, Aus	0.50-m f/6.8	ML16200	3072×2048×9µm	*R*	28×42	0.81
T32	Coonabarabran, Aus	0.43-m f/6.8	Moravian G4-16000	4096×4096×9µm	Lum	43×43	0.64
CHI-1	Rio Hurtado, Chile	0.61-m f/6.8	QHY 600M Pro	9576×6382×3.8µm	*r′*	31×21	0.395

Table II. Telescopes and Cameras. Filters: *R*: Cousins *R*; *r′*: Sloan *r′*; Lum: Luminance; Clear: Clear-uv block.

Acknowledgements

The remote observations were funded by the Union College Faculty Research Fund grant to FPW. We are grateful to iTelescope.net for a free one-hour observation near full moon.

References

Binzel, R.P. (2024). “Call for Observations of the Patroclus and Menoetius Mutual Events: Support for the NASA Lucy Mission to the Trojan Asteroids.” *Minor Planet Bull.* **51**, 212.

Brozović, M.; Jacobson, R.A.; Park, R.S.; Descamps, P.; Berthier, J.; Pinilla-Alonso, N.; Popescu, M.; Licandro, J. (2024). “Orbit of the Patroclus-Menoetius Binary System and Predictions for the 2024/2025 Mutual Events Season.” *Astron. J.* **167**, 104, 12 pp.

Collins, K.A.; Kielkopf, J.F.; Stassun, K.G.; Hessman, F.V. (2017). “AstroImageJ: Image Processing and Photometric Extraction for Ultra-precise Astronomical Light Curves.” *Astron. J.* **153**, 77-89.

Levison, H.F.; Olkin, C.B.; Noll, K.S.; Marchi, S.; Bell III, J.F.; Bierhaus, E.; Binzel, R.; Bottke, W.; Britt, D.; Brown, M.; Buie, M.; Christensen, P.; Emery, J.; Grundy, W.; Hamilton, V.E.; Howett, C.; Mottola, S.; Pätzold, M.; Reuter, D.; Spencer, J.; Statler, T.S.; Stern, S.A.; Sunshine, J.; Weaver, H.; Wong, I. (2021). “Lucy Mission to the Trojan Asteroids: Science Goals.” *Planetary Science J.* **2**:171, 13pp.

Morbidelli, A.; Levison, H.F.; Tsiganis, K.; Gomes, R. (2005). “Chaotic capture of Jupiter's Trojan asteroids in the early Solar System.” *Nature* **435**, 462-465.

Nesvorný, D.; Vokrouhlický, D.; Morbidelli, A. (2013) “Capture of Trojans by Jumping Jupiter.” *Astrophys. J.* 768, **45**, 8pp.

LIGHTCURVE PHOTOMETRY OPPORTUNITIES: 2025 JANUARY - APRIL

Brian D. Warner
Center for Solar System Studies (CS3)
446 Sycamore Ave.
Eaton, CO 80615 USA
brian@MinPlanObs.org

Alan W. Harris
Center for Solar System Studies (CS3)
La Cañada, CA 91011-3364 USA

Josef Ďurech
Astronomical Institute
Charles University
18000 Prague, CZECH REPUBLIC
durech@sirrah.troja.mff.cuni.cz

Lance A.M. Benner
Jet Propulsion Laboratory
Pasadena, CA 91109-8099 USA
lance.benner@jpl.nasa.gov

(Received: 2024 October 19)

We present lists of asteroid photometry opportunities for 2025 Jan-April. The extended four-month listing continues the changes announced in MPB 51-4 (Warner et al., 2024). Extending to the month beyond the usual quarter-year allows better observation planning, especially for those working in wide-spread collaborations. With the massive input of survey photometry, even if mostly sparse data, the small telescope researcher's role is moving away generic studies to those concentrating on specific needs and targets and so, we hope, leading to even more fulfilling and fruitful efforts.

We refer the reader to the lightcurve photometry opportunities article in *Minor Planet Bulletin* 51-4 (Warner et al., 2024) for a detailed discussion on the evolution of the lists presented here and the purpose behind each one. In addition, we refer the reader to other prior releases of this paper (e.g., Warner et al., 2023) for more detailed discussions about the requirements and considerations for the targets in the lists and to Warner et al. (2021a; 2021b).

An Improved Planning Tool

The ephemeris generator on the *https://MinorPlanet.info* web site allows creating custom lists for numbered objects reaching V ≤ 18.0 during a given month from 2020 through 2035 by setting search parameters based on a number of parameters.

https://www.minorplanet.info/php/callopplcdbquery.php

The updated page added data for the minimum phase angle of any object included in the search: the date (0.001 d), the minimum phase angle (0.1°), and the declination. Searches can limit results to a phase angle range between 0-120°. Also new is limiting the results to a range of rotation periods and so, for example, one can look for only long, or especially short, period objects.

Important and Useful Web Sites

The dates and values given on the MinorPlanet.info site are very good estimates in most cases. NEAs are sometimes an important exception. Use the site for preliminary planning for objects and then confirm those plans using the Minor Planet Center or JPL Horizons web sites.

MPC: *http://www.minorplanetcenter.net/iau/MPEph/MPEph.html*
JPL: *https://ssd.jpl.nasa.gov/sb/orbits.html*

Those doing work for modeling should contact Josef Ďurech at the email address above. If looking to add lightcurves for objects with existing models, visit the Database of Asteroid Models from Inversion Techniques (DAMIT) web site.

https://astro.troja.mff.cuni.cz/projects/damit/

to see what, if any, information it has on a chosen target.

For near-Earth asteroids in particular, check the list found on the Goldstone planned targets schedule at

http://echo.jpl.nasa.gov/asteroids/goldstone_asteroid_schedule.html

and keep in touch with Lance Benner at the email above. The radar team often needs updated astrometry and photometry (rotation period) prior to observing. Keep in mind as well that the *MinorPlanet.info* site opposition database includes only numbered objects. Keep a close eye on the MPC NEA pages.

Once you've obtained and analyzed your data, it's important to publish your results. Papers appearing in the *Minor Planet Bulletin* are indexed in the Astrophysical Data System (ADS) and so can be referenced by others in subsequent papers. It's also important to make the data available at least on a personal website or upon request. We urge you to consider submitting your raw data to the ALCDEF database. This can be accessed for uploading and downloading data at

http://www.alcdef.org

The database contains about 10.69 million observations for 24,454 objects (as of 2024 May 27), making it one of the more useful sources for raw data of *dense* time-series asteroid photometry.

The Planning Lists

The lists, excluding the one for NEAs, are usually restricted to objects reaching V ≤ 15.5 during the covered months. To include every object within a list that met this criterium alone resulted in far too many targets than the known community of asteroid photometrists could possibly handle, so only the "better" candidates are included. This is entirely subjective and the reader is encouraged to visit the *https://MinorPlanet.info* web site and use all the planning tools available there should our preferences not match yours.

Don't presume that something rated U ≥ 3– doesn't need more work nor, at the other end, that something not rated at all or 1– < U < 2+ or has a long period should be skipped in lieu of an "easier" project. The often-heard saying, "Past performance is not a guarantee of future results" should be part of your work ethic. Someone's "certain" result may not be so certain after all, especially if it's based on data that are minimal in quantity and/or quality.

<u>Favorable Apparitions</u> includes objects reaching one of the five brighter (favorable) apparitions from 1995 and 2050 and rated U < 3– in the LCDB (Warner et al., 2009).

<u>No Pole Solutions</u> includes objects rated U > 2+ but do not have a pole indicated on the LCDB summary line. This is list is the most likely needing further confirmation by checking the DAMIT web site, which grows in spurts large and small quite frequently and so the LCDB can lag considerably.

<u>Poor Pole Solutions</u> includes objects rated U < 3– that have a pole solution on the summary line. In this case, the period is often based on using sparse survey data, with or without support of dense lightcurve data. An additional set of dense data may help elevate both the U rating and the quality of the pole solution.

<u>Low Phase Angles</u> includes objects, regardless of U rating or even having a period, that reach a solar phase angle < 1°. You should refer to Warner et al. (2023) to review important information about low solar phase angle work.

<u>Long Periods</u> includes objects with $P \geq \sim 24$ hours. These are often overlooked because they are very difficult for a single-station campaign. However, they are ideal for collaborations, especially those with stations well-separated in longitude.

<u>NEAs (aka Radar Target)</u> is limited to *known* near-Earth asteroids that might be on the radar team's radar (pun intended). It is common for newly discovered objects to move into or out of the list. We recommend that you keep up with the latest discoveries by using the Minor Planet Center observing tools.

The List Data

If the list includes the "Fam" column, this is the orbital group (> 9000) using criteria from the LCDB or the collisional family (< 9000) based on Nesvorny et al. (2015) and Nesvorny (2015). To convert the number to a name, see the LCDB documentation on the LCDB web site or use the One Asteroid Lookup page on the site:

https://www.minorplanet.info/php/lcdb.php
https://minorplanet.info/php/oneasteroidinfo.php

<u>Table Columns</u>

Num	Asteroid number, if any.
Name	Name (or designation) assigned by the MPC.
Fam	Orbital group or collisional family.
BMD	Date of maximum brightness (to 0.1 d precision).
BMg	Approximate V magnitude at brightest.
BDC	Approximate declination at brightest.
PD	Date of minimum phase angle (to 0.001 d precision).
PMn	Phase angle at minimum (solar elongation > 90°).
PDC	Approximate declination at minimum phase angle.
P (h)	Synodic rotation period from summary line in the LCDB summary table. An * indicates a sidereal period.
U	LCDB solution quality (U) from 1 (probably wrong) to 3 (secure).
Notes	Comments about the object.

Some asteroids may appear in more than one list. The reader is referred to the latest LCDB release and, where and when necessary, the original reference source should be used. The Notes column is rarely used, for now, except for the NEAs list.

Favorable Apparitions (U < 3-)

Num	Name	Fam	BMD	BMg	BDC	PD	PMn	PDC	P (h)	U	Notes
18513	1996 TS5	701	01 12.6	15.5	+27	01 12.226	2.8	279.7492			
7186	Tomioka	9104	01 14.5	15.2	+22	01 14.017	0.2	227.3092			
4176	Sudek	602	01 17.5	15.4	+21	01 18.356	0.2	218.1642			
4683	Veratar	602	01 20.4	15.5	+19	01 21.076	0.5	1929.3912			
2843	Yeti	9104	01 25.4	15.2	+11	01 25.063	3.9	11156.718		2	
4107	Rufino	9104	02 08.3	14.4	+10	02 08.728	2.7	1022.3712			
4133	Heureka	502	02 12.5	15.3	+15	02 11.148	0.3	153.7262-			
2020	Ukko	606	02 15.5	15.1	+12	02 16.637	0.2	1225.4782+			
5438	Lorre	527	03 14.0	14.7	-40	03 13.600	20.1	-4025.302+			
2030	Belyaev	9104	03 16.5	15.4	+3	03 15.282	0.3	22.7382+			
5802	Casteldelpiano	9104	03 21.4	14.9	+1	03 21.914	0.8	12.9702+			
2045	Peking	401	03 21.5	14.7	+2	03 21.506	1.0	2158.72			
9369	1993 DB1	410	03 25.5	15.3	-1	03 24.795	0.3	-154.3352			
4350	Shibecha	9105	03 30.8	15.1	+5	03 31.734	4.2	52.8902+			
1287	Lorcia	606	04 02.4	15.0	-7	04 02.576	0.9	-78.8782			
1841	Masaryk	9106	04 04.4	15.0	-5	04 05.675	0.6	-47.53 2+			
85953	1999 FK21	9101	04 05.0	14.6	+34	03 31.001	30.1	1128.082			
1512	Oulu	9107	04 08.5	14.3	-8	04 06.829	0.3	-8132.32+			
1101	Clematis	2012	04 15.5	14.9	-8	04 13.453	0.3	-834.3 2			
1155	Aenna	9104	04 16.1	14.0	-7	04 15.971	1.4	-78.07 2+			
992	Swasey	9106	04 17.4	14.0	-12	04 16.987	0.6	-1213.3052+			
3815	Konig	517	04 22.0	15.1	-8	04 22.053	1.7	-86.2392			
9871	Jeon	9104	04 25.0	15.4	-21	04 24.821	4.0	-2194 2			
3857	Cellino	2004	04 30.5	15.1	-14	04 29.850	0.5	-143.6572Sidereal			

Table I. A partial list of numbered asteroids reaching a favorable apparition and with an LCDB rating U < 3-. Objects in bold text are near-Earth asteroids.

Spin Axis and Modeling (Favorable Apparition, U > 2+, No LCDB pole, not in DAMIT)

Num	Name	Fam	BMD	BMg	BDC	PD	PMn	PDC	P (h)	U	Notes
1302	Werra	602	01 02.4	14.1	+24	01 03.961	0.4	+248.1833-			
3335	Quanzhou	502	01 13.1	15.0	+15	01 13.284	2.7	+156.15643			
3048	Guangzhou	2004	01 14.0	15.2	+18	01 14.054	1.8	+183.8113-			
862	Franzia	9106	01 17.4	13.2	+21	01 18.685	0.3	+217.5233			
4440	Tchantches	9102	01 20.3	15.3	+4	01 19.827	8.6	+042.78833			
1342	Brabantia	9104	02 13.3	12.8	+4	02 12.375	5.0	+044.17543			
469	Argentina	9106	02 14.5	12.1	+15	02 14.019	0.9	+1517.5727		3	
1318	Nerina	701	03 09.5	13.9	+16	03 08.507	6.1	+162.52803			
75079	1999 VN24	701	03 11.1	15.3	-1	03 12.020	2.6	-006.6323-			
137170	1999 HF1	9101	03 22.6	14.6	+44	05 15.366	57.3	+632.31923			
298	Baptistina	403	04 10.2	13.3	-10	04 10.347	1.2	-1016.233			

Table II. A partial list of numbered asteroids reaching a favorable apparition that have high-quality periods solutions but do not have a pole solution in the LCDB or DAMIT databases.

Spin Axis and Modeling (Any Apparition, U < 3–, Pole in LCDB/DAMIT)

Num	Name	Fam	BMD	BMg	BDC	PD	PMn	PDC	P (h)	U	Notes
3140	Stellafane	606	01 23.5	15.4	+25	01 23.818	2.00	+2533.072			
1684	Iguassu	602	01 30.5	15.5	+20	01 29.406	0.64	+206.4162			
2045	Peking*	401	03 21.5	14.7	+2	03 21.506	0.98	+2158.72Favorable			
1055	Tynka	402	03 30.9	15.0	+2	03 30.340	2.44	+211.8932+			
2345	Fucik	606	04 23.5	15.5	-25	04 23.860	4.21	-2517.122			

Table III. A partial list of numbered asteroids reaching brightest magnitude that have a reported pole position but the LCDB rating is U < 3-.

Low Phase Angle (V ≤ 15.0, phase angle α ≤ 1.0°)

Num	Name	Fam	BMD	BMg	BDC	PD	PMn	PDC	P (h)	U	Notes
140	Siwa	9106	01 04.4	12.9	+22	01 05.870	0.1	+2234.4453			
1254	Erfordia	9106	01 05.0	14.8	+24	01 03.864	0.3	+2412.2873			
1067	Lunaria	633	01 10.4	13.9	+21	01 11.688	0.3	+216.0573			
240	Vanadis	9105	01 14.4	11.6	+21	01 15.023	0.0	+2110.5653			
862	Franzia	9106	01 17.4	13.2	+21	01 18.685	0.3	+217.5233			
1076	Viola	9104	02 05.4	14.4	+15	02 06.119	0.3	+157.3363			
2258	Viipuri	9105	02 05.9	14.9	+15	02 06.830	0.2	+153.8343			
300	Geraldina	9106	02 07.6	14.2	+16	02 09.197	0.3	+166.84233			
987	Wallia	9106	02 09.4	14.9	+14	02 11.295	0.1	+1410.0813		3	
282	Clorinde	9104	02 14.4	13.4	+13	02 14.967	0.2	+1349.3503-			
526	Jena	602	02 18.0	13.6	+12	02 19.054	0.3	+1211.8772			
271	Penthesilea	9106	02 27.4	14.1	+7	03 01.244	0.2	+0718.7873			
2159	Kukkamaki	9104	03 02.7	14.7	+7	03 03.864	0.3	+073.8673			
1079	Mimosa	605	03 08.4	14.8	+4	03 09.912	0.2	+0464.6 2-			
108	Hecuba	601	03 10.5	12.0	+5	03 09.150	0.1	+0514.2563			
491	Carina	9106	03 15.4	13.5	+2	03 17.040	0.2	+0214.8363			
313	Chaldaea	415	03 16.4	10.8	+1	03 17.251	0.2	+018.3923			
358	Apollonia	9106	03 17.4	13.0	+1	03 19.125	0.2	+0150.6 3-			
954	Li	602	03 18.5	14.9	+2	03 16.065	0.1	+027.2073			
1409	Isko	9105	03 19.0	14.7	+1	03 19.366	0.2	+0111.6392+			
48	Doris	9106	03 19.4	11.3	-1	03 20.742	0.2	-0011.893			
139	Juewa	9106	03 20.4	10.5	+0	03 21.188	0.2	+0020.9913			
160	Una	9106	03 22.4	12.6	-1	03 24.040	0.2	-0111.0333			
497	Iva	9106	03 23.4	14.8	-1	03 24.357	0.1	-014.6203			
229	Adelinda	9106	03 24.5	14.5	+1	03 22.189	0.3	+016.60 3			
60	Echo	9104	03 28.4	11.0	-4	03 28.921	0.2	-0425.2083			
3394	Banno	9104	03 31.4	14.4	-5	03 31.972	0.2	-057.3213			
175	Andromache	9106	04 03.5	13.7	-3	03 31.940	0.2	-048.3243			
1512	Oulu	9107	04 08.5	14.3	-8	04 06.829	0.3	-08132.32+			
1101	Clematis	2012	04 15.5	14.9	-8	04 13.453	0.3	-0834.3 2			
510	Mabella	9105	04 16.5	12.6	-9	04 15.233	0.3	-0919.4 3			
2052	Tamriko	606	04 18.5	14.9	-12	04 19.714	0.3	-127.4693			
1675	Simonida	402	04 23.4	14.6	-14	04 24.056	0.3	-145.28853			
468	Lina	602	04 26.5	14.6	-13	04 24.059	0.1	-1316.333			
1060	Magnolia	402	04 28.5	14.5	-15	04 28.055	0.3	-152.9113			

Table IV. A partial list of numbered asteroids reaching a minimum phase angle α ≤ 1.0°.

Long Period (Favorable Apparition, $P \geq 24$ h, U < 3)

Num	Name	Fam	BMD	BMg	BDC	PD	PMn	PDC	P (h)	U	Notes
887	Alinda	9101	01 12.1	9.3	+24	01 13.416	8.5	+26	28.41	3-	
4683	Veratar	602	01 20.4	15.5	+19	01 21.076	0.5	+19	29.391	2	
2843	Yeti	9104	01 25.4	15.2	+11	01 25.063	3.9	+11	156.718	2	
741	Botolphia	9106	01 29.7	13.4	+24	01 29.551	2.6	+24	23.9101	3	
282	Clorinde	9104	02 14.4	13.4	+13	02 14.967	0.2	+13	49.350	3-	
2020	Ukko	606	02 15.5	15.1	+12	02 16.637	0.2	+12	25.478	2+	
7564	Gokumenon	9106	03 01.4	15.1	+9	03 01.677	0.7	+09	30.58	3	
5438	Lorre	527	03 14.0	14.7	-40	03 13.600	20.1	-40	25.30	2+	
2045	Peking	401	03 21.5	14.7	+2	03 21.506	1.0	+02	158.7	2	
9369	1993 DB1	410	03 25.5	15.3	-1	03 24.795	0.3	-01	54.335	2	
85953	1999 FK21	9101	04 05.0	14.6	+34	03 31.001	30.1	+11	28.08	2	
1512	Oulu	9107	04 08.5	14.3	-8	04 06.829	0.3	-08	132.3	2+	
1101	Clematis	2012	04 15.5	14.9	-8	04 13.453	0.3	-08	34.3	2	
2014	Vasilevskis	701	04 19.3	14.4	-8	04 18.685	1.8	-08	32.16	3-	
9871	Jeon	9104	04 25.0	15.4	-21	04 24.821	4.0	-21	94	2	

Table V. A partial list of numbered asteroids reaching a favorable apparition and with a reported period $P \geq 24$ hours.

NEAs (aka Radar) Reaching Brightest for Year (Any Apparition, $V \leq 17.0$, $\alpha \leq 90°$)

Num	Name	Fam	BMD	BMg	BDC	PD	PMn	PDC	P (h)	U	Notes
459462	2013 AY52	9101	01 07.0	17.0	-16	01 17.514	26.4	+17			
	2020 BC6	9101	01 07.4	15.4	-46	01 19.925	20.3	+06		PHA	
887	Alinda	9101	01 12.1	9.3	+24	01 13.416	8.5	+26	28.41	3-	
137805	1999 YK5	9101	01 19.9	16.7	+73	01 10.837	36.9	+70	3.930	3-	
103067	1999 XA143	9101	01 20.6	15.9	+31	01 17.633	5.5	+26	9.8490	3	
6239	Minos	9101	01 22.7	15.9	+48	11 01.189	5.0	+22	3.5558	3	
265196	2004 BW58	9101	01 28.4	15.3	-4	02 20.648	27.6	+39	6.479	3	PHA
1627	Ivar	9101	01 29.5	15.9	+17	01 28.900	0.4	+17	4.795	3	
5332	Davidaguilar	9101	02 01.1	14.3	-8	02 10.604	25.4	+07	5.803	3	
16834	1997 WU22	9101	02 05.9	15.9	-22	10 05.186	21.8	+32	9.345	3	
496869	2000 QU7	9101	02 16.7	16.6	+22	02 26.349	3.1	+13			
	2015 BK509	9101	02 23.0	16.8	-21	12 04.899	8.8	+37	0.0741	3	Pravec (2020)
535844	2015 BY310	9101	03 02.3	16.0	-18	07 23.488	5.3	-28	0.09267	3	NHATS
66008	1998 QH2	9101	03 02.7	15.9	-68	09 19.536	31.4	+22	7.09	2+	
137126	1999 CF9	9101	03 05.0	14.1	+1	10 20.958	3.9	+03		PHA	
143678	2003 SA224	9101	03 16.7	16.4	+41	12 31.	9.0	-29	35.2		
137170	1999 HF1	9101	03 22.6	14.6	+44	05 15.366	57.3	+63	2.3192	3	
85709	1998 SG36	9101	03 28.1	16.0	-2	01 01.848	33.6	-32	3.573	3-	
	2014 TN17	9101	03 28.5	17.1	-21	-	-	-			
85953	1999 FK21	9101	04 05.0	14.6	+34	03 31.001	30.1	+11	28.08	2	
152754	1999 GS6	9101	04 09.6	16.9	-32	04 24.276	8.3	-22	8.021	2	
223456	2003 UB10	9101	04 10.2	16.8	+8	08 11.472	2.1	-18			
462959	2011 DU	9101	04 21.2	16.0	+35	12 29.403	5.4	+15	10.290	3	PHA
436030	2009 JO2	9101	04 25.8	16.7	+67	06 04.872	50.0	+29			
9058	1992 JB	9101	04 26.3	14.8	-15	05 05.449	30.5	+01			
85818	1998 XM4	9101	04 28.1	17.0	+13	12 31.	22.4	+33	19.451	3	

Table VI. A list of near-Earth asteroids known as of 2024 Oct 10. Green bar lines are on the Goldstone list of planned targets. PHA: Potentially Hazardous Asteroid. NHATS: Near-Earth Object Human Space Flight Accessible Targets Study. BA: Binary asteroid. This is not necessarily a complete list of Goldstone targets. Check their web site.

References

Nesvorny, D. (2015). "Nesvorny HCM Asteroids Families V3.0." NASA Planetary Data Systems, id. EAR-A-VARGBET-5-NESVORNYFAM-V3.0.

Nesvorny, D.; Broz, M.; Carruba, V. (2015). "Identification and Dynamical Properties of Asteroid Families." In Asteroids IV (P. Michel, F. DeMeo, W.F. Bottke, R. Binzel, Eds.). Univ. of Arizona Press, Tucson, also available on astro-ph.

Pravec, P.; Wolf, M.; Sarounova, L. (2020). *http://www.asu.cas.cz/~ppravec/neo.htm*

Warner, B.D.; Harris, A.W.; Pravec, P. (2009). "The Asteroid Lightcurve Database." *Icarus* **202**, 134-146. Updated 2023 Oct. *http://www.minorplanet.info/lightcurvedatabase.html*

Warner, B.D.; Harris, A.W.; Durech, J.; Benner, L.A.M. (2021a). "Lightcurve Photometry Opportunities: 2021 January-March." *Minor Planet Bull.* **48**, 89-97.

Warner, B.D.; Harris, A.W.; Durech, J.; Benner, L.A.M. (2021b). "Lightcurve Photometry Opportunities: 2021 October-December." *Minor Planet Bull.* **48**, 406-410.

Warner, B.D.; Harris, A.W.; Durech, J.; Benner, L.A.M. (2023). "Lightcurve Photometry Opportunities: 2023 July-September." *Minor Planet Bull.* **50***,* 240-244.

Warner, B.D.; Harris, A.W.; Durech, J.; Benner, L.A.M. (2024). "Lightcurve Photometry Opportunities: 2024 October - 2025 January." *Minor Planet Bull.* **51**, 379-384.

IN THIS ISSUE

This list gives those asteroids in this issue for which physical observations (excluding astrometric only) were made. This includes lightcurves, color index, and H-G determinations, etc. In some cases, no specific results are reported due to a lack of or poor-quality data. The page number is for the first page of the paper mentioning the asteroid. EP is the “go to page” value in the electronic version.

THE MINOR PLANET BULLETIN (ISSN 1052-8091) is the quarterly journal of the Minor Planets Section of the Association of Lunar and Planetary Observers (ALPO, http://www.alpo-astronomy.org). Current and most recent issues of the *MPB* are available on line, free of charge from:

https://mpbulletin.org/

The Minor Planets Section is directed by its Coordinator, Prof. Frederick Pilcher, 4438 Organ Mesa Loop, Las Cruces, NM 88011 USA (fpilcher35@gmail.com). Robert Stephens (rstephens@foxandstephens.com) serves as Associate Coordinator. Dr. Alan W. Harris (MoreData! Inc.; harrisaw@colorado.edu), and Dr. Petr Pravec (Ondrejov Observatory; ppravec@asu.cas.cz) serve as Scientific Advisors. The Asteroid Photometry Coordinator is Brian D. Warner (Center for Solar System Studies), Palmer Divide Observatory, 446 Sycamore Ave., Eaton, CO 80615 USA (brian@MinorPlanetObserver.com).

The Minor Planet Bulletin is edited by Professor Richard P. Binzel, MIT 54-410, 77 Massachusetts Ave, Cambridge, MA 02139 USA (rpb@mit.edu). Brian D. Warner (address above) is Associate Editor. Assistant Editors are Dr. David Polishook, Department of Earth and Planetary Sciences, Weizmann Institute of Science (david.polishook@weizmann.ac.il) and Dr. Melissa Hayes-Gehrke, Department of Astronomy, University of Maryland (mhayesge@umd.edu). The *MPB* is produced by Dr. Pedro A. Valdés Sada (psada2@ix.netcom.com).

Effective with Volume 50, the *Minor Planet Bulletin* is an electronic-only journal; print subscriptions are no longer available. In addition to the free electronic download of the *MPB* as noted above, electronic retrieval of all *Minor Planet Bulletin* articles (back to Volume 1, Issue Number 1) is available through the Astrophysical Data System:

http://www.adsabs.harvard.edu/

Authors should submit their manuscripts by electronic mail (rpb@mit.edu). Author instructions and a Microsoft Word template document are available at the web page given above. All materials must arrive by the deadline for each issue. Visual photometry observations, positional observations, any type of observation not covered above, and general information requests should be sent to the Coordinator.

* * * * *

The deadline for the next issue (52-2) is January 15, 2025. The deadline for issue 52-3 is April 15, 2025.

THIS PAGE INTENTIONALLY LEFT BLANK